amU
Aix Marseille Université

NNT : 0000AIXM0000

THÈSE DE DOCTORAT

Soutenue à Aix-Marseille Université
le 18 décembre 2024 par

Coleen Roger

IRM multi-contrastes pour l'étude des noyaux hypothalamiques dans les troubles liés au poids : Une étude trans-espèces

Multi-contrast MRI for the study of hypothalamic nuclei in weight-related disorders : A trans-species study

Discipline
Biologie santé

Spécialité
Neurosciences

École doctorale
ED62 – Sciences de la vie et de la sante

Laboratoire/Partenaires de recherche
- CRMBM-CEMEREM, Marseille
- IMCB-*A*Star, Singapore*

Composition du jury

Renaud Lopes	Rapporteur
CI2C, Hôpital universitaire de Lille	
Fabien Schneider	Rapporteur
TAPE, Université Jean Monnet St Etienne	
Laura M. Holsen	Examinatrice
Harvard Medical School, Brigham and Women's Hospital	
Anne Dutour	Présidente du jury
C2VN, AP-HM, Aix-Marseille Université	
Jean-Philippe Ranjeva	Directeur de thèse
CEMEREM-CRMBM, CNRS, Aix-Marseille Université	
Yu Fu	Co-directeur de thèse
*IMCB A*Star, National University of Singapore*	

Affidavit

I, undersigned, Coleen Roger, hereby declare that the work presented in this manuscript is my own work, carried out under the scientific supervision of Pr Jean-Philippe Ranjeva and Dr Yu Fu, in accordance with the principles of honesty, integrity and responsibility inherent to the research mission. The research work and the writing of this manuscript have been carried out in compliance with both the French national charter for Research Integrity and the Aix-Marseille University charter on the fight against plagiarism.

This work has not been submitted previously either in this country or in another country in the same or in a similar version to any other examination body.

Place Marseille, date 22 octobre 2024



Cette œuvre est mise à disposition selon les termes de la Licence Creative Commons Attribution - Pas d'Utilisation Commerciale - Pas de Modification 4.0 International.

List of publications and meetings

1) Publications related to the PhD work

The Role of the Human Hypothalamus in Food Intake Networks: An MRI Perspective.
Roger C, Lasbleiz A, Guye M, Dutour A, Gaborit B, Ranjeva JP.
Front Nutr. 2022 Jan 3;8:760914. doi: 10.3389/fnut.2021.760914. PMID: 35047539; PMCID: PMC8762294.

Specific macro- and micro-structural alteration of individual HT nuclei in young women with Obesity and Anorexia Nervosa: An in vivo 7T MRI study.
Coleen Roger, Adèle Lasbleiz, Hugo Dary, Lauriane Pini, Patricia Ancel, Anezka Kovarova, Marie-Pierre Ranjeva, Bénédicte Gaborit, Fu Yu, Patrick J Cozzone, Maxime Guye, Anne Dutour and Jean-Philippe Ranjeva. Accepted February 3, 2025

Functional reorganization of hypothalamic networks in young women living with Obesity and Anorexia Nervosa – a 7T MRI study. **Coleen Roger**, Adèle Lasbleiz, Hugo Dary, Lauriane Pini, Patricia Ancel, Anezka Kovarova, Marie-Pierre Ranjeva, Bénédicte Gaborit, Fu Yu, Patrick J Cozzone, Maxime Guye, Anne Dutour and Jean-Philippe Ranjeva. Submitted

2) Oral and poster presentations related to the PhD work

Gordon Research Conference (GRC 2022), Ventura, California US.
'Role of palatability level on hypothalamus activation during food cue paradigm: an fMRI study'.
Scientific poster presented by **Coleen Roger**, Adèle Lasbleiz, Maxime Guye, Fu Yu, Patrick Cozzone, Anne Dutour, Bénédicte Gaborit and Jean-Philippe Ranjeva.

International Society for Magnetic Resonance in Medicine (ISMRM 2024), Singapore.
'Morphological and microstructural modulation of Hypothalamic nuclei by eating disorder: a 7T MRI study'.
Digital scientific poster presented by **Coleen Roger**, Adèle Lasbleiz, Hugo Dary, Lauriane Pini, Patricia Ancel, Marie-Pierre Ranjeva, Maxime Guye, Anne Dutour, Bénédicte Gaborit and Jean-Philippe Ranjeva.

Organization of Human Brain Mapping (OHBM 2024), Seoul, South Korea.
'Functional and structural characterization of Human hypothalamic nuclei in eating disorders'.
Scientific poster presented by **Coleen Roger**, Adèle Lasbleiz, Maxime Guye, Anne Dutour, Bénédicte Gaborit and Jean-Philippe Ranjeva. Abstract Book 3: OHBM 2024 Annual Meeting. *Aperture Neuro*. 2024;4(Suppl 1). doi:10.52294/001c.120593

Résumé

Compte tenu du rôle central de l'hypothalamus (HT) dans la régulation de l'équilibre énergétique, les altérations de cette structure sont depuis longtemps suspectées comme étant la principale cause des troubles liés au poids. Par conséquent, ma thèse a cherché à étudier l'organisation des réseaux de comportement alimentaire chez la souris et l'humain, avec le HT au cœur de cette investigation.

Le premier axe de mes recherches, mené à Singapour, visait à examiner les changements de connectivité fonctionnelle et structurelle dans un modèle murin de consommation alimentaire par conditionnement, en établissant le protocole opératoire standard d'IRM pour les acquisitions d'IRMf au repos in vivo et de DTI ex vivo. Je me suis particulièrement concentré sur le noyau tubéral (TN), un noyau orexigène de l'HT récemment découvert, impliqué dans la prise alimentaire non homéostatique. Le connectome fonctionnel obtenu a révélé que le TN est hyperconnecté à des régions cérébrales impliquées dans la mémoire, la récompense et l'olfaction.

Le deuxième axe de mon travail, mené à Marseille, consistait à caractériser les changements structurels et fonctionnels des noyaux hypothalamiques humains dans les troubles liés au poids à l'aide de l'IRM 7T. Nous avons observé une augmentation des volumes de certains noyaux de l'HT tant chez les patients anorexiques que chez les patients obèses, associée aux niveaux plasmatiques de leptine/ghréline, à la gravité des troubles alimentaires, à la dépression et à l'anxiété. Des altérations de l'organisation fonctionnelle et des schémas d'activation ont été observées au sein du réseau interne de l'HT et entre les noyaux de l'HT et les régions appartenant au réseau de la saillance. Enfin, un ralentissement des dynamiques dans les réseaux internes de l'HT a été observé chez les patients obèses.

Mon travail illustre que l'IRM à ultra-haut champ est désormais suffisamment mature pour étudier efficacement les troubles du poids chez différentes espèces.

Mots clés : consommation alimentaire par conditionnement, équilibre énergétique, fonctionnel, hypothalamus, IRM 7T, noyau tubéral, réseaux de comportement alimentaire, structurel, troubles liés au poids.

Abstract

Given the central role of the hypothalamus (HT) in the control of energy balance, alterations in this small inhomogeneous structure have long been hypothesized to be the leading cause of weight-related disorders. Therefore, my thesis sought to investigate the organization of eating behavior networks in mice and humans, with HT at its core.

My first axis of research in Singapore aimed at investigating the functional and structural connectivity changes in a mouse model of contextual feeding conditioning (CFC), establishing from the ground up the MRI standard operating protocol for the in-vivo resting-state fMRI and ex-vivo DTI acquisitions. I specifically focused my attention on the tuberal nucleus (TN), a newly discovered orexigenic HT nucleus, involved in non-homeostatic food intake. The functional connectome obtained revealed that TN is hyperconnected to brain regions involved in memory, reward and olfaction.

The second axis of my work conducted in Marseille consisted in characterizing structural and functional changes of Human HT nuclei in weight-related disorders using 7T MRI. We found increased volumes of specific HT both in AN and OB, with an association with leptin/ghrelin plasmatic levels, severity of eating disorders, depression and anxiety. Altered functional organization and activation patterns were observed in the inner-HT network and between HT nuclei and regions belonging to the salience network. Finally, a slow-down of dynamics in inner HT networks was observed in OB.

My work illustrates that ultra-high field MRI has now matured enough to effectively study weight-disorders over different species.

Keywords : 7T MRI, contextual feeding conditioning, eating behavior networks, energy balance, functional, hypothalamus, structural, tuberal nucleus, weight-related disorders.

Aknowledgement

"Now I know that if you open the right door at the right time, you might finally find a place where you belong" Every heart a doorway, Seanan McGuire

I found my door almost 10 years ago, when I entered 'Introduction to Neurosciences' class during my first year of bachelor's degree. What started as an inspiring class, turned into devouring every neuroscience book I could find, getting my first volunteered internship in a neuroscience lab, and ultimately being accepted in third year Neuroscience at Aix-Marseille University only 2 years later. There, what was initially a passion turned into a dream of making this my career one day. Being a student in the neuroscience program, I got the huge privilege to participate in the summer research program at Wellesley College (MA) which sparked the idea of doing research abroad and the richness that international diversity brings to a lab environment brings (Thank you to Dr Wiest and my lab mates), and ultimately led me to opt for an internationally co-directed PhD when the opportunity came. The path that leads to a PhD is challenging and takes a village. Here is the opportunity to thank my village.

First and foremost, I want to thank my PhD supervisors. To start with, I am incredibly grateful for your invaluable guidance and unwavering support throughout this PhD journey. Thank you for trusting me with this amazing project, it was a privilege to work with you.
Pr Jean-Philippe Ranjeva, your kindness, patience, and genuine dedication have not only guided me through this PhD but have also inspired me to grow both academically and personally and made this journey exceptionally meaningful. Thank you for you positivity, I will never forget your famous saying 'Allez ça va le faire !', which encouraged and motivated me throughout this journey.
To my co-supervisor Dr Fu Yu, I wish to thank you for our regular "thesis meetings" and for your infectious passion for eating behavior. I am truly lucky to have been working alongside you and your team at Astar.
I also want to thank Dr Patrick Cozzone without whom this collaboration between Singapore and Marseille would not have existed. Finally, I am grateful for the funding of Neuroschool and the Astar institute without whom this collaboration wouldn't have been possible.

Then, I want to thank my jury members: Dr Renaud Lopes, Dr Fabien Schneider, Dr Laura M. Holsen and Dr Anne Dutour. Thank you for giving your time to read and evaluate this research work, and for our enlightening discussions during my PhD defense.
I would also like to give special thanks to Professor Vincent Prévot, as well as Dr. Pierre-Yves Jacob, for having supported me throughout my thesis. I am extremely grateful for all your advice and encouragement during the thesis committees.

To my colleagues in Singapore at IMCB, Dr Esra Senol, Dr Hasan Mohammad, Dr Sarah Luo, Dr Kenneth Lum, Shi Ying Tor, Christine Chiam, Zhi Yin and Dr Yongjuan Xin, I want to thank you for having led the ground of my project here and for your help in the lab and insightful advice during lab meetings.
I also want to say a huge thanks to the MRI team in Singapore directed by the Dr Lee Kuan Jin, with whom I have spent most of my time in the lab. From spending our whole day scanning mice, sometimes falling to, but always learning from it and thriving to make it better, and to all our meetings, full of important teaching. Dr Lee Kuan Jin, Xing Qi, Dr Redha Boubertakh, Dr

Sanjay Verma, and Isaac Huen, I learned the most from you. Specific thanks to Xing Qi, who was like a big sister to me, your kindness and drive to better yourself inspires me, I hope we will see each other soon lah!

A mes collègues de Marseille, tout d'abord merci à l'ensemble de l'équipe du CEMEREM et CRMBM, pour les discussions enrichissantes autour d'un café ou vos questions pertinentes pendant la réunion CNS qui ont rendu ma réflexion scientifique meilleure. Je tiens à remercier l'ensemble des investigateurs de l'étude HYPOTHALNET qui m'ont permis de participer à ce projet formidable : Adèle Lasbleiz, Anne Dutour, Bénédicte Gaborit, Arnaud Le troter, Maxime Guye, Patrice Darmon, Sylviane Confort-Gouny, Marie-Pierre Ranjeva et Monique Bernard.
Un grand merci également au NeuroSchool PhD program, plus particulièrement Dr Wafa Zaaraoui, pour m'avoir fait confiance et pour ton implication sans faille auprès des étudiants en Neurosciences. Merci aux manipulateurs radio et aux ingénieurs, Lauriane Pini, Claire Costes, Shirley Corela et Hugo Dary pour votre expertise, patience et savoir-faire. Un merci tout particulier à mes collègues de bureau, devenues des amis chères à mon cœur, Soraya gherib, Mikael Azilinon et Roy Haast pour n'en citer que quelques-uns. À mon acolyte Dr Samira Mchinda, merci pour ton soutien sans failles tout au long de cette aventure, et à nos fameuses pauses madeleine, ces moments précieux remplis de fous rires.

A mes amis qui ont vécus avec moi les montagnes russes que représente une thèse : Kimberley Aubert, Marion Ristorcelli, Thibaut Piquemal, Nolwenn Poupine et Halla Redjdal.
To my friends met in Singapore who made these 2 years even more beautiful: Mendelsohn Chan, Chelsea Robas Park, May Parks and Nicolas Christie just to name a few.

A mes parents et ma grand-mère, mes piliers. Je vous dédie tous mes accomplissements, car avant d'y croire moi-même, vous en étiez persuadés.

Moving to Asia was not only a valuable scientific experience, but it also led me to find my husband. Chester, thank you for your unwavering support, patience and love throughout my thesis journey. Not only have you been there for me emotionally, but you've also kept me nourished with your delicious meals, making sure I could focus on my work, and for that, I am beyond grateful. Thank you for always being my rock and giving me the comfort of home during this challenging time.

Table of contents

Affidavit 2
List of publications and meetings 3
Résumé 4
Abstract 5
Acknowledgement 6
Table of contents 8
List of figures 13
List of abbreviations 14
1 General introduction 15
1.1 Motivation 15
1.2 Context of the thesis 17
2 General overview 18
2.1 Energy homeostasis 18
2.1.1 Hypothalamic central control of food intake 20
2.1.2 Peripheral signaling of food intake 22
2.1.2.1 Short term regulation 24
2.1.2.1.1 Sensory signals 24
2.1.2.1.2 Glucagon-Like Peptide 1 (GLP-1) 24
2.1.2.1.3 Cholecystokinin (CCK) 24
2.1.2.2 Long-term regulation 25
2.1.2.2.1 Leptin 25
2.1.2.2.2 Insulin 26
2.1.2.2.3 Ghrelin 26
2.1.2.2.4 Peptide tyrosine-tyrosine (PYY) 26
2.1.3 Extra-hypothalamic central control of food intake 27
2.1.3.1 Sensory cortex 28
2.1.3.2 Limbic system 28
2.1.3.3 Cortex 32
2.2 General anatomy of the Hypothalamus 33
2.2.1 Human hypothalamus 33
2.2.2 Mouse hypothalamus 34

2.2.2.1 Principal hypothalamic nuclei involved in food-intake regulation 36
2.2.2.1.1 Arcuate nucleus (ARH) 36
2.2.2.1.1.1 Role 36
2.2.2.1.1.2 Connectivity 36
2.2.2.1.2 Lateral hypothalamus (LH) 36
2.2.2.1.2.1 Role 36
2.2.2.1.2.2 Connectivity 37
2.2.2.1.3 Dorsomedial Nucleus (DM) 37
2.2.2.1.3.1 Role 37
2.2.2.1.3.2 Connectivity 37
2.2.2.1.4 Paraventricular nucleus (PaVN) 38
2.2.2.1.4.1 Role 38
2.2.2.1.4.2 Connectivity 38
2.2.2.1.5 Ventromedial Nucleus (VM) 38
2.2.2.1.5.1 Role 38
2.2.2.1.5.2 Connectivity 39
2.2.2.1.6 Tuberal nucleus (TN) 39
2.2.2.1.6.1 Role 39
2.2.2.1.6.2 Connectivity 40
2.3 Weight-related disorders associated to dysfunction of eating behavior networks 41
2.3.1 Obesity 41
2.3.1.1 Definition 41
2.3.1.2 Epidemiology 41
2.3.1.3 Etiology 44
2.3.1.3.1 Environment 44
2.3.1.3.2 Genetic 45
2.3.1.3.3 Dopaminergic system 45
2.3.1.3.4 Hypothalamic pathways implicated in the disruption of energy homeostasis 45
2.3.2 Anorexia nervosa 47
2.3.2.1 Definition 47
2.3.2.2 Epidemiology 47
2.3.2.3 Etiology 48
2.3.2.3.1 Environment 48
2.3.2.3.2 Genetic 49
2.3.2.3.3 Dopaminergic system 50
2.3.2.3.4 Hypothalamic pathways implicated in the disruption of energy homeostasis 50

2.4 Assessment of eating behavioral disturbances in weight-related disorders 52
2.4.1 Animal models of weight-related disorders 52
2.4.1.1 Activity-based anorexia nervosa (ABA) 52
2.4.1.1.1 Model induction 52
2.4.1.1.2 Lipostat alterations in ABA 52
2.4.1.1.3 Appetite regulation hormone levels alterations in ABA 53
2.4.1.2 High-fat diet-induced obesity (HFD) 54
2.4.1.2.1 Model induction 54
2.4.1.2.2 Lipostat and Appetite regulation hormone levels alterations in HFD 54
2.4.1.3 Contextual feeding conditioning (CFC) 55
2.4.1.3.1 Model induction 55
2.4.1.3.2 Contextual feeding conditioning paradigm (CFC) mechanism 56
2.4.2 Assessment of eating behavior in Human 57
2.4.2.1 SCOFF (Sick, Control, One, Fat, Food) 57
2.4.2.2 Eating Attitudes Test-26 (EAT-26) 57
2.4.2.3 Yale Food Addiction Scale 2.0 (YFAS) 57
2.4.2.4 Hospital Anxiety and Depression Scale (HADS) 57
2.4.2.5 Beck Depression Inventory (BECK) 58
2.5 Contributions of brain imaging in the study of weight-related disorders 59
2.5.1 Foreword 59
2.5.2 Manuscript 59
2.5.3 Concluding remarks 87
3 Hypotheses and Objectives 89
4 Structural and Functional study of the hypothalamic tuberal nucleus in mice using high-resolution MRI and its modulation in a model of cue-triggered food consumption, contextual feeding conditioning (CFC), in mice 91
4.1 Foreword 91
4.2 Animal model 94
4.2.1 Anaesthesia and animal preparation 94
4.2.2 Monitoring of animal physiology 95
4.2.3 Recovery after scan 95
4.3 Adaptation of a mouse Atlas for MRI studies 97
4.4 Resting-state fMRI 99
4.4.1 MRI Set up 99
4.4.2 Analysis 100
4.4.2.1 Data processing 100

4.4.2.2 Preprocessing 100
4.4.2.3 Preprocessing quality control 102
4.4.2.4 Confound correction 104
4.4.2.5 Statistical analysis of functional connectivity 104
4.5 Ex-vivo DTI MRI 105
4.5.1 Transcardial perfusion and brain preparation 105
4.5.2 MRI Setup 105
4.5.3 Analysis 105
4.5.3.1 Data preparation 105
4.5.3.2 preprocessing 106
4.5.3.3 Statistical analysis 107
4.6 Preliminary results 108
4.6.1 Functional connectome of the TN in mice 108
4.6.1.1 Functional connectivity of the TN in control mice 108
4.6.1.2 Hyperconnectivity of the TN in CFC mice 112
4.6.1.3 Hypoconnectivity of the TN in CFC mice 115
4.6.2 Structural connectome of the Tuberal Nucleus in control mice 117
4.7 Multi-modal brain-wide circuit analysis reveals neural mechanisms of conditioned feeding behavior 120
4.7.1 Foreword 120
4.7.2 Manuscript 120
5 Structural alterations of individual hypothalamic nuclei in young women with Obesity and Anorexia Nervosa: An in vivo 7T MRI study 127
5.1 Foreword 127
5.2 Manuscript 127
5.2.1 Questionnaires 134
5.2.2 *Participants* 134
5.2.3 *Image acquisition* 136
5.3 Concluding remarks 170
6 Functional reorganization of hypothalamic networks in young women with Obesity and Anorexia Nervosa – a 7T MRI study 171
6.1 Foreword 171
6.2 Manuscript 171
6.2.1.1 Whole-brain network dynamics 182
6.2.2 EAT-26 correlations 183
7 General conclusion 207
8 Bibliography 210

9 Appendix 276

List of figures

Figure 1 : Schematic representation of the consequences of hypothalamic inflammation on energy homeostasis. 19
Figure 2 : Schematic representation of the consequences of hypothalamic inflammation on energy homeostasis. 23
Figure 3 : Long-acting adiposity signals and short-acting meal-related signals that contribute to energy balance. 25
Figure 4 : Coordination of eating behavior by multiple brain regions. 27
Figure 5 : Cortical and Subcortical connections to Hypothalamus. 28
Figure 6 : Mesocorticolimbic-hypothalamic circuitry and functions. 30
Figure 7 : Structural organization of HT and its nuclei. 33
Figure 8 : Schematic representation of hypothalamic subdivisions in a midsagittal section of the mouse brain 35
Figure 9 : Evolution of the prevalence of obesity by age groups between the 1997-2012 and the 2020 42
Figure 10 : Evolution of the prevalence of obesity (BMI ≥ 30 kg/m2) by professional category. 42
Figure 11 : Evolution of the prevalence of obesity (BMI ≥ 30 kg/m2) by professional category, ... 43
Figure 12 : Foresight's Tackling Obesities: Future Choices report, UK. 44
Figure 13 : Schematic representation of the consequences of hypothalamic inflammation on energy homeostasis. 46
Figure 14 : Trends in the incidence of anorexia nervosa in women of all ages for hospital admission studies 48
Figure 15 : Environmental risk factors that can trigger the onset of eating disorders. 49
Figure 16 : Schematic of the CFC paradigm. 55
Figure 17 : ^{TN}SSTneurons in the mouse can be activated by hunger signals, including ghrelin. 91
Figure 18 : Full resting-state pipeline. 92
Figure 19 : Full DTI pipeline. 93
Figure 20: Timeline of anaesthesia during the scan. 95
Figure 21: Timeline (A) and physiological monitoring (B) of recovery. 96
Figure 22: Comparison of the original and compacted bilateral Allen Brain Atlases. 97
Figure 23: Masks of the different mouse tissue types used in the resting stare data preprocessing. 98
Figure 24: Scan timeline. 99
Figure 25: Preprocessing steps used in Rabies pipeline. 101
Figure 26 : Automatically generated outputs for preprocessing quality control from one CFC subject preprocessed with RABIES. 103
Figure 27: Registration of the brain mask and atlas to DTI data 106
Figure 28: Quality control of DTI preprocessing 107
Figure 29: Circos plot of the TN functional connectome in control mice. 111
Figure 30 : Circos plot of the hyperconnectivity of TN in conditioned mice. 114
Figure 31: Circos plot of the TN functional connectome in control sup conditioned mice. 116
Figure 32: Circos plot of the TN structural connectome in control mice. 119

List of abbreviations

AgRP	Agouti-related protein
AHA	Anterior Hypothalamic Area
α-MSH	Alpha-melanocyte stimulating hormone
AN	Anorexia nervosa
ARH	Arcuate hypothalamic Nucleus
AVPV	Anteroventral periventricular preoptic nuclei
BLA	Basolateral amygdala
BMI	Body mass index
BNST	Bed Nucleus of Stria Terminalis
CART	Cocaine- and amphetamine-regulated transcript
CCK	Cholecystokinin
CEA	Central amygdala
CFC	Contextual feeding conditioning
DM	Dorsomedial hypothalamic nucleus
DPEH	Dorsal Periventricular Hypothalamic nucleus
FX	Fornix
GLP-1	Glucagon-Like Peptide 1
HC	Healthy control
HT	Hypothalamus
LH	Lateral hypothalamus
MM	Mammillary bodies
MnPO	Median preoptic nuclei
MPO	Medial preoptic nuclei
MT	Mammillothalamic tracts
NAc	Nucleus accumbens
NST	Nucleus of the solitary tract
NPY	Neuropeptide Y
OB	Obesity
OFC	Orbitofrontal Cortex
PaVN	Paraventricular Hypothalamic nucleus
PeVN	Periventricular hypothalamic nucleus
PAG	Periaqueductal gray
PFC	Prefrontal cortex
PH	Posterior nuclei
PM	Premammillary nuclei
POA	Preoptic area
POMC	Proopiomelanocortin
PVpo	periventricular preoptic nuclei
PVT	Paraventricular thalamus
SC	Suprachiasmiatic hypothalamic nucleus
SCN	Suprachiasmatic
SON	Supraoptic optic nucleus
SuM	supramammillary nucleus
TM	Tuberomammillary nucleus
TN	Tuberal nucleus
VLPO	Ventrolateral preoptic nuclei
VM	Ventromedial hypothalamic nucleus
VP	Ventral pallidum
VTA	Ventral tegmental area
WHO	World Health Organization
ZI	Zona Incerta

1 General introduction

1.1 Motivation

Energy expenditure is a continuous process, whereas energy replenishment through food intake is inherently intermittent. Despite this finely tuned system, significant weight variations can occur, leading to an imbalance in energy equilibrium. The origin of this disorder is complex and multifactorial, with a behavioral component that explains the disturbance in eating habits. Given its central role in the control of energy balance, alterations in the hypothalamus (HT) have long been hypothesized to be the leading cause of weight-related disorders.

In Human, most neuroimaging studies have largely overlooked the hypothalamus or considered it as one homogeneous structure. Although the HT is a small brain region (around 1 cm^3), it is organized into highly distinct nuclei. Indeed, rodent studies have demonstrated that food intake behavior is primarily regulated by five key nuclei within the hypothalamic circuit known as the lipostat, which is responsible for managing and maintaining energy balance.
First, the Arcuate hypothalamic Nucleus (ARH) initiates food intake, the Lateral (LH) and Dorsomedial hypothalamic nucleus (DM) stimulate food intake, while the Paraventricular (PaVN) and Ventromedial hypothalamic nuclei (VM) exert an inhibitory effect on feeding behavior when satiation is reached (J. Zhang et al., 2020).

Apart from this well-characterized circuit, a new aspect of food intake involving mechanisms governing non-homeostatic processes was found. A recent animal study showed that the LH and the Tuberal nucleus (TN) are implicated in non-homeostatic feeding driven by contextual cues, 'contextual feeding conditioning' (CFC) (Mohammad et al., 2021), with TN specifically involved in the approach of palatable food. This work, led by my colleagues in Singapore, revealed a novel circuit mechanism that explains how environmental information is processed by hypothalamic orexigenic neurons, which directly influence feeding behavior. These findings suggest that the presence of palatable food activates additional circuits to facilitate context-dependent feeding. These circuits may play a crucial role in how TN and LH respond to food. However, it remains unclear how these neurons are activated by palatable food. Furthermore, neural circuit mechanisms of context-induced feeding are particularly relevant to human behavior, as such feeding patterns are observed in individuals with obesity and likely contribute to eating disorders, such as compulsive and binge eating (Schachter, 1968; Wardle, 1990).
In sum, although multiple HT nuclei have been identified, their differential participation in the behavioural response to food intake remains enigmatic. Understanding the specific functions of these nuclei and how their alterations contribute to weight-related disorders could provide crucial insights into the mechanisms underlying weight-related disorders.

Moreover, translation of the cellular mechanisms observed in animal models to Human *in vivo* is not straightforward. In that context, ultra-high field (7T) MRI has appeared as a game changer to explore eating behavioral networks and the consequences of their dysregulation from an anatomical, functional or even metabolic point of view (Florent et al., 2020a; Neseliler et al., 2017; Salem & Dhillo, 2015a). Bridging this translational gap using MRI is the core of my project.

Since the dysregulation of feeding behaviour seems to contribute to the rising prevalence of obesity, as well as the severity of restrictive anorexia nervosa, this thesis sought to investigate the organization of the food intake network in mouse and Human. To do so, we studied the functional and structural alterations of individual hypothalamic nuclei, both involved in homeostatic and non-homeostatic regulation of food intake, to assess their respective roles in the behavioral changes observed in weight-related disorders in vivo.

This PhD work focuses on the two most frequent chronic weight-related disorders resulting from maladaptive eating behaviors: obesity and restrictive anorexia nervosa.

Defined by a body mass index (BMI) over 30 resulting from to abnormal fat accumulation presenting a risk to health (World Health Organization, WHO), obesity is rapidly increasing the morbidity and mortality rates of chronic diseases, particularly cardiovascular disease, type 2 diabetes mellitus, and mental health disorders (Takizawa et al., 2015). In France alone, the prevalence of obesity keeps increasing, with estimation at 8,5 % in 1997, 15 % in 2012 and 17 % in 2020 (Charles et al., 2008; Fontbonne et al., 2023).

In contrast, restrictive anorexia nervosa represents the most common eating disorder and holds the highest mortality rate of any psychiatric disease. Restrictive anorexia nervosa is specifically characterized by chronic food restriction, which may or may not be associated with intense physical exercise, leading to a severe weight loss associated with metabolic disturbances, infertility, osteopenia, and osteoporosis.

We believe that studying the HT at the nuclei level using UHF MRI will facilitate the translation of findings from mouse studies and enable more detailed profiling of individual hypothalamic nuclei in both species. Understanding how both normal and maladaptive eating behaviors develop and persist is essential for creating effective interventions or treatments. This concept could substantially advance personalized monitoring for patients with weight-related disorders, improve their outcomes, and support the development of tailored nutritional interventions based on their specific neural profiles.

1.2 Context of the thesis

This manuscript describes the work accomplished throughout my 4-year PhD period.
A general background will be established, followed by the thesis objectives and hypothesis. The next three chapters will be dedicated to the three scientific articles produced as part of this thesis. The first one is part of a collaborative study investigating the connectivity changes in a mouse model of context using Lightsheet and multi-modal MRI. The last two characterized the structural and functional alterations of hypothalamic nuclei in weight-related disorders. In the last chapter, the outcomes of my PhD work and their limitations will be discussed, concluding with remarks and future perspectives.

Clinical work was conducted at the Magnetic Resonance Center for Metabolic Exploration (CEMEREM-CRMBM, APHM, AMU-CNRS), on a 7T MRI system. Pre-clinical work was conducted at the Institute of Molecular and Cell Biology (IMCB) at the A*Star institute of Singapore, equipped with 11.7T and 9.4T MRI systems.

My PhD was co-funded by the Neuroschool PhD Program (*ANR-17-EURE-0029)* in Marseille and by the A*STAR Research Attachment Program (ARAP) in Singapore. The team of Pr Patrice Darmon and Anne Meyer-Dutour at the Department of Endocrinology, Public Assistance-Hospitals of Marseille (AP-HM) of La Conception Hospital was a valuable partner throughout my thesis.

2 General overview

2.1 Energy homeostasis

Energy expenditure appears as a continuous process, while energy refilling through food intake is by nature discontinuous. To keep the body fat mass stable, a system in which the hypothalamus (HT) is one of the key structures, provides efficient balance between energy expenditure and energy intake (**Figure 1**). The regulation of energy balance relies on a complex and continuous communication between homeostatic system controlled by the HT (2.1.1) through its integration of hormonal and metabolic signals (2.1.2), as well as other central structures which can be divided into 3 systems following the hierarchical model of taste processing: reward, cognitive control and encoding of gustatory, visual, auditory, and somatosensory palatability (2.1.3) (Rolls, 2004, 2015, 2016a, 2016b).

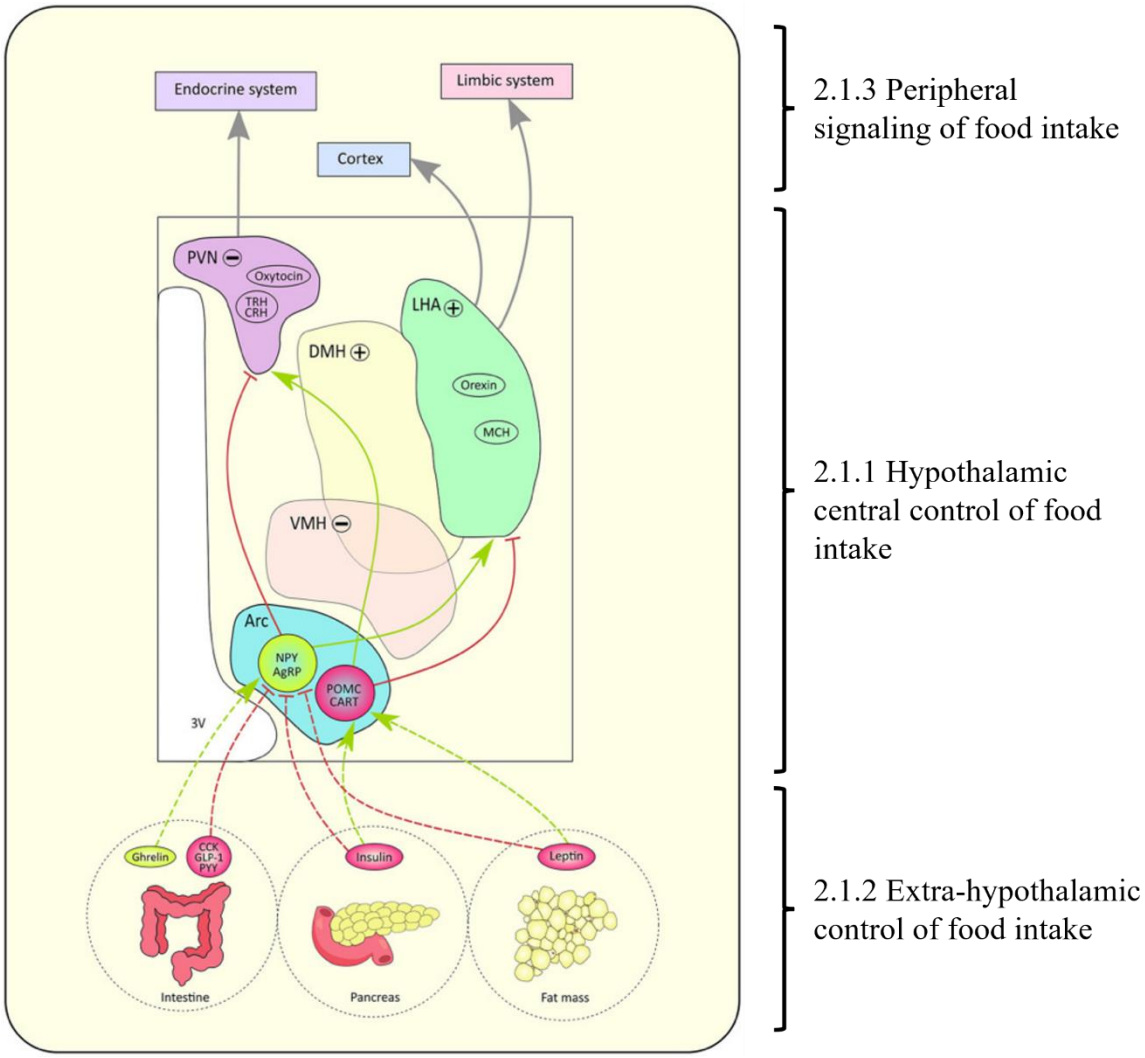

Figure 1 : Schematic representation of the consequences of hypothalamic inflammation on energy homeostasis.

According to hunger state, hormones are released by the intestine, pancreas and fat mass. Those signals directly influence neuronal activity in the hypothalamus through their action on antagonistic neurons located in the arcuate nucleus (Arc): orexinergic neurons expressing neuropeptide Y (NPY)/ agouti-related peptide (AgRP) and anorexinergic neurons expressing pro-opio-melanocortine (POMC)/ cocaine- and amphetamine- regulated transcript (CART). Gut hormones such as cholecystokinin (CCK), peptide YY (PYY), glucagon-like peptide 1 (GLP-1) inhibit NPY/AgRP neurons while ghrelin stimulates NPY/AgRP neurons. The pancreas secretes insulin while leptin is secreted by fat mass cells. Both hormones trigger the inhibition of NPY/AgRP neurons but the stimulation of POMC/CART neurons. Red arrows represent inhibitory connections, green arrows represent stimulatory connections, gray connections represent indirect pathways. The paraventricular nucleus (PVN) hosts neurons expressing oxytocin, thyrotropin-releasing hormone (TRH) and corticotropin-releasing hormone (CRH), while the lateral hypothalamic area (LHA) contains neurons expressing orexin and melanin-concentrating hormone (MCH). The '+' sign means the nucleus has an orexinergic effect on food intake when activated, whereas the '−' sign indicates that the nucleus has an anorexinergic effect on food intake when activated. Indeed, when activated, the dorsomedial hypothalamus (DMH) and lateral hypothalamic area (LHA) have an orexinergic action while the ventromedial hypothalamus (VMH) and paraventricular nucleus (PVN) have an anorexinergic action on food intake. Finally, the PVN sends information to the endocrine system while the LHA carries input to the cortex and limbic systems. 3V, third ventricle (Roger et al., 2022).

2.1.1 Hypothalamic central control of food intake

Ablation studies first brought focus on the hypothalamus's role in feeding and energy metabolism. While lesions in the ventromedial HT led to hyperphagia and ultimately obesity, lesions in the lateral hypothalamus caused decreased food intake and significant weight loss (Hetherington & Ranson, 1940). These discoveries led to the conclusion that there were hypothalamic 'centers' regulating satiety and hunger in distinct ways.

It was later discovered that the ventromedial lesion included the arcuate nucleus (ARH), a small structure playing a central role in signaling peripheral signals to other brain structures. Indeed, located near the third ventricle, the neuronal populations of ARH are the first to receive circulating blood signals, serving as the primary hypothalamic relay between peripheral organs and the central nervous system. Therefore, it is accessible to appetite-regulating hormones such as leptin, insulin and ghrelin, which cannot cross the blood-brain barrier in other areas of the brain. By binding to their respective receptors in the ARH, these hormones alter the activity of hypothalamic neurons and contribute to the regulation of energy status. The ARH contains the cell bodies of first order neuronal populations involved in regulating food intake: (i) orexigenic neurons expressing the Agouti-related protein (AgRP) and neuropeptide Y (NPY), (ii) anorexigenic neurons expressing proopiomelanocortin (POMC), a protein precursor of two classes of peptide, cocaine- and amphetamine-regulated transcript (CART) and alpha-melanocyte stimulating hormone (α-MSH) (Sainsbury & Zhang, 2010).

The HT depends on a complex network of circuits to regulate energy balance. Indeed, first order neurons located in the ARH also send intra-hypothalamic projections to second order neurons. ^{ARH}AgRP neurons activate neurons in the LH that express melanocortin hormones and orexin, leading to increased food intake. In contrast, satiety is mainly regulated by ^{ARH}POMC neurons, which project to PaVN neurons to release α-melanocyte-stimulating hormone and reduce food intake (Berthoud, 2002a; Harris, 2017a). Second-order neurons in the PaVN, VM, DM, and LH also play an active role in regulating energy homeostasis through their extended intra- and extrahypothalamic projections (Harris, 2017a).

Numerous morphological studies have shown that interactions occur between the two neuronal populations present in the ARH (Csiffáry et al., 1990). Indeed, when energy levels are low, ^{ARH}AgRP can directly inhibit ^{ARH}POMC neurons to effectively block satiation (Timper & Brüning, 2017). Thus, the first-order neurons in the ARH serve as a crucial link between the periphery and the central nervous system, with their activity being modulated in response to peripheral signals.

The hypothalamic nuclei are intricately interconnected, allowing for the coordinated regulation of energy balance, reproduction, sleep-wake cycles, stress responses, thermoregulation, osmoregulation, and blood pressure. In sum, reciprocal communication between first order neurons co-existing in the ARH and between first order and second order neurons allows for the coordination and balance of their activity. These key neural circuits ultimately enable the increase of hunger sensation and motivation to eat when energy balance is negative and, conversely, decrease these responses when energy balance is positive (Csiffáry et al., 1990).

Additionally, the HT is recognized as a central hub for integrating signals from gut-derived hormones and microbiota metabolites. The next part is dedicated to the different peripheral signals which activate or inhibit these hypothalamic neuronal populations depending on the body's energy status.

2.1.2 Peripheral signaling of food intake

As previously reported, energy homeostasis relies on feedback between the peripheral system and specific hypothalamic neuronal populations. These neurons respond to hormonal and metabolic signals, interacting to maintain short- and long-term energy balance (**Figure 2**). Short-term regulation of energy balance is governed by feedback from intestinal hormones ensuring appropriate food intake, while long-term regulation is linked to adipose tissue ensuring adequate energy stores (Andermann & Lowell, 2017). These various mechanisms enable precise regulation of eating behavior throughout life in most humans.

- In a fasting state, ghrelin levels increase while leptin, insulin, Glucagon-Like Peptide 1 (GLP-1), and PYY levels decrease which activates central orexigenic pathways and produces a sensation of hunger (Friedman & Halaas, 1998). The low plasma leptin levels simultaneously activate ^{ARH}AgRP neurons and inhibit ^{ARH}POMC neurons. In contrast, the enhanced secretion of ghrelin activates ^{ARH}NPY/AgRP neurons while inhibiting anorexigenic neurons (Berthoud & Morrison, 2008a).

- In a satiation state, ghrelin is inhibited and secretion of leptin, GLP-1, and PYY is enhanced, which activates central anorexigenic pathways and generates a feeling of satiety (Friedman & Halaas, 1998). The elevated plasma leptin levels increases ^{ARH}POMC neuronal activity while inhibiting ^{ARH}AgRP neurons by lifting their GABAergic inhibition on anorexigenic neurons which has the effect of inhibiting food intake and increasing energy expenditure (Elias et al., 1998; M. W. Schwartz et al., 1996). Additionally, insulin causes hyperpolarization and reduced firing in both neurons ^{ARH}NPY/AgRP neurons, while stimulating POMC neurons (Berthoud & Morrison, 2008a).

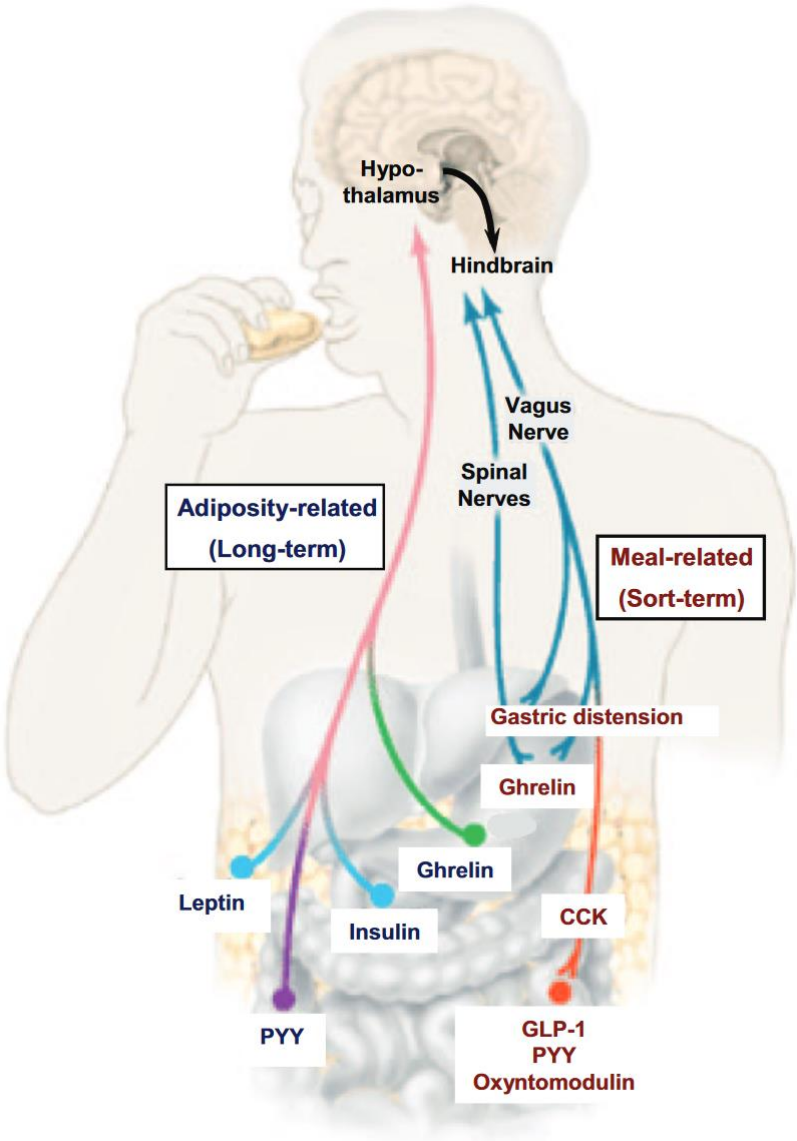

Figure 2 : Schematic representation of the consequences of hypothalamic inflammation on energy homeostasis.

Ingested food stimulates gastric distention as well as a set of intestinal peptides that act in unison to cause satiation and promote meal termination, largely signaling through neural connections to the hindbrain. Long-acting adiposity hormones, such as leptin and insulin, augment satiation signals through several mechanisms, including hypothalamus-to-hindbrain pathways, direct actions on hindbrain sites receiving visceral vagal input, and enhancement of vagal responsiveness to relevant gut peptides. Secretion of the orexigenic peptide ghrelin, primarily from the stomach, is stimulated before individual meals and also in response to weight loss. Ghrelin acts on the hypothalamus, hindbrain, vagus nerve, and mesolimbic reward centers to increase food intake and body weight (Foster-Schubert & Cummings, 2006).

2.1.2.1 Short term regulation

Short-term regulation of energy balance involves meal initiation and termination, directly influenced by food intake signals during digestion and nutrient metabolism. These signals affect meal volume and duration, satiety, and duration of satiation.

2.1.2.1.1 Sensory signals

Sensory signals, primarily from sight and smell, trigger physiological responses before food ingestion. Taste, temperature, and texture then influence food palatability, affecting how much is consumed. This palatability determines whether food intake is prolonged and increased or stops early if sensations turn unpleasant. These sensory inputs include learned associations and various cues beyond direct food identification, such as auditory and somatosensory inputs. Once in the mouth, taste and mechanical sensations play key roles in ingestive behavior, sending neural or hormonal signals to the brain via vagal afferents or the bloodstream (Berthoud & Morrison, 2008a).

2.1.2.1.2 Glucagon-Like Peptide 1 (GLP-1)

GLP-1 is an anorexigenic peptide produced in the ileum, which enhances satiation and reduces food intake (Hoyt et al., 1996). GLP-1 is secreted in response to arrival of nutrients into the intestine proportionally to the meal's energy content. The active form of GLP-1 reduces short-term food intake and appetite (D.-H. Kim et al., 2009). Peripherally, GLP-1 regulates digestion and enhances insulin secretion (Nauck et al., 1997). GLP-1's effects on pancreatic hormone secretion and gastric emptying make it a potent regulator of glycemic homeostasis (Schirra & Göke, 2005). Centrally, GLP-1 acts through the activation of its receptor, GLP-1R, predominantly found in the ARH and PaVN, as well as in the brainstem (Turton et al., 1996).

2.1.2.1.3 Cholecystokinin (CCK)

CCK is a peptide hormone secreted by the enterocytes of the proximal part of the small intestine (duodenum and jejunum). Secretion of CCK is triggered by the arrival of proteins or lipids. Although it is believed that CCK main action is to reduce food intake, its concentration in the bloodstream can remain elevated for up to 5 hours after a meal.
Peripherally, CCK regulates intestinal motility and stimulates pancreatic and gastric secretions. Its satiety effect is potentiated by stomach distension or the secretion of leptin (Moran & Kinzig, 2004). Centrally, CCK acts on the LH, DM, PaVN, and solitary tract nucleus (Bi et al., 2001).

2.1.2.2 Long-term regulation

Long-term regulation of energy balance ensures the maintenance of energy stores and is primarily hormonal. It modulates the impact of short-term signals on brain regions by directly influencing hypothalamic pathways that control energy balance. These signals can be divided into factors triggering hunger and those maintaining satiety: orexigenic signals like ghrelin, a marker of hunger and meal initiation, versus anorexigenic signals like leptin, insulin and PYY.

2.1.2.2.1 Leptin

Leptin is a digestive hormone secreted in the bloodstream predominantly by the adipose tissue when lipid reserves are high (Y. Zhang et al., 1994). It is commonly known as 'the satiety hormone' because it regulates fat storage by controlling the sensation of fullness, which ultimately reduces food intake in both the short and long term (van Dielen et al., 2001). The concentration of circulating leptin reflects both the body's energy reserves and food intake. Indeed, leptin baseline level is positively correlated with adipose tissue mass (**Figure 3**), explaining its high levels in obese patients (Chapelot et al., 2000).

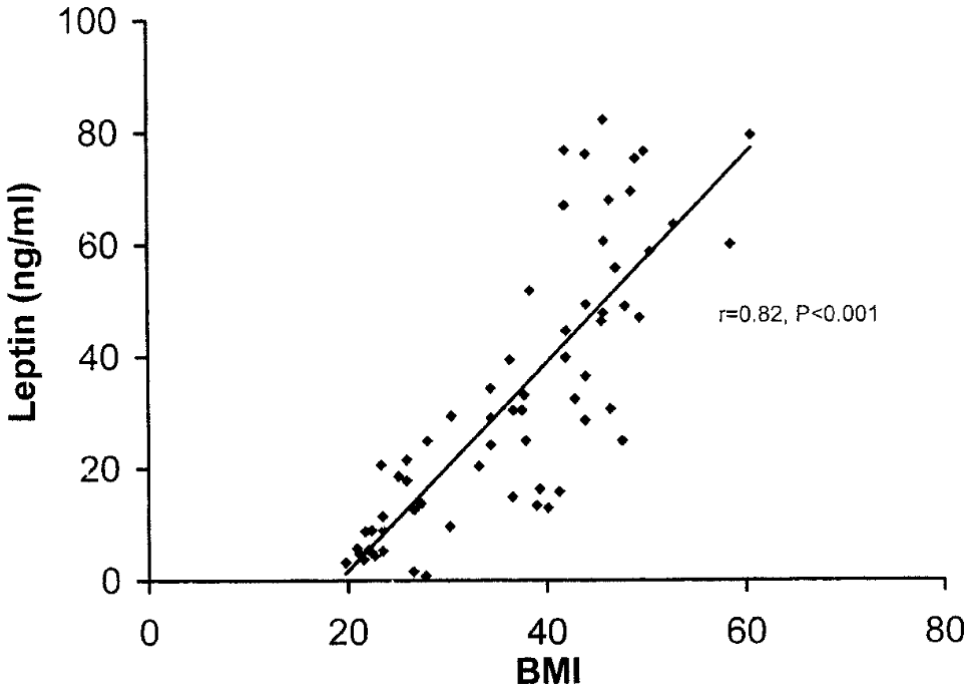

Figure 3 : Long-acting adiposity signals and short-acting meal-related signals that contribute to energy balance (van Dielen et al., 2001).

2.1.2.2.2 Insulin

Insulin regulates blood sugar levels and energy substrate usage, with its plasma levels varying throughout the day, primarily rising after carbohydrate-rich meals. Insulin plays an active role in short-term regulation by responding to postprandial increases in blood sugar levels. However, it also plays a role in long-term regulation because fasting plasma insulin levels correlate positively with adiposity.

2.1.2.2.3 Ghrelin

Ghrelin is the only peripherally secreted hormone with a stimulatory effect on appetite. It is secreted from the mucosa of the empty stomach and duodenum seems to stimulate appetite by inhibiting activity of vagal afferents.
Ghrelin acts centrally to stimulate food intake and food-motivated behavior (Wren et al., 2001) (Skibicka et al., 2012).
Ghrelin circulating levels are high when fasting and peak just before a meal. Its concentration rapidly drops upon the ingestion of food, proportionally to the energy consumed and the content of specific macronutrients, with proteins having a greater inhibitory effect on its secretion than carbohydrates (Cummings, 2006).
Ghrelin decreases the secretion and anorexigenic effect of leptin, while leptin reduces the secretion and orexigenic effect of ghrelin, forming a feedback loop known as the 'ghrelin-leptin tango' (Cummings & Foster, 2003).

2.1.2.2.4 Peptide tyrosine-tyrosine (PYY)

Peptide tyrosine-tyrosine (PYY) is secreted mainly in the ileum, colon, and rectum in response to food intake, and its concentration remains high for up to 6 hours after the meal. Its release into the bloodstream is primarily influenced by the caloric density and composition of the food bolus, with lipids being the most potent stimulators. PYY plays a crucial role in satiation through the stimulation of α-MSH release and inhibition of NPY in the ARH (Batterham et al., 2002; Strader & Woods, 2005).

Interestingly, appetite regulation hormones, such as leptin and insulin, also have receptors in other central nervous system structures involved in energy homeostasis, which communicate reciprocally with the HT. These connections support circuits involved in reward, salivation, smell, hunger, and the physical act of foraging, ensuring that behavioral decisions align with an individual's emotional state and environment.
Indeed, the hypothalamus (HT) functions are highly influenced by the sensory and emotional information it integrates from its extensive neural connections with other brain regions. This integration is crucial for understanding complex behaviors like feeding.
The next section will focus on the extra-hypothalamic centers, in the cortex and subcortex, contributing to the central control of food intake through their connection with the HT.

2.1.3 Extra-hypothalamic central control of food intake

The communication between the HT and higher-order brain regions are equally necessary for the complex regulation of feeding. To coordinate eating behavior, the HT in conjunction with other brain regions such as the insular cortex, receives interoceptive information (orexigenic and anorexigenic peripheric signals), which is processed alongside external cues (environmental, sensory and emotional information) by various cortical and subcortical areas (**Figure 4**). The hypothalamus receives (Top-Down) and sends (Down-Top) axonal projections to higher-order brain regions to integrate sensory information, crucial for appetite control and behavior, and ultimately projects to midbrain and brainstem areas that regulate behavior (**Figure 5**).

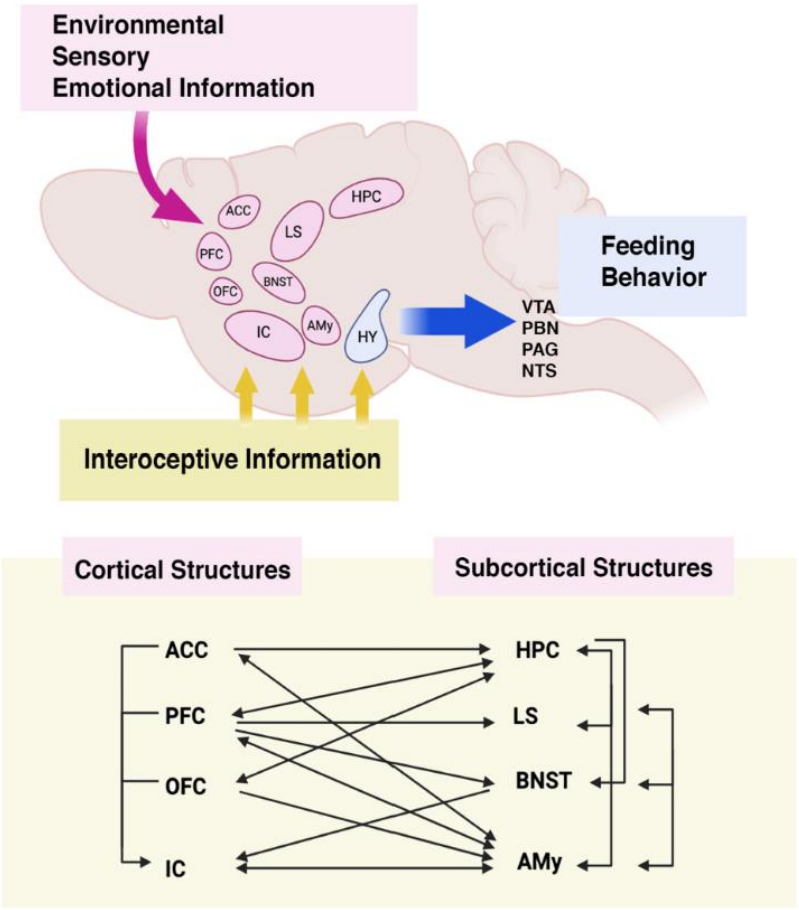

Figure 4 : Coordination of eating behavior by multiple brain regions.

Together with the hypothalamus, the insular cortex and other brain regions receive interoceptive information from peripheral organs. This information is processed along with environmental, sensory and emotional information by other cortical and subcortical areas, ultimately leading to changes in food intake. The hypothalamus ultimately projects to midbrain and brainstem areas controlling behavior (VTA: ventral tegmental area; PBN: parabrachial nucleus; PAG: periaqueductal gray; NTS: nucleus tractus solitarius). Many of the cortical (ACC: anterior cingulate cortex, PFC: prefrontal cortex, OFC: orbitofrontal cortex, IC: insular cortex) and subcortical (HPC: hippocampus, LS: lateral septum, BNST: bed nucleus of stria terminalis; Amy: Amygdala) are reciprocally connected and control information outflow (Azevedo et al., 2022).

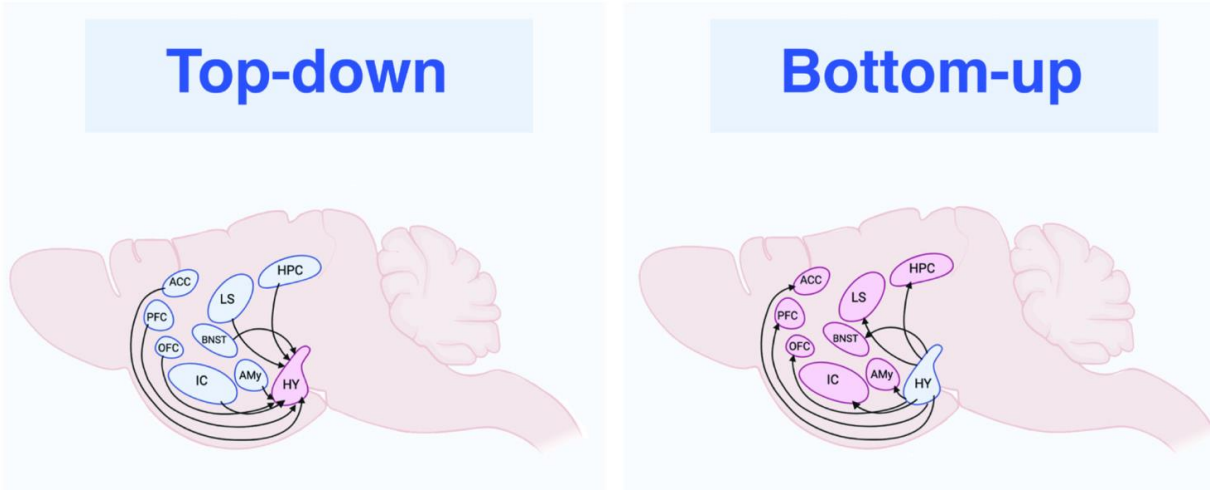

Figure 5 : Cortical and Subcortical connections to Hypothalamus.
Efferent and afferent projections from the hypothalamus to many cortical and subcortical structures are summarized in this figure. Many of these projections are important in the regulation of hypothalamic activity and appetite control. OFC: orbitofrontal cortex; IC: insular cortex: HPC: hippocampus, HY: hypothalamus, PFC: prefrontal cortex, ACC: anterior cingulate cortex; LS: lateral septum; BNST: bed nucleus of stria terminalis; Amy: Amygdala (Azevedo et al., 2022).

2.1.3.1 Sensory cortex

Gustatory responses are processed in the insula taste cortex, the parvocellular part of the ventroposteromedial thalamus, and the nucleus of the solitary tract. The primary taste cortex in the insula and frontal operculum handles taste intensity, temperature, and texture, but not taste-specific satiety. Olfactory responses are processed by the olfactory bulb and pyriform cortex. Visual responses are processed in V1, V2, V4, and the inferior temporal cortex. Auditory responses are encoded in the primary auditory cortex. Somatosensory responses are handled by the ventral posterolateral nucleus, primary somatosensory cortex, and SII, including the frontal and pericentral opercula (Rolls, 2004, 2015, 2016a, 2016b). Interestingly, hunger was associated with reduced activity in regions responsible for somatosensory and visual processing, such as the postcentral and lingual gyri, as well as in the cerebellar Crus I, which is involved in homeostatic regulation (E. Y. Chen & Zeffiro, 2020a).

2.1.3.2 Limbic system

The limbic system links cognitive functions, emotions, and adaptive responses, enabling memory formation, learning, and behavior adjustments based on environmental cues. Key hypothalamic-limbic connections include hippocampal circuits, which regulate episodic memory via the fornix, amygdala circuits, which process mood and emotions through connections with the stria terminalis and thalamus (Risold et al., 1997a) as well as the mesocorticolimbic circuit involved in rewarding aspect of food (Castro et al., 2015).

The following is a brief overview of the limbic system structures involved in regulating food intake.

Hippocampus

While the hippocampus is well-known for its crucial role in learning, memory, and spatial navigation, it is also involved in food intake regulation. It helps inhibit hunger and arousal, as seen in studies where hippocampal damage led to increased eating (Milgram, 1969). Recent research shows that the hippocampus connects spatial and reward information, linking specific locations with rewards, which influences foraging and food intake (Davidson et al., 2009; Hebben et al., 1985; Rozin et al., 1998). Additionally, it integrates sensory and internal signals related to eating, highlighting its role beyond just spatial navigation.
The hippocampus is also responsive to ghrelin and glucagon-like peptide-1 (GLP-1) which modulate food intake in rodents (Hsu et al., 2018; Kanoski et al., 2013). Specific neuronal populations in both the ventral and dorsal hippocampus were found to regulate food intake, avoidance behavior, and food-place memory through projections to the septum (Azevedo et al., 2019). Additionally, both hippocampal regions may regulate appetite through Fornix connections to the HT, particularly the LH (Azevedo et al., 2019; Sweeney & Yang, 2015).
In sum, the hippocampus plays a key inhibitory role in controlling appetite through its connection to HT and integration of appetite-regulating hormones.

Amygdala

The amygdala plays an important role in learning, memory, and emotion management and coordinates the body's response to fear and aggression. Bilateral lesions of the amygdala in rats followed by changes in food intake revealed the important role of this brain region in appetite regulation (N. B. Schwartz & Kling, 1964). It was later discovered that the amygdala influences appetite through the stria terminalis connections to numerous HT nuclei, specifically the VM, DM and LH, involved in behaviors such as aggression, stress responses, and eating (Krettek & Price, 1978). Additionally, through its connection to the hippocampus, the amygdala links spatial and sensory information with the emotional significance of experiences, influencing food-related behaviors (Janak & Tye, 2015; Zheng et al., 2017). Interestingly, primates with amygdala lesions are less selective and choose foods that healthy animals typically avoid, suggesting the amygdala also affects food preferences and helps in avoiding unpalatable foods (Machado & Bachevalier, 2007).
In sum, the amygdala appears to integrate hedonic, visceral, and external signals to regulate feeding behaviors.

Basal Ganglia

The interaction between the mesocorticolimbic system involving the nucleus accumbens (NAc) and ventral pallidum (VP) with the LH seems to regulate hunger/satiety modulation of food motivation and reward (Kenny, 2011). More specifically, LH, VP and NAc mediate distinct ‘wanting’ and ‘liking’ aspects of food reward (**Figure 6**). Indeed, if activation of LH neurons in rodents triggers an increase in food consumption, it does not enhance ‘liking’ reactions to sweetness (Castro et al., 2015).
However, the VP and NAc both contain a hedonic ‘hotpsot’ where opioid and related signals enhance ‘liking’ for food rewards and a ‘coldspot’ which suppresses positive hedonic impact.

Therefore, while intrinsic LH neurons primarily modulate food intake (‘wanting’), LH projections to VP and NAc enhance the positive hedonic impact of food (‘liking’).
LH neurons form monosynaptic connections with dopamine neurons in the ventral tegmental area (VTA), a brain region playing a critical role in reward processing (Watabe-Uchida et al., 2012; Wise, 2004). The VTA also sends projections back to the LH, both directly and indirectly via other regions such as the nucleus accumbens, amygdala, hippocampus and ventral pallidum (Barone et al., 1981; Beckstead et al., 1979; H. Simon et al., 1979). Different components of the LH-VTA circuit process different aspects of a reward-related task to maintain an adaptive balance between motivating behavior and appropriately regulating appetite-driven actions. Indeed, a subpopulation of VTA projecting LH neurons modulate reward-seeking actions in conditioned feeding task but not the activity during food consumption whereas another subpopulation encode reward expectation (Nieh et al., 2015). Interestingly these findings indicate that activating the LH-VTA pathway increases feeding behavior in fully-fed (sated) mice. This behavior is comparable to the compulsive overeating or binge eating observed in humans diagnosed with these disorders (DSM-V).
Another HT nucleus, the PaVN, projects to dopaminergic neurons of the VTA (Beier et al., 2015). Interestingly, this effective connectivity was found to be associated with a greater tendency in participants toward food-seeking behavior (Ogawa et al., 2022).

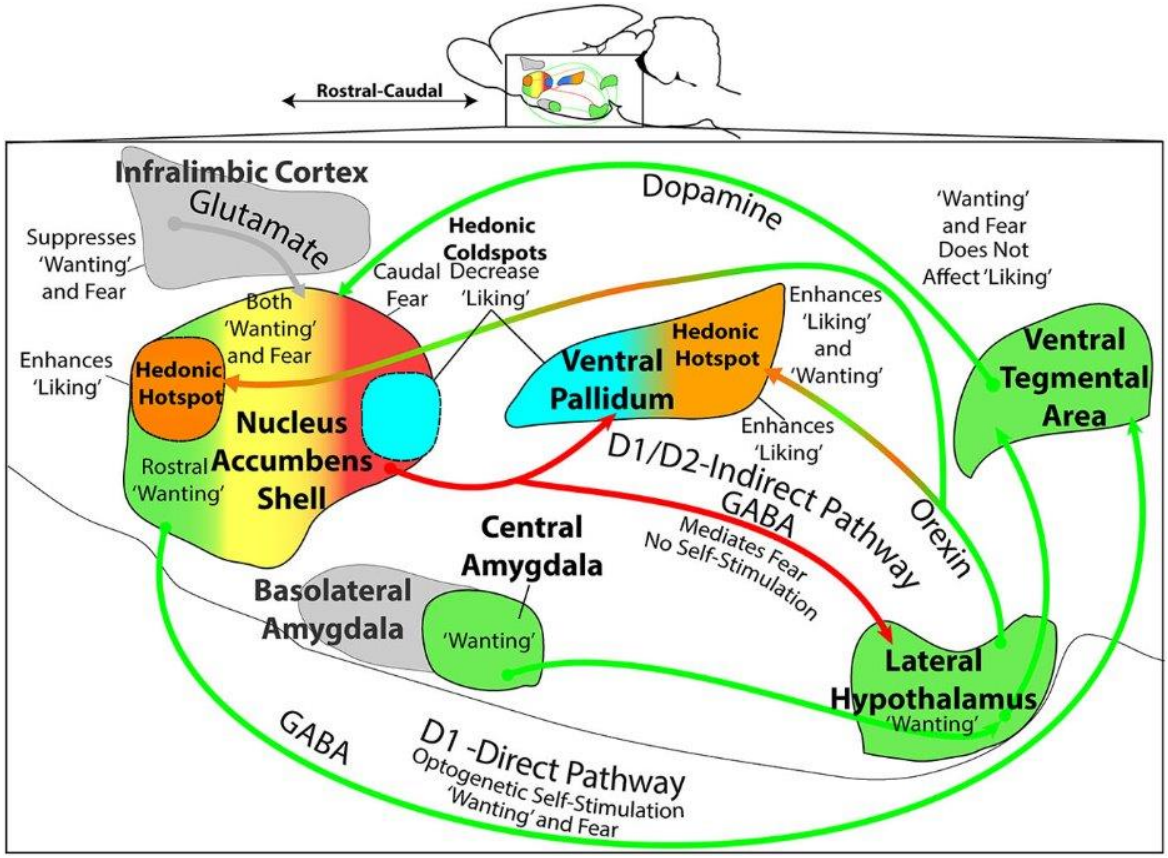

Figure 6 : Mesocorticolimbic-hypothalamic circuitry and functions.

Sagittal view depicts structures and circuitry underlying “liking”, “wanting”, and “fear” functions discussed in text. The NAc medial shell contains a hedonic hotspot in the rostral half, where opioid and related stimulation increases “liking” reactions to sucrose taste. Conversely, NAc shell contains a caudal hedonic coldspot, where opioid stimulation suppresses “liking” reactions to sweetness. These functional sites overlap with the NAc shell motivational keyboard for GABAergic/glutamatergic microinjections, in which rostral sites produce desire (e.g.,

eating, place preference, etc.), caudal sites produce fear (e.g., antipredator reactions, distress calls and bites, and place avoidance). Furthermore, NAc glutamatergic generation of appetitive behavior by DNQX microinjection requires endogenous dopamine stimulation of D1 receptors on direct path neurons that project directly to ventral tegmental area (VTA). Optogenetic stimulation of NAc D1-expressing neurons also supports appetitive self-stimulation behavior throughout the entire medial shell. By contrast, NAc glutamatergic generation of fearful behaviors requires additional dopamine stimulation of D2-receptors, implicating indirect path neurons that project to the VP and lateral hypothalamus (LH). The posterior half of VP contains an opioid hedonic hotspot, whereas the rostral half of VP contains a coldspot where mu opioid stimulation suppresses "liking" reactions to sucrose taste. Optogenetic stimulation of the VP hotspot, or of its lateral hypothalamic inputs, may produce enhanced "liking" and "wanting". Colors denote implication in "wanting" (green), fear (red), mixed "wanting" and fear (yellow), suppression of "wanting" or "fear" (gray), "liking" (orange), or suppression of "liking" (blue).

2.1.3.3 Cortex

Early studies found that a disruption in cortical activity could affect eating and drinking by altering lateral hypothalamic activity (Buresova, 1956). Indeed, the cortex can control feeding behavior, even in already satiated animals, highlighting its role in regulating hypothalamic circuits involved in hunger (Huston & Bures, 1970).

Orbitofrontal Cortex (OFC)

On one hand, OFC is a convergence site for sensory information that passes through the primary cortical areas for taste, smell, vision, and somatosensorial (Rolls, 2004). OFC houses the major cortical representation of tastes such as sweet, salty, bitter, and sour, and its neurons receive gustatory and olfactory stimuli and respond to specific tastes and odors (Rolls, 2004).
On the other hand, OFC integrates satiety-related visceral signals associated with satiety and modulates the representation of food (Rolls, 2004). These taste representations can act as positive or negative reinforcers for the reward system (Rolls, 2004). Therefore, its ability to encode rewards likely influences food selection (Zald, 2009). Indeed, an fMRI study showed differential activation of this region when participants imagined consuming palatable versus unpalatable food (Stice et al., 2010), which suggests that OFC is involved in the assessment of food's pleasantness.

Prefrontal Cortex (PFC)

Despite being highly differentiated among mammals, the PFC consistently plays a crucial role in regulating food intake across species (Carlén, 2017).
In mice, stimulation of dopamine receptor-1 neurons in the mice homologue of the PFC (the prelimbic/infralimbic cortex), and their axon terminals in the basolateral amygdala (BLA), which ultimately connect to the HT, increases food consumption, while inhibition reduces food intake (Oh et al., 2014). In Human, the PFC has a complex role in decision-making related to eating, encompassing self-regulation and the cognitive control of cravings.

Insular Cortex

The insular cortex, or insula, plays a significant role in various autonomic and endocrine processes. The insula influences eating behavior by responding to environmental cues and palatable foods (Baldo et al., 2016; Stern et al., 2021), with studies showing that optogenetic stimulation of the insular cortex can lead to a decrease in food consumption (Gehrlach et al., 2020; Zhang-Molina et al., 2020). It also regulates conditioned taste aversion, encoding both attractive and aversive stimuli to adjust eating responses (Yiannakas & Rosenblum, 2017).
Thus, the insula integrates interoceptive and exteroceptive information, providing top-down control of eating behavior through its connections to limbic structures.

In sum, homeostatic inputs from the HT are combined with hedonic feeding signals from mesolimbic pathways and signals from higher decision-making centers to create a coordinated response for regulating feeding.

2.2 General anatomy of the Hypothalamus

2.2.1 Human hypothalamus

As its name suggests, the HT is located below the thalamus, just above the brainstem, and forms the ventral part of the diencephalon. This small brain region about the size of an almond (1.4 cm^3) and representing only 1% of the brain, contains the integrative systems that support life (Lemaire et al., 2013a; Rasmussen, 1938).

Indeed, the HT plays a crucial integrative role by gathering various sensory inputs to make vital decisions regarding fundamental life functions. It compares these inputs to ideal setpoints for parameters like body temperature, blood sodium, glucose levels, and hormone levels. To maintain these setpoints (homeostasis) or address stressors (allostasis), the hypothalamus triggers autonomic, endocrine, and behavioral responses.

It is composed of four sub-regions: pre-optic, anterior, tuberal, and mammillary regions. These regions host numerous nuclei with distinct physiological and anatomical characteristics (**Figure 7**). Along the rostral-caudal axis, the HT comprises: (i) anteriorly: preoptic nuclei (lateral and medial), anterior hypothalamic nuclei, paraventricular nuclei, anteroventral periventricular nuclei, supraoptic nuclei, and suprachiasmatic nuclei; (ii) medially: dorsomedial nuclei, ventromedial nuclei, and arcuate nuclei; (iii) laterally: lateral nucleus; and (iv) posteriorly: posterior nucleus and mammillary bodies (see Figure 1). These nuclei play specific roles in maintaining homeostasis, regulating energy, food intake, thirst, as well as temperature, sexual dimorphism, sleep, and circadian rhythm. HT is an integrative hub, connecting central structures and peripheral signals, enabling adjustments in food intake and energy equilibrium through feedback mechanisms (Schwartz *et al.*, 2000).

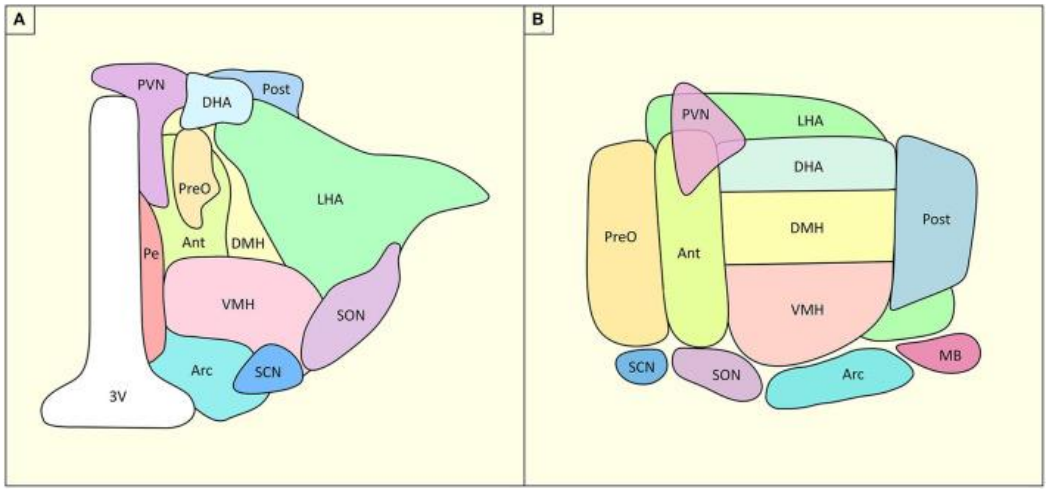

Figure 7 : Structural organization of HT and its nuclei.

(A) *Coronal slice of the hypothalamus,* ***(B)*** *Sagittal slice of the hypothalamus. Ant, anterior hypothalamus; Arc, arcuate nucleus, DHA, dorsal hypothalamic area; DMH, dorsomedial hypothalamus; LHA, lateral hypothalamic area; MB, mammillary body; Pe, periventricular nucleus; Post, posterior hypothalamic nucleus; PreO, preoptic nucleus; PVN, paraventricular nucleus; SCN, suprachiasmatic nucleus; SON, supraoptic nucleus; VMH, ventromedial hypothalamus; 3V, third ventricle. (Roger et al., 2022).*

2.2.2 Mouse hypothalamus

The mouse HT is anatomically comparable to the human HT, with similar nuclei architecture and similar neuropeptide-expression profiles. Indeed, cross-species comparisons revealed a remarkable degree of conservation, with 105 of 108 human neuron subtypes having a corresponding subtype identified in mice (Herb et al., 2023). This conclusion makes sense considering that the HT is a primitive brain region that existed before the vertebrate brain evolved and is responsible for the most fundamental survival functions, such as feeding, energy expenditure, thermoregulation or even reproduction (Saper & Lowell, 2014). Although there might be human-specific cell populations at finer levels of resolution, the high degree of cross-species conservation of cell types supports the validity of translating findings from mice to humans.

The mouse HT is located rostroventrally to the thalamus and constitutes part of the floor and walls of the third ventricle. Its more rostral portion is flanked by the globus pallidus, internal capsule, and entopeduncular nucleus, while the caudo-dorsal portion is bordered by the subthalamus, nucleus of the fields of Forel, and cerebral peduncle.
The hypothalamus is symmetrically duplicated on each side of the brain, with the third ventricle in the midline forming a boundary between the two sides. Along the rostral-caudal axis, the HT is divided into four regions: the preoptic, anterior, tuberal, and mammillary regions, each further subdivided into lateral, medial, and periventricular zones (**Figure 8A**) (Fong et al., 2023).
(i) The most rostral part, the preoptic area (POA), includes the median (MnPO), medial (MPO), ventrolateral (VLPO), anteroventral periventricular (AVPV), and periventricular (PVpo) preoptic nuclei. (ii) The anterior region consists of the anterior hypothalamus (AHA) along with the supraoptic (SON), suprachiasmatic (SCN), and paraventricular (PaVN) nuclei. (iii) Ventral to the tuberal hypothalamus lies the median eminence (ME) and pituitary stalk, with the tuberal region containing the lateral hypothalamic area (LH), dorsomedial (DM), ventromedial (VM), arcuate (ARH), and tuberal (TN) hypothalamic nuclei. (iv) Lastly, the mammillary region is composed of the premammillary (PM), supramammillary (SuM), tuberomammillary (TM), and posterior hypothalamic (PH) nuclei (**Figure 8B-E).**

Each of these hypothalamic divisions hosts distinct nuclei with significant functional overlap and extensive coordination (**Figure 8F**). Distinct aspects of feeding, energy balance, and thermoregulation are heavily regulated by neurons within the tuberal hypothalamus (Arc, VM, DM, LH, TU) while also involving circuits within the MnPO, VLPO, PaVN, AH, and PM. Similarly, corticotropin-releasing hormone (CRH) neurosecretory cells in the PaVN play a central role in stress responses, integrating inputs from the MPO, DM, LH, and PH (Herman et al., 2016). Additionally, sleep-wake cycles are orchestrated by the SCN, the main circadian pacemaker, in coordination with the VLPO, MnPO, PaVN, DM, VM, LH, TM, and SuM (Scammell et al., 2017).

The overlap of circuits involved in a single fundamental function highlights the challenging task of precisely mapping the hypothalamic cell types and circuits that regulate complex behaviors. Furthermore, the diverse range of functions attributed to a single nucleus can be attributed to the heterogeneous population of neurons it contains.

For example, subtypes of orexigenic agouti-related peptide neurons in the arcuate nucleus (^{ARH}AgRP) show distinct transcriptional responses to fasting, suggesting they may represent separate populations that respond specifically to different energy states (Campbell et al., 2017). Similarly, the diverse populations of neurons in the LH enable this nucleus to coordinate a range of essential behaviors, including sleep, wakefulness, feeding, stress, and motivated actions (Mickelsen et al., 2019).

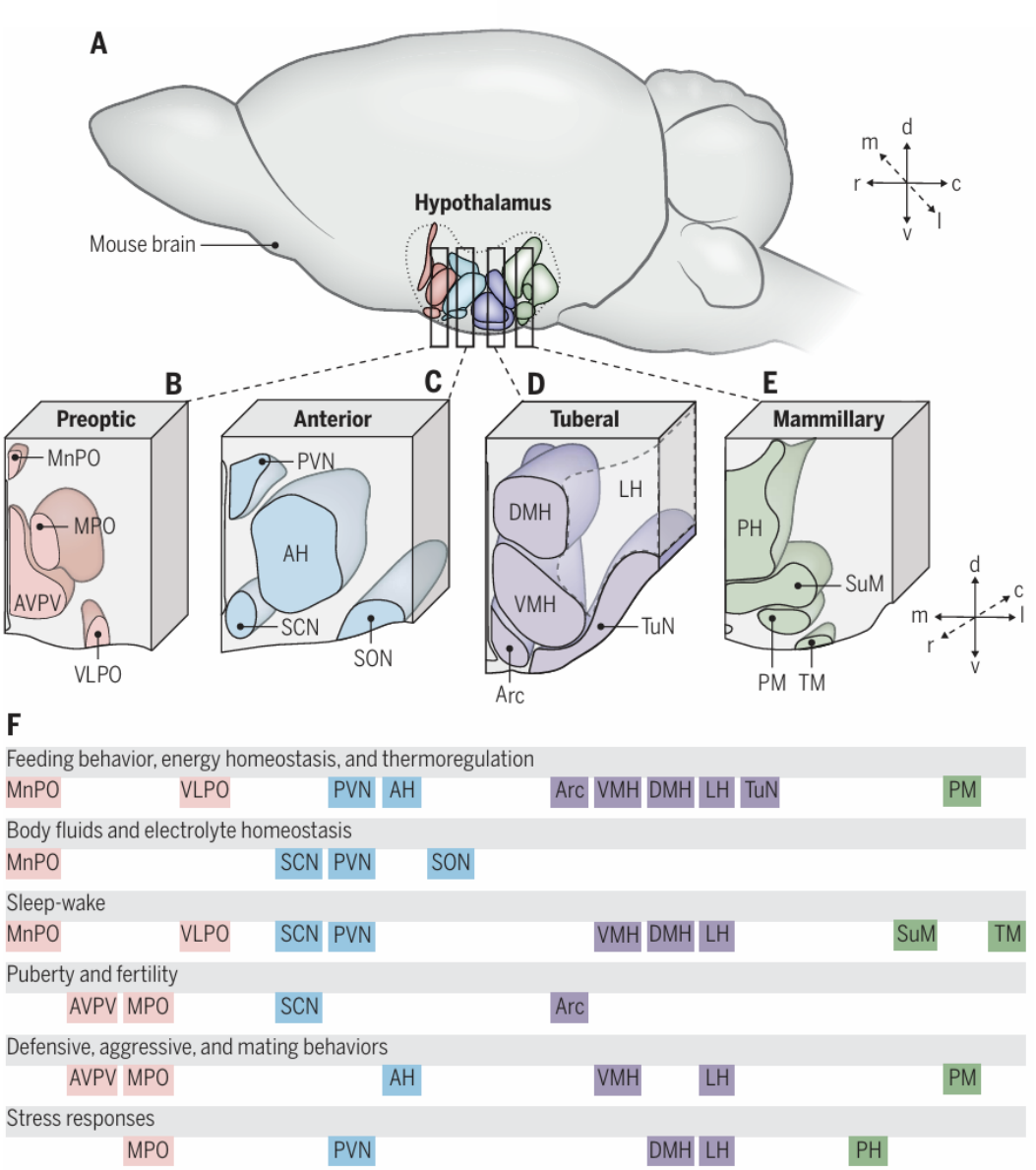

Figure 8 : Schematic representation of hypothalamic subdivisions in a midsagittal section of the mouse brain.

(A) The hypothalamus resides at the base of the brain, with its nuclei forming a complex 3D patchwork around the third ventricle across four rostral-caudal regions. (B to E) Representative coronal sections of the preoptic (B), anterior (C), tuberal (D), and mammillary (E) regions demonstrate the diversity and intercalation of hypothalamic nuclei. (F) The hypothalamic control of diverse physiologies and behaviors critical to survival involves coordinated activity across multiple nuclei (Fong et al., 2023).

2.2.2.1 Principal hypothalamic nuclei involved in food-intake regulation

2.2.2.1.1 Arcuate nucleus (ARH)

2.2.2.1.1.1 Role

Ablation of the AgRP expressing neurons in the mouse ARH (^{ARH}AgRP) significantly impacts their food consumption and leads to death by starvation (Luquet et al., 2005). Furthermore, chemogenetic inhibition of these neurons in fasted mice leads to a decrease in food intake while optogenetic and chemogenetic activation induces feeding behavior in well-fed mice (Aponte et al., 2011; Krashes et al., 2011). Additionally, the level of ^{ARH}AgRP activity correlates with the amount of food intake in these mice (Aponte et al., 2011). These findings suggest that ^{ARH}AgRP neurons generate an appropriate magnitude of behavioural response corresponding to the physiological need level. Subsequently, ^{ARH}AgRP neurons activity in fasted mice rapidly decrease in response to sensory detection of the food or food predictive auditory cue and that their activity is low during food consumption (Betley et al., 2015; Y. Chen et al., 2015). On the contrary, the same studies showed that activation of ^{ARH}AgRP neurons enhances feeding-related motivated behaviours, such as motivation to seek and obtain food (Atasoy et al., 2012). These results suggest that ^{ARH}AgRP neurons are not involved in the consumption step of feeding behavior, but rather participates in food-seeking.
Furthermore, the motivational role of ^{ARH}AgRP neurons also influences learning by attributing valence to a specific context. Indeed, a high activity level of ^{ARH}AgRP neurons transmits a negative valence in fed mice while a low activity triggers a positive valence in fasted mice (Betley et al., 2015). In sum, these findings indicate that ^{ARH}AgRP neurons not only initiate food intake but also participate in the regulation of feeding-related motivated behaviours.

2.2.2.1.1.2 Connectivity

Certain subsets of ^{ARH}AgRP neurons, including PaVN, bed nucleus of the stria terminalis (BNST), LH, and the paraventricular thalamus (PVT), are sufficient to promote feeding (Betley et al., 2013). However, stimulating ^{ARH}AgRP axonal terminals in specific areas, such as the periaqueductal gray (PAG) and the central amygdala (CEA), does not induce food intake. ^{ARH}AgRP neurons also receive monosynaptic inputs from the dorsomedial hypothalamus (DM), PaVN, ventromedial hypothalamus (VM) and forebrain nuclei (D. Wang et al., 2015). The ARH is also highly connected to the brainstem, specifically to the nucleus of the solitary tract (NST), which plays a crucial role by integrating and relaying neural information from the digestive tract via the vagus nerve (Berthoud et al., 2006).

2.2.2.1.2 Lateral hypothalamus (LH)

2.2.2.1.2.1 Role

The LH is known as the ‘feeding center’, since its ablation results in a complete cessation of food intake associated with an important weight loss leading to death (Anand & Brobeck, 1951a; Hetherington & Ranson, 1940) and its electrical stimulation leads to an increase in food intake (Coons & Cruce, 1968; Delgado & Anand, 1953; Mogenson & Stevenson, 1967). Subsequent experiments on the LH revealed its role in adjusting self-stimulation behavior based on feeding suggesting its involvement in reward-seeking behavior (Hoebel & Teitelbaum, 1962). Furthermore, the LH seems to contribute to the processing of the palatability of food

since it is involved in forming conditioned preferences or aversions to tastes based on gustatory stimuli (Ferssiwi et al., 1987; J. X. Li et al., 2013; Touzani & Sclafani, 2001). However, intrinsic LH neurons don't seem to directly influence the hedonic impact of palatable food since electrical stimulation of the LH does not enhance positive hedonic reactions to sucrose in rodents (Berridge & Valenstein, 1991). In sum, LH seems to be involved in various aspects of feeding behavior, first the feeding regulation particularly of palatable food intake and second the reward-seeking and taste preference formation.
The orexinergic action of the LH operates via its neurons expressing orexin and melanin-concentrating hormone (MCH).

2.2.2.1.2.2 Connectivity

LH-projecting BNST neurons promote feeding (Jennings et al., 2013). LH neurons also project to extra-hypothalamic brain regions, such as the cortex, brainstem and limbic systems. ^{LH}VGAT projections to VTA were found to be highly involved in food-related tasks (Marino et al., 2020; Nieh et al., 2015, 2016). Stimulating activating neurons expressing dopamine receptor 1 (Drd1) in the NAc specifically inhibits ^{LH}VGAT neurons and decreases food intake (O'Connor et al., 2015). LH glutamatergic neurons are primarily targeted, and their activity reduced by inhibitory synaptic inputs from the extended amygdala (Jennings et al., 2013). Through its connection to substantia nigra (SN) neurons, LH neurons also seem to be involved in motor actions associated with feeding behaviour (Travers et al., 1997).

2.2.2.1.3 Dorsomedial Nucleus (DM)

2.2.2.1.3.1 Role

The Dorsomedial nucleus (DM) is involved in the maintenance of energy balance. Lesion of the DM led to hypophagia, hypodipsia, reduced body weight and decreased linear growth (Bellinger & Bernardis, 2002). Additionally, DM is also implicated in energy expenditure since chemical stimulation of these neurons triggers nonshivering thermogenesis and elevates core body temperature (Dimicco & Zaretsky, 2007; Morrison & Nakamura, 2011).
As a critical component of the hypothalamic circadian timing system, DM is implicated in food-entrainable circadian rhythms. Indeed, restricted feeding schedules synchronize the daily rhythm of DM cellular activity, adjusting behavioral and physiological rhythms to anticipate food availability (Gooley et al., 2006).
Moreover, DM leptin receptor-expressing (^{LepR}DM) neurons specifically take part in the control of body weight, adiposity, and diurnal rhythms. through regulating feeding times and metabolic rhythms. Indeed, silencing these neurons in adult mice led to increased body weight, phase-advanced feeding and metabolism into the light cycle, reduced dark-cycle locomotor activity, and a failure to adapt to restricted food availability (Faber et al., 2021). Finally, DM also seems to be involved in the regulation of the emotional response to stress (DiMicco et al., 2002).

2.2.2.1.3.2 Connectivity

Finally, DM also seems to be involved in the regulation of the emotional response to stress through its projections to PaVN (DiMicco et al., 2002; H. Y. Li & Sawchenko, 1998).

The DM receives input from various hypothalamic and brainstem nuclei, which are believed essential for regulating feeding, body weight, and metabolism (Elmquist et al., 1999; Fulwiler & Saper, 1984; Thompson & Swanson, 1998; Zigman & Elmquist, 2003). For example, DM neurons have direct projections to orexin neurons in the LH, playing a key role in the expression of food-entrained behavioral rhythms (Mieda et al., 2006). Furthermore, the DM also sends robust projections to the PaVN which control the circadian release of corticosteroids from the adrenal glands (Chou et al., 2003; Elmquist et al., 1999; Thompson & Swanson, 1998).

2.2.2.1.4 Paraventricular nucleus (PaVN)

2.2.2.1.4.1 Role

The paraventricular nucleus (PaVN), located bilaterally around the third ventricle, plays a critical role in energy homeostasis. Ablation of the PaVN in rats resulted in hyperphagia and obesity with hyperinsulinemia (Sims & Lorden, 1986), due to PaVN MC4R neurons strongly suppressing food intake (B. P. Shah et al., 2014). Additionally, the PaVN receives monoaminergic signals, particularly serotonin, which has an anorexigenic effect by inhibiting NPY. The PaVN also acts as the primary endocrine control center of the brain since it hosts neurons expressing oxytocin (OXT), corticotropin releasing hormone (CRH), thyrotropin releasing hormone (TRH), arginine vasopressin (AVP), which are involved in endocrine and CNS functions (Affinati & Martin G. Myers, 2021).

2.2.2.1.4.2 Connectivity

The exchange of information between the ARH and the PaVN is essential for translating nutritional signals received by the HT into actionable signals that induce metabolic alterations (Hill, 2012). By receiving direct melanocortin input, along with other integrated signals regarding energy balance, the PaVN is a key output nucleus for the HT. Indeed, the PaVN sends integrated information to various effector systems, including the pituitary gland, the autonomic nervous system, and behavioral control circuits, to control feeding and energy expenditure (Affinati & Martin G. Myers, 2021; Sutton et al., 2016).
Additionally, as the primary driver of hypothalamo–pituitary–adrenocortical (HPA) responses, PaVN seems to be involved in handling the demands of chronic stress exposure (Herman et al., 2016).

2.2.2.1.5 Ventromedial Nucleus (VM)

2.2.2.1.5.1 Role

The ventromedial nucleus (VM) plays a crucial role in various neuroendocrine functions, including glucose regulation, thermogenesis, and behaviors related to appetite, social interactions, and sexual behaviors. It has been recognized as an anorexigenic nucleus, since its lesion led to an increase in body weight (Hetherington & Ranson, 1940). Furthermore, SF1 knockout mice, which lack the development of a VM, and mice with SF1 cell-specific deletion of leptin receptors (LepR) exhibit modest increased body weight and fat accumulation (Dhillon et al., 2006; Majdic et al., 2002). However, when the VM LepR knockout mice are given a high-fat diet, their obesity significantly worsens. Unlike normal mice, these knockout mice do not reduce their food intake or increase energy expenditure through thermogenesis in response

to the high-fat diet. This finding seems to indicate that ^{SF1}VM neurons play a crucial role in counteracting the effects of an obesogenic diet by regulating food intake and energy expenditure. Additionally, chemogenic manipulation of ^{SF1}VM neurons activity affects food intake and body fat over several weeks (Viskaitis et al., 2017). Behavioral studies suggest that when food is absent, low ^{SF1}VM neuron activity promotes exploration and food-seeking behavior (Viskaitis et al., 2017). Conversely, activation of ^{SF1}VM neuron this behavior and leads to food avoidance (Viskaitis et al., 2017).
Electrical stimulation of the VM increases glucose production and uptake, decreases circulating insulin, and increases glucagon, corticosterone, and norepinephrine levels, ultimately countering hypoglycemia (Borg et al., 1994; Frohman & Bernardis, 1971; Shimazu et al., 1978). Interestingly, optogenetic inhibition of ^{SF1}VM neurons in adult mice does not affect fasting blood glucose levels but hinders the mice's ability to recover from mild insulin-induced hypoglycemia (Meek et al., 2016). This finding suggests that VM has a major role of protection against hypoglycemia through its complex interactions with various hormones and neuronal pathways.

2.2.2.1.5.2 Connectivity

Despite the various endocrine functions of the VM, it was shown that ^{NOS1}VM projections to the anterior bed nucleus of the stria terminalis (aBNST) are involved in glucose counter-regulation, while ^{NOS1}VM projections to the PAG elicits defensive behaviors such as freezing immobility (Faber et al., 2018). It is also hypothesized that ^{PACAP}VM neurons could play a crucial role in regulating hepatic glucose production during hypoglycemia and stress, through its connection to the PaVN neurons which express corticotropin-releasing hormone (CRH) (Grinevich et al., 1997).

2.2.2.1.6 Tuberal nucleus (TN)

2.2.2.1.6.1 Role

The Tuberal nucleus is a newly found orexinergic neuronal population located in the lateral posterior part of the HT. Indeed, TN neurons expressing somatostatin (^{TN}SST), a GABAergic neuropeptide crucial for brain function (Schettini, 1991), were found to be involved in regulating food intake in mice (Luo et al., 2018). It was reported that the recently identified ^{TN}SST neurons, activated during fasting and chemogenetic activation, promote feeding whereas inhibition of this population reduced food intake. Additionally, genetic ablation of ^{TN}SST led to a decreased weight gain and food intake, which suggests this population has a long-term effect on energy homeostasis.
Furthermore, ^{TN}SST are the only orexigenic neurons to show preferential response to palatable food. Indeed, they are the only neurons among the four major types of hypothalamic orexigenic neuron, to show a higher percentage of c-Fos-positive neurons when mice were consuming palatable food after overnight fasting (Mohammad et al., 2021). It was also reported that different sub populations of ^{TN}SST neurons respond to different types of palatable food, with none to little overlap (Mohammad et al., 2021).
Furthermore, chemogenetic experiments showed that activating ^{TN}SST neurons significantly increased HFD consumption while inhibiting TNSST neurons significantly decreased HFD consumption in sated mice (Mohammad et al., 2021).

However, ^{TN}SST neurons seem to be implicated in food approach rather than food consumption. Indeed, in an arena containing normal chow diet, palatable food (HFD or sweet chocolate pellets), a plastic food-mimic and an empty bowl in its four corners, ^{TN}SST neurons responded at the exact moment the mice entered the palatable corner, even before they consumed the food. Additionally, ^{TN}SST neurons were similarly activated by gavage of palatable food, a technique which bypasses the food consumption process. This further supports the conclusion that ^{TN}SST neurons respond to palatable food mainly through a pre-consumption mechanism. The present findings all seem to support the crucial role of ^{TN}SST neurons in the approach rather than the consumption of palatable food.
^{TN}SST can sense metabolic signals such as ghrelin to modulate feeding, and its orexigenic effect orexigenic effect (Luo et al., 2018).
Interestingly, newly published data revealed that ^{TN}SST neurons are necessary for non-homeostatic feeding driven by contextual cues, 'contextual feeding conditioning' (CFC). Indeed, CFC relies on the activation of ^{TN}SST neurons associated to a context as well as glutamatergic inputs from the vSub. More specifically, pairing a context to palatable food significantly increased synaptic transmission between the vSub and ^{TN}SST neurons, leading to CFC, which was suppressed only by inhibiting ^{TN}SST neurons or the vSub. These results suggest the involvement of ^{TN}SST in the overconsumption of food, the leading factor for obesity in our modern world (Swinburn *et al.*, 2009)

2.2.2.1.6.2 Connectivity

^{TN}SST neurons have projections to many brain regions such as the PaVN, LH, BNST, CEA and PAG (Luo et al., 2018). While optogenetic activation of PVH or BNST projecting ^{TN}SST neurons terminals promote feeding activation, activation of CEA or PAG projecting ^{TN}SST neurons is not sufficient to drive food consumption (Luo et al., 2018).

Building on this understanding of the anatomy of the Human and mouse HT, the next section will explore how dysregulation within these circuits contributes to the development of weight-related disorders, such as obesity and anorexia nervosa.

2.3 Weight-related disorders associated to dysfunction of eating behavior networks

Eating behavior is finely regulated to ensure an energy balance that maintains a constant level of fat mass. Although the regulation system is successful in most cases, this equilibrium can be disrupted. Indeed, eating behavior is complex and can be affected by neurobiological, psychopathological aspects, as well as familial and cultural influences. Disruption of this system can ultimately lead to eating disorders and consequent weight gain or loss.

2.3.1 Obesity

2.3.1.1 Definition

Obesity is characterized by a body mass index (BMI) over 30, resulting from an abnormal fat accumulation presenting a risk to health (WHO). Characterized as a chronic disease, obese individuals are more susceptible to developing mental health disorders, such as anxiety and depression, as well as type 2 diabetes, and cardiovascular disease in later life (Takizawa et al., 2015).

2.3.1.2 Epidemiology

According to the WHO, 650 million people were affected worldwide by obesity in 2016, which makes it a real public health problem. In Europe, obesity affects 23% of the population (WHO European Regional Obesity Report 2022; WHO Regional Office for Europe: Copenhagen, Denmark, 2022). Although numerous efforts have been made to combat the obesity epidemic since the Agenda for Sustainable Development was introduced in 2015, there has been no progress in reducing its prevalence or that of related conditions such as type 2 diabetes (*A/RES/70/1 Transforming Our World: The 2030 Agenda for Sustainable Development*, 2030).

In France, the prevalence of obesity (**Figure 9**) keeps increasing, with estimation at 8,5 % in 1997, 15 % in 2012 and 17 % in 2020 (Charles et al., 2008; Fontbonne et al., 2023). Prevalence of obesity was found to be higher in women (17.4%) than men (16.7%) (Fontbonne et al., 2023).

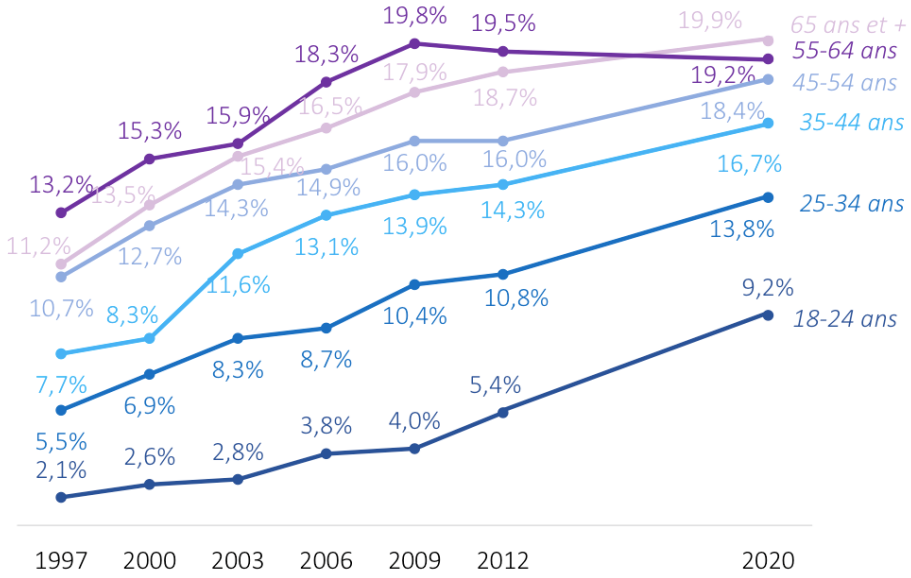

Figure 9 : Evolution of the prevalence of obesity by age groups between the 1997-2012 and the 2020 *(Charles et al., 2008; Fontbonne et al., 2023).*

Obesity also seems to be dependent on socioprofessional factors (**Figure 10**), with a negative relation to the qualification of the occupation (Charles et al., 2008).

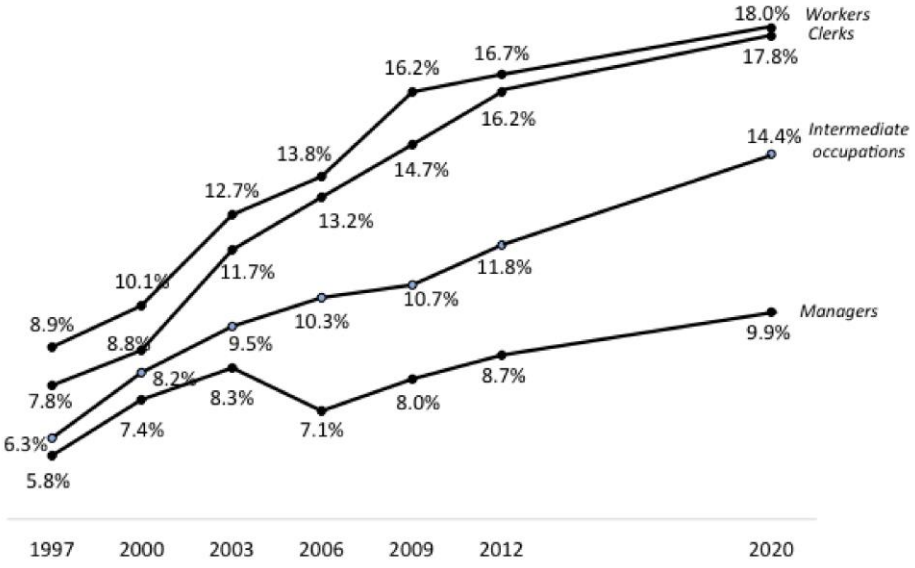

Figure 10 : Evolution of the prevalence of obesity (BMI ≥ 30 kg/m2) by professional category *Obepi-Roche 1997–2012 with addition of LCO 2020 Obepi-Roche study (Fontbonne et al., 2023).*

Obesity prevalence is higher (over 20%) in the northern and northeastern regions of France (**Figure 11**), and lowest (under 14.5%) in the Paris region (Ile-de-France) and the lower Loire region (Pays de la Loire). Globally, there seems to be a decreasing gradient in obesity prevalence from north to south (Fontbonne et al., 2023).

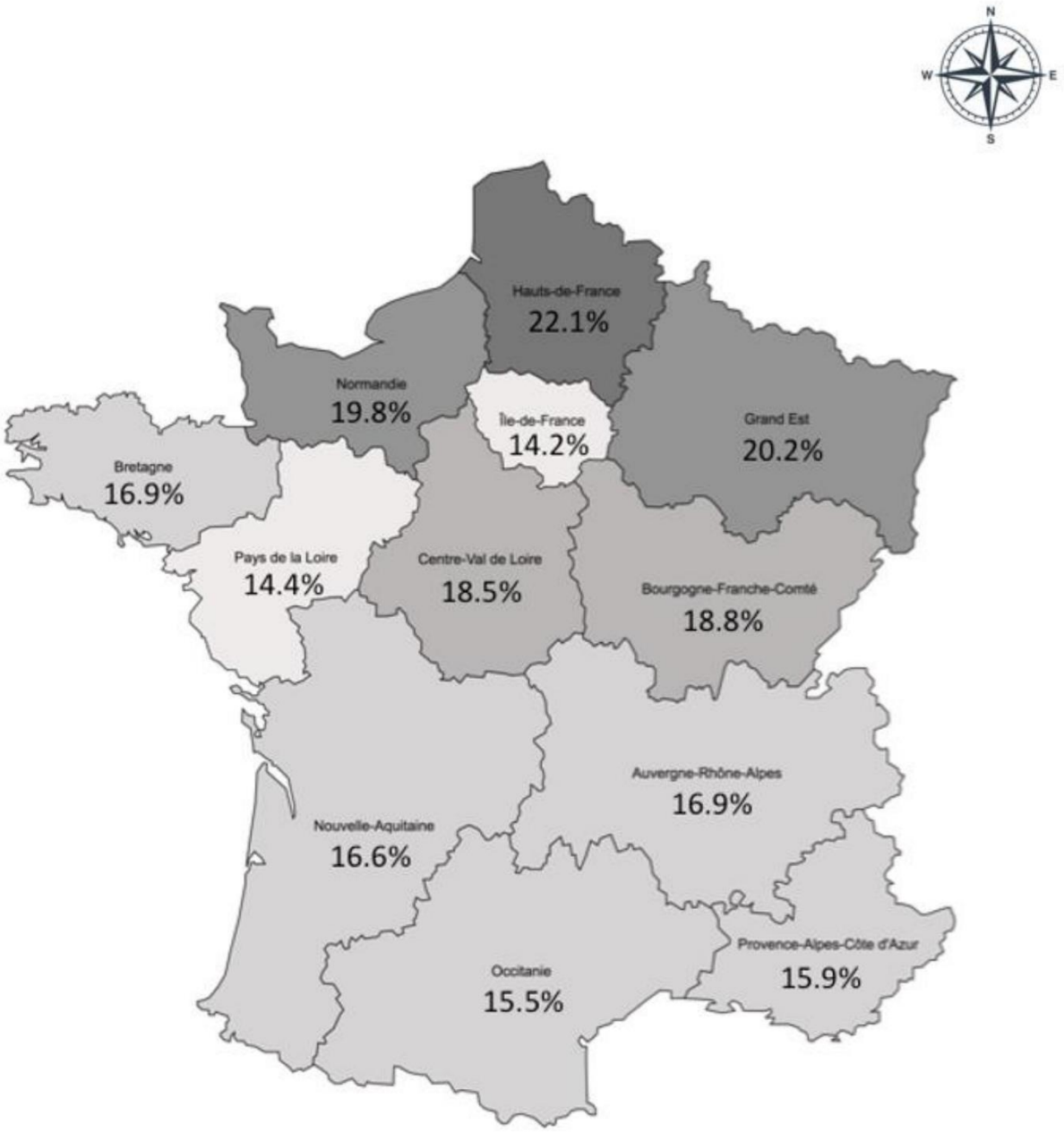

Figure 11 : Evolution of the prevalence of obesity (BMI ≥ 30 kg/m2) by professional category,
Obepi-Roche 1997–2012 with addition of LCO 2020 Obepi-Roche study (Fontbonne et al., 2023).

2.3.1.3 Etiology

As highlighted by the obesity foresight map (**Figure 12**), obesity is a chronic pathology with a multitude of causes, all intertwined into a complex web of social, cultural, political, and economic factors (Foresight's Tackling Obesities: Future Choices report, UK). Several factors have been recognized to play a role in the development as well as the maintenance of obesity, such as diet, physical activity, automation, urbanization, genetic susceptibility, medications, mental disorders, economic policies, endocrine disorders, and exposure to endocrine-disrupting chemicals (WHO, Bleich *et al.*, 2008; Yazdi *et al.*, 2015; Kassotis *et al.*, 2020). The development of obesity is influenced by a combination of genetic predisposition to weight gain and environmental factors.

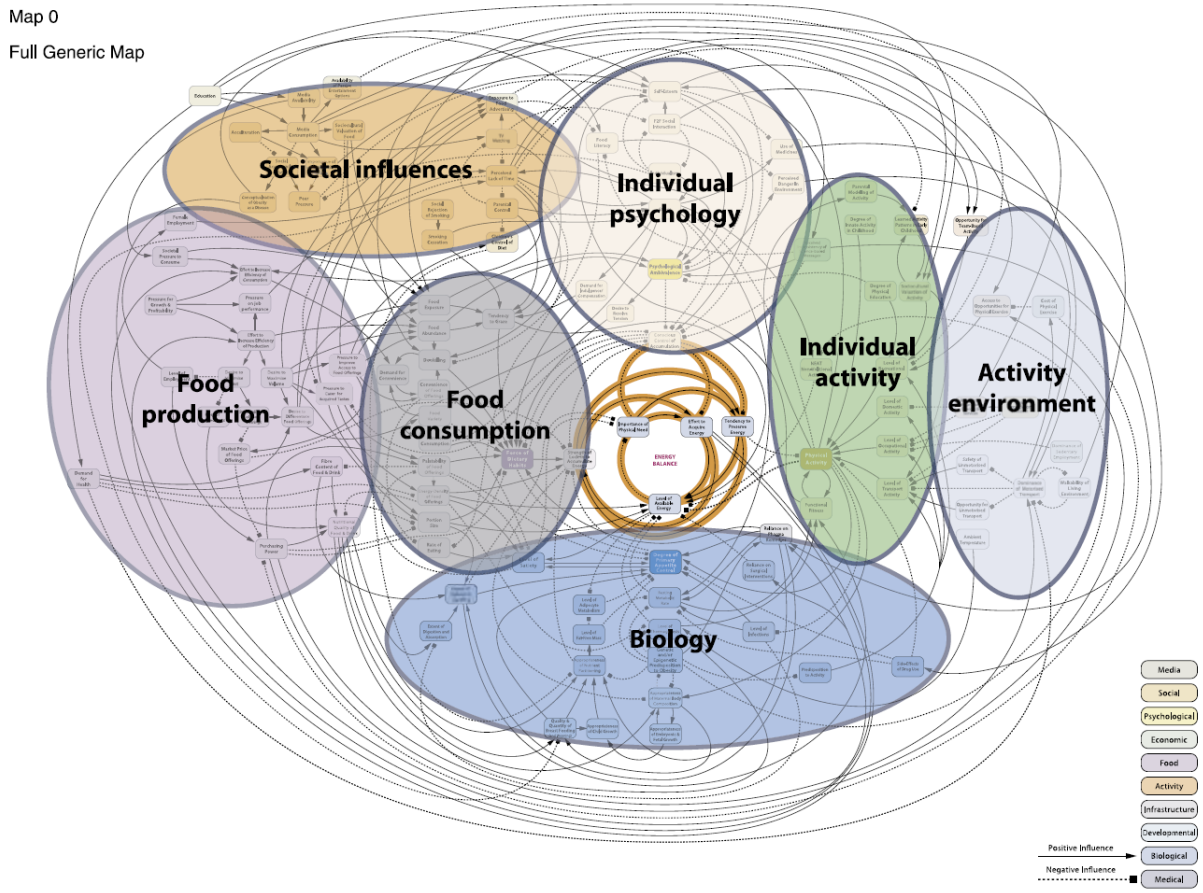

Figure 12 : Foresight's Tackling Obesities: Future Choices report, UK.

2.3.1.3.1 Environment

Our modern world is characterized by easy access to highly palatable, calorie-dense foods and an environment that promotes sedentary lifestyles (Pimentel et al., 2014). This obesogenic

environment disrupts energy balance and is a major factor in pathological food intake, leading to conditions such as obesity. Indeed, food intake is influenced by non-homeostatic factors Furthermore, neuromarketing tools increasingly exploit food cues that target emotions and cognitive functions (Berthoud, 2012a). This leads to higher consumption of high-fat, high-sugar foods, which not only increases calorie intake but may also impair brain systems involved in nutrient sensing, pleasure, motivation, and cognitive processing.

2.3.1.3.2 Genetic

Genetic predisposition plays a critical role in obesity pathogenesis since an individual has 2 to 8 times higher risk of becoming obese if their family members are also obese. Genetic studies have uncovered various several major monogenic mutations causing hyperphagia and severe, early-onset obesity (Farooqi & O'Rahilly, 2006). For example, some single gene defects involved in the leptin-melano-cortin pathway were shown to trigger severe obesity in humans. Other minor genes have a more variable impact on weight and fat distribution, affecting factors such as the age of onset and severity of obesity. However, from the known genetic defects, only a small fraction accounts for variations in body weight. Obesity seems to follow a polygenic model since the known major and minor genes account for only a small fraction of the variations in body weight within the population (Wareham et al., 2008).

2.3.1.3.3 Dopaminergic system

Malfunction of the reward system was also associated with obesity. Indeed, a lower Striatal dopamine D2 receptor availability was found in adults with obesity. Additionally, the availability of dopamine D2 receptor (D2R) was negatively correlated with BMI (Jf et al., 1999). Since Dopamine regulates motivation and reward circuits, a deficiency in dopamine among obese individuals may influence overconsumption of food to compensate for the reduced activation of these circuits.

2.3.1.3.4 Hypothalamic pathways implicated in the disruption of energy homeostasis

Numerous works have established a robust link between obesity and low-grade inflammation (Pimentel et al., 2014). In rodents, only a few days of high-fat calorie-dense diet (HFD) suffice to induce an inflammatory response in hypothalamic neurons (Thaler et al., 2012a). Indeed, both reactive gliosis and markers indicative of neuron injury were observed in the hypothalamic ARH of rodents within the first week of high-fat diet. The inflammation observed in the ARH might be attributed to its permeability to certain saturated fatty acids (SFAs) such as palmitate, which can pass through the partially incomplete blood-brain barrier. The presence of SFAs in the HT was found to trigger neuronal responses, leading to increased expression of inflammatory cytokines, production of reactive oxygen species (ROS), endoplasmic reticulum stress, and recruitment of microglia (Cai & Khor, 2019a).
HFD-induced obesity in rats was also associated with resistance to anorexigenic signals such as the insulin and leptin (Ávalos et al., 2018a; De Souza et al., 2005a).
In obesity, leptin secretion remains high before and after meals (Farr et al., 2015; Tschöp et al., 2001). However, leptin does not seem to reach its hypothalamic target due to leptin resistance, which disrupts hunger and satiety signals (Izquierdo et al., 2019). However, evidence suggests

that high-fat diet-induced obesity is also linked to reduced circulating ghrelin levels as well as an impaired ability of ghrelin to stimulate food intake via the ^{ARH}AgRP/NPY neurons (Briggs et al., 2010; Castañeda et al., 2010).

In obesity, there seems to be a maladaptive mechanism in which inflammation (**Figure 13**) triggers the CNS to enhance food intake and decrease energy expenditure, thereby providing additional nutrients to the growing adipose tissue (Pimentel et al., 2014).

In Human, the onset of leptin resistance and the ineffectiveness of leptin treatment in individuals living with obesity are also crucial traits associated with obesity (Heymsfield et al., 1999). Indeed, local inflammation was found in the mediobasal hypothalamus (including the AN, the anterior part of the PaVN, and the ME) (Kreutzer et al., 2017).

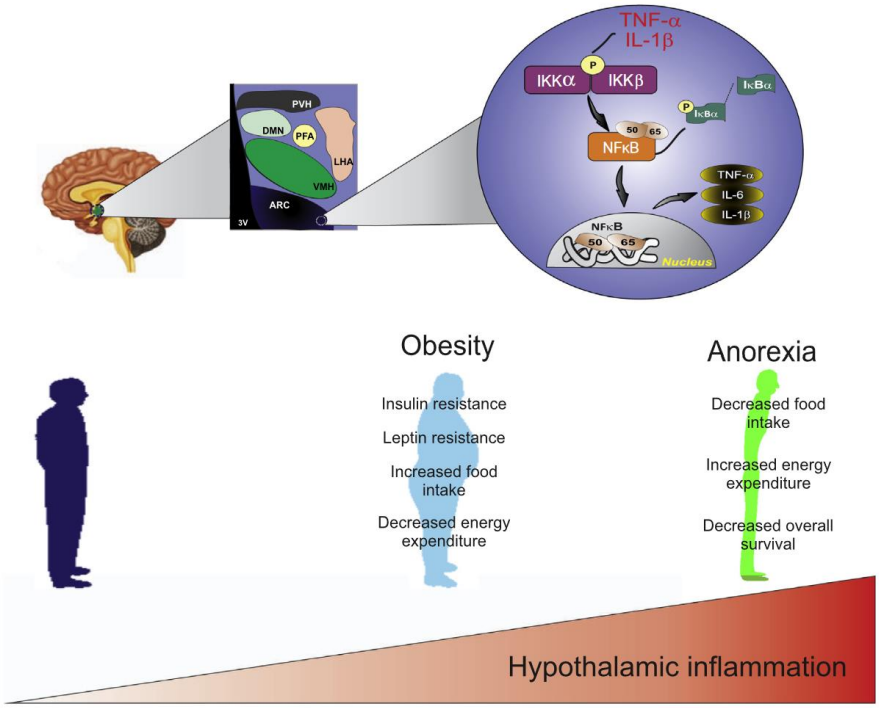

Figure 13 : Schematic representation of the consequences of hypothalamic inflammation on energy homeostasis.

Hypothalamic low-grade inflammation promotes the activation of intracellular signaling pathways that suppress insulin and leptin signaling to promote obesity. Whereas, high-grade inflammation, such as that which occurs in cancer, directly induces anorexia. Notably, the same inflammatory mediators that are associated with obesogenesis are also involved in the development of anorexia. However, the *exact hypothalamic inflammation threshold that makes the central nervous system change from a program that induces obesity to one that elicits anorexia is still unclear*. ARC: arcuate nucleus; DMN: dorsomedial nucleus; IjB: inhibitor of nuclear transcription factor; LHA: lateral nucleus; NFjB: nuclear factor-kappaB; PVH: paraventricular nucleus; VMH: ventromedial nucleus *(Pimentel et al., 2014)*.

2.3.2 Anorexia nervosa

2.3.2.1 Definition

Anorexia nervosa is the most common eating disorder and holds the highest mortality rate of any psychiatric disease. According to the DSM-5, it is characterized by an important self-inflicted restriction of food intake leading to a BMI below 17.5, intense fear of gaining weight, as well as altered body perception influencing self-esteem and causing denial of the severity of current thinness (http://www.dsm5.org/meetus/pages/eatingdisorders.aspx). Anorexia nervosa is frequently associated with various psychiatric comorbidities, including depression, anxiety, obsessive-compulsive disorder, personality disorders, and substance abuse (Erdur et al., 2012). Our study focused on young women with the restrictive subtype of anorexia nervosa, representing the third largest cause of chronic illness in teenagers of industrialized countries (Lucas et al., 1991). Restrictive anorexia nervosa is specifically characterized by chronic food restriction, which may or may not be associated with intense physical exercise, leading to a severe weight loss associated with metabolic disturbances, infertility, osteopenia, and osteoporosis.

2.3.2.2 Epidemiology

Traditionally, anorexia nervosa was believed to be primarily prevalent in affluent Western countries, where access to food was abundant. However, this stereotype no longer holds true; the disorder can affect individuals across all social strata. In France, its annual incidence varies from 2 to 8 cases per 100,000 individuals. Its incidence appears to increase during adolescence, specifically among young women aged 10 to 24, with an average onset age of 17 and two prevalence peaks in early and late adolescence (Smink et al., 2016). Although anorexia nervosa affects both young men and women, the disorder disproportionally affects females. Indeed, it was estimated that 4% of females and only 0.3% of males will develop the disorder over the course of their lifetime (van Eeden et al., 2021).
While the overall incidence of anorexia nervosa has remained relatively stable over the past few decades, there has been an increase in cases (**Figure 14**), among younger individuals aged under 15 years (van Eeden et al., 2021). Generally, the earlier the onset of anorexia nervosa, the more severe the prognosis.

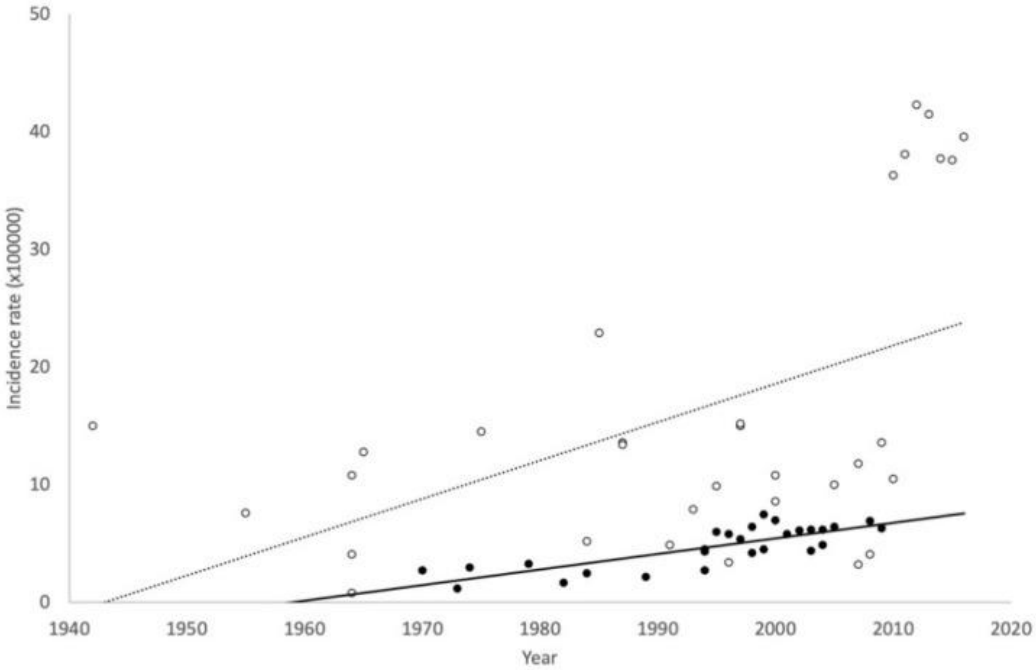

Figure 14 : Trends in the incidence of anorexia nervosa in women of all ages for hospital admission studies.
(Black circle and continuous line) and outpatient healthcare services (OHS) studies (White circle and dotted line) (Martínez-González et al., 2020).

2.3.2.3 Etiology

Anorexia nervosa arises from an interplay of various factors, where environmental influences and genetic susceptibility are closely interwoven.

2.3.2.3.1 Environment

Environmental factors are crucial in the development of anorexia nervosa, which usually starts with harmless dietary restrictions that leads to malnutrition (Connan et al., 2003; Klump et al., 2001). Several studies showed that eating disorders are more common in environments where an idealized body is central to the profession, such as among dancers, models, and high-level athletes, where a thin and controlled body image represents mastery of sensations and physical and intellectual performance, often at the expense of emotional exchanges.
Early life experiences involving stress and traumas such as separation or loss, are important triggers in eating disorders. Puberty is a crucial phase for the development of anorexia nervosa since it is characterized by changes in relationships with others and self-perception, often placing a strong emphasis on body image.
The family framework of anorexic patients appears to play a crucial role, often characterized by hyper-protectiveness, rigidity, conflict avoidance, and poor problem-solving capabilities (Selvini-Palazzoli & Viaro, 1988). Certain personality traits are also commonly found in anorexic young women, such as perfectionism, personal dissatisfaction, low self-esteem, anxiety or depression.
Environmental factors influence the development of anorexia nervosa through epigenic processes. These biochemical mechanisms lead to changes in gene regulation through

modifications of DNA, histones, or non-coding RNAs. Previous works have suggested that the interaction between genetic risk factors and environmental stressors may contribute to the onset of eating disorders (Hübel et al., 2019) (**Figure 15**).

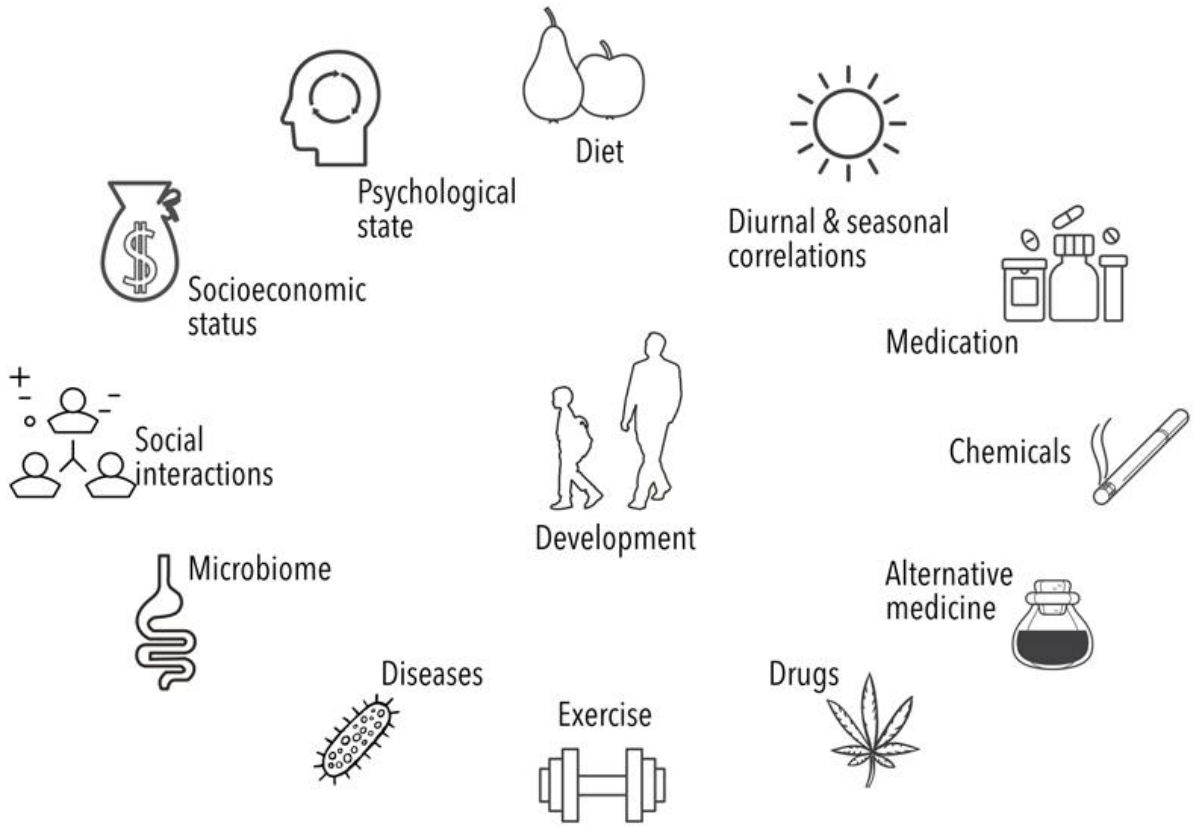

Figure 15 : Environmental risk factors that can trigger the onset of eating disorders *(Hübel et al., 2019).*

2.3.2.3.2 Genetic

For many years, anorexia nervosa was viewed as a culture-bound disorder, heavily influenced by family and sociocultural factors. However, family and more specifically twin studies have demonstrated the crucial role of genetic factors in the susceptibility to this disorder (Klump et al., 2001). Anorexia nervosa is a heritable eating disorder (50–60%), women whose parents have had an eating disorder are at 6 to 10 times higher risk of developing an eating disorder compared to the general population incidence (Yilmaz et al., 2015).

Various Genome-Wide Association Studies (GWAS) have scanned the entire genome to identify genetic variations, such as single-nucleotide polymorphisms (SNPs), that are associated with anorexia nervosa. A first study has associated a SNP with an increased risk of restrictive-type anorexia nervosa (K. Wang et al., 2011). This SNP was located in the HTRD1 gene, which encodes a serotonin receptor, and the OPRD1 gene, which encodes an opioid receptor. The study suggests that both SNPs and rare cases of copy-number variations (CNPs) contribute to the risk of anorexia nervosa. More recently, another GWAS involving a larger number of anorexia nervosa cases identified 8 significant loci at risk involved in metabolic dysregulation (Watson et al., 2019). Nowadays, 58 novel risk loci for anorexia nervosa have

been identified (Bang et al., 2023). A genetic overlap was also identified between anorexia nervosa and major psychiatric disorders, such as schizophrenia, bipolar disorder and major depression (Bang et al., 2023). However, no single gene has been found to directly cause anorexia nervosa. Therefore, it is currently believed that anorexia nervosa falls into an additive gene model, where multiple genes may contribute to the apparition of the pathology.

2.3.2.3.3 Dopaminergic system

Many of the common primary characteristics of anorexia nervosa, such as food obsession combined with food restriction, weight loss, heightened physical activity, and strong associations with mood disorders like anxiety or depression, strongly suggest a potential alteration in the central dopaminergic reward system.

The restrictive diet coupled with intense physical activity followed by individuals with anorexia induces stress which seems to increase dopamine levels in the nucleus accumbens and stimulate dopamine in the mesolimbic reward centers (A & Y, 2014; Bergh & Södersten, 1996a; Fladung et al., 2010). In turn, this seems to reinforce these behaviors, as individuals with anorexia nervosa derive significant satisfaction from their thinness and the control they have over their bodies.

Interestingly, the mesolimbic pathway plays a crucial role in addictive behaviors associated with both drugs and dietary habits (Avena & Bocarsly, 2012). It was theorized that this increased dopaminergic response can turn behaviors usually perceived as rewarding, like dieting and exercise, into habits comparable to substance addiction (Södersten et al., 2016). Indeed, 35% of patients with the restrictive anorexia nervosa subtype have substance-use disorders, indicative of an addictive disorder (M et al., 2012).

Rodent studies showed that administration of D2/3 receptor (D2/3R) antagonists to rodent models of anorexia nervosa, such as the activity-based anorexia (ABA) model, decrease weight loss, hypophagia and increase survival rates (Klenotich et al., 2015a).

Additionally, aPET imaging study showed an increase in D2/3R binding in the striatum of recovered anorexia nervosa patients compared to control subjects, which suggests that D2/3R density or affinity may be higher in patients with anorexia nervosa (G. K. Frank et al., 2005a). Recovered individuals compared to those currently affected with anorexia nervosa also showed reduced concentrations of the major metabolite of dopamine in humans (homovanillic acid) in the cerebrospinal fluid (Kaye et al., 1999). Moreover, measure of blink rate, which is a peripheral measure of central dopaminergic activity, was found to be abnormally high in restricting-type anorexia nervosa patients compared to control subjects and was positively correlated to the duration of illness (Barbato et al., 2006). Genetic studies are also in line with the existence of a dysfunction of the dopaminergic system in anorexia nervosa, since specific combinations of DRD2 and DRD4 gene variants seem to predispose individuals to both eating disorders and certain addiction-related psychopathologies (Bergen et al., 2005; Ceccarini et al., 2022; E et al., 2007).

2.3.2.3.4 Hypothalamic pathways implicated in the disruption of energy homeostasis

Anorexia nervosa has been associated to high-grade inflammation (Figure 13) and substantial alterations in the release of key hormones involved in energy balance and feeding regulation (Gautron & Layé, 2010; Hasan & Hasan, 2011). Indeed, leptin levels are low and ghrelin levels are high, both in fasting and satiated states (Föcker et al., 2011; Troisi et al., 2005). The rise in

plasma ghrelin levels in individuals with anorexia nervosa appears paradoxical considering their restricted eating habits, indicating a potential adaptive response to the condition. In addition, the postprandial secretion of PYY is delayed, and autoantibodies may target α-MSH, which lead to disrupted satiety signals (Fetissov et al., 2002; Kaye et al., 1990).

2.4 Assessment of eating behavioral disturbances in weight-related disorders

2.4.1 Animal models of weight-related disorders

2.4.1.1 Activity-based anorexia nervosa (ABA)

The severe weight loss observed in patients with AN is accompanied by significant changes in hormones involved in energy balance, feeding behavior, and bone formation, all of which can be replicated in animal models.

2.4.1.1.1 Model induction

In the late sixties, the activity-based anorexia (ABA) model was created to explore the physiopathology of anorexia nervosa (Routtenberg & Kuznesof, 1967). This model consists in giving rats access to a running wheel (22–24 h) while restricting their food intake (< 2 h feeding period/day with standard chow and *ad libitum* access to water). This combination leads to increasing hyperactivity and decreasing food intake over time. The ABA protocol is typically followed until a specific weight loss criterion is met, often defined as a weight loss between 15% and 30%. ABA relies on the natural mechanism that wheel running interferes with adaptation to the feeding schedule, which is usually avoided when the feeding schedule is introduced before the running wheel. Hyperactivity allows animals to reach areas with stable food sources, thereby ensuring their survival, suppress appetite and help avoid a drop in body temperature. Indeed, anorexia nervosa patients show a drive for hyperactivity that is positively correlated with anxiety, suggesting that increasing activity is a way to reduce anxiety. Through the ABA model studies, numerous brain alterations, hormonal changes as well as adaptations of the immune system were characterized.

2.4.1.1.2 Lipostat alterations in ABA

In comparison to *ad libitum* fed female rats, ABA was correlated with c-Fos expression in the ARH and supraoptic nucleus (Scharner et al., 2016). Food-anticipatory activity in the running wheel was correlated with c-Fos expression in the DM (Verhagen, Luijendijk, de Groot, et al., 2011). In the same study, ABA rats also exhibited a negative correlation between neuronal activity in the ARH and body weight loss (Verhagen, Luijendijk, de Groot, et al., 2011).
More importantly, they showed that anorexic-like conditions disrupt hypothalamic circuitry, with alterations of neuropeptides such as AgRP, NPY, POMC, and CART in first order neurons which can impair energy balance.
Depending on the progression of ABA, POMC protein expression showed a transient up-regulation of POMC mRNA levels in the ARH during development of ABA (Hillebrand et al., 2006), followed by a 2-fold reduction in case of a chronic food restriction (Rijke et al., 2005). ABA was also associated with elevated melanocortin receptor expression in the VM, which is involved in POMC signaling (Kas et al., 2003). Interestingly, the injection of AgRP, an inverse agonist of melanocortin 3 and 4 receptors, increased the survival rate by reducing physical hyperactivity and preventing the drastic reduction of food intake usually associated with development of ABA (Flier, 2006; Kas et al., 2003). On the contrary, repeated injections of alpha-melanocyte stimulating hormone (α-MSH), an agonist of melanocortin 3 and 4 receptors, triggered wheel running hyperactivity and a reduction of food intake, which made them more susceptible to developing ABA (Hillebrand, Kas, et al., 2005; Saneyasu et al., 2011).

Higher protein expression of the AgRP, NPY and POMC was found in the AN, which was negatively correlated to body weight and white adipose tissue mass (Boersma et al., 2016; Rijke et al., 2005). Interestingly, the combination of food restriction and physical hyperactivity in male mice elevated hypothalamic protein expression of AgRP, while food restriction alone increased both NPY and AgRP (Byerly et al., 2013).

2.4.1.1.3 Appetite regulation hormone levels alterations in ABA

As it was observed in anorexia nervosa patients, ABA studies also found alterations in appetite regulation hormone levels (Schalla & Stengel, 2018; Stroe-Kunold et al., 2016). Indeed, reduced circulating leptin levels and increased ghrelin levels were observed in male ABA rats (Pardo et al., 2010).

In male ABA rats, chronic leptin infusion during the initiation of food restriction suppressed the significant increase in baseline physical activity observed in restrictively fed control animals, whereas chronic subcutaneous leptin administration after the onset of semi-starvation-induced hyperactivity abolished this behavior (Exner et al., 2000).

In female ABA rats, chronic leptin treatment decreased running wheel activity, reduced food intake, and increased energy expenditure through thermogenesis (Hillebrand, Koeners, et al., 2005). Furthermore, acute central leptin injections into the lateral ventricle and microinjection of leptin into the ventral tegmental area also reduced hyperactivity, which suggests that decreased leptin signaling may play a role in hyperactivity (Verhagen, Luijendijk, & Adan, 2011).

On the contrary, food-anticipatory activity in the running wheel was correlated with plasma ghrelin levels in female ABA mice (Verhagen, Egecioglu, Luijendijk, et al., 2011). Interestingly, daily intraperitoneal injection of ghrelin, either alone or combined with IgG from obese mice, prevented ABA in male mice by reducing physical activity during feeding periods without affecting body weight loss or food-anticipatory behavior (Legrand et al., 2016).

2.4.1.2 High-fat diet-induced obesity (HFD)

Although the role of high-fat diets in human adiposity is debated, it is evident that animals exposed to high-fat (HF) diets (HFD) often develop obesity (Willett & Leibel, 2002).

2.4.1.2.1 Model induction

The HFD model consists in randomizing 3-month-old C57BL/6J mice into two groups, fed with either control diet (chow) or HFD (60% of calorie from fat) for 12 weeks, while their weight and food intake is monitored (Z. Liu et al., 2015).

2.4.1.2.2 Lipostat and Appetite regulation hormone levels alterations in HFD

In comparison to the control group, the HFD group showed increased body weight starting from week 3. This weight increase was associated with higher fasting glucose- and insulin levels in plasma, lower glucose tolerance, and higher HOMA-IR values (Z. Liu et al., 2015).
After only a few days of HFD exposure, the central sensitivity to insulin and leptin was reduced (Banks et al., 2004; Benoit et al., 2009). Indeed, HFD seems to directly affect the hypothalamic signaling pathways, resulting in alterations in neuropeptide expression.
Concurrently, HFD-induced obesity led to a chronic low-grade HT inflammation (De Souza et al., 2005a).

2.4.1.3 Contextual feeding conditioning (CFC)

Rodents' studies have shown that environmental context can trigger non-homeostatic feeding in sated animals through Pavlovian conditioning, although the specific neural circuitry involved remains unclear (Petrovich, 2011; Stern et al., 2018). A way to investigate the importance of context in eating behavior is to use a Contextual feeding conditioning paradigm (CFC) (**Figure 16**). The CFC protocol was created by my colleagues at IMCB Astar (Mohammad et al., 2021) adapted from a previously published hunger-induced CFC protocol (Azevedo et al., 2019) based on the observation that palatable food can drive CFC (Stern et al., 2018).

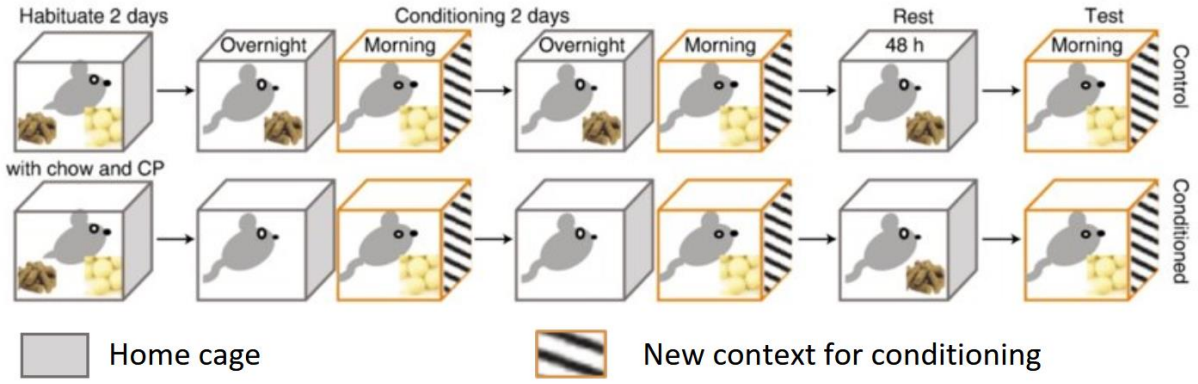

Figure 16 : Schematic of the CFC paradigm.
(grey boxes represent the home cage, orange boxes with stripes represent the new context for conditioning). Adapted from (Mohammad et al., 2021) .

2.4.1.3.1 Model induction

First, mice are given CPs in their home cage and handled for 2 days to prevent neophobia. Mice are habituated for 1h to the food (chow or CPs) in the PhenoTyper chambers for 2 days while their food intake is monitored. For conditioning, the mice are categorized as either "control" or "conditioned". The conditioned mice are then fasted for 23h after habituation, whereas controls have unrestricted access to chow.
On conditioning day 1, both sated (control) and fasted (conditioned) mice are placed in a new context with food (chow or CPs) for 1 hour. The conditioned mice continue to be fasted for another 23h and controls have ad libitum access to chow. On conditioning day 2, both groups are provided with food in the same context.
Following this, both groups are allowed unrestricted access to chow for 48 hours before testing start.
During the testing phase, both groups are exposed to the same context for 1h with CPs or chow provided. Food intake is then measured by weighing the food cup after each 1-hour session during each phase.

2.4.1.3.2 Contextual feeding conditioning paradigm (CFC) mechanism

Hasan and colleagues work suggests that ^{TN}SST neurons may serve as a crucial hub for integrating metabolic signals with environmental context information, likely through projections from the ventral subiculum, to regulate feeding behavior (Mohammad et al., 2021). Indeed, the synaptic connection between the vSub and ^{TN}SST is strengthened after pairing palatable food with an environmental context. This finding demonstrates a synaptic plasticity mechanism that explains how, during conditioning, an environmental context can override nutritional needs to trigger non-homeostatic feeding. Activation of ^{LH}VGAT neurons also induced CFC and receive inputs from the vSub, despite these neurons not being strongly activated by palatable food. Interestingly, rats with bilateral neurotoxic lesions of the medial prefrontal cortex (vmPFC) cancelled CFC (Petrovich et al., 2007). This conditioned potentiation of feeding mechanism also seems to involve connections between the vmPFC and the LH, which suggests that decision-making or sensory processing might be involved. Noteworthy, activating either ^{TN}SST or ^{LH}VGAT neurons in a context without food did not trigger context-induced feeding. Additionally, activating vSub neurons alone did not enhance feeding behavior.

While the precise complete neural mechanisms remain incompletely understood, there is a suggestion that a swift decrease in AgRP neuronal activity is crucial for a learning process that facilitates successful food-seeking (Sternson & Eiselt, 2017). Hence, it is plausible that the suppression of negative-valence AgRP neural activity, followed by the activation of positive-valence ^{TN}SST neural activity, collaboratively ensures effective food-seeking and consumption. Palatable food notably suppresses AgRP neural activity to a greater extent (Y. Chen et al., 2015) and activates ^{TN}SST neurons more significantly, aligning with its potentially prominent role in conditioning.

While many of the molecular, cellular, and mesoscopic mechanisms underlying eating behavior can only be investigated through animal models, human studies employing tools like questionnaires and MRI have proven effective in two ways. First, they allow for initial screening of behavioral processes, and second, they enable the investigation of the anatomo-functional roles of specific brain regions involved in eating behavior circuits. Recent studies have particularly focused on exploring the HT and its subregions, which play critical roles in different aspects of food intake regulation.

2.4.2 Assessment of eating behavior in Human

Questionnaires have been designed for the self-assessment by subjects of their degrees of eating behavioral disturbances. Thus, the participants respond independently, without intervention from the examiner, following the instructions provided on the questionnaire. This can be in a dichotomous format (true/false, or yes/no), or in a graded manner, with various levels of response.

2.4.2.1 SCOFF (Sick, Control, One, Fat, Food)

The SCOFF is a quick 5 items questionnaire developed to detect eating disorders such as AN and Bulimia (Jf et al., 1999). It is considered positive when a participant responds affirmatively to at least two questions. We used the French version of SCOFF, the 'SCOFF-F', because it is the most appropriate for our cohort of young women. Indeed, it has demonstrated a high sensitivity (94.6%) and specificity (94.8%) among French female students. Furthermore, the SCOFF-F has been recommended by the French National Health Authority (HAS) since 2011, for screening eating disorders (Morgan, Reid et al. 1999).

2.4.2.2 Eating Attitudes Test-26 (EAT-26)

EAT-26 measures several aspects of a person's eating behavior, including whether they experience periods of food restriction, episodes of binge eating, preoccupation with food, or if they exert control over their food intake (Garner et al., 1982). Each question in the EAT-26, relating to an eating habit, always offers the same 6 responses: always, usually, often, sometimes, rarely, and never. Participants scoring 20 or higher meet the diagnostic criteria for an eating disorder. It is commonly used to screen for eating disorder risk among high school students, college students, and other groups at elevated risk, such as athletes.

2.4.2.3 Yale Food Addiction Scale 2.0 (YFAS)

The YFAS was created to detect risks of food addiction by measuring the number of food addiction symptoms present in the past 12 months (Brunault et al., 2014). It consists of 35 items (either Likert-type or dichotomous), based on the seven substance dependence criteria from the DSM-IV-TR. The test is considered positive when the participant meets at least 2 of the 7 criteria and fulfills the "marked distress" criterion. For a criterion to be considered "positive," at least one of its items must have a significant score.

2.4.2.4 Hospital Anxiety and Depression Scale (HADS)

HADS was developed to detect and quantify the presence of depression and anxiety (Herrmann, 1997). It requires participants to reflect on their mood over the past week, with 7 items focusing on depression (inability to experience pleasure, feelings of sluggishness and appearance) and 7 items assessing the anxiety (autonomic arousal, tension and restlessness). Each item is rated on a 4-point scale, a score above 11 in either group of 7 items suggests the presence of anxiety or depression.

2.4.2.5 Beck Depression Inventory (BECK)

We used the abridged version of BECK which measures the severity of depressive feelings, in adults as well as in adolescents over 13 years old, through 13 items related to specific behavioral manifestations of depression (Beck & Beamesderfer, 1974). Each item is graded from 0 to 3 through a series of 4 statements reflecting the severity of the symptom.
The total score ranges from 0 to 39, a score between 0 to 3 suggests an absence of depression, 4 to 7 a mild depression, 8 to 15 a moderate to moderately severe depression, and above 16 a severe depression.

2.5 Contributions of brain imaging in the study of weight-related disorders

2.5.1 Foreword

This sub-chapter consists of my first publication of the thesis (literature review), issued in the journal Frontiers in Nutrition on January 3, 2021.
In this literary review, we exposed an overview of the last advances in the neuroimaging domain including in vivo parcellation of hypothalamus, its structural and functional connectivity, as well as functional MRI using various paradigms, in healthy subjects, as well as individuals living with obesity and anorexia nervosa. We also provided new directions for a better use of such imaging methods, which we believe will prove to be of interest in deepening our knowledge on weight-related disorders.
As experts in the field of magnetic resonance imaging and principal investigators of a study on the characterization of the organization of hypothalamic networks related to food intake, we felt relevant to combine the existing knowledge regarding the neuroimaging of hypothalamus.
Despite the large amount of neuroimaging studies investigating food intake networks, we noticed a lack of review summarizing and criticizing all this information, especially regarding the role of the hypothalamus. As new neuroimaging projects surrounding the issue of obesity are currently flourishing, we believed this paper was of great necessity.

2.5.2 Manuscript

On october 2024, this literary review was cited 27 times and holds a total of views and download of more than 18k, which is more views than 94% of all Frontiers articles.

The role of the Human hypothalamus in food intake networks: an MRI perspective

Coleen Roger [1,2*], Adèle Lasbleiz [2,3], Maxime Guye [1,2], Anne Dutour [3], Bénédicte Gaborit [3], Jean-Philippe Ranjeva [1,2]

1) Aix Marseille Univ, CNRS, CRMBM, Marseille, France
2) AP-HM, Timone University Hospital, CEMEREM, Marseille, France
3) AP-HM, La Conception Hospital, Department of Endocrinology, Marseille, France

***Correspondence:**

Coleen Roger

coleen.roger@etu.univ-amu.fr

Abstract

Hypothalamus (HT), this small structure often perceived through the prism of neuroimaging as morphologically and functionally homogeneous, plays a key role in the primitive act of feeding. The current paper aims at reviewing the contribution of magnetic resonance imaging (MRI) in the study of the role of the HT in food intake regulation. It focuses on the different MRI techniques that have been used to describe structurally and functionally the Human HT. The latest advances in HT parcellation as well as perspectives in this field are presented. The value of MRI in the study of eating disorders such as anorexia nervosa (AN) and obesity are also highlighted.

Keywords: MRI, hypothalamus, networks, anorexia, obesity, resting state, diffusion

Introduction

Energy expenditure appears as a continuous process, while energy refilling through food intake is by nature discontinuous. In order to keep the body fat mass stable, a mechanism guaranteeing an efficient balance between energy expenditure and energy intake is therefore needed (Morton et al., 2014). Modern ways of life in developed countries tend to disturb such energetic balance. Indeed, this phenomenon is leading to drastic increases in the prevalence of eating disorders such as obesity, often referred as “globesity” (WHO, 2001) or AN, which holds the highest mortality rate of any mental illness (Arcelus et al., 2011). Although it is true that eating behavior is influenced by our lifestyle, it is the result of the complex association of genetic, metabolic and neurological alterations that have not been completely elucidated to date.

One key structure in the control of the energetic balance is the hypothalamus (HT), a small and complex deep brain structure. HT is composed of four sub-regions: the pre-optic, anterior, tuberal and mammillary regions. These regions project to the autonomous system, and the primary and associative systems. They each host multiple nuclei which bear different physiological-anatomical characteristics. Along the rostral-caudal axis, HT is composed by, i) at the anterior level: the preoptic nuclei (lateral and medial), the anterior hypothalamic nuclei, the paraventricular nuclei (PVN), the anteroventral periventricular nuclei, the supraoptic nuclei and the suprachiasmatic nuclei; ii) at the medial level: the dorsomedial nuclei, the ventromedial nuclei, and the arcuate nuclei; iii) laterally: the lateral nucleus and iv) and at the posterior level: the posterior nucleus and the mammillary bodies (Figure 1). Each of these nuclei has specific roles in homeostatic regulation of energy, food intake, thirst but also temperature, sexual dimorphism, sleep and circadian rhythms (Saper & Lowell, 2014).

Most of the knowledge regarding the functional role of HT nuclei in food intake processes have been derived from animal studies (Anand & Brobeck, 1951b; Krieg, 1932; P. M. Smith & Ferguson, 2008). Figure 2 is an attempt to summarize the current knowledge on such networks. Pioneer works in rats showed that bilateral lesions of the ventromedial HT (VMH) induced hyperphagia while bilateral lesions of the lateral hypothalamic area (LHA) provoked hypophagia (Hetherington & Ranson, 1940) . These early lesion approaches led to the definition of VMH as the "center of satiety", responsible for the food intake inhibition, and LHA as the "center of hunger", whose role is to stimulate food intake (Hetherington & Ranson, 1940). The PVN sends information to the endocrine system while the LHA carries input to the cortex and limbic systems (Berthoud, 2002b).

Advances in deciphering such mechanisms were also possible through the characterization of a network called the ‘hypothalamic lipostat’, which refers to the neuronal pathways involved in

the integration of information related to food intake (Jais & Brüning, 2017). HT ensures energy balance in the long term by integrating factors circulating by humoral or vagal pathways such as satiety signals and adipokines (see (De Silva et al., 2012a) for review). More recently, the 'gut-brain axis' was also associated to the regulation of food intake. Indeed, serotonin-secreting cells found in the gut, communicate with the brain through the vagus nerve (Mawe & Hoffman, 2013; O'Mahony et al., 2015). Visceral signals from the gut activate neurons in the nucleus of the solitary tract (NTS), which excites regions known to mediate feeding behaviour, such as the lateral parabrachial nucleus (PBN) in the pons (Roman et al., 2016). The gut-brain axis is also involved in food reward (de Araujo et al., 2020) and sugar preference (Tan et al., 2020).

Five hypothalamic nuclei have been associated to food intake regulation: the lateral, ventromedial, dorsomedial, PVN and arcuate nuclei (Koutcherov et al., 2003). The arcuate nuclei host first order neurons, which impose antagonistic effects on food intake. On one hand, neurons expressing the neuropeptide Y (NPY) and neuropeptide agouti-gene related peptide (AgRP) project to second order neurons localized in the PVN to stimulate appetite (Berthoud, 2002b). On the other hand, neurons expressing proopiomelanocortin (POMC) and the neuropeptide cocain and amphetamine related transcript (CART) project to second order neurons contained in the LHA in order to inhibit food intake (Berthoud, 2002b), although POMC neurons' role seems more contrasted than previously described (see (Quarta et al., 2021) for review). Depending on energetic state, different types of signals activate or inhibit these neurons. Indeed, when lipid reserves are high, plasmatic leptin concentration increases (Considine et al., 1996). Leptin is an anorexigenic hormone, which acts on food intake in the long term. It reduces appetite by increasing the activity of POMC/CART neurons and inhibiting NPY/ AgRP neurons (Berthoud & Morrison, 2008b). The regulation of food intake is ensured in the short and medium term by insulin as well. After a meal, insulin secretion rises and exercises an anorexigenic effect (Berthoud & Morrison, 2008b). Intestinal peptides also modulate appetite. For example, cholecystokinin (CCK), PYY 3-36 and glucagon-like peptide-1 (GLP-1) stimulate satiety whereas ghrelin promotes food intake (Berthoud & Morrison, 2008b). New hypothalamic regions have recently been shown to be involved in food intake mechanisms. For example, the tuberal lateral nucleus seems to promote an orexigenic effect on food intake by inhibiting the PVN through somatostatin (SST) interneuron signaling (Luo et al., 2018).

In addition, food intake is subjected to a non-homeostatic control influenced by the palatability of food as well as environmental and emotional influences (Berthoud, 2012b). Second order hypothalamic neurons constitute intermediate relays to some regions of the limbic system such

as the amygdala, the hippocampus, the insula, the striatum and the orbitofrontal cortex (OFC). These structures, already known to be involved in emotions, memory or addictions, seem to have an important role in modulating eating behavior (Berthoud & Morrison, 2008b). Furthermore, the limbic system undergoes an inhibitory control from the prefrontal cortex which promotes meal termination (Gautier et al., 2001).

HT dysfunction has long been implicated in eating disorders such as obesity (Thaler & Schwartz, 2010) and anorexia nervosa (AN). With 650 million people affected worldwide in 2016, obesity is defined by a body mass index (BMI) over 30, resulting from an abnormal fat accumulation, which presents a risk to health (WHO). Rat studies showed that obesity induced by high fat diet led to a chronic low-grade HT inflammation with insulin and leptin resistance which promoted weight gain (Ávalos et al., 2018b; De Souza et al., 2005b). Besides, obese individuals showed T_2 hyperintensity in the mediobasal HT, reflecting gliosis (Thaler et al., 2012b). More generally, HT appears to be an open window for some macronutrients (saturated fatty acids (SFAs)) such as palmitate passing through the partially incomplete blood brain barrier in the ARC and the median eminence (Morselli et al., 2014; Posey et al., 2009; Valdearcos et al., 2014). Furthermore, it was shown that the presence of SFAs in HT induce neuronal responses leading to stimulated inflammatory cytokine expression, ROS production, endoplasmic reticulum stress and microglia recruitment (see (Cai & Khor, 2019b) for review). These findings collectively support the hypothalamic inflammatory hypothesis. Malfunction of the reward system has also been associated to a decreased availability of dopamine D2 receptor (D2R) proportionally to the BMI of patients (G. J. Wang et al., 2001).

Concurrently, AN affects approximately 4% of females and 0.3% males during their lifetime (van Eeden et al., 2021). This pathology is characterized by an important self-inflicted restriction of food intake leading to a BMI below 17.5, intense fear of gaining weight, as well as altered body perception influencing self-esteem and causing denial of the severity of current thinness (Diagnostic and Statistical Manual of Mental Disorders 5th Ed. (DSM-5) criteria http://www.dsm5.org/meetus/pages/eatingdisorders.aspx). In comparison to obesity, the cellular mechanisms and physiological substrates of AN have not been as thoroughly characterized yet (Rask-Andersen et al., 2010). However, the administration of D2/3 receptors (D2/3R) antagonists to a rodent model of AN, the “activity-based anorexia” (ABA) model, was found to reduced weight loss and hypophagia, and increased survival (Klenotich et al., 2015b). Furthermore, D2/3R density or affinity seem to increase in AN patients (G. K. Frank et al., 2005b). As it is the case for obesity, this result support the existence of a dysfunction of the dopaminergic system in AN. Therefore D2/3R appear to be interesting therapeutic targets for

AN. Furthermore, serotonin levels have been associated to almost all the behavioral changes observed in AN patients, such as extreme dieting weight loss, hyperactivity, depression/anxiety, self-control, and behavioral impulsivity (Haleem, 2012). However, one of the most interesting hypothesis on the pathophysiology of AN is that chronic food restriction alters the ghrelin signaling pathway and leads to the development of abnormal behaviors such as addiction to food starvation (Méquinion et al., 2013). Overall, translation of the cellular mechanisms observed in animal models to Human is not easy and straightforward. In that context, neuroimaging has appeared as a game changer to explore food intake and the consequences of its deregulation from an anatomical, functional or even metabolic point of view (Florent et al., 2020b; Salem & Dhillo, 2015b) . However, in order to define the precise function of each hypothalamic nucleus in human, it is necessary to clarify their location and their respective roles within the different functional brain networks. Given the small size of the HT, its location and the large number of hypothalamic nuclei, fine characterization of HT is still ongoing. This paper gives an overview of the different neuroimaging studies which have attempted to characterize HT *in-vivo*, as well as the different ways to progress in the field. We will also highlight the undeniable value of MRI in the study of eating disorders such as AN and obesity.

Anatomical MRI characterization, parcellation and morphometry of HT

HT is generally poorly defined or individualized in the numerous subcortical brain atlases proposed in the literature (Brodmann, 1909; Desikan *et al.*, 2006; Lancaster *et al.*, 2007; Mai *et al.*, 2015; Pauli *et al.*, 2018; Tian *et al.*, 2020). Despite the fact that brain MRI stands out as the most suitable tool in the study of central nervous system, the poor contrasts between hypothalamic nuclei has led to consider the HT as a single homogeneous structure, which prevents the precise morphological characterization of each nuclei. Moreover, hypothalamic MRI is subject to artefacts as a consequence of the vicinity of HT with sinuses and bones (Salem & Dhillo, 2015b). Nevertheless, standardized guidelines have been proposed for manual HT delineation as a single structure (Nieuwenhuys et al., 1988). Recently, few MRI studies aimed at characterizing hypothalamic sub-regions based on anatomical references. The first neuroimaging atlas of the HT was based on 3D-MRI acquired at 1.5T in twenty healthy subjects (Baroncini et al., 2012). Thus, by combining anatomical, histological and magnetic resonance images, the human HT was parcellated into PVN, VMH, arcuate nuclei, LHA and the posterior hypothalamic area (Baroncini et al., 2012).

One year later, combination of *in vivo* 1.5T MRI and *ex vivo* 7T MRI data allowed Makris and co-workers to individualize five hypothalamic sub-regions: the lower anterior HT, the upper

anterior HT, the lower tuberical HT, the upper tuberical HT and the posterior HT (Makris et al., 2013). This approach was sufficiently robust to perform quantitative morphometry of HT sub-parts, showing an overall larger HT in men relative to women after correction for brain size. Indeed, significant differences in sizes were reported bilaterally in the five HT subregions, especially in the tuberal region which includes the LHA, infundibular, PVN, VMH and supraoptic nucleus (Makris et al., 2013).

A more detailed parcellation was proposed by Lemaire and collaborators, based on a 1.5T MRI database (Lemaire et al., 2013b). Using precise anatomical landmarks, especially the white matter (WM) bundles neighboring the HT, most internal hypothalamic structures were located: posterior nucleus, dorsomedial nucleus, infundibular nucleus, lateral nucleus, mammillary body, PVN, preoptic nuclei, suprachiasmatic nucleus, supraoptic nucleus, tuberomamillaris nucleus and VMH (Lemaire et al., 2013b).

More recently, the first digital human brain atlas to gather neuroimaging, high-resolution histology, and chemo-architecture was created (Ding et al., 2016). This atlas has the particularity to be based on 7T MRI and 3T diffusion-weighted imaging (DWI) scans, as well as 1,356 large-format cellular resolution (1 μm/pixel) Nissl and immunohistochemistry anatomical plates from a complete adult female brain. Using this strategy enabled the description of every hypothalamic nuclei, including the most challenging structures to describe such as the suprachiasmatic nucleus.

However, a step forward was reached recently by Neudorfer and colleagues (Neudorfer et al., 2020a) who proposed a template based on a large set of 3T data composed by 990 3D-MPRAGE T_1-weighted MRI (isotropic voxel size 1 mm^3) of healthy controls from the Human Connectome Project database (https://www.humanconnectome.org/study/hcp-young-adult/document/1200-subjects-data-release). Using state-of-the-art multiscale template-building methods including non-linear registration procedures (ANTS, http://stnava.github.io/ANTs (B. B. Avants et al., 2008)), the authors proposed the first complete high-resolution in-vivo anatomical atlas of the human HT with a spatial resolution up to 0.25mm × 0.25mm × 0.25 mm voxel size. Based on this high resolved template, three experts were able to delineate the thirteen hypothalamic nuclei and individualized them. Projection to individual subjects using non-linear registration showed differences in volumes of hypothalamic nuclei which are dependent on brain hemisphere and subject gender in healthy subjects. These improvements in delineation and quantification were highly dependent on the artificially increased spatial resolution brought by the use of a large number of exams, which limited partial volume effects and allowed for a better contrast between HT nuclei.

In this context, spatially more resolved raw data, brought by in vivo ultra-high field (UHF) 7T MRI, should play a major role in the finer characterization of HT nuclei at the individual level. Indeed, it should open new opportunities to better understand individual structural organization of tiny HT sub-structures. Thus, unbiased MP2RAGE acquisitions performed at 7T (Marques et al., 2010) should provide T_1 weighted images and unbiased quantitative T_1 maps at high spatial resolution (typically 0.6mmx0.6mmx0.6mm) and allow for a better description of HT sub-structures. As an example, projection of the Neudorfer hypothalamic atlas to a home-made 7T MP2RAGE Uni-Den template one a single subject is presented in Figure 3.

Figure 4 compares two different parcellation processes of the human HT using MRI.

In line with these technological improvements regarding acquisition and post-processing methods, the finer structural characterization of HT nuclei using UHF MRI should play a major role in the depiction of structural abnormalities in the different HT nuclei of patients with eating disorders.

Anatomical characterization of HT in Obesity and Anorexia Nervosa

Very few structural hypothalamic abnormalities have been observed in obesity, while whole brain morphometry showed subtle gray matter (GM) atrophy in some regions of the frontal lobe implicated in behavioral control such as the post-central gyrus, the frontal operculum as well as the putamen which is involved in the regulation of taste and reward (Dekkers et al., 2019; Pannacciulli et al., 2006; Yokum et al., 2012). BMI has been positively associated with GM volume in the right middle occipital gyrus involved in visual processing and systematically activated in food-cue task (Yokum et al., 2012). Such high GM volumes of occipital regions observed in obese individuals could be associated to the selective attention bias toward appetitive food cue (Yokum et al., 2011) and could constitute a predictor of future weight gain (Yokum et al., 2012). In contrast, total body fat appeared negatively correlated with volumes of subcortical GM structures, with greater associations in men compared to women (Dekkers et al., 2019).

On the other hand, a lot of structural hypothalamic abnormalities were found in AN. HT GM volume has been found to be correlated with BMI in AN patients (Boghi et al., 2011). Moreover, while a higher decrease in GM volume was observed in the cerebellum of AN patients with longer disease duration (> 9 years), lower hypothalamic GM was found significant only in AN patients with shorter disease duration (< 3 years) (Boghi et al., 2011).

Furthermore, a meta-analysis of voxel-based morphometry in AN revealed regional GM decreases in the left HT and other areas implicated in somatosensory perception and appetite, such as the left inferior parietal lobe, right lentiform nucleus and right caudate (Titova et al., 2013). Nevertheless, and surely due to the lack of spatial resolution, the largest variations were observed outside HT, with enlargement of ventricles, cortical sulci (Artmann et al., 1985), interhemispheric fissure and generalized volume reduction (Miles et al., 2018) associated with cortical thinning (King et al., 2015). GM atrophy has been specifically observed in somatosensory and reward regions which could explain abnormal reward responses to food stimuli and distortion of body perception (Titova et al., 2013). However, the nutritional status in AN affects cortical folding (Bernardoni et al., 2018), and a longitudinal study on adolescent and young adults with acute and recovered AN patients reported that weight restoration seems to have a rapid reversible effect on cortical thinning (Bernardoni et al., 2016).

Structural connectivity of hypothalamus

The appetitive and self-control brain networks underlying food intake regulation can be represented by three interconnected sub-networks. First, the 'lipostat' regulating energy balance signals including the HT, the ventral tegmental area (VTA) and the Substantia Nigra (SN) participating in the dopaminergic system. Second, the 'limbic system' receiving sensory inputs and programming action to fulfill energy. This sub-network is composed by the amygdalar and hippocampal formations (memory, emotion, learning), the insula (ingestive cortex), the OFC, and the ventromedial prefrontal cortex (VMPFC) (eating value), the accumbens nuclei and the striatum (motivation and value to action). Finally, the 'control system' is composed by the dorsolateral prefrontal cortex (DLPFC) and the anterior cingulate cortex (ACC) which participates in self-regulation (Harris, 2017b). Through the participation of its numerous nuclei and their WM connections, HT appears as central node for each of these different sub-networks.

Diffusion-weighted MRI has helped to better characterize *in vivo* this organization. Kamali and coworkers showed that the stria terminalis connects the amygdala to the anterior HT (Kamali et al., 2015). The stria terminalis projects to the mammillary body region as well as multiple septal and hypothalamic nuclei, which could not be identified due to the lack of spatial resolution (Kamali et al., 2015).. Atlases of human neuroanatomy reported that the ventral amygdalo-fugal fibers originating from the basolateral and central nucleus of the amygdala, project to the nucleus accumbens, basal forebrain, medial dorsal nucleus of the thalamus

(Noback et al., 2007). The ventral amygdalo-fugal fibers also reach the septal nuclei, LHA, lateral preoptic, anterior and tuberal nuclei of the HT (Kamali et al., 2016; Nolte & Sundsten, 2002).

The fornix originates from the hippocampal formation and links the hippocampus to major structures involved in the homeostatic (HT), hedonic valence (amygdala) and reward control (OFC, nucleus accumbens) of food intake (Berthoud, 2002b; Kamali et al., 2015; Metzler-Baddeley et al., 2013a). The fornix fibers were also shown to terminate in the region of mammillary bodies and septal nuclei (Kamali et al., 2015). The pathway connecting the hippocampus to the HT might be involved in the motivated and conditioned pattern of food intake (Tracy et al., 2001). Recently, Kamali's team was the first to reconstruct the dorsal thalamo-hypothalamic tract, revealing in the meantime the existence of a direct connection between the dorsal thalamus to the ventral hypothalamic nuclei (Kamali, Karbasian, et al., 2020). The authors hypothesized that since the thalamus constitute a hub for somatosensory information, the dorsal thalamic nuclei could carry sensory information from the thalamus to the limbic system, in particular to the HT. These findings are in line with studies done in rats suggesting the association of the thalamus and the HT with eating behavior, food motivation/ reward and the circadian rhythms (Kelley et al., 2005; Moga et al., 1995; Poulin & Timofeeva, 2008). A high-spatial and angular resolution diffusion weighted tractography technique revealed the detailed pathway of the parieto-occipito-hypothalamic tract. The parieto-occipito-hypothalamic tract seems to allow for visuosensory information to be carried from the parietal and occipital cortices to the limbic system, especially the HT and the bed nucleus of the stria terminalis. This finding stresses the point that many limbic functions, such as hunger, fear or circadian rhythm rely on visuo-sensory information (Kamali, Ghazi Sherbaf, et al., 2020).

The cerebellum might be involved in the locomotor and foraging aspects of eating behavior (Risold et al., 1997b). Lesional animal studies showed that ablation of the cerebellar nuclei induced degeneration in the HT, reflecting the existence of a cerebello-hypothalamic connection (Jacobs, 1965; Martin et al., 1974). In human, high-resolution diffusion-weighted tractography at 3T revealed that the cerebellar-ponto-hypothalamic tract is responsible for the reciprocal communication between the cerebellum and the limbic system, especially the HT and the septum (Kamali et al., 2018). More recently, a direct cerebello-hypothalamic tract was described in Human. Indeed, DTI results reported fibers projecting from the cerebellar nuclei to the contralateral anterior HT and ipsilateral posterior HT (Çavdar et al., 2020). The cerebellar-hypothalamic connection seems to allow for the convergence of non-limbic information to the limbic system through the hypothalamic and septal nuclei. Numerous animal

studies support the modulatory action of the cerebellum on food intake through its action on the HT (Zhu & Wang, 2008). Therefore, these findings suggest that the cerebellar-ponto-hypothalamic tract might carry the modulatory action of the cerebellum on hypothalamic feeding centers.

Finally, structural connectivity derived from DTI tractography was been used to parcel HT by studying the orientations and projections of the different efferent and afferent WM fibers connecting HT to other brain areas. Lemaire and co-workers characterized parts of the macroscopic internal structure of the HT and its extrinsic connectivity with deep brain and cortical regions (Lemaire et al., 2011). Thus, preoptic, anteroventral and lateral hypothalamic regions were shown to predominantly project to the right frontal hemisphere, largely involved in behavioral control (Lemaire et al., 2011). Using color coded directional fractional anisotropy (FA) maps of HT, three different subregions of HT were defined: an anteromedial region with dorsoventral diffusion direction, a posteromedial region with rostro-caudal direction, and a lateral region with mediolateral direction (Schönknecht et al., 2013). The anteromedial region was assigned to the PVN, anterior, and dorsomedial hypothalamic nucleus and part of the LHA, the lateral region to the VMH and supraoptic nucleus and finally the posteromedial region to the suprachiasmatic, infundibular, VMH, posterior hypothalamic, medial and lateral mammillary nucleus.

Altered structural connectivity in Obesity and Anorexia Nervosa

Obesity has been associated with abnormal WM volume and microstructure as well as microstructural brain diffusion changes in HT and other structures involved in satiety and hunger (Van den Eynde & Treasure, 2009)**.** Indeed, DWI studies revealed that the apparent diffusion coefficients (ADC) of HT, hippocampal gyrus, amygdala, insula, cerebellum and midbrain were significantly increased in obese patients. More specifically, hypothalamic longitudinal diffusivity λ_1, a DTI metric related to axonal integrity, has been found to be negatively correlated with fat mass in obese subjects (Puig et al., 2015). Furthermore, altered hypothalamic microstructure, characterized by a higher mean diffusivity (MD) within the HT, have been associated with a higher BMI (Thomas et al., 2019). Indeed, alteration in the hypothalamic microstructure visible on DTI has been associated with the presence of inflammatory factors, such as C-reactive protein (CRP) or lipopolysaccharide-binding protein (LBP) (Puig et al., 2015). However, there is no consensus regarding the sign of the correlations between BMI and WM volumes. Most studies have established an increases of WM volumes in the frontal, temporal, parietal and occipital lobes, fusiform and parahippocampal gyri,

brainstem and cerebellum in obese relative to lean participants (Haltia et al., 2007; Walther et al., 2010). On the contrary, a decrease in WM volumes has been reported in overweight and obese older adults within the frontal lobe, anterior cingulum and corona radiata (Raji et al., 2009). The percentage of total body fat has been positively associated with global FA in men and women, and negatively associated with global MD in women. These results suggest that obese women globally present higher integrity but lower magnitude of WM microstructure, showing differential gender effects of obesity on WM microstructure (Dekkers et al., 2019). Generally, the association between markers of obesity and diffusion parameters seems stronger in women than in men (Mueller et al., 2011). However, regionally, obese individuals demonstrate a negative correlation between BMI and FA in the corpus callosum and fornix (Stanek et al., 2011). Furthermore, BMI was found to be negatively associated with the microstructural integrity of numerous WM bundles such as callosal and limbic tracts (Xu et al., 2013). Interestingly, obese subjects show partial recovery of WM volumes after only six weeks of dieting (Haltia et al., 2007).

Alteration of WM microstructure has also been observed in AN patients (Miles et al., 2020). DTI studies reported low FA and/or high MD of the fornix, amygdala and the prefrontal region in AN (Martin Monzon et al., 2016). Low FA was also found in the lateral part of the cerebellum of AN patients (Nagahara et al., 2014; Zhu & Wang, 2008). This result is in line with animal studies stating that cerebellar nuclei would modulate lateral hypothalamic response to satiety and hunger through interaction with gastric vagal nerves (E. Y. Chen & Zeffiro, 2020b).
Using a probabilistic tracking algorithm, the same team who implemented the first 3D-MRI atlas of the HT (Baroncini et al., 2012) found a significant reduction in the number of fibers in the arcuate nucleus of AN patients and leanness controls compared to normal-weight controls but higher connectivity of LHA in AN compared to leanness and normal-weight controls (Florent et al., 2020b). In the same study, high basal levels of HT glutamatergic markers (Glutamate-Glutamine/Cr ratios) derived from magnetic resonance spectroscopy (MRS) dropped abnormally following food intake in AN compared to controls (Florent et al., 2020b). Therefore, lower BMI seems associated with a specific altered structural connectivity of the arcuate nucleus and LHA as well as a different HT metabolic response to food intake (Florent et al., 2020b).

Moreover, AN seems to be characterized by a disrupted fronto-accumbal structural connectivity since a longitudinal neuroimaging study revealed that the abnormal increase in structural connectivity within the fronto-accumbal network found in AN patients persisted even after weight recovery (Cha et al., 2016a).

However, the full structural connectome of HT nuclei is far from being entirely described, both at the intra-HT and extra-HT connectivity levels. DTI techniques cannot provide crucial information such as the afferent or efferent nature of fiber tracts. Only significant improvements in DWI acquisitions and models including high angle resolution diffusion imaging (HARDI), orientation diffusion functions, multi-shell acquisitions and/or UHF protocols increasing spatial resolution (Fritz et al., 2019), and correlation with post-mortem data should allow for the full characterization of these complex hypothalamic networks. In that sense, improvement of post-processing pipelines validated in large cohorts (Glasser et al., 2013) will help to correct distortion artifacts (eddy currents, susceptibility effects, motions…) in UHF DWI and will allow for high quality data to be accurately overlaid with HT nucleus structural atlases.

Functional connectivity of hypothalamus

Appetite networks have also been explored through the prism of functional connectivity (FC) by using resting-state functional MRI (rs-fMRI). rs-fMRI consists in recording temporal correlations of low frequencies blood oxygen level dependent (BOLD) fluctuations between various brain areas during a 'resting' period (Biswal et al., 1995a). This technique is commonly used to identify functional networks when no task is performed (Scaife et al., 2017).

Such paradigm was used to explore the effect of fasting and satiation on the FC patterns in healthy subjects (Wright et al., 2016). Interestingly, variations of blood glucose levels between scans accounted for numerous altered functional connectivities. Indeed, FC between the left HT and inferior frontal gyrus strengthened during fasting whereas FC increased between the right HT and the superior parietal cortex during satiation (Wright et al., 2016).

In healthy subjects, a depleted energy state seems to favor connectivity of the HT with the inferior frontal gyrus, which is implicated in suppressing the desire for food and preventing temptation to eat (Hollmann et al., 2012; Lopez et al., 2014). On the contrary, satiation is associated with a stronger connectivity between the HT and the superior parietal cortex, which is hypothesized to be involved in decreasing the eating drive by being less distracted by thoughts of food or eating (Wright et al., 2016). Thus, the HT connectivity seems to be lateralized and to depend on the energy state.

Hunger may increase effective connectivity (EC) from posterior insula to anterior insula while EC from the anterior insula to posterior insula may be decreased (Al-Zubaidi et al., 2020). Therefore, individuals' energy states affect the strength and directionality of connections between sub-regions of the insula. However, this same study failed to provide evidence of an effect of hunger on the connection between the HT and the insula.

Seed-based resting-state connectivity maps derived from a 3T MRI database of 49 healthy subjects were generated from the LHA (Kullmann, Heni, et al., 2014a) considered as the hunger center, and from the medial HT (including the VMH) considered as the satiety center (Hetherington & Ranson, 1940; Mayer & Barrnett, 1955). The LHA was shown to be strongly connected to the dorsal striatum (caudate, putamen), anterior cingulum, thalamus, and frontal operculum, regions involved in goal-directed behavior (Dosenbach et al., 2006), and to the lateral OFC implicated in coding stimulus reward value (O'Doherty, 2004). The LHA was also shown to receive preferentially inputs from the lateral OFC (Hirose et al., 2016). In contrast, the medial HT showed stronger connections with the ventral striatum (nucleus accumbens), the medial OFC and the occipital gyrus, regions involved in reward and motivation (Tomasi & Volkow, 2013) and with the medial OFC (Hirose et al., 2016).

Improvement of statistical power through a better temporal resolution and higher spatial resolution available with UHF MRI scanners (Gulban et al., 2018) should be a game changer in the study of functional reorganization of HT networks in healthy subjects and eating disorders patients.

Modulation of FC in Obesity and Anorexia Nervosa

Functional connectivity is altered in obese patients when compared to healthy subjects. On one hand, high BMI subjects show a decreased global brain connectivity (GBC) in the lateral and prefrontal cortices, the insula and the limbic system (P. Geha et al., 2017), and a reduced FC between HT and regions involved in cognitive control such as the superior parietal lobule (T. M. Le et al., 2020a). On the other hand, obese patients show increased global brain connectivity in the visual, parietal, and premotor cortices (P. Geha et al., 2017). Functional connectivity of the LHA with the ventral striatum, anterior insula and OFC were found to be enhanced in obese compared to healthy individuals (Martín-Pérez et al., 2019). In addition, high BMI subjects show increased FC between HT and regions involved in motivation processes (insula, thalamus, globus pallidus, cerebellum) (T. M. Le et al., 2020a), and increased FC between medial HT and regions involved in reward processing such as OFC and nucleus accumbens (Kullmann, Heni, et al., 2014a). Therefore, BMI is positively associated with FC between HT and brain regions involved in motivated feeding, reward processes and motricity, while FC between HT and areas involved in cognitive control of food intake is negatively correlated to BMI (T. M. Le et al., 2020a).

Modulation of hunger states showed that obese patients exhibit higher connectivity between the HT and the medial prefrontal cortex (PFC) and the dorsal striatum when fasted compared to

lean subjects (Lips et al., 2014). Furthermore, in contrast to lean subjects, FC between HT and the PFC did not decrease when fed, which could explain the increased craving for food obese individuals experience during a fast (Lips et al., 2014). Additionally, lower FC was found between the HT and brainstem in response to glucose administration in obese compared to normal-weight control (J. J. Simon et al., 2020a). These results stress the presence of FC alterations between the HT and regions involved in the inhibition of the eating drive, thus limiting the control of the balance between energy intake and expenditure (Lips et al., 2014). However, weight loss surgery allowed reversibility of FC abnormalities within HT networks, with restored lower FC between the HT and the OFC and somatosensory cortices (van de Sande-Lee et al., 2011).

Even though numerous resting-state fMRI studies were conducted in AN, most of them did not look at HT connectivity. Indeed, they rather focused on altered local- and large-scale-connectivity of 'conventional' resting state networks (RSN) such as the default mode network (DMN), the visual network and auditory networks, as well as the reward and cognitive control systems. The DMN is a network associated with stimulus-independent thoughts and self-reflection (Cowdrey et al., 2014). Within this network, increased FC was observed between the dorsal ACC and regions such as the precuneus and the retro-splenial cortex, which was positively correlated with body shape questionnaire scores (Lee et al., 2014). Such FC increase could represent a supplementary effort of the cognitive control system to restrain appetite (K. R. Kim et al., 2012). Data driven approach using independent component analysis (ICA) showed increased FC between the angular gyrus and the frontoparietal network in AN, which was also correlated with stronger cognitive control scores (Boehm et al., 2014). In AN patients compared to healthy subjects, EC was increased from the bilateral orbitofrontal gyrus to the right IFG and from the bilateral insula to the left IFG while EC was decreased from the right inferior frontal gyrus to the mid-cingulum (Kullmann, Heni, et al., 2014a). These findings suggest that connectivity within the control network is reduced whereas connectivity between salience-related systems is increased in AN.

The ventral attentional circuit was also shown to be abnormally highly connected in AN, especially the inferior frontal gyrus (Collantoni et al., 2016). Since the ventral attention circuit allows for the implementation of appropriate behavioral responses, especially when an unexpected or salient stimulus occurs, its alteration could be responsible for lower interoceptive sensations awareness and struggles in adapting one's behavior to environmental needs (Corbetta & Shulman, 2002).Visuospatial and auditory processing involved in self-body image have also appeared to be disturbed in AN patients, with reduced FC within the lateral visual

cortices and the auditory network (Scaife et al., 2017), and between the sensorimotor and visual circuits (Phillipou et al., 2016).

Furthermore, hyperconnectivity in AN of the dorsal caudate with prefrontal regions involved in motor and cognitive functions (Di Martino et al., 2008), have been interpreted as altered habit learning deficiencies responsible for the maintenance of AN symptoms (Steinglass & Walsh, 2016).

Within the reward system, AN patients showed increased FC between the left nucleus accumbens and the left medial OFC compared to control subjects (Cha et al., 2016a). Moreover, the connectivity within the ventral fronto-striatal circuit also seems to be dysfunctional in AN. Furthermore, hypoconnectivity between nucleus accumbens and superior frontal gyrus, found in AN, correlated with greater cognitive eating disorder symptoms (Eating Disorder Examination Global scores). Collectively, these findings suggest that FC is altered in AN in key brain regions involved in reward processing, homeostatic communication and habit.

Half of the AN individuals who received medical care need to be re-hospitalized within a year of discharge (Pike, 1998). Given the persistence and high risk of relapse of this long-term disease, the study of the resting state functional connectivity (rsFC) in weight-recovered AN individuals is particularly important.

Complete restoration of rsFC in weight-recovered AN individuals for at least 12 months has been observed in the PFC, sensorimotor, precuneal, insular, left parietal and left temporal cortices (Lotter et al., 2021). In contrast, altered FC persists after 6 months recovery in the frontoparietal network with reduced FC with the DLPFC and increased FC with the angular gyrus and between the precuneus and DLPFC (Boehm et al., 2016). Overall, rsFC alterations in AN tend to normalize after weight restoration, with the noticeable exception of the cognitive control network, which could in part explain the high risk of relapse of this disease.

However, more resting-state studies are needed since findings on the same networks are inconsistent (Gaudio et al., 2016). Moreover, undernutrition was found to alter reward and habit learning related networks (Zink & Weinberger, 2010) as well as to influence rsFC results (Al-Zubaidi et al., 2020). Therefore, rsFC AN studies might observe the consequence of starvation and not the neuronal correlates of AN (Haynos et al., 2019). On the other hand, it can be hypothesized that a malfunction of the reward system could be the trigger of AN in genetically predisposed individuals exposed to certain environmental conditions such as emotional shock or diet (see (Keating et al., 2012) for review). Furthermore, most studies did not take into

account the different subtypes of AN (restrictive and binge eating/purging), although they were not found to influence results (Cha et al., 2016a).

Task related fMRI of eating disorders and hypothalamus

Different methods of functional imaging have been used to study appetite networks. Tracking variations of BOLD signal (fMRI), regional cerebral blood flow (rCBF) (PET or fMRI) or ADC (diffusion weighted MRI) have been conducted i) during different hunger states, ii) before, during and after glucose (or other nutriment) ingestion, or iii) during different food cue image display paradigms, including (or not) different satiety states.

Hunger was shown to enhance BOLD signal and rCBF within the HT, the ACC, the insula, the parahippocampal gyrus, and the hippocampus, core regions of the limbic system (Tataranni et al., 1999). Concurrently, during satiation, increase in rCBF was observed in the VMPFC, the DLPFC, and the inferior parietal lobe, which are all involved in the control of food intake (Tataranni et al., 1999).

Glucose ingestion in healthy subjects induce a dose-dependent decrease in the BOLD signal within the PVN and the VMH, which have an anorexigenic role (Matsuda et al., 1999). Besides, oral glucose intake triggers two peaks of response in healthy subjects: one just after the ingestion, followed by another peak approximately 10 min later (Y. Liu et al., 2000). This delayed response was found to be associated with a negative response in the medial HT, and the fasting plasma insulin concentrations (Y. Liu et al., 2000) reflecting the important role of HT in the modulation of insulin secretion to regulate glucose levels (Benzo, 1983).

The type of ingestion may also play a role since both sweet taste and energy content are necessary to trigger a hypothalamic response (Smeets et al., 2005). However, the limited spatial resolution of these techniques may prevent the ability to detect such changes in HT during glucose ingestion due to the different roles and activity patterns (stimulatory or inhibitory) of close-by hypothalamic nuclei (Purnell et al., 2011).

However, more recently, Osada and colleagues described the glucose metabolism of individual major HT nuclei by using areal parcellation based on areal profiles of resting state functional connectivity (Osada et al., 2017). They observed a decreased activity in the VMH but an increased activity in the LHA between 10 and 40 minutes after glucose ingestion. Furthermore, the decrease in activity found in the arcuate nucleus was followed by a rise in blood insulin during the first 10 minutes after glucose ingestion (Osada et al., 2017).

Sun and colleagues demonstrated that the amygdala response to the administration of a milkshake predicted weight in satiated but not in hungry individuals (Sun et al., 2015). Looking at EC, sated subjects showed an unidirectional gustatory input from basolateral amygdala to the HT, whereas during hunger, HT drove bilateral connectivity with the amygdala (Sun et al., 2015).

Another popular neuroimaging method commonly used to investigate appetite networks is food-cue reactivity paradigms, which consist in presenting images of food under various forms and energy-content as well as non-related food images. Comparison of BOLD signals between conditions helped to decipher appetite processes. Indeed, high-calorie food were shown to trigger a significant bilateral activation of the HT (Killgore et al., 2003a; Schur et al., 2009a), the medial and DLPFC, the medial dorsal thalamus, the cingular cortex, and the cerebellum compared to the non-food condition (Killgore et al., 2003a). The cerebellum was also shown to be activated when viewing high fat relative to low fat food images (Killgore et al., 2003a). Furthermore, numerous animal studies revealed that the cerebellum modulates the activity of the LHA through its connections with gastric vagal nerves involved in hunger and satiety signaling (E. Y. Chen & Zeffiro, 2020b).

Similarly to results obtained during the glucose ingestion, presentation of rewarding food tastes and images during satiation decreased BOLD signal in the reward system, including the HT, vmPFC, nucleus accumbens, OFC, and insula but increased BOLD response in the DLPFC, which is part of the control network (Thomas et al., 2019). Similar manipulation of food types through hunger states showed that presentation of high-energy food during fasting might activate the HT and ventral striatum to a greater extent compared to low-energy food (van der Laan et al., 2011). fMRI is also used in the study of emotional connotation of food, which could be a factor in unhealthy food choices. One of this studies found an association between lower food healthiness evaluation of food in a food-cue task, and higher activation in the amygdala (Herwig et al., 2016). Therefore, the ability to differentiate healthy from unhealthy foods is affected by emotional state.

Nevertheless, reproducibility across these studies appears to be highly dependent on various external factors, limiting the fine characterization of the role of HT within food intake networks. One meta-analysis (van der Laan et al., 2011) revealed that no more than 41% of experiments contributed to the activated voxel clusters for the contrast between food and non-food pictures, which could be explained by biases of subject selection according to age (Killgore & Yurgelun-Todd, 2005b), BMI scores (Killgore & Yurgelun-Todd, 2005a), sex, hunger states (Uher et al., 2006), emotional state (Killgore & Yurgelun-Todd, 2006), dietary restriction (Coletta et al.,

2009) and subject genotype (Kaurijoki et al., 2008). Minimization of potential biases relative to menstrual cycle, which could trigger cravings, has been proposed through the recommendation of performing MRI scans during the follicular phase (Buffenstein et al., 1995). Indeed, mean diffusivity and metabolism of HT appear to be modulated by artificial menstrual cycle, leading to a decrease in ADC and increase in Choline/NAA ratios after oral contraceptive use compared to pill free period in young healthy women (Baroncini et al., 2010).

Regarding study designs, food paradigms differ between studies in the nature and nutritional properties of the food presented, in task instruction and even in sample sizes, which are generally small, and differences in the acquisition and analyses methods (van der Laan et al., 2011). In regard to these irregularities, which hinder the understanding of the role of the HT in the regulation of food intake, standardized databases of food and non-food images have been implemented (Blechert et al., 2014; Charbonnier et al., 2016). Moreover, the duration of the fasting period before scan sessions should be harmonized to create a more homogenous hunger state in subjects across studies.

Recent studies have tried to minimize the bias related to individuals' food preferences. Some studies take into account the participant's preferred food in their script (Jastreboff et al., 2013), while others ask them to rate the appetence of the presented food (Mehta et al., 2012). One study even had volunteers rate their hunger, satiety, thirst, fullness and emptiness, before and after the scanning session (Chin et al., 2018). However, taking into account those ratings did not refine the model fit in this food-cue reactivity study.

Functional imaging in Obesity

During satiation, obese individuals showed deactivation of the precuneus and the superior parietal cortex, with lower rCBF in the HT, cingulate, nucleus accumbens, in the limbic and paralimbic regions (parahippocampal gyrus, insular cortex, amygdala), caudate nucleus, frontal and temporal regions relative to controls (Gautier et al., 2000, 2001). In contrast, sated obese women exhibited significantly higher rCBF in the ventral PFC and frontal operculum (Gautier et al., 2000, 2001). These findings are in agreement with the hypothesis that the PFC is implicated in the termination of a meal by its inhibiting action on limbic and paralimbic areas (Gautier et al., 2001).

Concurrently, glucose ingestion in obese patients relative to controls induced a delayed and attenuated dose-dependent decrease in BOLD signal in the PVN and VMH (Matsuda et al., 1999). In addition, the decrease of rCBF in HT during a meal associated with normal satiety processes in healthy subjects has appeared to be attenuated in obese patients (Gautier et al., 2000).

When administered a liquid meal, obese and former obese who succeeded in decreasing their BMI from at least 35 to a BMI of 25 kg/m2 and in keeping their weight stable for no less than 3 months before the start of the study, exhibited an increased rCBF in the middle insular cortex while no change in activity was registered in lean individuals (DelParigi et al., 2004). Additionally, when given a satiating amount of the same liquid, obese presented a different neural response in the posterior hippocampus, posterior cingulate cortex and amygdala. Indeed, the posterior hippocampus rCBF decreased in a similar manner in obese and former obese while it increased in lean individuals (DelParigi et al., 2004).

Persisting differential activities in regions implicated in gustation and rewarding/ hedonic aspect of food (insular cortex) or enteroception and learning/memory (hippocampus) could partly explain the high risk for relapse of former obese. Interestingly, a study on smokers and non-smokers revealed that the hypothalamic response to oral intake of milkshake in non-smokers was lower, which is associated with long-term weight change in this population (P. Y. Geha et al., 2013).

Food-cue task fMRI studies reported elevated responsivity of somatosensory (Rolandic operculum), gustatory (insula, frontal operculum) and reward brain areas (caudate, putamen, amygdala, OFC) in obese subjects compared to lean individuals when presented with palatable food cues (Rothemund et al., 2007; Stice et al., 2008; Stoeckel et al., 2008a). Abnormal activity patterns in obese patients have been found in the HT, PFC, parietal and temporal cortex, cingulate cortex, nucleus acumens, amygdala, midbrain, insula, and OFC (DelParigi et al., 2004; Gautier et al., 2001).

During high-calorie food cue, obesity has been associated with hyperactivation of the right putamen, left caudate body, left anterior insula, left hippocampus, and the left parietal lobe relative to control, while low-calorie food cue elicited exacerbate responses in the left superior frontal, right middle and inferior frontal gyrus, middle occipital gyrus, and left superior temporal gyrus in obese compared to healthy controls (Rothemund et al., 2007). Thus, BMI was positively associated with higher response to high-calorie in brain regions involved in the processing of taste information (anterior insula, lateral OFC), motivation (OFC), emotions and memory (posterior cingulate cortex), salience-guided orienting (claustrum) and reward anticipation (dorsal striatum) (Rothemund et al., 2007; J. B. Smith et al., 2019). BMI is also positively associated with selective attention toward appetitive food-cue and higher responsivity in reward regions such as the ventrolateral prefrontal cortex (VLPFC), lateral OFC, temporal operculum and anterior insula (Batterink et al., 2010a; Yokum et al., 2011). However, when asked to inhibit responses to high-calorie food images, obese individuals exhibit less

activation in frontal inhibitory regions, such as the superior and middle frontal gyrus, VLPFC and VMPFC, and OFC, relative to lean individuals, which is consistent with behavioral evidence of impulsivity often found in overweight individuals (Batterink et al., 2010a). These findings suggest that a higher weight is preferably linked to hypo-activation of inhibition control regions and hyper-activation of reward regions in response to palatable food. Failure of inhibition control regions to inhibit reward regions when presented with appetitive food could increase the susceptibility to overeat (G.-J. Wang et al., 2009). Moreover, obese-like activity in the middle insular cortex and hippocampus persists in former obese (DelParigi et al., 2004). These results suggest that higher activation in reward and somatosensory regions in response to food-cue constitute a risk for future weight gain.

During reduced weight maintenance, obese individuals show high FC between the HT and visual (occipital fusiform and temporal fusiform areas, superior lateral occipital cortex and cuneus), memory (hippocampus) and attention areas (dorsal ACC, left middle and inferior frontal gyri) when viewing food compared to non-food images (Hinkle et al., 2013). Moreover, the inferior frontal gyrus, implicated in inhibitory control (Swick et al., 2008), has been found to be more activated by food images in people able to maintain their weight loss than in obese or lean subjects (Sweet et al., 2012) and its activation in satiation is lower in obese than in normal weight participants (D. S. N. T. Le et al., 2009). These results suggest that during weight loss, obese patients have a higher sensitivity to food cues. Furthermore, the inhibitory action of the inferior frontal gyrus seems to be necessary to maintain weight loss (Sweet et al., 2012).

Overall, obesity seems to be associated with a concurrent blunted hypothalamic reactivity to glucose ingestion and an exacerbated hedonic reactivity, which do not coincide with homeostatic state and lead to overconsumption of high fat food.

Functional imaging in Anorexia Nervosa

Considering the ability of AN patients to fight against the natural instinct to feed oneself, the hypothesis of a dysregulation in hypothalamic glucose-sensitivity was investigated. AN and controls exhibited the same decrease in neuronal activity when administered with a glucose solution (van Opstal et al., 2015). Therefore, the hypothalamic reactivity to glucose does not seem to be altered in AN. However, contrary to normal-weight controls and obese subjects, AN patients did not display an increase of FC between the HT and brains regions implicated in reward processes (amygdala, nucleus accumbens) during infusion of water when compared to glucose infusion, with the exception of the posterior insula (J. J. Simon et al., 2020a). As

opposed to control, AN did not show deactivation in the mesocorticolimbic reward circuit including structures such as the caudate nucleus, putamen, insular cortex, medial OFC, and inferior operculum after glucose administration (J. J. Simon et al., 2020a).

Furthermore, AN exhibited a higher FC between the HT and the left ventral striatum in response to glucose administration relative to normal-weight controls and obese (J. J. Simon et al., 2020a). The abnormal hyper-activation of the ventral striatum is a neural signature of patients suffering from AN and is hypothesized to be involved in the onset and maintenance of this illness (Bergh & Södersten, 1996b). Interestingly, a study comparing the response to pictures of underweight women demonstrated a higher activation in the left ventral striatum in AN patients compared to lean control (Fladung et al., 2013).

Moreover, patients with AN do not show satiety state–dependent connectivity between the HT and meso-corticolimbic reward circuit that is commonly found in normal-weight controls. This observation could explain the reduced hedonic coding aspect of food associated with AN (J. J. Simon et al., 2020a). AN individuals show hypoactivation of food motivation network in response to high-calorie foods (Holsen et al., 2012a). Indeed, both fasted women with weight-restored (maintenance of 90%–110% ideal body weight for at least 6 months) and active AN exhibited hypoactivity in the HT, amygdala and anterior insula in response to high-calorie foods versus objects when compared to control. Hypoactivation in the anterior insula persisted in women with active disease after they were served a meal (18% calories from protein, 23% from fat and 59% from carbohydrates).

In contrast, weight-restored AN women show similar activation to controls after a meal (Holsen et al., 2012a). Compared with controls, women with active disease show hypoactivation in the HT, amygdala, hippocampus, OFC and anterior insula when fasted and in the amygdala and insula after they ingested a meal (Holsen et al., 2012a). Interestingly, activations in the HT, amygdala and anterior insula are significantly associated with appetite (hunger) and appetence ratings (how appealing is the food) in controls and weight-restored AN women but not in those with active disease (Holsen *et al.*, 2012). The authors provided evidence for dysfunction of the food motivation network, including the HT, in women with active AN, which tend to persist even after weight-restoration. AN has been shown to be associated with lower food-cue processing activity in brain structures implicated in reward and salience (HT, striatum, hippocampus, amygdala, cerebellum, insula) but greater activity in regions involved with cognitive control (dorsolateral PFC, mPFC, OFC, ACC) (Brooks, Rask-Andersen, et al., 2012; Sanders et al., 2015). To sum up, AN has been associated with a reduced hypothalamic

reactivity and connectivity with the reward system, which could be responsible for the repressed motivational responses to food cue, in relation with an alteration in food reward processing.

Conclusion

Despite the important progress in the neuroimaging of HT and the better characterization of its functional activation pattern across different hunger states or eating disorders, its role within the structural and functional food-intake networks remains to be elucidated. UHF MRI combined with the use of the highly resolved atlases (Neudorfer et al., 2020a) should allow for a better understanding of the role of each hypothalamic nuclei in a normal and pathological context. Indeed, advanced magnetic resonance (MR) techniques provide new significant anatomical, functional metabolic and connectomic insights of the HT, through the improvement of quantitative MRI, spectral/spatial resolution of MRS, spatial resolution of anatomic MRI, diffusion and functional MRI. Furthermore, the current paper briefly mentioned the possible contribution of metabolic MRI in the study of obesity. In addition, MRI is an undeniable interesting tool in the study of the effectiveness of treatments for eating disorders in humans since this technic is non-invasive and partially replace for the lack of AN animal models. Finally, combining the study of the HT at the structural, functional and metabolic levels could bring new perspectives to better understand and better treat patients with eating disorders, as it is already done in the study of pathologies such as Alzheimer (Schouten et al., 2016) or epilepsy (Chang et al., 2019).

Funding

Coleen Roger has received a PhD grant from the Neuroschool, a support from the French government under the Programme Investissements d'Avenir, Initiative d'Excellence d'Aix-Marseille Université via A*Midex (AMX-19-IET-004) and ANR (ANR-17-EURE-0029) funding.

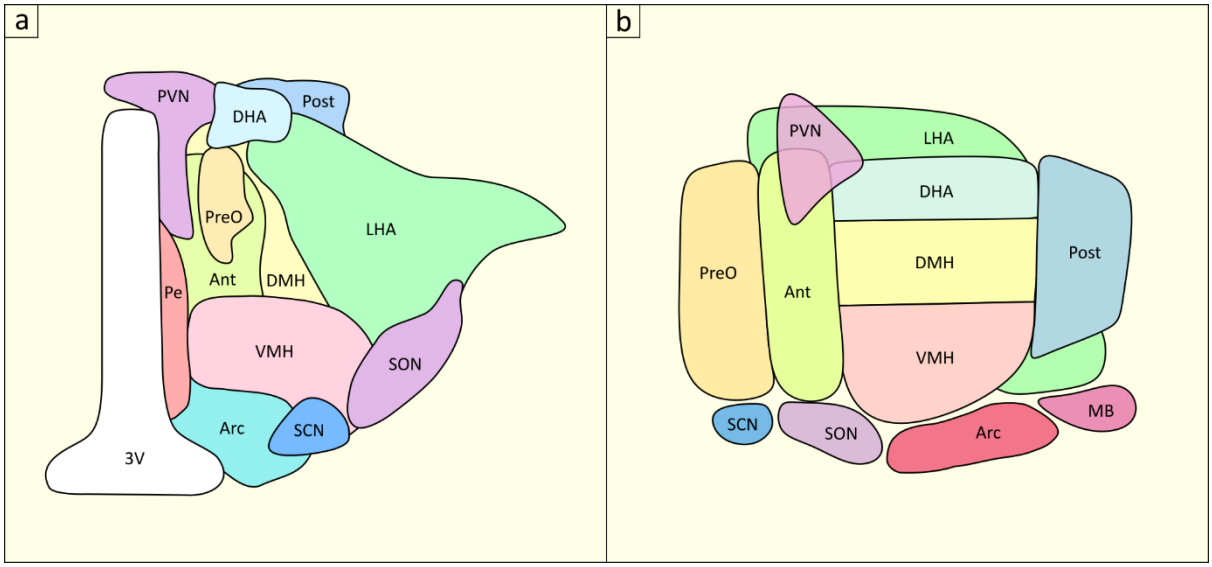

Figure 1: Structural organization of HT and its nuclei.

a) coronal slice of the hypothalamus, b) sagittal slice of the hypothalamus. Ant: anterior hypothalamus, Arc: arcuate nucleus, DHA: dorsal hypothalamic area, DMH: dorsomedial hypothalamus, LHA: lateral hypothalamic area, MB: mammillary body, Pe: periventricular nucleus, Post: posterior hypothalamic nucleus, PreO: preoptic nucleus, PVN: paraventricular nucleus, SCN: suprachiasmatic nucleus, SON: supraoptic nucleus, VMH: ventromedial hypothalamus, 3V: third ventricle. Based on ((*Atlas of the Human Hypothalamus - 1st Edition*, n.d.; Neudorfer et al., 2020a)).

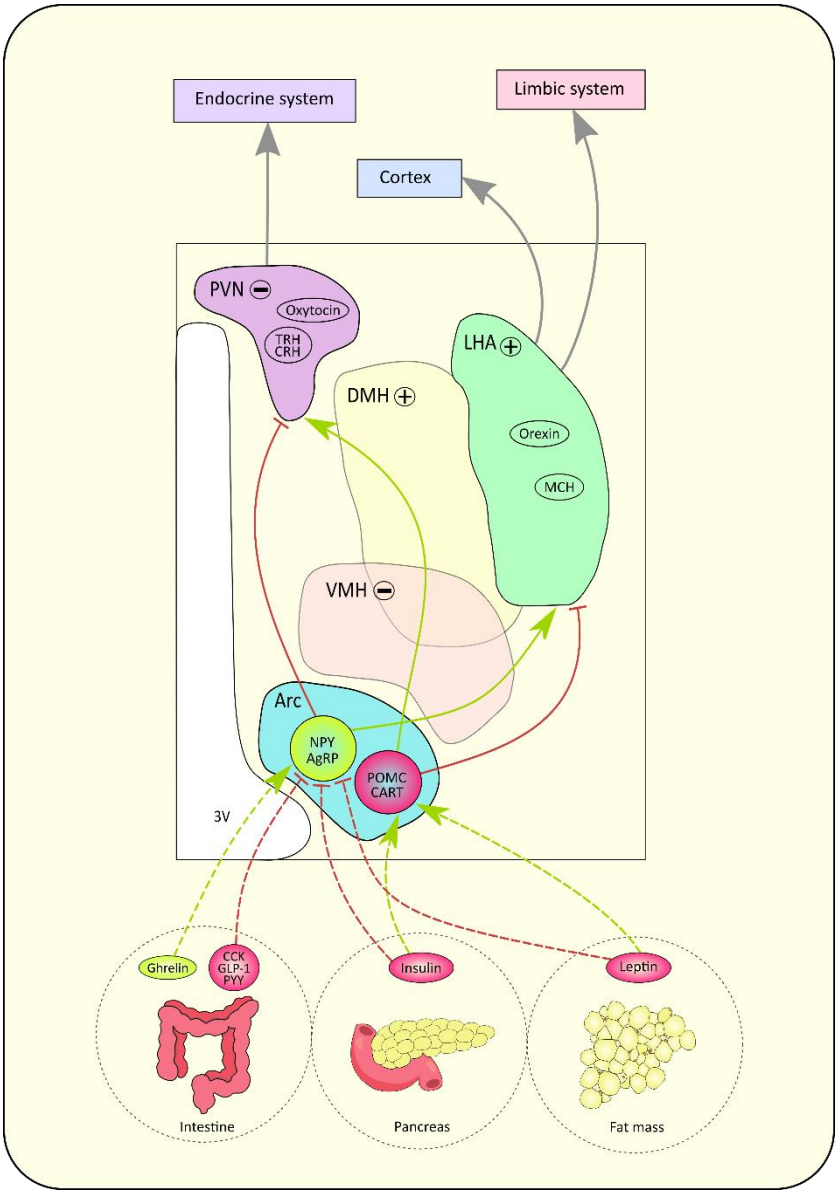

Figure 2: Schematic pathway of the lipostat and its peptidergic circuitry.

According to hunger state, hormones are released by the intestin, pancreas and fat mass. Those signals directly influence neuronal activity in the hypothalamus through their action on antagonistic neurons located in the arcuate nucleus (Arc): orexinergic neurons expressing neuropeptide Y (NPY)/ agouti-related peptide (AgRP) and anorexinergic neurons expressing pro-opio-mélanocortine (POMC)/ cocaine- and amphetamine-regulated transcript (CART).

Gut hormones such as cholecystokinin (CCK), peptide YY (PYY), glucagon-like peptide 1 (GLP-1) inhibit NPY/AgRP neurons while ghrelin stimulates NPY/AgRP neurons. The pancreas secretes insulin while leptin is secreted by fat mass cells. Both hormones trigger the inhibition of NPY/AgRP neurons but the stimulation of POMC/CART neurons. Red arrows represent inhibitory connections, green arrows represent stimulatory connections, grey connections represent indirect pathways. The '+' sign means the

nucleus has an orexinergic effect on food intake when activated, whereas the '-' sign indicates that the nucleus has an anorexinergic effect on food intake when activated. Indeed, when activated, the dorsomedial hypothalamus (DMH) and lateral hypothalamic area (LHA) have an orexinergic action while the ventromedial hypothalamus (VMH) and paraventricular nucleus (PVN) have an anorexinergic action on food intake. Finally, the PVN sends information to the endocrine system while the LHA carries input to the cortex and limbic systems (Berthoud, 2012b). 3V: third ventricle.

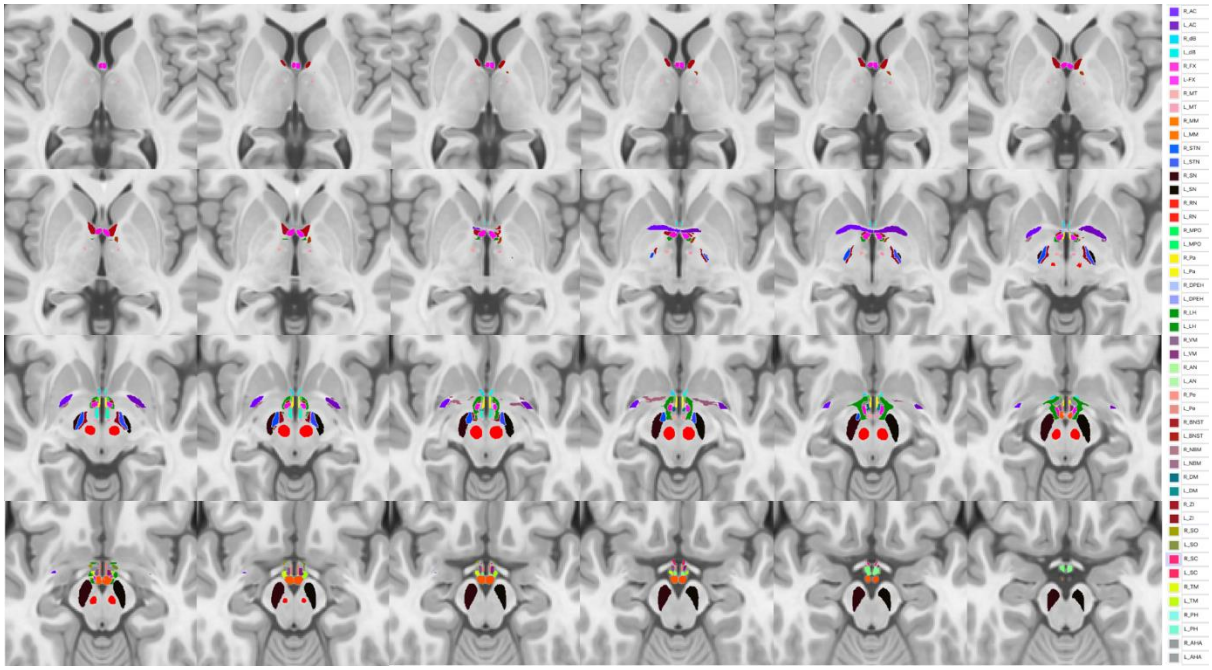

Figure 3: Projection of the Neudorfer hypothalamic atlas into a homemade 7T MP2RAGE Uni-Den template.

Ac: anterior commissure, AHA: anterior hypothalamic area, AN: arcuate nucleus, BNST: bed nucleus of stria terminalis, dB: diagonal band of Broca, DM: dorsomedial hypothalamic nucleus, DPEH: dorsal periventricular hypothalamus, FX: fornix, LH: lateral hypothalamus, MM: mammillary bodies, MPO: medial preoptic nucleus of the hypothalamus, MT: mammillothalamic tract, NBM: nucleus basalis of Meynert, Pa: paraventricular nucleus, Pe: periventricular nucleus, PH: posterior hypothalamus, RN: red nucleus, SC: suprachiasmatic nucleus, SN: substantia nigra, SO: supraoptic nucleus, STN: subthalamic nucleus, TM: tuberomammillary nucleus, VM: ventromedial nucleus, ZI: zona incerta.

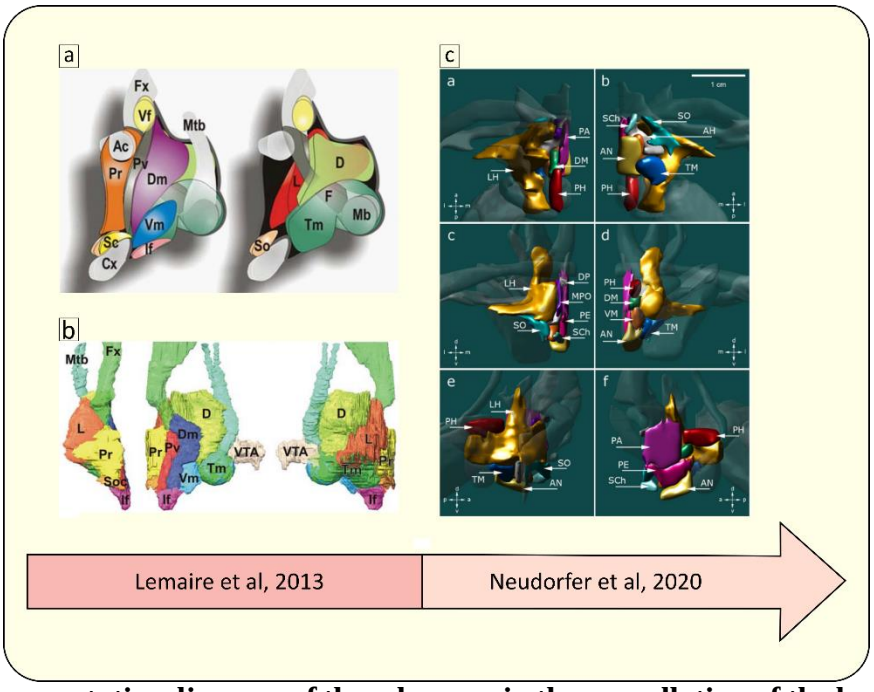

Figure 4: Representative diagram of the advances in the parcellation of the hypothalamus.

A. Schematic drawing of hypothalamic nuclei, lateral view from the midline. Left: nuclei directly located under the wall of the third ventricle, right: more deeply located nuclei up to the lateral region (Lemaire et al., 2013b). B. 3D overview of hypothalamic nuclei, constructed from a 3D high-field MRI data set. Left: frontal view, middle: lateral view, right: medial view. VTA: ventral tegmental area, Ac: anterior commissure, D: dorsal or posterior nucleus, Dm: dorsomedial nucleus, Fx: fornix, F: fornix nuclei, If: infundibular (arcuate) nucleus, L: lateral nucleus, Mb: mammillary body, Mtb: Fmillo-thalamic bundle, Cx: optic chiasma, Pv: paraventricular nucleus, Pr: preoptic nuclei, Sc: suprachiasmatic (ovoid) nucleus, Vf: ventricular foramen, So: supraoptic (tangential) nucleus, Tm: tuberomamillaris (mamilloinfundibularis) nucleus, Vm: ventromedial (tuber principal) nucleus (Lemaire et al., 2013b). C. 3D reconstruction of hypothalamic nuclei and their neuroanatomical relationships. (a) top view, (b) bottom view, (c) frontal view, (d) occipital view, (e) sagittal view depicting the outer surface of hypothalamic nuclei, (f) sagittal view depicting the inner surface of hypothalamic nuclei. AH: anterior hypothalamic area, AN: arcuate nucleus, DP: dorsal

periventricular nucleus, DM: dorsomedial hypothalamic nucleus, LH: lateral hypothalamus, MPO: medial preoptic nucleus, PA: paraventricular nucleus, PE: periventricular nucleus, PH: posterior hypothalamus, SCh: suprachiasmatic nucleus, SO: supraoptic nucleus, TM: tuberomammillary nucleus, VM: ventromedial nucleus (Neudorfer et al., 2020a).

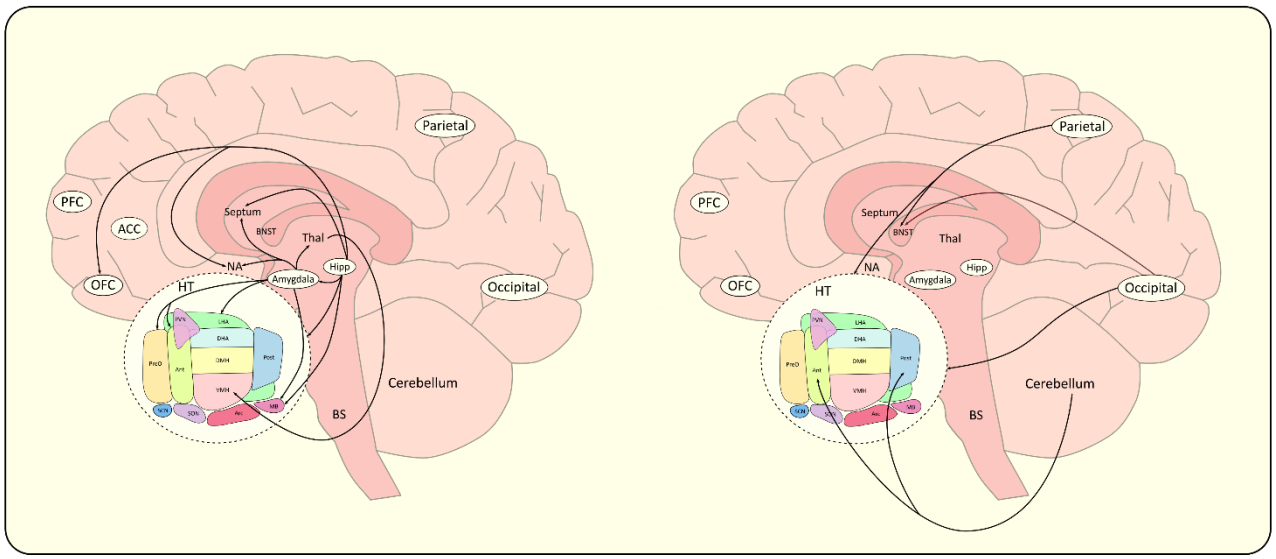

Figure 5: Schematic representations of extra-hypothalamic networks of food intake.

For clarity concern, extra-hypothalamic connections reported in the literature have been divided in an appetitive network (left) and a control network (right). ACC: anterior cingulate cortex, BNST: bed nucleus of the stria terminalis, BS: brain stem, Hipp: hippocampus, HT: hypothalamus, NA: nucleus accumbens, Parietal: parietal cortex, PFC: prefrontal cortex, Occipital: occipital cortex, OFC: orbitofrontal cortex, Thal: thalamus. The schematic sagittal slice of the hypothalamus (HT) includes, Ant: anterior hypothalamus, Arc: arcuate nucleus, DHA: dorsal hypothalamic area, DMH: dorsomedial hypothalamus, LHA: lateral hypothalamic area, MB: mammillary body, Pe: periventricular nucleus, Post: posterior hypothalamic nucleus, PreO: preoptic nucleus, PVN: paraventricular nucleus, SCN: suprachiasmatic nucleus, SON: supraoptic nucleus, VMH: ventromedial hypothalamus.

2.5.3 Concluding remarks

Neuroimaging techniques are invaluable tools for the precise *in vivo* study of brain structure and function. However, there is a significant lack of data focusing on the hypothalamic homeostatic control of food intake. In the future, neuroimaging could evolve into a powerful diagnostic tool to differentiate between various types of eating disorders by analyzing the distinct anomalies observed in MRI scans among individuals with anorexia Nervosa, obesity, and normal weight. Additionally, it may offer insights into tracking the remission process through neuroanatomical changes observed during weight recovery stages. The next section summarizes and updates the most recent developments and publications in the field.

Anatomical MRI characterization, parcellation and morphometry of HT

A new release of one High-resolution 3D Mapping of the Human Hypothalamus has been proposed to improve the precision of the parcellation of hypothalamic nuclei. Indeed, this new high-resolution cytoarchitectonic map of the human HT capture the shape and extent of the hypothalamic nuclei with cellular precision and will help to bridge the gap between microscopical level of organization of the HT with the macrolevel (provided in MR imaging). Both the high-resolution maps in the BigBrain and the probabilistic maps are part of the integrative framework of the Julich-Brain atlas and are available as a FAIR data via EBRAINS (Amunts et al., 2020; Mapping, 2024).

Anatomical Characterization of HT in Obesity and Anorexia Nervosa

Level of structural analyses of HT has gained in granularity. HT is now widely studied at the subregional level, rather than being viewed as a single, uniform structure. Accordingly, regional morphological alterations of HT partitions were reported in obesity and anorexia nervosa. For example, volumes of the left anterior-inferior, and the right posterior parts of HT were found to be increased in adults living with obesity relative to normal weight adults (Brown et al., 2023). Another study reported increased HT volume in young women with obesity and atrophy in the inferior-tubular subregion in patients with anorexia nervosa (Alzaid *et al.*, 2024). The same study also reported that structural alterations in specific HT regions were linked to changes in appetite-regulating hormone levels. Specifically, larger volumes in the posterior HT subregions correlated with elevated leptin levels in the obesity group, while ghrelin levels showed a negative association with overall HT volume across all participants (anorexia, obesity, and control groups).

Functional Connectivity of Hypothalamus

A recent study explored hypothalamic functional connectivity (FC) in response to high-calorie food images, focusing on the effects of hunger and body weight (Kullmann et al., 2023). They found that in the sated state, the HT exhibited stronger FC with brain regions related to reward, taste, and executive function compared to the fasted state. Notably, overweight individuals or living with obesity showed reduced HT FC with the right dorsolateral prefrontal cortex (DLPFC) when fasted. Higher FC between the HT and brain regions such as the caudate, insula, and inferior frontal cortex was observed in the sated state. An interaction between hunger state and BMI revealed that participants with normal weight had stronger HT-DLPFC FC in the

fasted condition compared to overweight individuals or living with obesity. The study suggests that hypothalamic connectivity is influenced by both hunger and palatability, with disrupted hypothalamic-DLPFC communication in individuals with obesity potentially promoting overeating.
Using rs-fMRI, another study uncovered a new pathway from the medial prefrontal cortex (mPFC) to the lateral hypothalamus (LH) (Clarke et al., 2023). The same study further explored the physiological function of this glutamatergic pathway, revealing that it is activated during acute stress and is suppressed during eating. Inhibition of this circuit resulted in increased feeding and sucrose-seeking behavior under mild stress but not under non-stressful conditions, while its activation is sufficient to suppress food intake and sucrose seeking in mice. Therefore, the mPFC-LH seems to be a stress-sensitive anorexigenic pathway involved in food regulation and motivation.

Task Related fMRI of Eating Disorders and Hypothalamus

A recent study found a significant effect of Appetitive state (premeal vs postmeal) in BOLD activation to high-calorie foods versus objects characterized by hyperactivation of the right hypothalamus, right amygdala, bilateral nucleus accumbens, and right caudate in individuals with anorexia nervosa and healthy controls (Eddy et al., 2022).

Another study examining the hypothalamic activity in response to forced choice between Food versus rewarding non-Food stimuli (Money) reported hypoactivation of the PaVN and LH (Ogawa et al., 2022). Furthermore, dynamic causal modeling showed unidirectional connections from the PaVN the midbrain and ventromedial prefrontal cortex. This finding suggests the presence of a dual HT pathway from the PaVN to reward-related, involved in regulating reward evaluation for decision making.

Synthesis

A precise in vivo assessment of the specific anatomo-functional roles of hypothalamic (HT) nuclei in humans is crucial for translating molecular insights from in vitro studies into a deeper understanding of weight-related disorders. Advances in spatial and temporal resolution achieved with in vivo UHF MRI now appear sufficiently mature to bridge the gap between the cellular scale (e.g., lightsheet microscopy) and the mesoscopic scale in preclinical MR imaging of rodents. This progress allows a shift from viewing the hypothalamus (HT) as a homogeneous structure to a robust parcellation of individual HT nuclei in humans using 7T MRI, which I aimed to accomplish in my PhD work and is detailed in the following chapters.

3 Hypotheses and Objectives

My PhD work aimed at characterizing the neural network of eating behaviors using a translational approach, both in vivo and in vitro in mice, and in vivo in humans. The objectives of my thesis were dual but complementary and correspond to the two internships conducted in Singapore and Marseille.

The first objective was to better understand at the mesoscale the role of the hypothalamic tuberal nucleus (TN) in feeding processes. Previous studies conducted by Yu Fu's Lab uncovered a new circuit mechanism for feeding regulation involving orexigenic ^{TN}SST neurons. Using a paradigm called the 'contextual feeding conditioning' (CFC) (Mohammad et al., 2021; Stern et al., 2020), a model of cue-driven food overconsumption, they found that ^{TN}SST neurons showed preferential response to palatable food and are involved in the non-homeostatic food intake. Nevertheless, the connectivity of this newly described hypothalamic nucleus and its modulation in CFC was not fully characterized yet.

Therefore, I established from the ground up the MRI standard operating protocol for the in-vivo and ex-vivo acquisitions, combined with precise pre- and post-processing. My objective for this preclinical work was to characterize the structural and functional connectomes of TN in the CFC model.
To do so, I first studied the in-vivo functional connectivity using resting-state fMRI data acquired on a preclinical 11.7T MRI scanner. Then, I investigated the ex-vivo structural connectivity using DTI data acquired on a preclinical 9.4T MRI scanner.
Concurrently, my colleagues have implemented the VITALISTIC (viral tracing assisted by light sheet and tissue clearing) pipeline to investigate the brain-wide input changes of ^{TN}SST neurons.
Combining MRI and viral tracing-based methods is an attempt at proving a more comprehensive and reliable method to investigate potential neural circuit mechanisms that drive a specific conditioned behavior.

My hypothesis was that CFC increases brain connectivity and specifically affects the TN connectivity with brain regions involved in olfaction, reward and memory.

The second objective of my PhD work was to determine if the morpho-functional characterization of individual hypothalamic nuclei could also be addressed in vivo in humans. Translation from rodent to human required first to optimize MRI protocol at 7T. We also set up on clinical trial at CEMEREM in collaboration with the department of endocrinology (APHM Marseille) with the support of the A*STAR (Singapore) and optimize the post-processing pipeline. The main objectives were to evaluate the ability of 7T MRI to characterize the morpho-functional variations of individual HT nuclei in young women with anorexia nervosa and young women living with obesity relative to young women with normal weight.
We aimed at providing with an unprecedented precision, an *in vivo* and non-invasive mapping of the microstructure, connectivity and functional organization of individual hypothalamic

nuclei involved in food intake networks and their modulations in weight-related disorders in humans. To achieve this, we used Ultra-Hight Field (UHF) MRI (≥7T).

We first investigated the morpho-structural variations of HT nuclei and their association to BMI, hormone levels and behavioral scores using high resolution quantitative 3D-T_1 MRI in well-characterized cohorts of young women living with obesity (OB) or restrictive anorexia nervosa (AN) or healthy control with normal-weight (HC).

The hypothesis was that the volume and/or T1 signal of the global HT, as well as specific food-related HT nuclei, might be altered in OB and AN relative to HC.

In the same cohort, we then studied the functional alterations of brain regions involved in food intake network, including HT nuclei. To do so, we have investigated their activation patterns in response to a food-cue reactivity paradigm during a fasting period using very high spatial/temporal resolution BOLD fMRI. Using this paradigm, we have also studied the impact of environmental context related to food on brain activity. Both static and dynamic FC variations of HT nuclei, and their association to BMI and behavioral scores were also assessed using resting-state fMRI through network-based analysis (NBS), graph theory metrics as well as typical dynamic FC.

We hypothesized that OB would exhibit decreased activation of the control network and increased activation of the reward network, whereas AN might show decreased activation of the reward system and increased activation of the emotional system. Regarding the HT nuclei, we speculated that the improved spatial and temporal resolution of images acquired at 7T would allow us to visualize activations of different hypothalamic nuclei in response to the food cue presented, as well as show altered connectivity with the reward system and cognitive control networks in AN and OB.

4 Structural and Functional study of the hypothalamic tuberal nucleus in mice using high-resolution MRI and its modulation in a model of cue-triggered food consumption, contextual feeding conditioning (CFC), in mice

4.1 Foreword

The context of this work is to enhance the understanding of the tuberal nucleus (TN), an understudied brain region, and its role in appetite regulation. Luo and colleagues from Fu Yu's lab recently discovered a new mechanism of feeding regulation which operates through orexigenic GABAergic tuberal neurons expressing somatostatin (^{TN}SST). This new discovery provides a new perspective for understanding appetite changes (Luo et al., 2018). ^{TN}SST neurons are activated by hunger and by the hunger-regulating hormone ghrelin (**Figure 17**). Activation of ^{TN}SST neurons promotes feeding, whereas inhibition reduces it through projections to the PaVN and BNST. Ablation of TNSST neurons reduced body weight gain and food intake.

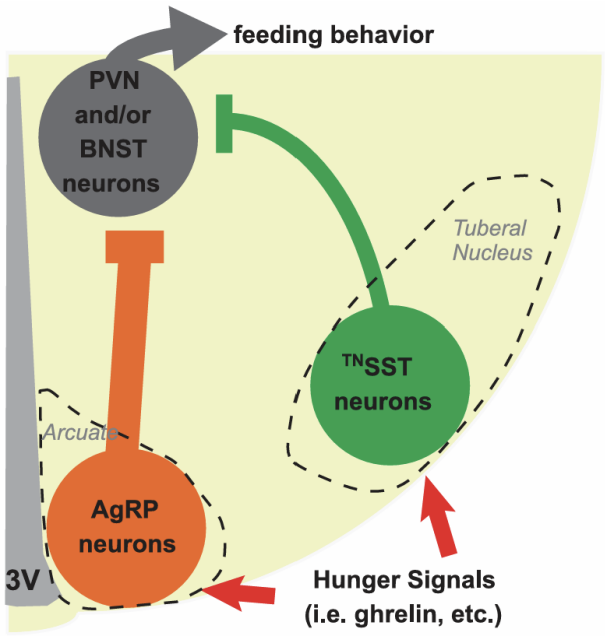

Figure 17 : ^{TN}SSTneurons in the mouse can be activated by hunger signals, including ghrelin.
Activation of ^{TN}SST neurons stimulates feeding through inhibiting downstream neurons in the PVN and BNST, a mechanism similar to the activation of AgRP neurons in the arcuate area (Luo et al., 2018).

The objective of the first part of my PhD work was to demonstrate that such mechanisms observed at the cellular level, using chemogenetics and viral tools to label and manipulate specific neural circuits for functional probing, can also be associated to mesoscopic observations obtained from in vivo ultra-high field MR imaging. This should help bridge the gap across different scales, enabling the characterization of brain networks in living animals.
In this context, our goal was to combine viral-based whole-brain neural circuit mapping with MRI to investigate potential neural circuit mechanisms underlying contextual feeding conditioning, to gain a more comprehensive understanding of the neural processes involved.
In this large-scale project, my first mission was to set up from ground up the fMRI (**Figure 18**) and DTI (**Figure 19**) protocol and processing pipeline to enable the definition of the structural and functional connectome of the TN in mice. To address this, I have created a tailored brain atlas that includes all hypothalamic nuclei and other relevant brain regions, ensuring compatibility with MRI studies in terms of spatial precision of parcels and adequate signal-to-noise ratio for reliable MR imaging. I have then extracted the functional and structural connectomes of the TN derived from MRI data in control and conditioned mice, to enable their comparisons and investigate their association to cellular connectomes derived from VITALISTIC (viral tracing assisted by light sheet and tissue clearing) obtained by colleagues.

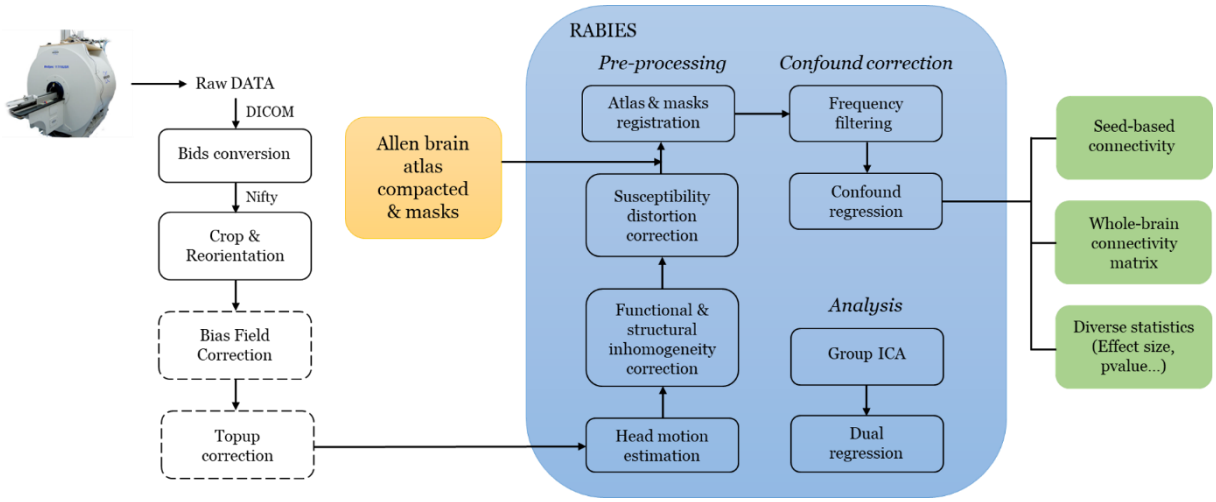

Figure 18 : Full resting-state pipeline.

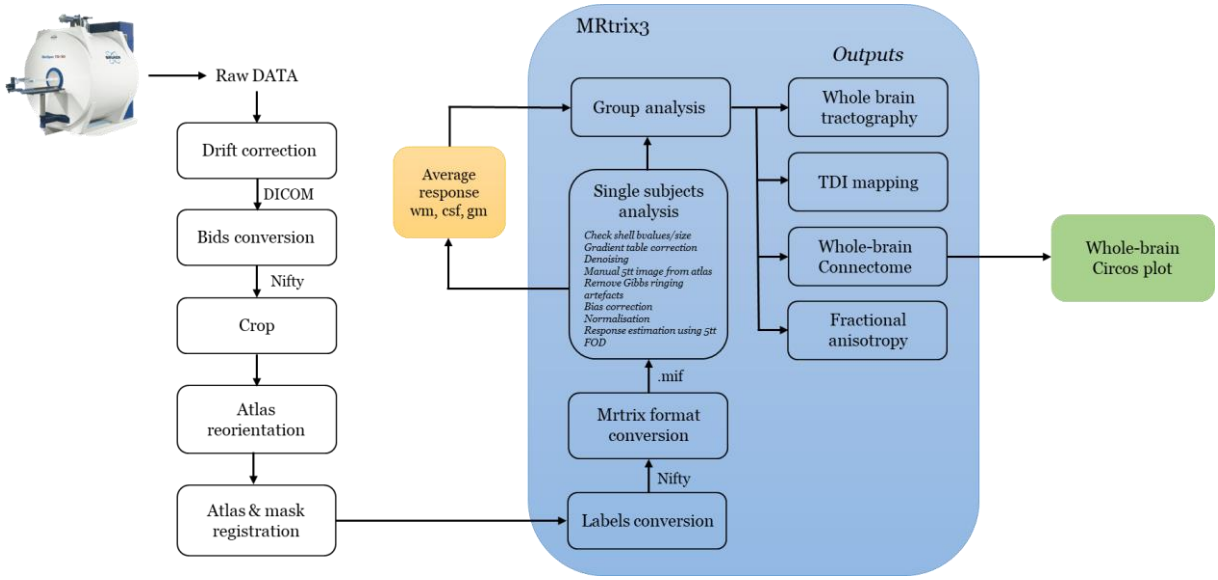

Figure 19 : Full DTI pipeline.

4.2 Animal model

All experimental procedures involving use of animals were approved by the Institutional Animal Care and Use Committee of the Agency for Science, Technology and Research (A*STAR) of Singapore. Animals were housed in a standard 12-hour light-dark cycle with access ad libitum to water and standard mouse chow (Teclab Global 18% protein rodent diet). For the fMRI acquisition, 29 male wildtype C57BL/6J mice (purchased from Jackson Laboratories) between 4 and 8 months were used in this study. The control mice had *ad libitum* access to water and standard mouse chow, weighted 30.7±2.7 g at the date of scan. The obese mice aged 8 to 10 weeks were placed on HFD (60% fat) for 3 to 6 months and were 49±9.5 g at the time of the scan.

4.2.1 Anaesthesia and animal preparation

The mouse was initially anesthetized in a chamber with 3-4% isoflurane in 0.5L/min air and oxygen (ratio 1:1). When the animal did not show reaction to the pinch test, the mouse was securely installed to an intubation stand, and isoflurane was reduced to 3% to avoid overdose. First, a gavage needle coated with 2% lidocaine gel (Pifzer, United States) was inserted, to prevent laryngospasm. An endotracheal PE tube (Scientific Commodities, Inc. Catalog #BB31695-PE/3, 0.023" I.D x 0.039" O.D, cut to length of 30mm) was then inserted for artificial ventilation using a guide wire (Rivera et al., 2005). The mouse was then connected to the ventilator set up at 90 bpm in pressure mode, with air/oxygen (2% isoflurane), flow at 500 ml/min and a pressure of 18 cm H_2O; if intubation is successful the abdominal breathing should synchronize with the ventilator. After performing a pinch test to ensure the mouse is fully anesthetized, the mouse was transferred to the MR cradle and connected to the ventilator set up at 90 bpm in pressure mode, air/oxygen (ratio 8:2; and 2% isoflurane), flow at 1000 ml/min, pressure of 18 cm H_2O. After flushing the infusion line (Scientific Commodities, Inc. Catalog #BB31695-PE/1, 0.011" I.D x 0.025" O.D.) and calibrating the pump (<3% standard error), the 30G needle of the infusion line was inserted subcutaneously to flank of the mouse.
Following the anesthetic regimen, a bolus of 0.05 mg/kg Medetomidine (Domitor, medetomidine hydrochloride; Pfizer Pharmaceuticals, Sandwich, UK) and 0.10 mg/kg Pancuronium (Sigma-Aldrich, Steinheim, Germany) was delivered, and 5 min later, isoflurane was reduced and maintained at 0.5%. The bolus was followed 10 min later by an infusion of 0.10 mg/kg/h Medetomidine, 0.20 mg/kg/h Pancuronium. The infusion was stopped, and isoflurane increased to 2% at the end of the resting state and top up sequences. **Figure 20** summarizes the timeline of anaesthesia during the scan.

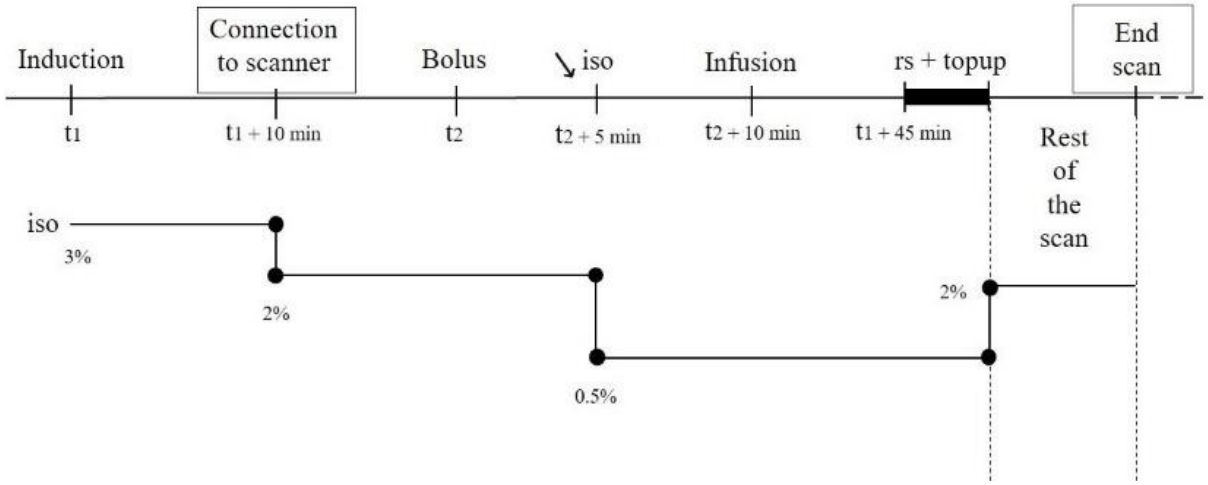

Figure 20: Timeline of anaesthesia during the scan.

4.2.2 Monitoring of animal physiology

Inside the cradle, the head of the animal was securely attached by ear bars and the teeth hooked on the tooth loop. A respiratory pillow recording heart rate in bpm (I4SA, SAII Gating and Monitoring Systems for Small Animals, United States) was installed under the abdomen of the mouse and an oximeter sensor measuring O2 saturation PhysioSuite® for Mice & Rats, Kent Scientific, United State) was clipped on the animal left hind paw. The rectal temperature probe was coated with Vaseline before insertion into the mouse. To keep the animal at a constant temperature of 36.5±0.5 °C, a heating tube (SAII, United States) is placed near the animal, aligned to the opening of the cradle. Ophthalmic ointment was applied on the mouse's eyes and the cradle was placed into the bore. The temperature, heart rate and SpO2 were monitored closely during the whole scan. Under anesthesia, the mouse's heart rate should lie between 200-400 bpm, with most mice with a heart rate of 300 bpm during scan. If the heart rate exceeds 400 bpm, it suggests the mouse is not sufficiently sedated.

4.2.3 Recovery after scan

Upon completion of imaging, the mouse was removed from the MR cradle and placed on a heating pad set at 38˚C. It was then reconnected to a ventilator set at 90 bpm in pressure mode, with a 1:1 air/oxygen ratio and 0.5% isoflurane. At this stage, the mouse should be unresponsive to the pinch test (**Figure 21 Phase 1**). Gradually, the mouse would regain its pinch reflex. The endotracheal tube was occasionally disconnected from the ventilator to check if the mouse could regain muscle activity and breathe independently (**Figure 21 Phase 2**). Once the mouse demonstrated the ability to breathe independently for an extended period without gasping, with an increased respiration rate and maintained high SpO2, an injection of 0.05 mg/ml Atipamezole was administered subcutaneously (**Figure 21 Phase 3**). Following this, the mouse would typically show a righting reflex. The mouse was then supervised for an additional 5 minutes before being returned to its cage. The entire recovery process typically lasts about 2 hours.

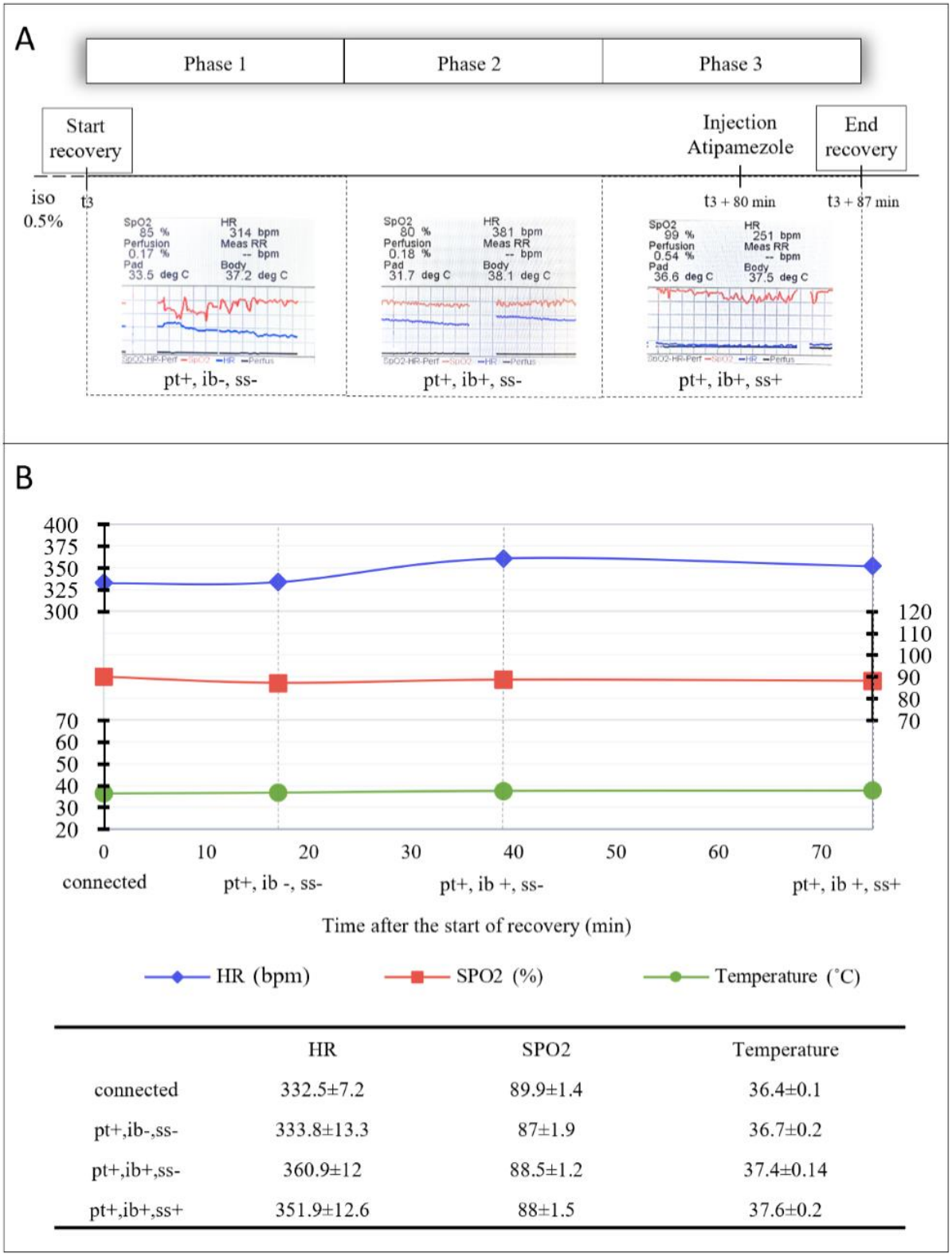

	HR	SPO2	Temperature
connected	332.5±7.2	89.9±1.4	36.4±0.1
pt+,ib-,ss-	333.8±13.3	87±1.9	36.7±0.2
pt+,ib+,ss-	360.9±12	88.5±1.2	37.4±0.14
pt+,ib+,ss+	351.9±12.6	88±1.5	37.6±0.2

Figure 21: Timeline (A) and physiological monitoring (B) of recovery.
pt= pinch test, ib= independent breathing, ss= sustained breathing, += positive check, -= negative check.

4.3 Adaptation of a mouse Atlas for MRI studies

With the development of ultra-high-field (UHF) preclinical MRI (11.7 T), the investigation of small brain regions is now possible. Therefore, we needed a mouse atlas matching the granularity of individual hypothalamic nuclei as well as regions with size compatible with sufficient signal/noise ratio at 11.7T. Several atlases could have served as a starting point:

1) The DSURQUE atlas is a bilateral mouse atlas compatible with MRI studies (356 labels, 40 µm) (http://repo.mouseimaging.ca/repo/DSURQE_40micron_nifti/). However, it lacks sufficient granularity for our study and does not include HT division at the nuclei level.
2) The Allen Brain Atlas (ABA) mouse brain connectome is one of the most comprehensive attempts to map mouse brain connectivity and includes data from nearly 500 unique anterograde viral neuronal tracer injections in the wild-type C57BL/ 6 mouse brain (Q. Wang et al., 2020). However, the ABA is way too granular (10 µm isotropic resolution) to be appropriate for MRI studies (130 µm for 11.7 T). Nevertheless, its precision makes it suitable for tailoring.

Therefore, I have created a compacted version of the ABA in which smaller regions are condensed with other nearby regions with the same function/ structural identity (**Figure 22**). For example, all the different layers of the primary motor area are compacted in one unique label called 'primary motor area'. Furthermore, we have created a bilateral version of ABA by splitting labels along the midline to generate separate label sets for the left and right hemispheres of the brain. To achieve this, we created a homemade python script following multiple steps: (i) Registration of the DSURQUE atlas to ABA (Allen2DSURQUE), (ii) Inversion of the registration to get DSURQUE2Allen, (iii) Apply transform to DSURQUE labels.

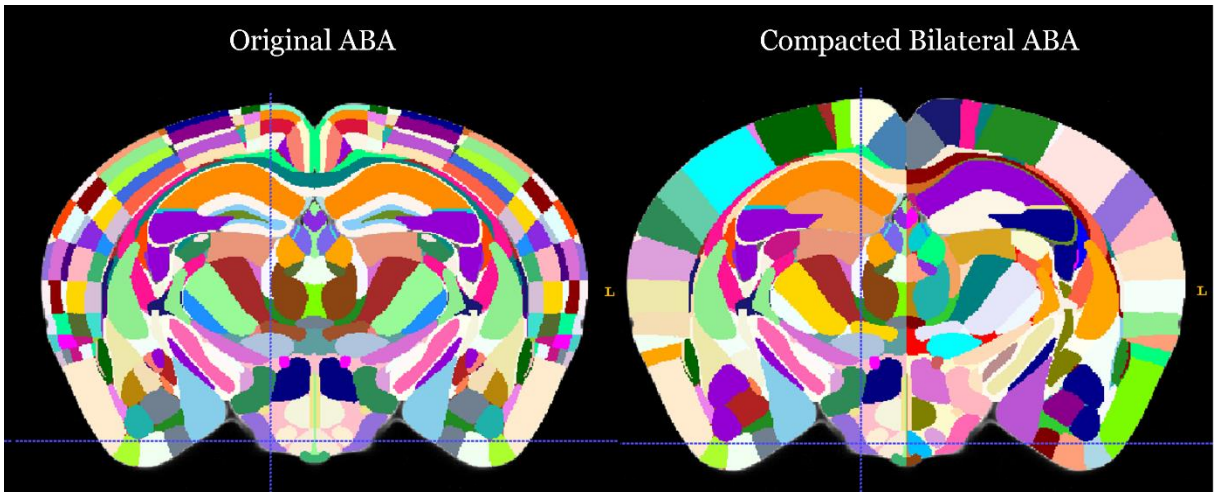

Figure 22: Comparison of the original and compacted bilateral Allen Brain Atlases.

I also used compacted WM labels to create the WM mask and the ABA atlas to create a brain mask (**Figure 23**). I used the vascular mask from the DSURQE atlas and registered it to ABA using linear registration (flirt).

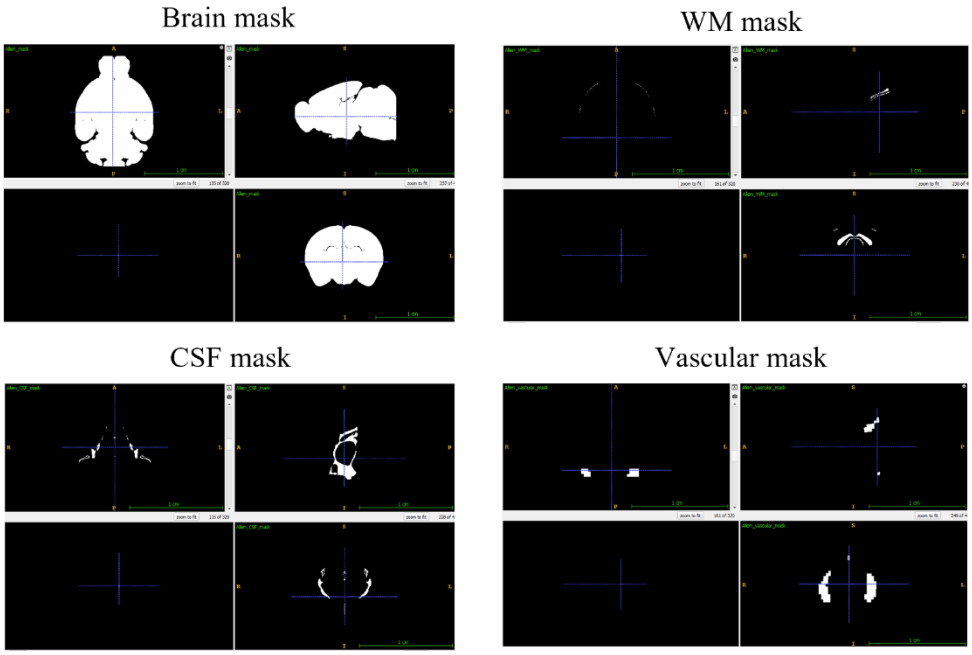

Figure 23: Masks of the different mouse tissue types used in the resting stare data preprocessing.

At this stage, I have designed a tailored MRI atlas and template of the mouse brain with parcel precisions that are compatible with the characterization of HT nuclei, as well as cortical and subcortical regions to build accurate functional and structural connectomes derived from rs-fMRI and Diffusion weighted MRI.

4.4 Resting-state fMRI

4.4.1 MRI Set up

MRI experiments were conducted using a 11.7 T Bruker Biospec scanner (117/16 Ultra Shielded Refrigerated (USR) system) with a 15.5 cm horizontal bore running Paravision 6.0.1, equipped with a radiofrequency coil setup of 72mm ^{1}H volume coil and Cryocoil Sweep width: 10.000 MHz. Anatomical images were acquired with a TurboRARE-T2w sequence. Functional resting state data were acquired for 16 minutes, using a GE-EPI sequence: resolution (mm^3)= 0.130 × 0.130 × 0.500, field of view (FOV) = 22 × 22 mm2, repetition time (TR) = 1125 ms, echo time (TE) = 15 ms, average=8, flip angle (FA)= 30˚ (**Figure 24**).

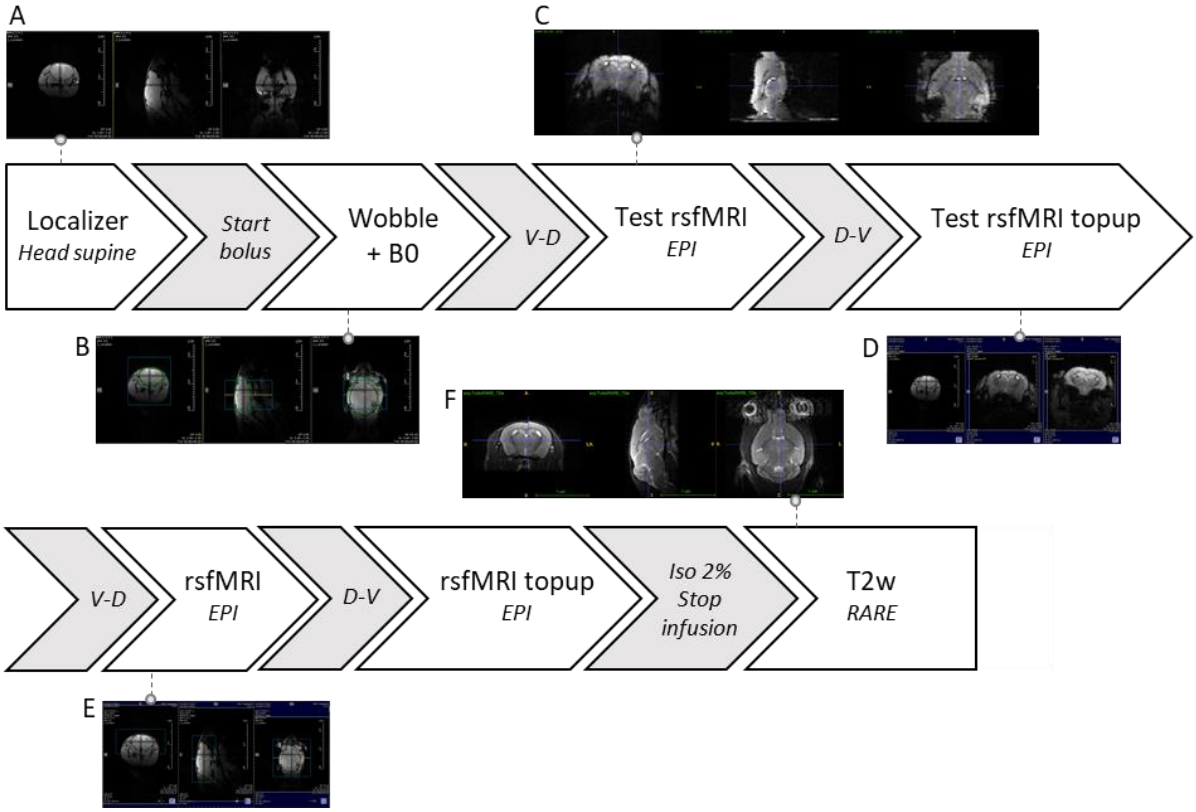

Figure 24: Scan timeline.

4.4.2 Analysis

4.4.2.1 Data processing

Scans were converted from DICOM to NIfTI and organized according to the Brain Imaging Data Structure (BIDS) format (Gorgolewski et al., 2016) with an homemade python script using dcm2niix (https://github.com/rordenlab/dcm2niix), bidskit (https://github.com/jmtyszka/bidskit), bids validator (https://github.com/bids-standard/bids-validator) and numpy (https://numpy.org/).
Subsequently, data was reoriented using an homemade linux script requiring AFNI (https://afni.nimh.nih.gov/pub/dist/doc/htmldoc/background_install/install_instructs/steps_linux_ubuntu18.html).

4.4.2.2 Preprocessing

Rodent Automated Bold Improvement of EPI Sequences (RABIES; publicly available to the community https://github.com/CoBrALab/ RABIES), is a new pipeline that has been developed for preprocessing, confound correction, and analysis, tailored for rodent neuroimaging. RABIES integrates the latest computational framework and has already been successfully applied in recent publications (Grandjean et al., 2022, 2023).
Pre-processing was performed on a high-performance computing cluster (HPC Fujitsu, Intel 8268 48-Cores @ 2.9 GHz Nvidia V-100) using RABIES 0.4.6 (Desrosiers-Gregoire et al., 2022) by applying autobox (Cox, 1996), motion correction, a non-linear registration between functional and anatomical scans (B. Avants et al., 2009) and between anatomical scan and template, as well as a common space resampling (**Figure 25**). Autobox automatically crops out extra tissue, which was helpful since the intensity of tissue outside the brain was provoking registration failures.
Anatomical and bold images were subjected to intensity inhomogeneities twice, which correct for non-uniformities in the magnetic field that can lead to signal variations across the brain.
Structural images were registered together by generating an unbiased data-driven template, which is then registered to ABA to provide both an anatomical segmentation and a common space.
Motion artefacts during fMRI acquisition were estimated by registering each raw 4D EPI images to a volumetric 3D EPI target reference image with a rigid registration using ANTs' antsMotionCorr algorithm (B. Avants et al., 2009).
The EPI images were registered non-linearly to their associated anatomical image and corrected for susceptibility distortions (S. Wang et al., 2017). The preprocessed bold timeseries are concatenated into common space and resampled to ABA. The atlas was registered using RABIES scale-independent registration algorithm, wrapped around antsRegistration (B. Avants et al., 2009), which automatically adapts parameters to species-specific physical dimensions (affine, SyN) (Desrosiers-Gregoire et al., 2022). summarizes the different steps of the preprocessing pipeline, from inhomogeneity correction to the registration of the Atlas.

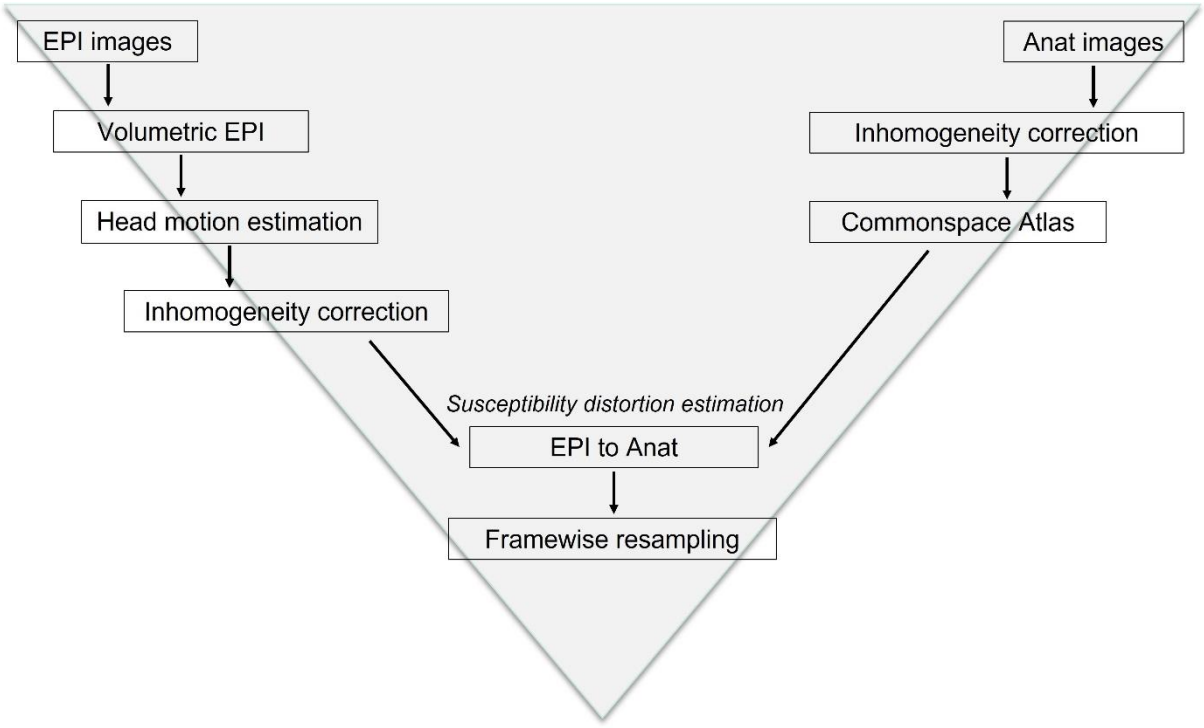

Figure 25: Preprocessing steps used in Rabies pipeline.

4.4.2.3 Preprocessing quality control

The quality of the preprocessing was visually inspected using the automated Quality Control report provided by RABIES.

The inhomogeneity correction was assessed for every single subject and the masking was deemed successful and the intensity homogenate (**Figure 26A-B**). Indeed, performing the inhomogeneity correction twice, which uses dataset-specific template, improved the robustness of masking.

The non-linear alignment of the anatomical images with their respective EPI images was validated after thorough inspection (**Figure 26C**).

The registration of the inhomogeneity-corrected anatomical scan to the dataset-generated unbiased average (**Figure 26D**), as well as the registration of the unbiased average template and the ABA were validated (**Figure 26E**).

The provided ABA and its different masks were visually checked to ensure that the proper template files were used during preprocessing (**Figure 26F**).

Temporal features diagnosis demonstrated that the scan was uncorrupted (**Figure 26G**). The 6 translation and rotation head motion parameters tracking the head position across scan duration, as well as the framewise displacement, which quantifies the timing and amplitude of spontaneous motion, were very small. In addition, the spatial map of the signal variability at each voxel (STD) was small and the temporal signal-to-noise ratio (tSNR) was appropriately high.

The connectivity of some well-known connected brain regions was checked. Following Grandjean and colleagues' suggestions (Grandjean et al., 2020, 2023), we looked at indexes of accurate FC identification. The first criterion was the strong connectivity between inter-hemispheric sensory cortices (barrel field, S1bf). Indeed, sensory–motor networks, both in humans and animals, have a bilateral homotopic organization (Biswal et al., 1995b). Our data shows a positive correlation between the barrel field (S1bf) left and right (r= 0.25), which validates the first criterion.

The second criterion was a weak or anti-correlation between S1bf and the anterior cingulate area (ACA). Indeed, task-positive (S1bf) and task-negative network (ACA) are generally non-correlated or anti-correlated (Fox et al., 2005). Our data shows a correlation inferior to 0.1 (r=0.09) between the barrel field S1bf and the ACA, which validates the second criterion.

The absence of outliers was validated by calculating the mean correlation coefficient of the 25 subjects. The mean correlation coefficient of the control and treatment showed similar standard error (SE control= 0.0047 vs SE treatment= 0.0050), with a higher mean for the treatment group.

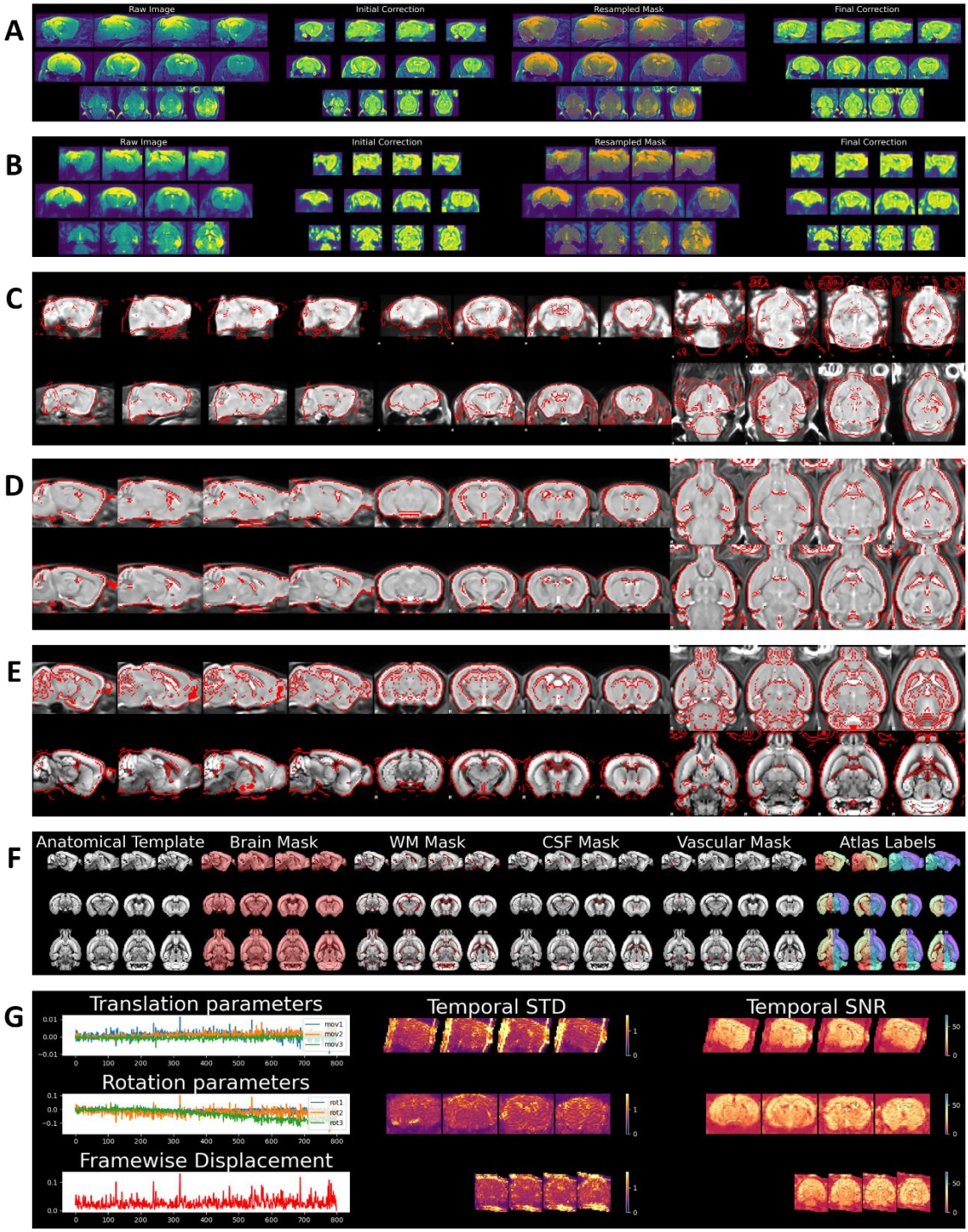

Figure 26 : Automatically generated outputs for preprocessing quality control from one CFC subject preprocessed with RABIES.

A)Masking of the anatomical scan for inhomogeneity correction. The four columns show 1) the raw image before correction, 2) the image after an initial correction prior to registration, 3) the mask brain mask obtained for the final correction and 4) the final inhomogeneity correction. The sagittal, coronal and transverse slices are shown from top to bottom for each column. B) Same as A), but for the EPI image. C) Alignment of the EPI image to its associated anatomical image of the same scanning session. D) Quality control for the registration of the inhomogeneity-corrected anatomical scan (top row) to the dataset-generated unbiased average (bottom row). E) Same as D), but for the unbiased average template (top) and the ABA (bottom). F) overlap of the ABA with it's associated masks and labels. The G) Temporal features including (left to right), 1) timecourse of the 6 head motion realignment parameters and framewise displacement, 2) spatial map of the signal variability at each voxel (STD), 3) temporal signal-to-noise ratio (tSNR).

4.4.2.4 Confound correction

Frequency filtering (highpass, lowpass) was applied using a 3rd-order Butterworth filter where 30 seconds are removed at each edge of the timeseries to account for edge artefacts following filtering. Remaining confound effects were eliminated using ordinary least squares (OLS) linear regression of the nuisance regressors (CSF signal, WM signal) onto the BOLD timeseries. ICA AROMA (Pruim et al., 2015), a well-used motion-detection algorithm in the human fMRI literature was not used during the confound correction. AROMA is not deterministic and introduced inhomogeneity in the results and was not necessary since the present data is absent of any significant head motion (4.4.2.3).

4.4.2.5 Statistical analysis of functional connectivity

Statistical analyses were conducted using MATLAB (Mathworks, Natick, MA) on a high-performance computer (HPC). The matlab function 'ffpermutationtest' was used to produce p-value using Fisher-Pitman permutation test of independent values.
Seed based analysis at the ROI level was computed using two-sample t-test which tests the null hypothesis that the data in vectors x and y comes from independent random samples from normal distributions with equal means and equal but unknown variances, as well as one-sample t-test which tests the null hypothesis that the sample data comes from a normal population with mean equal to zero and unknown variance. MRIcroGL software was used to create the exploded brain figures.

4.5 Ex-vivo DTI MRI

4.5.1 Transcardial perfusion and brain preparation

A solution of Xylazine/Ketamine solution (0.1 mL/ 10 g) was given intraperitoneally to the animal. After full surgical plane of anaesthesia was reached, the animal was secured over a downdraft table, the chest cavity was opened to expose the heart, and a 25G needle connected to a pump (Ecoline/Ismatec), was inserted into the left ventricle. After the right atrium was pierced, an intracardial perfusion with Phosphate Buffered Saline solution (PBS, 40ml) was delivered, followed by 40mL of 4% paraformaldehyde in PBS with gadolinium (6.5% (v/v), Magnevist®, Bayer), an injectable contrast medium for magnetic resonance imaging, known to enhances signal in T1 weighted images. After the perfusion, the skull was dissected out for ex-vivo MR scan. The skull was then placed in a 50mL falcon tube filled with 4% PFA (at least 10 x volume of the tissue) and kept at 4°C for 24h. The skull was then washed with PBS and incubated in 100mL of PBS and kept 4°C on an orbital shaker for 72h. The skull was then placed in a 10mL BD plastic syringe and covered with 3M™ Fluorinert™ Electronic Liquid FC-40. Bubbles were removed and the syringe was sealed with a blue tack (Bostic, Australia). Data were acquired with the brain inside the skull to reduce the structural deformation associated with death and fixation (Aggarwal et al., 2009; Calabrese et al., 2015).

4.5.2 MRI Setup

Acquisitions were conducted on a 9.4 T magnet (BioSpec 94/30) equipped with a 40mm volume coil and using ParaVision 6.0.1.
Since injecting Gadolinium causes reduction in tissue T1 and T2 relaxation times, the experiment design was optimized. Relaxation times were minimized by having a low flip angle, long TR (T1 min= 400 ms) and a short TE (T2* min= 24 ms).
Brains stained with 6.5% Gadolinium were scanned for 53 hours. DTI was acquired with 3D single spin-echo echo magnetic resonance imaging sequence which removes greatly the risk of susceptibility distortion (frequency encode nose-tail direction, isotropic resolution= 0.250 mm^3, flip angle= 90 degrees, TR/TE= 400/16.897 ms, average= 1, SliceThickness= 0.25). Diffusion-weighting was applied in 60 directions per bvalue (hemispheric direction diffusion) with 2 b-values of 1000 and 2000 s/mm^2. 5 B0 images were acquired at the beginning of scan.
Quantitative T1 RARE (T1 estimation: 200 ms, Variable TR), and T2 Multi Slice Multi Echo (fixed TR) were acquired.

4.5.3 Analysis

4.5.3.1 *Data preparation*

Since data acquisition took several days, due to imperfections and heating of the scanner, the images were subject to "drift" slightly with time. Therefore, Drift correction was performed post-acquisition to minimize artifacts and align images, ensuring data consistency and accuracy. DICOM data was then converted to nifty images in bids format, before cropping the brain.
The ABA atlas was rotated to match the orientation of DTI data before an optimized 3 steps registration was performed. First, the atlas was aligned to DTI using FLIRT; then, ANTs SyN

registration was performed using FLIRT transform as the initial starting point; finally, ANTs transform was applied to the atlas mask and label files (B. B. Avants et al., 2011) (**Figure 27**).

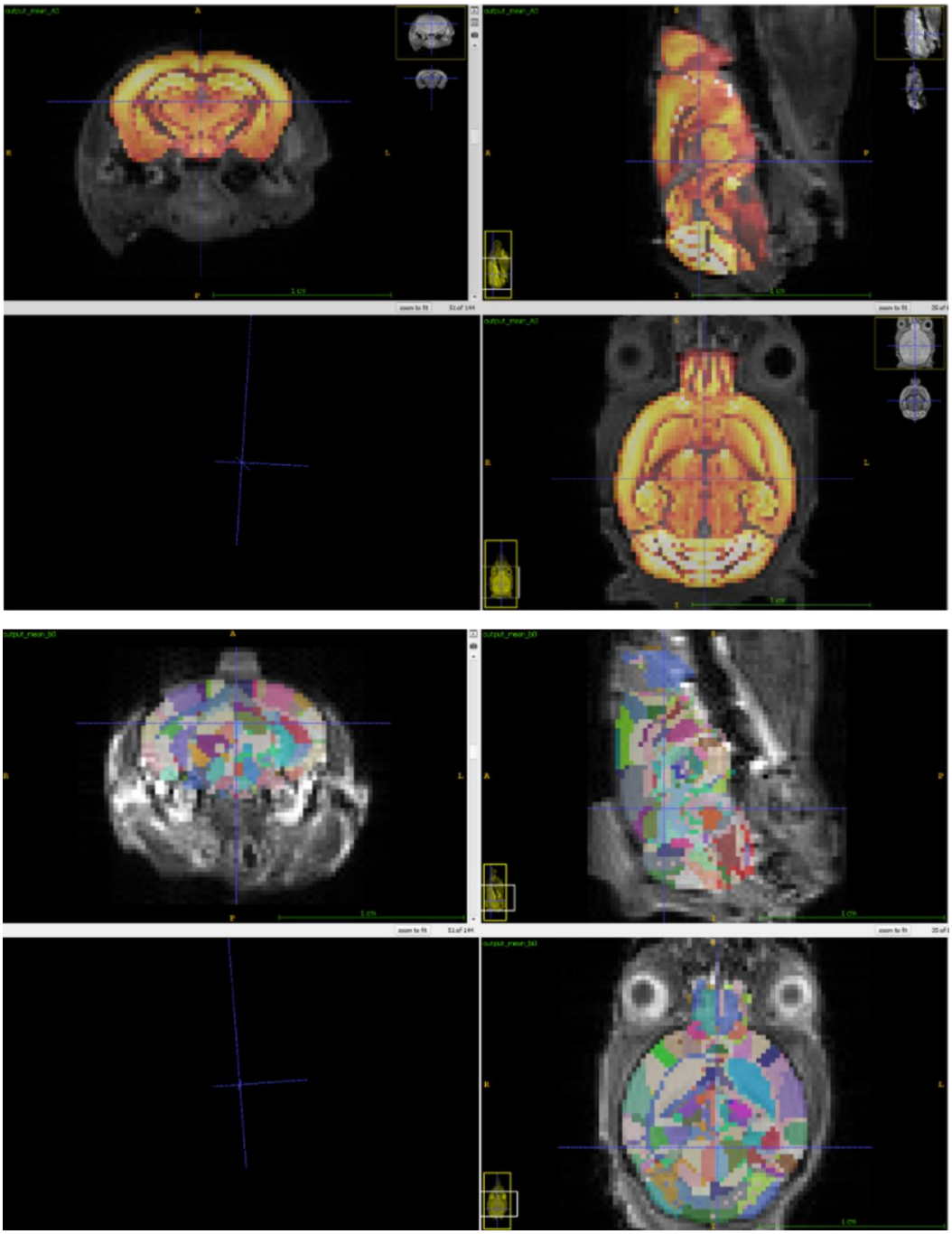

Figure 27: Registration of the brain mask and atlas to DTI data.

4.5.3.2 preprocessing

Preprocessing of diffusion MRI data was performed using MRtrix3 (Tournier et al., 2019) (http://www.mrtrix.org/). After checking the consistency of the gradient information in

diffusion-weighted MRI images, diffusion data were denoised and Gibbs ringing artefacts were removed. Multi-shell, multi-tissue constrained spherical deconvolution (CSD) was performed, generating fiber orientation distributions (FODs) for each tissue type. B1 field inhomogeneity was corrected using N4BiasFieldCorrection before global intensity normalisation was performed. A Spherical-deconvolution Informed Filtering of Tractograms (SIFT) was used to assign weights to each streamline, matching the streamline density to the underlying fiber orientation distributions (FODs) for improved quantitative accuracy (**Figure 28**). A matrix of connection strength normalized by the volume of the seed was performed as well as a whole-brain probabilistic streamline tractography producing 10 million streamlines per subject.

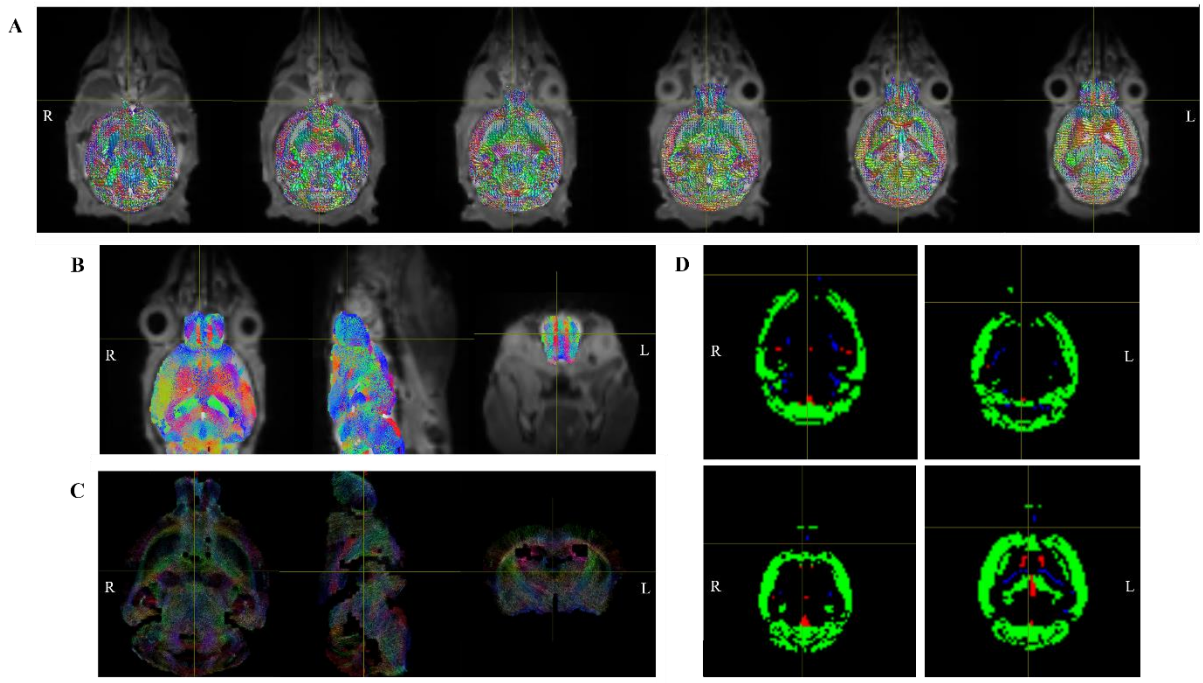

Figure 28: Quality control of DTI preprocessing.
A) fiber orientation distributions (FODs), B) Results of streamline creation, displayed as an overlay on the DW image. The tracks are color-coded (red: streamlines from right to left, green: from anterior to posterior, blue: from superior to inferior), C) Track Density Imaging (TDI) , D) Different tissue type masks (Green: Grey matter, Blue: White matter, Red: CSF).

4.5.3.3 Statistical analysis

A connectome group-wise statistics at the edge level was conducted using threshold-free network-based statistics (TFNBS, n= 5000) (Baggio et al., 2018), with family-wise error (FWE) correction applied to the whole-connectome p-values.

4.6 Preliminary results

4.6.1 Functional connectome of the TN in mice

4.6.1.1 Functional connectivity of the TN in control mice

The functional connectomes of the right TN (up) and left TN (down) of control mice (p_{uncorr} <0.05) are presented in (**Figure 29**). TN showed both inner-HT connections and extra-HT connections that appeared different between the right and the left TN.

Inner-hypothalamic network

The Primary connection of the TN was the HT (rTN-rHT p= 0.0052; rTN-lHT p= 0.0263; lTN-lHT p= 0.0013), including reciprocal TN connections (p= 0.0101), as well as connections to the PeVN (rTN-rPVi p= 0.0002; lTN-rPVi p= 0.0024; lTN-rPVa p= 0.0337), ARH (rTN-rARH p= 0.0007; rTN-lARH p= 0.0126; lTN-lARH p= 0.0057), DM (rTN-rDM p= 0.0003; rTN-lDM p= 0.0318; lTN-lDM p= 0.0134), Mammilary body (rTN-right Medial mammillary nucleus MM p= 0.0005; rTN-lMM p= 0.0065; lTN-rMM p= 0.0039; rTN-left Tuberomammillary nucleus TM, p= 0.0114; lTN-lTM p= 0.0106; lTN-left Lateral mammillary nucleus LM, p= 0.0009), Dorsal premammillary nucleus (PMd, rTN-rPMd p= 0.0263; rTN-lPMd p= 0.0067; lTN-rPMd p= 0.0026), Ventral premammillary nucleus (PMv, rTN-lPMv p= 0.0013; lTN-rPMv p= 0.0087; lTN-lPMv p= 0.0010), Ventromedial hypothalamic nucleus (VM, rTN-rVM p= 1.8525e-05; rTN-lVM p= 0.0025; lTN-rVM p= 0.0098; lTN-lVM p= 0.0001), LH (rTN-rLH p= 0.0008; rTN-lLH p= 0.0055; lTN-rLH p= 0.0348) (**Figure 29**). The rTN presented connections with the right PaVN (p= 0.0226), the right Anterior hypothalamic nucleus (AHA, p= 0.0025) and the right Lateral preoptic area (LPO, p=0.0446). Meanwhile, the lTN was connected to the left Anterodorsal preoptic nucleus (ADP, p= 0.0329), left Retrochiasmatic area (RCH, p= 0.0019) and left Subthalamic nucleus (STN, p= 0.0364).

Extra-hypothalamic network

Isocortex

The TN is also deeply connected to the Isocortex, including the Retrosplenial area (rTN-lRSPd p= 0.0178; lTN-lRSPv p= 0.0421; lTN-rRSPv p= 0.0019). The rTN is especially connected to the right Anteromedial visual area (VISam, p= 0.0409), left Primary somatosensory area upper limb (SSp-ul, p= 0.0373) and left ventral part of the Agranular insular area (AIv, p= 0.0243). However, the lTN is strongly connected to orbital areas (rORBl p= 0.0092; lORBl p= 0.0098; rORBm p= 0.0147; rORBvl p= 0.0402), right olfactory areas (OLF, p= 0.0441), left Secondary motor area (MOs, p= 0.0169), left infralimbic areas (ILA, p= 0.0388), left Temporal association areas (TEa, p= 0.0433).

Midbrain

The midbrain also served as a major connection for the TN, such as the reticular part of the Substantia nigra (SNr, rTN-rSNr p= 0.0150; rTN-lSNr p= 0.0467; lTN-rSNr p= 0.0012), right Ventral tegmental area (VTA, rTN p= 0.0137; lTN p= 0.0146). In addition, while the rTN shows a connection to the right Pedunculopontine nucleus (PPN, p= 0.0284), the lTN demonstrated more diverse connections, such as with the right Inferior colliculus (IC, p= 0.0337), right Supraoculomotor periaqueductal gray (Su3p= 0.0301), right Edinger-Westphal nucleus (EW, p= 0.0064), right Ventral tegmental nucleus (VTN, p= 0.0222) and left Paratrochlear nucleus (Pa4, p= 0.0037).

Pons

The rTN, and to a lesser extent the lTN, are also highly connected to the Pons (rTN- rP p= 0.026161; rTN-right Principal sensory nucleus of the trigeminal PSV, p= 0.0293; rTN-right Supratrigeminal nucleus SUT, p= 0.0322; rTN-right Tegmental reticular nucleus TRN, p= 0.0198; lTN-rTRN p= 0.0284; rTN-right Peritrigeminal zone P5, p= 0.0466; rTN-right Nucleus raphe pontis RPO, p= 0.0135; lTN-rRPO p= 0.0135; rTN-right Intertrigeminal nucleus I5, p= 0.0054; rTN-left Laterodorsal tegmental nucleus LDT, p= 0.0459; lTN-left Koelliker-Fuse subnucleus KF, p= 0.0082; lTN-left Pontine central gray PCG, p= 0.0171).

Thalamus

The rTN is equally more connected to the thalamus compared to the lTN (rTN-left Thalamus TH, p= 0.0446; rTN-right Xiphoid thalamic nucleus Xi, p= 0.0046; lTN-rXi p= 0.0307; rTN-right ventral medial nucleus of the thalamus VM, p= 0.0004; rTN-right Ventral posterolateral nucleus of the thalamus VPL, p= 0.0397; rTN-left Mediodorsal nucleus of thalamus MD, p= 0.0494; rTN-left Nucleus of reuniens RE, p= 0.0064; rTN-left Intergeniculate leaflet of the lateral geniculate complex IGL, p= 0.0426; lTN-right Peripeduncular nucleus PP, p= 0.0379; lTN-right Posterior complex of the thalamus PO, p= 0.0025).

Olfactory areas

Another significant connection of the TN is the Cortical amygdalar area (COA, rTN-rCOAa p= 0.0261; rTN-lCOAa p= 0.0211; rTN-lCOApm p= 0.0332; lTN-lCOApm p= 0.0474; lTN-lCOApl p= 0.0149), as well as other olfactory areas (rTN-left Taenia tecta ventral part TTv, p= 0.0367; lTN-Right Main olfactory bulb MOB, p= 0.0149; lTN-right Accessory olfactory bulb AOB, p= 0.0279; lTN-left Dorsal peduncular area DP, p= 0.0013).

Medulla

The rTN also shows more connection to the medulla than the lTN (rTN-right Magnocellular reticular nucleus MARN, p= 0.0026; rTN-right Lateral vestibular nucleus LAV, p= 0.0385; rTN-left Nucleus of the trapezoid body NTB, p= 0.0301; rTN-left Nucleus prepositus PRP, p= 0.0108; rTN-left Parapyramidal nucleus PPY, p= 0.0065; lTN-right Gigantocellular reticular nucleus GRN, p= 0.0488; lTN-right Parvicellular reticular nucleus PARN, p= 0.0156; lTN-left Spinal nucleus of the trigeminal oral part SPVO, p= 0.0182).

Cortical subplate

The TN also presented connections to the cortical subplate (rTN-right Claustrum CLA, p= 0.0095; rTN-left Cortical subplate CTXsp, p= 0.0138; Endopiriform nucleus dorsal part EPd, p= 0.0055), the Striatum (rTN-right Lateral septal nucleus LS, p= 0.0389; rTN-lLS p= 0.0413; lTN-lLS p= 0.0317; rTN-right Central amygdalar nucleus CEA, p= 0.0052; rTN-left Septofimbrial nucleus SF, p= 0.0447; lTN-left Caudoputamen CP, p= 0.0259) and cerebellum (rTN-right Declive (VI) DEC, p= 0.0491; rTN-left Uvula (IX) UVU, p= 0.0118; rTN-left Ansiform lobule Crus 1 ANcr1, p= 0.0423; rTN-left Fastigial nucleus FN, p= 0.0081; lTN-right Flocculus FL, p= 0.0172).

Hippocampal region

Finally, only the rTN showed connection to the Hippocampal region (right Entorhinal area lateral part ENTl, p= 0.0026; right Parasubiculum PAR, p= 0.0012; right Postsubiculum POST, p= 0.0114; right Area prostriata APr, p= 0.0089).

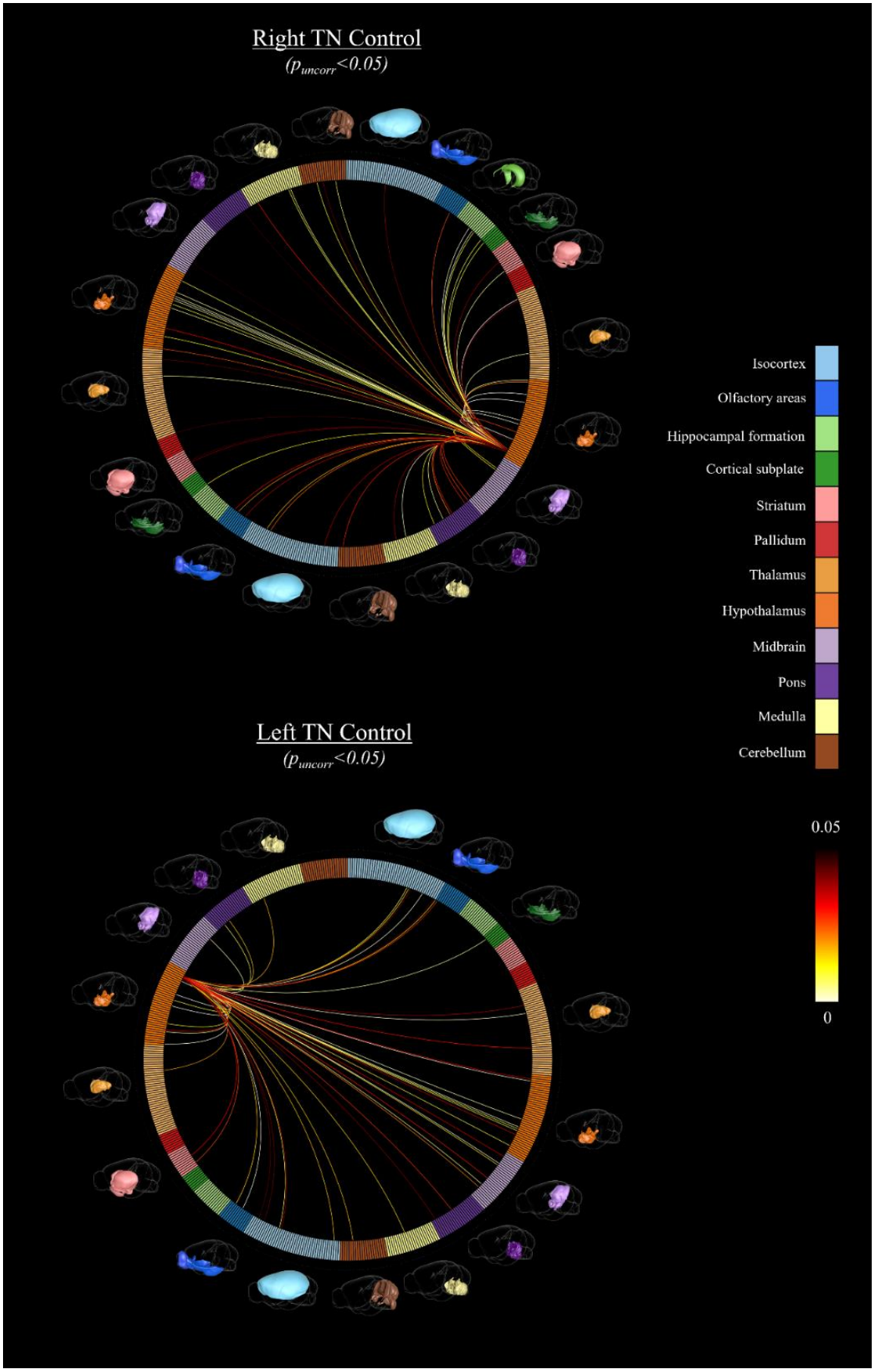

Figure 29: Circos plot of the TN functional connectome in control mice.

4.6.1.2 Hyperconnectivity of the TN in CFC mice

The functional connectomes of the right TN (up) and left TN (down) **hyperconnectivity** in CFC mice (p_{uncorr} <0.05) are presented in (**Figure 30**).

Inner-hypothalamic network

CFC mice showed hyperconnectivity within the HT, with the rTN more connected to the right Anteroventral preoptic nucleus (AVP, p= 0.0410), right Median preoptic nucleus (MEPO, p= 0.0412) and right Suprachiasmatic nucleus (SCH, p= 0.0188), while the lTN was more connected to the left Anterodorsal preoptic nucleus (ADP, p= 0.0466).

Extra-hypothalamic network

Isocortex

Both rTN and lTN show hyperconnectivity to visual areas (VIS, rTN-rVISpl p= 0.0328; lTN-rVISpl p= 0.0066; rTN-rVISpor p= 0.0262; rTN-lVISpor p= 0.0394), infralimbic areas (ILA, rTN-rILA p= 0.0452; lTN-rILA p= 0.0258; lTN-lILA p= 0.037), orbital areas (ORB, rTN-rORBm p= 0.0322; lTN-rORBl p= 0.0008; lTN-lORBl p= 0.0206; lTN-lORBm p= 0.003; lTN-rORBvl= 0.0406), agranular insula (AI, rTN-lAIv p= 0.0058; lTN-rAId p= 0.0326), Perirhinal area (PERI, rTN-lPERI p= 0.0034; lTN-rPERI p= 0.0148) and left ectorhinal area (ECT, rTN-lECT p= 0.0354; lTN-lECT p= 0.037). Additionally, lTN was more connected to the right isocortex (FRP, rFRP p= 0.0306), secondary motor area (MOs, rMOs p= 0.0372; lMOs p= 0.0282) and left ventral auditory area (AUDv, p= 0.044). The TN is also generally more connected to olfactory areas, especially the lTN (rTN-right Dorsal peduncular area DP, p= 0.0064; lTN-lDP p= 0.0002; rTN-right lateral olfactory tract NLOT, p= 0.0474; lTN-rNLOT p= 0.0254; rTN-left Piriform area, PIR p= 0.0194; lTN-rOLF p= 0.0078; lTN-rMOB p= 0.0248; lTN-rAOB p= 0.0186; lTN-r p= 0.0074; lTN-lTTd p= 0.0376; lTN-lTR p= 0.0246).

Hippocampal region

The rTN is hyperconnected, and the lTN to a lesser extent, to the hippocampus (rTN-rCA2 p= 0.0194; lTN-LCA1 p= 0.0264; lTN-lDG p= 0.0028; lTN-lHPF p= 0.0424), subiculum (rTN-lSUB p= 0.0418; rTN-lPRE p= 0.0194; rTN-rPOST p= 0.014; lTN-rPOST p= 0.0344; rTN-lProS p= 0.0162; lTN-lProS p= 0.0378) and Area prostriata (APr; rTN-rAPr p= 0.009; rTN-lAPr p= 0.0496; lTN-rAPr p= 0.027; lTN-lAPr p= 0.0028).

Pallidum

The TN also showed stronger connectivity to the pallidum, including the left Globus pallidus externe (GPe, rTN-lGPe p= 0.0468; lTN-lGPe p= 0.03), Substantia innominate (SI, lTN-rSI p= 0.0458; lTN-lSI p= 0.0404), right Medial septal nucleus (MS, lTN-rMS p= 0.032) and right Diagonal band nucleus (NDB, rTN-rNDB p= 0.0206).

Thalamus

The TN is also deeply hyperconnected to the thalamus (rTN-right Central medial nucleus of the thalamus CM p= 0.0264; rTN-right Parafascicular nucleus PF p= 0.049; rTN- left Dorsal part of the lateral geniculate complex LGd p= 0.0374; rTN-left Perireunensis nucleus PR p= 0.0492; rTN-left Intergeniculate leaflet of the lateral geniculate complex IGL p= 0.0002; lTN-lIGL p= 0.033; lTN-right Lateral dorsal nucleus of thalamus LD p= 0.004; lTN-left Lateral posterior

nucleus of the thalamus LP p= 0.0346; lTN-left Posterior complex of the thalamus PO p= 0.016; lTN-left Posterior limiting nucleus of the thalamus POL p= 0.0182; lTN- left Medial habenula MH p= 0.0358).

Midbrain

The lTN, and the rTN to a less extent, are also more connected to the midbrain (Midbrain reticular nucleus MRN, rTN-lMRN p= 0.018; lTN-rMRN p= 0.0308; Red nucleus RN, rTN-lRN p= 0.03; lTN-lRN p= 0.0074; Anterior tegmental nucleus AT, rTN-lAT p= 0.0266; lTN-lAT p= 0.0354; Nucleus sagulum SAG, rTN-lSAG p= 0.0282; Superior colliculus sensory related SCs, lTN-rSCs p= 0.033; Ventral tegmental nucleus VTN, lTN-rVTN p= 0.0082; Pedunculopontine nucleus PPN, lTN-rPPN p= 0.0078; Nucleus of the brachium of the inferior colliculus lTN-lNB p= 0.0368; Substantia nigra compact part, lTN-lSNc p= 0.035).

Pons

Both rTN and lTN are more connected to the right Nucleus raphe pontis (RPO, rTN p= 0.0164; lTN p= 0.03760).

Main lateralization connectivity differences

The rTN is more connected to the right claustrum (CLA, p= 0.0438) whereas the lTN is more connected to the Endopiriform nucleus (EP, right dorsal EP p= 0.0254; left ventral EP p= 0.0338). The TN is also strongly connected to the Medulla (rTN-right Lateral vestibular nucleus LAV, p= 0.003; rTN-left Nucleus prepositus PRP, p= 0.0014). In addition, while the rTN is highly connected to the Pons (left Supragenual nucleus SG, p= 0.0156; left Supratrigeminal nucleus SUT, p= 0.044; left Parvicellular motor 5 nucleus PC5, p= 0.0354; left Laterodorsal tegmental nucleus LDT, p= 0.0326) and the cerebellum (left Ansiform lobule crus 1, ANcr1 p= 0.0372), the lTN is hyperconnected to the striatum (right Nucleus accumbens ACB, p= 0.038; left caudoputamen CP, p= 0.046; left Central amygdalar nucleus CEA, p= 0.0414).

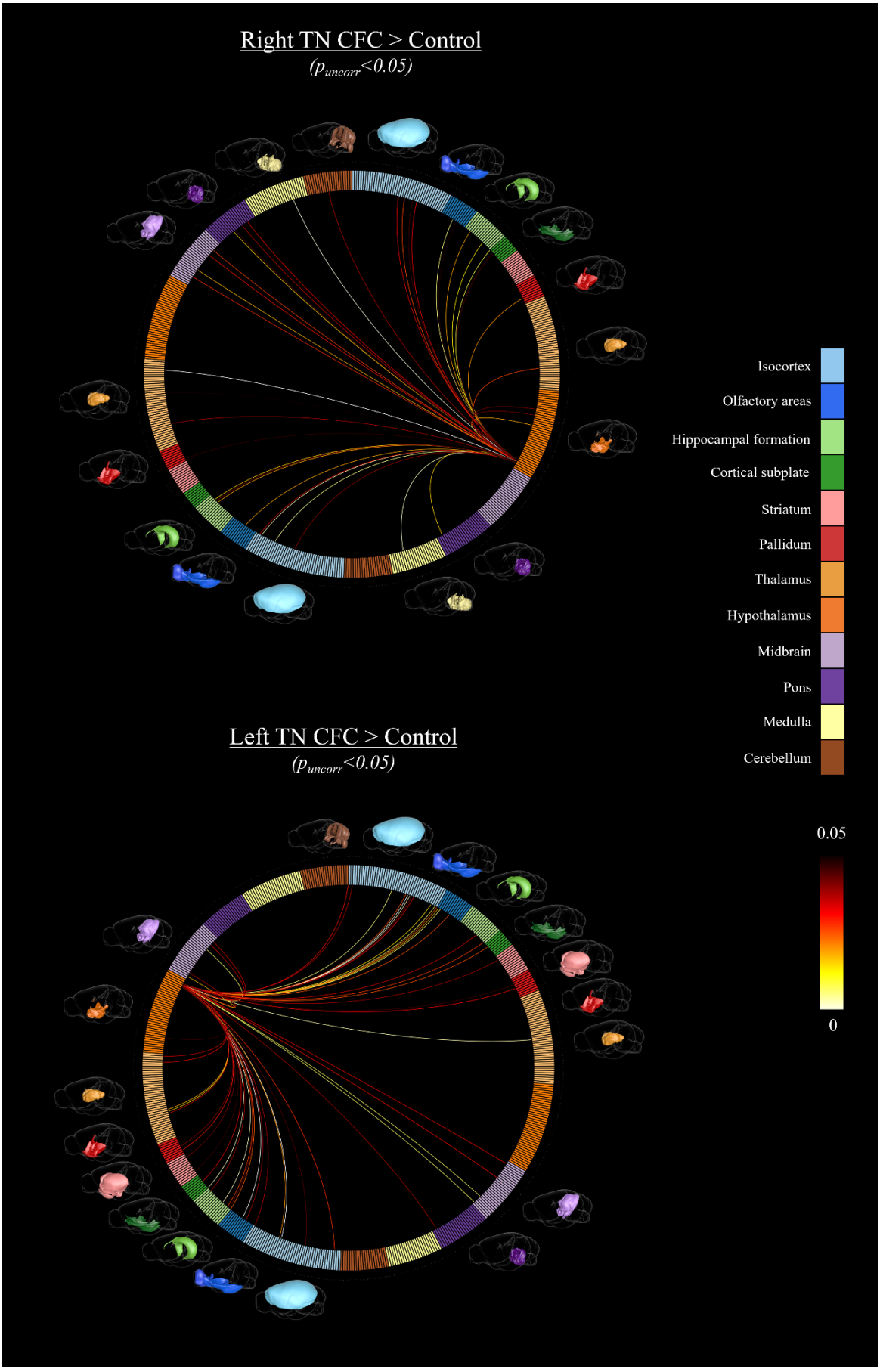

Figure 30 : Circos plot of the hyperconnectivity of TN in conditioned mice.

4.6.1.3 Hypoconnectivity of the TN in CFC mice

The functional connectomes of the right TN (up) and left TN (down) hypoconnectivity in CFC mice (p_{uncorr} <0.05) are presented in (**Figure 31**).

Inner-hypothalamic network

In CFC mice, both the rTN and lTN showed lower connectivity with the hypothalamic medial mammillary nucleus (MM, rTN p= 0.0022; lTN p= 0.003), the right paraventricular nucleus (PaVN, rTN p= 0.0012; lTN p= 0.0492), and the right dorsal premammillary nucleus (PMd, rTN p= 0.0094 and 0.0114), and subthalamic nucleus (STN, rTN-rSTN p= 0.0228; lTN-lSTN p= 0.0428). The rTN aslo showed less connections to the hypothalamic DM (DM, rDM p= 0.0012; lDM p= 0.026), the left medial mammillary nucleus (MM, p= 0.023) and the right anterior HT area (AHA, p= 0.0046). Meanwhile, the lTN had lower connectivity with the hypothalamic Lateral mammillary nucleus (LM, rLM p= 0.0344; lLM p= 0.0048) and right Posterodorsal preoptic nucleus (PD, p= 0.0426).

Extra-hypothalamic network

Medulla

Both showed hypoconnectivity with regions in the medulla, however while the rTN shows less connections to the left medulla (Nucleus of the trapezoid body NTB, p= 0.0052; Spinal nucleus of the trigeminal interpolar part SPVI, p= 0.024; Magnocellular reticular nucleus MARN, p= 0.0336; Parapyramidal nucleus PPY, p=0.0164), the lTN shows less connections to the right medulla (Gigantocellular reticular nucleus GRN, p=0.0134; Superior vestibular nucleus SUV, p= 0.02980).

Midbrain

The TN globally was hypoconnected to the right midbrain, with the rTN connected to the right ventral tegmental area (VTAp, p= 0.012) and right pedunculopontine nucleus (PPN, p= 0.0146), while the lTN showed less connections to the right reticular part of the Substansia nigra (SNr, p= 0.0416), right Supraoculomotor periaqueductal gray (Su3, p= 0.029) and left Paratrochlear nucleus (Pa4, p= 0.0296).

Pons

The TN was also less connected to the right Pons, such as the right Intertrigeminal nucleus (rI5, p= 0.0024) for the rTN and the right Tegmental reticular nucleus (TRN, p= 0.022) and left Peritrigeminal zone (lP5, p= 0.0288) for the lTN.

Main lateralization connectivity differences

However, only the rTN was hypoconnected to the cerebellum, including the Nodulus (NOD, rNOD p= 0.0352; lNOD p= 0.0392), Paraflocculus (PFL, rPFL=0.0212; lPFL p= 0.0098) and left Fastigial nucleus (FN, p= 0.0078), as well as the Left Primary somatosensory area barrel field (SSp-bfd, p= 0.0176), Left ventral part of the Taenia tecta (TTv, p= 0.0056) and the Left Cortical subplate (CTXsp, p= 0.01). Conversely, the lTN was less connected to the Left Globus pallidus internal segment (lGPi, p= 0.047).

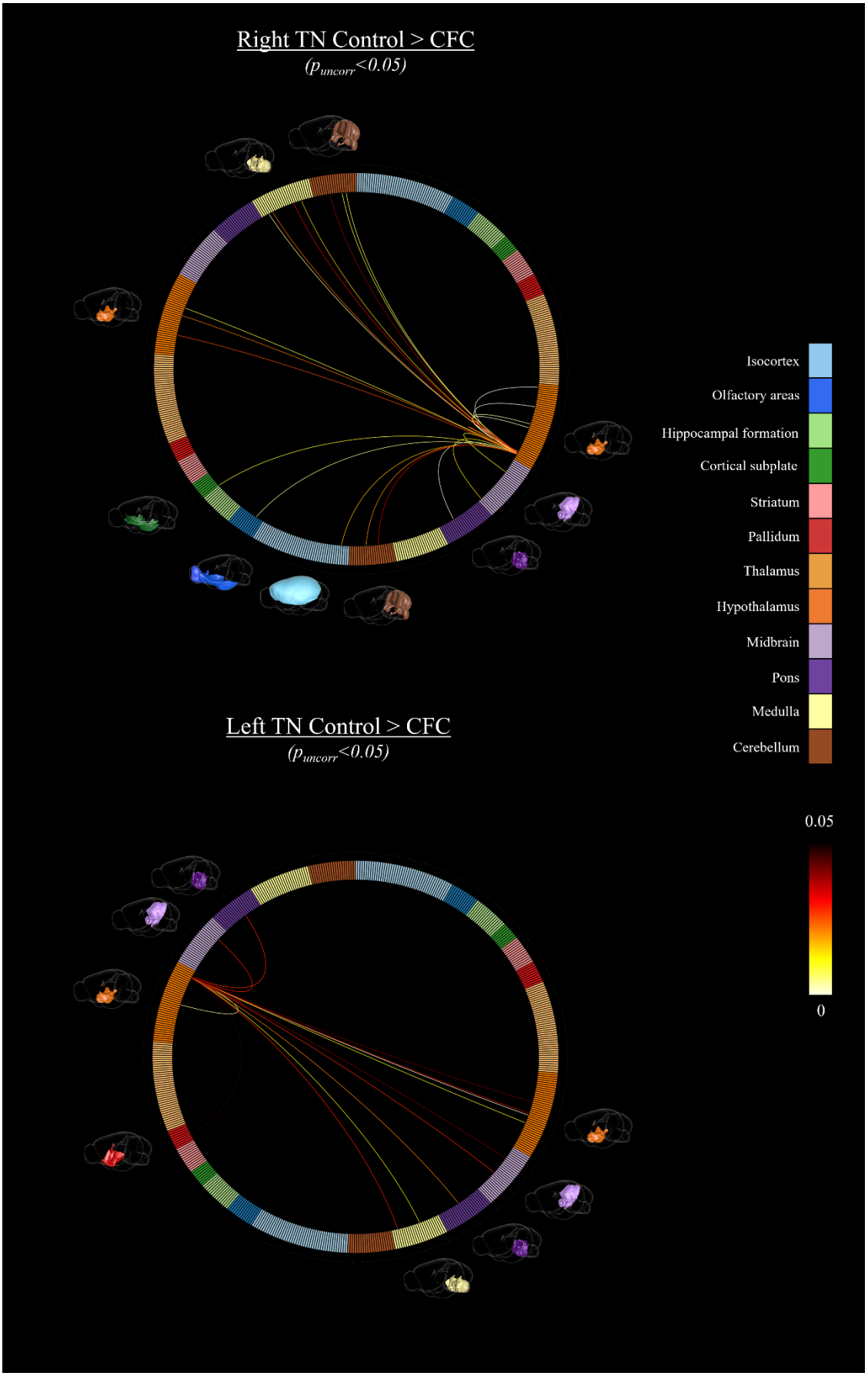

Figure 31: Circos plot of the TN functional connectome in control sup conditioned mice.

4.6.2 Structural connectome of the Tuberal Nucleus in control mice

The functional connectomes of the right TN (up) and left TN (down) of control mice (TFNBS p_{fwe} <0.05) are presented in (**Figure 32**).

Inner-hypothalamic network

The Primary connection of the TN is the HT (HT, rTN-rHT p= 0.0002; rTN-lHT p= 0.0002; lTN-rHT p= 0.0006; lTN-lHT p= 0.0044), including reciprocal TN connections (p= 0.0004), as well as connections with the left PaVN ((rTN-lPaVN p= 0.0154; lTN-lPaVN p= 0.0294), LH (rTN-rLH p= 0.0002; rTN-lLH p= 0.0294; lTN-lLH p= 0.0054), right ARH (rTN-rARH p= 0.0044; lTN-rARH p= 0.0028), Anterior hypothalamic nucleus (AHN, rTN-rAHN p= 0.0054; rTN-lAHN p= 0.0006; lTN-rAHN p= 0.0082; lTN-lAHN p= 0.0054), Medial preoptic area (MPO, rTN-rMPO p= 0.0154; lTN-rMPO p= 0.0294; lTN-lMPO p= 0.0044), Lateral preoptic area (LPO, rTN-rLPO p= 0.0006; lTN-lLPO p= 0.0154), Medial mammillary nucleus (MM, rTN-rMM p= 0.0002; rTN-lMM p= 0.0004; lTN-rMM p= 0.0006; lTN-lMM p= 0.0004), left Dorsal premammillary nucleus (PMd, rTN-lPMd p= 0.0006; lTN-lPMd p= 0.001), Tuberomammillary nucleus (TM, rTN-rTM p= 0.0294; rTN-lTM p= 0.006; lTN-rTM p= 0.0082; lTN-lTM p= 0.0054), VM (rTN-rVM p= 0.0154; rTN-lVM p= 0.006; lTN-rVM p= 0.0154), Supramammillary nucleus (SUM, rTN-rSUM p= 0.0154; rTN-lSUM p= 0.006; lTN-rSUM p= 0.0082), Posterior hypothalamic nucleus (PH, rTN-rPH p= 0.001; rTN-lPH p= 0.0006; lTN-rPH p= 0.0028), Suprachiasmatic nucleus (SCH, rTN-lSCH p= 0.0004; lTN-lSCH p= 0.0082).The rTN was connected to the DM (DM, rTN-rDM p= 0.0082; rTN-lDM p= 0.0016), Medial preoptic nucleus (MPN, rTN-rMPN p= 0.0028; rTN-lMPN p= 0.0054), Lateral mammillary nucleus (LM, rTN-rLM p= 0.0006; rTN-lLM p= 0.0442), left Anteroventral periventricular nucleus (AVPV, rTN-lAVPV p= 0.0016), left Ventrolateral preoptic nucleus (VLPO, rTN-lVLPO p= 0.0442), left Ventral premammillary nucleus (PMv, rTN-lPMv p= 0.001), left Perifornical nucleus (PeF, rTN-lPeF p= 0.001), left Retrochiasmatic area (RCH, rTN-lRCH p= 0.0154). Meanwhile, the lTN was more connected to the left preoptic part of the PeVN (PVpo, lTN-lPVpo p= 0.0442) and Anterodorsal preoptic nucleus (ADP, lTN-rADP p= 0.0442).

Extra-hypothalamic network

Olfactory areas

Then, the rTN and the lTN to a lesser extent are connected to olfactory areas (rTN-right Main olfactory bulb MOB, p= 0.0082; lTN-lMOB p= 0.0294; rTN-left ventral part of the Taenia tecta TTv, p= 0.0054; lTN-lTTv p= 0.0044; rTN-right Anterior olfactory nucleus AON, p= 0.0082; rTN-lAON p= 0.0082; rTN-right PIR, p= 0.0294).

Striatum

The TN showed connection to the Striatum (STR, rTN-rSTR p= 0.0154; rTN-lSTR p= 0.0154; lTN-rSTR p= 0.0082; lTN-lSTR p= 0.0082), including the Lateral septal nucleus (LS, rTN-rLS p= 0.0442; lTN-lLS p= 0.0006). While the lTN presented connections to the Septofimbrial nucleus (SF, lTN-rSF p= 0.0294; lTN-lSF p= 0.0154), left Nucleus accumbens (ACB, p=

0.0442) and left Olfactory tubercle (OT, p= 0.0442), the rTN showed connections to the right Caudoputamen (CP, p= 0.0082).

Pallidum

The TN also showed connections to the Pallidum, including the Diagonal band nucleus (NDB, rTN-lNDB p= 0.0028; lTN-rNDB p= 0.0442), with the rTN linked to the right Medial septal nucleus (MS, p= 0.006) and right Bed nuclei of the stria terminalis (BST, p= 0.0028), while the lTN linked to the Triangular nucleus of septum (TRS, rTRS p= 0.001; lTRS p= 0.0082).

Midbrain

The midbrain (MB, rTN-rMB p= 0.0004; rTN-lMB p= 0.0294) also represented a consequent connection of the rTN and the lTN to a lesser extent, such as the sensory related part of the Superior colliculus (SCs, rTN-rSCs p= 0.001; lTN-lSCs p= 0.0294). Additionally, the rTN was connected to the left reticular part of the Substantia nigra (SNr, p= 0.001), right motor related part of the Superior colliculus (SCm, p= 0.0442) and right Periaqueductal gray (PAG, p= 0.0044).

Main lateralization connectivity differences

The rTN also showed minor connections to the right Dentate Gyrus (DG, p= 0.0442) and right Laterodorsal tegmental nucleus (LDT, p= 0.0044), while the lTN present a connection to the cerebellum simple lobule (SIM, p= 0.0028).

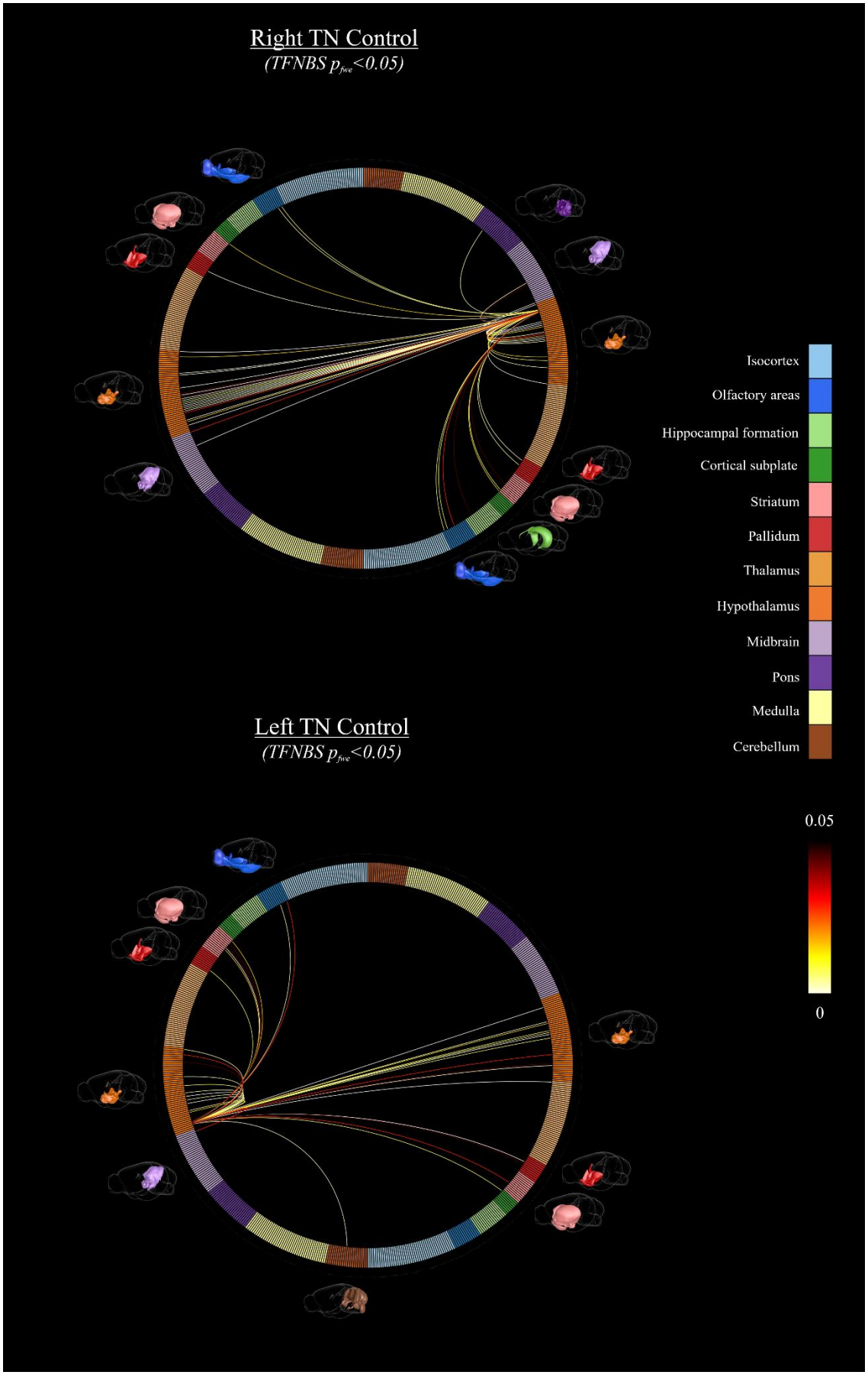

Figure 32: Circos plot of the TN structural connectome in control mice.

4.7 Multi-modal brain-wide circuit analysis reveals neural mechanisms of conditioned feeding behavior

4.7.1 Foreword

The previous functional and structural connectomes of TN derived from rs-fMRI and diffusion tractography have been compared to lighsheet microscopic results in the same CFC protocol. This first draft provides a detailed account of that comparison.

4.7.2 Manuscript

Multi-modal brain-wide circuit analysis reveals neural mechanisms of conditioned feeding behavior

Xiaoning Liu[1,#], Coleen Roger[1,2,3,#], Yi-fei Li[1,4,#], Han-yin Cheng[1,#], Menghan Wang[1,#], Joanes Grandjean[5] Kuan Jin Lee[1], Yu Fu[1,4,6,*]

[1] Institute of Molecular and Cell Biology, Agency for Science, Technology and Research (A*STAR), Singapore, 138673

[2] Aix Marseille Univ, CNRS, Centre de Résonance Magnétique Biologique et Médicale (CRMBM), Marseille, France

[3]Aix Marseille Univ, Assistance Publique-Hôpitaux de Marseille (AP-HM), Centre d'Exploration Métabolique par Résonance Magnétique (CEMEREM), Hôpital Universitaire de la Timone, Marseille, France

[4] Department of Physiology, Yong Loo Lin School of Medicine, National University of Singapore, Singapore, 117597

[5] Donders Institute for Brain, Cognition and Behaviour, Radboud University Medical Center, Nijmegen, The Netherlands

[6] Lee Kong Chian School of Medicine, Nanyang Technological University, Singapore, 308232

# contributed equally

* corresponding author: fu_yu@imcb.a-star.edu.sg

Abstract

Dynamic plastic changes of neural circuits enable flexible behavioral outcomes, including learning and memory, and also maladaptive behaviors. While it's tempting to claim that a specific neural circuit is critical for a specific behavior, we have to appreciate that the brain often engages multiple neural circuits to regulate specific or different aspects of a particular behavior. Therefore, it's often to note that several neural circuits could be reported by different researchers to regulate the same behavioral paradigm. While we can still examine the function of a specific neural circuit based on prior knowledge, there is a need to non-biasedly screen for potential circuit mechanisms using brain-wide neural circuit mapping methods such as whole brain neural circuit mapping and functional MRI (fMRI). Here we report the combination of viral-based whole-brain neural circuit mapping and fMRI for mapping potential neural circuit mechanisms of a specific behavior, contextual feeding conditioning, to have a more comprehensive understanding of the underlying neural mechanisms. Both brain-wide circuit mapping methods reveal common circuit changes, including both reported and novel circuits. Importantly, there is a significant positive correlation between the circuit changes revealed by viral-based mapping and fMRI mapping, providing the structural basis for the functional changes revealed by fMRI. Such multi-modal brain-wide neural circuit mapping represents a major advance in systems neuroscience research by providing a more comprehensive method for discovering potential circuit mechanisms of a specific conditioned behavior research

Main Text

The development of optogenetics, chemogenetics, in vivo imaging and viral tools greatly advanced neuroscience research, allowing people to precisely label and manipulate specific neural circuits for probing their functions. While we appreciate the functional importance of specific neural circuits, we also need to acknowledge that the brain develops complex mechanisms for ensuring proper functional outputs that are usually resilient to interferences. Therefore, it's not surprising to note that different neural circuits are reported to regulate similar behaviors. Given the complex neural mechanisms, it will be ideal if we can systematically map potential neural circuit mechanisms for a more comprehensive understanding of a specific behavior.

Functional MRI has been a powerful tool for studying the activity changes in the whole animal brain for suggesting potential neural mechanisms (Low et al., 2021). The fMRI has also been used for detecting connectivity strength of different brain regions by calculating the correlation of their activity time series. However, such connectivity is purely based on mathematical calculation without a guarantee that there is a direct neural connection between even highly correlated brain regions. Therefore, how to better use the connectivity changes inferred by fMRI for guiding neural circuit functional investigation is still in its infant stage. On the other hand, several technologies have enabled whole-brain neural circuit mapping based on viral or genetic tools and optical imaging methods, which may also be important for revealing critical neural circuit mechanisms (Beier et al., 2017; Gong et al., 2020; Nectow et al., 2017). However, the differentially changed brain regions revealed by optical methods often suffer low significance so that they may not survive stringent statistical tests for ensuring confidence in further functional tests. Therefore, it'll be ideal if we can combine different brain-wide neural circuit mapping technologies, such as optical based systems and fMRI, for cross-validating potential neural circuit changes with relatively lower significance level in either test for screening potential important circuits with a balanced consideration of stringent statistical tests and exploring more possible targets.

We implemented VITALISTIC (viral tracing assisted by light sheet and tissue clearing) pipeline for examining the brain-wide input changes to specific starter cells in a defined behavioral paradigm (Fig 1a), contextual feeding conditioning (CFC) that has been studied before as a model of cue-driven food oversumption (Mohammad et al., 2021; Stern et al., 2020). We previously found that subiculum (Sub) to tuberal nucleus somatostatin (^{TN}SST) circuit is potentiated by CFC, and plays a critical role in CFC (Mohammad et al., 2021). Since it was reported that a potentiated connection may enabling more labelling by rabies virus (Beier et al., 2017), we first examined whether the conditioned mice show increased percentage of rabies labelling. VITALISTIC method allowed us to quantify the percentage of input neurons of all brain regions (Fig 1b), and the percentage of ^{TN}SST input neurons in Sub was more than that in control mice (Fig 1c and 1d). The percentage of ^{TN}SST input neurons in Sub significantly correlated with the amount of food consumption on the test days (Fig 1d), supporting the reported function of this circuit in CFC.

Encouraged by the enhanced input labelling in Sub, we further examined the changes in all brain regions and found that the Sub input actually was one of the most significantly enhanced input regions, with other brain regions showing more modest changes (lower Hedge's g value) (Fig 1f, regions with g value bigger than 0.5 were labelled). Further analysis showed that the olfactory and hippocampal areas contained relatively more brain regions showing bigger enhancement in CFC, indicating the critical roles of olfactory and contextual inputs in CFC.

Therefore, using VITALISTIC method, we confirmed that Sub input is likely one of the most important inputs to ^{TN}SST neurons in mediating CFC, and further revealed other input regions that may also play a role in CFC.

To further investigate the circuit mechanisms of CFC, we also conducted resting state fMRI for both control and conditioned mice (Fig 2a). We first examined all potential neural connections that could be detected by fMRI (Fig 2b) and revealed some circuits that showed significantly higher connectivity after CFC (Fig 2b). We further examined structural neural circuit connectivity by diffusion tensor imaging (DTI), which revealed significant connections after CFC (Fig 2c). Such brain-wide analysis revealed too many targets which made subsequent functional testing/validation very challenging. Furthermore, mean activity of major brain regions suggested significantly enhanced activity in cingulate region, suggesting potential involvement of mPFC in CFC, which is corroborated by relatively bigger effect size of dorsal cingulate area (ACAd) input revealed by VITALISTIC method (Fig 1f, right panel).

To validate the feasibility of using fMRI based connectivity screening, we first examined whether there was significant increase of TN-Sub connectivity in conditioned mice. Interestingly, linear regression of the TN-Sub connectivity with the amount of food intake showed significant correlation (Fig 2e and 2f), supporting the potential role of this circuit in CFC. Next, we examined whether we can combine these two brain-wide circuit mapping tools, by plotting the Hedge's g values of all input regions to ^{TN}SST neurons revealed by VITALISTIC method with the g values of all connectivity with TN revealed by fMRI (Fig 2g). Interestingly, there was a significant positive correlation of the circuit connectivity changes revealed by VITALISTIC and fMRI, suggesting the potential feasibility of combining these two brain-wide circuit mapping tools.

The regions shown in the upper-right quarter are the ones showing relatively big positive changes in both imaging methods, and we reason that these regions are likely potentiated by CFC and are more likely to play important roles in CFC. Combining with the actual percentage of these input regions, we postulate that the inputs from AON, CA1, ACB and ACAv likely play important roles in CFC (Fig 2g). Although a group comparison of the average values of TN-CA1 and TN-ACB connectivity didn't show significant increase in conditioned mice, there was a significant correlation of these connectivity with the amount of food consumption on test days, suggesting that these circuits may play a role in CFC.

Discussion

In this study, we employed two different brain-wide neural circuit mapping tools, VITALISTIC and fMRI, for revealing neural circuits that are likely to play important roles in CFC, as a pilot

to explore a more comprehensive method to investigate neural circuit mechanisms of a defined behavior.

By examining the changes of the connectivity between Sub and TN, using both viral based optical method and fMRI, we showed that Sub-TN connectivity was positively correlated with the level of conditioned feeding behavior, which strongly supported our previous finding that Sub-^{TN}SST circuit plays a critical role in CFC. These findings indicate that such brain-wide mapping tools are useful in revealing the underlying neural circuit mechanisms.

Our finding that the changes revealed by VITALISTIC method was significantly correlated with the changes revealed by fMRI supported the feasibility of combining two such brain-wide circuit mapping tools in discovering neural circuit mechanisms. We have to emphasize that the circuits show relatively big change, revealed by the Hedge's g value, do not mean that such changes will pass stringent statistical tests; and combining two orthogonal brain-wide mapping tools is for helping us identify potential targets from two inherently noisy methods without using more stringent statistical methods, which are helpful for reducing type I error with the cost of increasing type II error. Such multi-modal imaging tools are useful as an exploratory tool, and the potential circuits revealed by these tools will need to be functionally tested for their actual relevance for a specific behavior.

We think that systematically utilising such multi-modal circuit mapping tools will greatly advance neuroscience research by providing a more comprehensive understanding of underlying mechanisms. Importantly, the circuits revealed by such methods are unbiased and not limited by any prior hypothesis. Therefore, such method will provide new neural circuit targets that may not be immediately obvious to test according to published literature, which will likely generate novel ideas and hypothesis that will advance our understanding of a specific behavior.

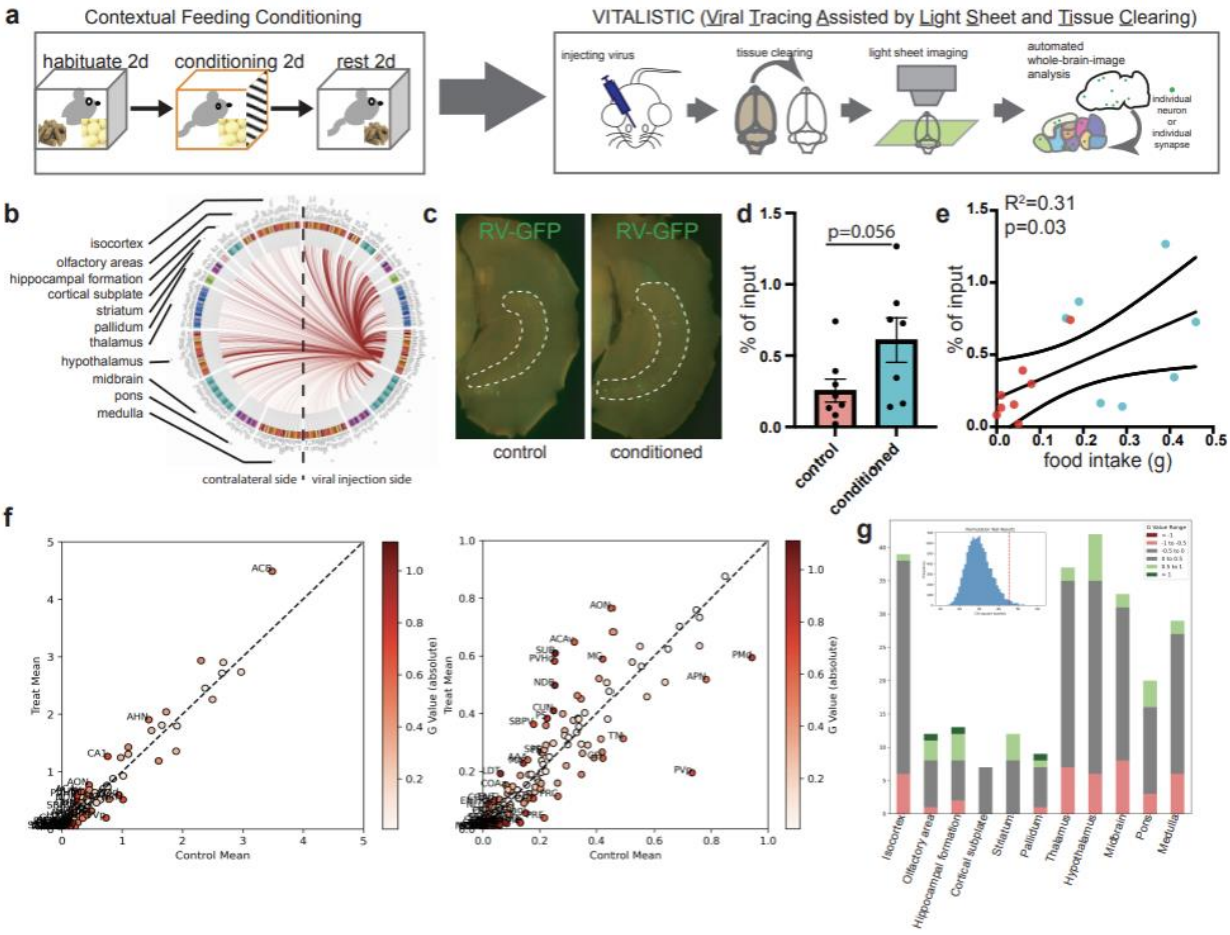

Figure 1. VITALISTIC mapping reveals tuberal nucleus related circuit changes in contextual feeding conditioning paradigm. **a**, Schematic diagram showing the simplified experimental paradigm of contextual feeding conditioning and subsequent VITALISTIC neural circuit mapping. **b**, The Circos map showing the brain-wide inputs to tuberal nucleus somatostatin (^{TN}SST) neurons. **c**, Representative coronal section images showing rabies virus labelled inputs neurons in subiculum. **d**, Quantification of the subiculum input neurons as a percentage of the whole brain inputs in both control and conditioned mice. **e**, Correlation of the subiculum input percentage and the food intake on the test day for examining the level of conditioned feeding. Simple linear regression was performed and the curved lines indicate 95% confidence intervals. f, (left) Scatter plot showing the correlation between the percentage of input in control and conditioned groups for all brain regions; (right) A zoomed in plot of the lower left corner of the left panel. Scatter plot showing the correlation between the percentage of input in control and conditioned groups for the inputs below 1%. The color indicates the Hedge's g value. **g**, Bar plot summarising the number of regions showing different level of changes of inputs (indicated by Hedge's g value) in major brain regions. The inserted plot showing the chance of observed changes after 5000 times of permutation of results.

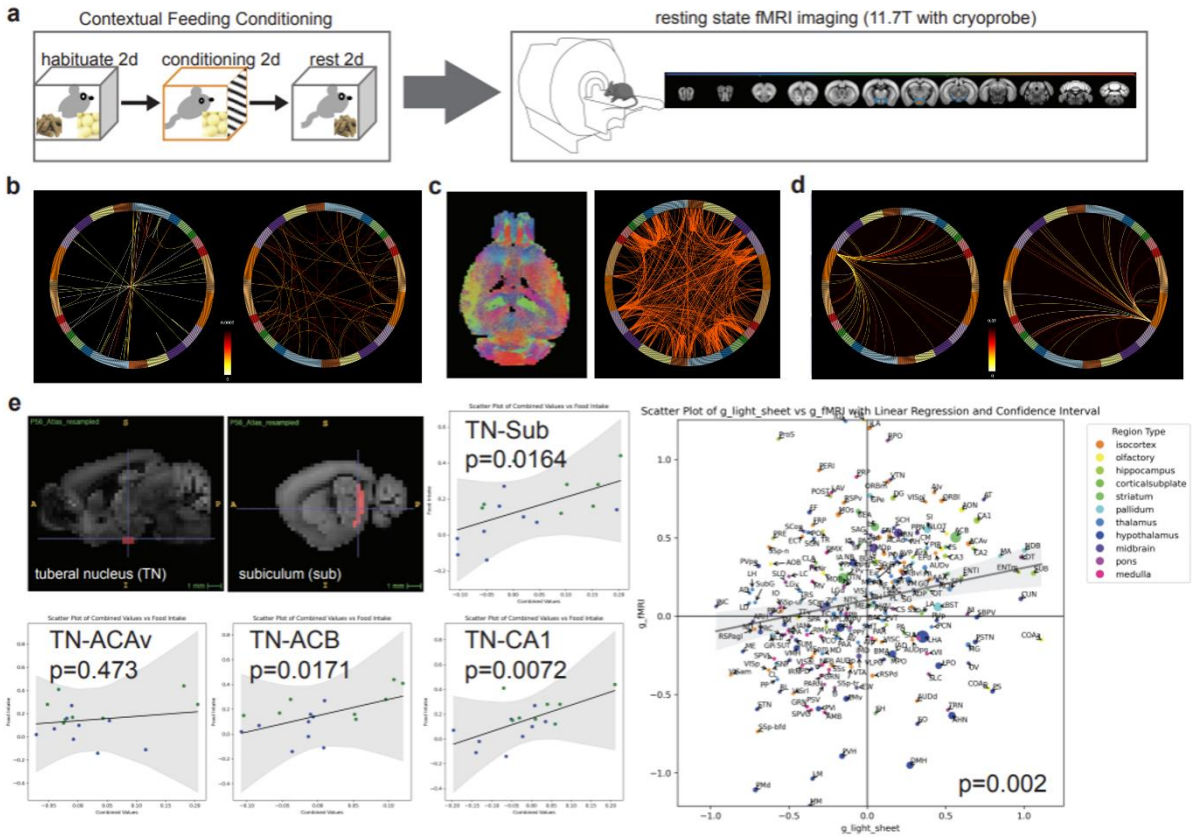

Figure 2. fMRI imaging reveals connectivity changes in contextual feeding conditioning paradigm. **a**, The schematic showing the contextual feeding conditioning paradigm and subsequent fMRI. **b**, The significant connections of all brain regions in conditioned mice (left); and the significantly changed neural connections (right). Color indicates p value. **c**, Representative image showing the DTI results of a mouse (left); significantly neural in CFC by DTI (right). **d**, The significantly changed neural functional connections of the left TN (left); and the right TN (right). **e**, Representative images showing the location of TN and sub in mouse brain. **f**, The scatter plot of the TN-sub connectivity value and the amount of food intake on test day, with linear regression analysis with 95% confidence intervals. **g**, The scatter plot of the Hedge's g values of all input regions to TN in VITALISTIC (x-axis value) and fMRI (y-axis value). The size of the dot represents the percentage of input in VITALISTIC method. **h**, The scatter plot of the TN-ACAv, TN-ACB and TN-CA1 connectivity in fMRI and the amount of food intake on test days, together with linear regression with 95% confidence intervals.

The second part of my PhD research focused on investigating whether the structural and functional organization of hypothalamic (HT) networks involved in eating behaviors could also be observed in vivo in humans, specifically at the granular level of HT nuclei. To address this, we implemented a clinical protocol in Marseille, utilizing 7T MRI to characterize the structural (both micro- and macro-level) and functional modulation of HT nuclei involved in eating behaviors in young females with restrictive anorexia nervosa or living with obesity.

5 Structural alterations of individual hypothalamic nuclei in young women with Obesity and Anorexia Nervosa: An in vivo 7T MRI study

5.1 Foreword

The second part of my PhD work consisted in determining if the structural and functional organization of HT networks involved in eating behaviors could also be observed in vivo in Human at the granular level of HT nuclei. Using 7T MRI, we have implemented in Marseille a clinical protocol aiming at characterizing the structural (micro- and macro-) and functional modulation of HT nuclei involved in eating behaviors in young women living with obesity or restrictive anorexia nervosa.

Despite the abundance of neuroimaging studies exploring food intake networks, we identified a resolution gap that hinders the examination of hypothalamic alterations at the nuclei level in pathological conditions in Human. Thus, we questioned the sensitivity of quantitative ultra-high field (7T) MRI to uncover the morpho-structural variations of hypothalamic nuclei and their association to BMI, hormone levels and eating behavioral scores using high resolution quantitative 3D-T1 MRI sequence in well-characterized cohorts of young women with normal weight, living with obesity and restrictive anorexia nervosa.
We reported that 7T MRI possesses the sensitivity to reveal both macro- and micro-structural changes in specific hypothalamic nuclei involved in eating behavior networks in individuals with restrictive anorexia nervosa or living with obesity.
Our results on specific hypothalamic nuclei implicated in eating behavior networks aim at developing a more detailed individual HT profiling, potentially useful for personalized monitoring of patients with weight-related disorders, improving their outcomes and tailoring nutritional interventions to their specific neural profiles. As new neuroimaging projects surrounding the issue of weight-related disorders are currently flourishing, we believe this paper will be of great interest for the readers of the American journal of clinical nutrition.

This work was the subject of a scientific poster presentation at the Organization of Human Brain Mapping (OHBM) Annual Meeting 2024 in Seoul, South Korea, as well as a digital scientific poster at the International Society for Magnetic Resonance in Medicine (ISMRM) Annual Meeting 2024 in Singapore. Finally, this work has been submitted as a scientific paper and is currently under review; it will be the focus of the next section.

5.2 Manuscript

Structural alterations of individual hypothalamic nuclei in young females with Obesity and Anorexia Nervosa - An *in vivo* 7T MRI study

Coleen Roger[1,2,3], Adele Lasbleiz[4,5], Hugo Dary[1,2], Lauriane Pini[1,2], Patricia Ancel[4], Anezka Kovarova[1,2,6,7], Marie-Pierre Ranjeva[1,2], Patrice Darmon[4,5], Benedicte Gaborit[4,5], Yu Fu[3], Patrick J Cozzone[1,2], Maxime Guye[1,2], Anne Dutour[4,5], Jean-Philippe Ranjeva[1,2]

1. Aix Marseille Univ, CNRS, Centre de Résonance Magnétique Biologique et Médicale (CRMBM), Marseille, France
2. Aix Marseille Univ, Assistance Publique-Hôpitaux de Marseille (AP-HM), Centre d'Exploration Métabolique par Résonance Magnétique (CEMEREM), Hôpital Universitaire de la Timone, Marseille, France
3. A*Star, Institute of Molecular and Cell Biology (IMCB), Singapore.
4. Aix Marseille Univ, INSERM, INRAE, Centre de recherche en CardioVasculaire et Nutrition (C2VN), Marseille, France
5. Aix Marseille Univ, Assistance Publique-Hôpitaux de Marseille (AP-HM), Département d'Endocrinologie, Hôpital de la Conception, Marseille, France
6. CEITEC – Central European Institute of Technology, Masaryk University, Brno, Czech Republic
7. Faculty of Medicine of the Masaryk University, First Department of Neurology, Brno, Czech Republic

Corresponding author:
coleen.roger@etu.univ-amu.fr

Abstract

Background: The Hypothalamus (HT) plays a crucial role in regulating eating behaviors. Disruptions in its function have been linked to the development of weight-related disorders. Nevertheless, its characterization remains a challenge.

Objective: We assessed the structural alterations of individual HT nuclei related to eating behaviors in patients with weight-related disorders, and their association with BMI and severity of eating disorders.

Methods: Forty-four young females with normal weight (HC, n=21), restrictive anorexia nervosa (AN, n=13) and living with obesity (OB, n=10) were explored *in vivo* using 7T high resolution (0.6mm isotropic voxel) T_1 quantitative MRI. Volumes and quantitative T_1 values of individual HT nuclei were compared after whole brain normalization using non-parametric tests (corrected for multiple comparisons for groups and regions). We investigated the parameters associated with BMI and eating disorders, such as MRI parameters of HT nuclei, ghrelin and leptin levels, depression, and anxiety using multivariate non-linear partial least square (NIPALS).

Results: Both AN and OB showed higher volumes of HT relative to HC (Zscores: 0.78±1.06; 1.43±1.51). AN showed significantly higher volumes and T_1 values of the right paraventricular nucleus (PaVN) (volume Zscore:1.82±1.45; T_1 Zscore: 3.76±4.67), and higher T_1 values of the left PaVN (Zscore: 2.25±2.37) and right periventricular nuclei (Zscore: 3.73±4.81). NIPALS models showed that lower BMI in AN was associated with structural alterations of the bilateral PaVN, right anterior commissure, and left fornix (FX). Higher BMI in OB was associated with structural alterations within the right PaVN, bilateral FX, left posterior hypothalamic nucleus, right lateral hypothalamus, and right anterior hypothalamic area. Finally, severity of eating disorders was associated with larger structural alterations within the bilateral PaVN, bilateral

arcuate hypothalamic nuclei, right bed nucleus of stria terminalis, left medial preoptic nucleus, and right tubero-mammillary hypothalamic nucleus.

Conclusions: Weight-related disorders are associated with significant micro and macrostructural alterations in HT nuclei involved in eating behaviors.

Keywords

Hypothalamus, obesity, restrictive anorexia nervosa, 7T, quantitative T_1 MRI, hypothalamic nuclei, volume, leptin, ghrelin, eating disorders.

Abbreviations

AC, anterior commissure; AHA, anterior hypothalamic area; AN, young females with anorexia nervosa; ARH, arcuate hypothalamic nucleus; BECK, Beck Depression Inventory ; BNST, bed nucleus of the stria terminalis; DM, dorsomedial hypothalamic nucleus; DPEH, dorsal periventricular hypothalamic nucleus; EAT-26, Eating Attitudes Test-26; FX, fornix; GM, grey matter; HADS, Hospital Anxiety and Depression Scale; HC, young females with normal weight; HT, hypothalamus; LH, lateral hypothalamus; MM, mammillary bodies; MPO, medial preoptic nucleus; MT, mammillothalamic tracts; NIPALS, Non-Linear Partial Least Square; OB, young females with obesity; PaVN, paraventricular hypothalamic nucleus; PeVN, periventricular hypothalamic nucleus; PH, posterior hypothalamic nucleus; SC, suprachiasmatic hypothalamic nucleus; SCOFF, Sick Control One Fat Food; TM, tuberomammillary hypothalamic nucleus; VM, ventromedial hypothalamic nucleus; WM, white matter; YFAS, Yale Food Addiction Scale; ZI, zona incerta.

Introduction

The prevalence of weight-related disorders is in constant augmentation and represents a real public health problem: obesity is now considered an epidemic (1), and anorexia nervosa has the highest mortality rate of all psychiatric disorders (2). The pathophysiology of weight-related disorders is complex, affecting both energy regulation systems (lipostat/energy balance) and non-homeostatic functions involving emotion, memory, reward, palatability value, and self-regulation (3,4).

Disturbance of energy homeostasis both in anorexia nervosa and obesity primarily stems from hormonal imbalance (5,6). The anorexigenic hormone leptin is reduced in anorexia nervosa and increased in obesity (7,8). The orexigenic hormone ghrelin is increased in anorexia nervosa and reduced in obesity (8–10). However, this physiological adaptation is undeniably not associated with normal homeostatic food consumption in weight-related disorders, because both patients with obesity and anorexia nervosa show a blunted responsivity to peripheral appetite regulation (11).

The key structure orchestrating the balance between these different functions is the hypothalamus (HT), a central small brain area organized in multiple nuclei exhibiting distinct physiological and anatomical characteristics. Rodents' studies have revealed that each HT nucleus possesses a specific role in homeostatic regulation of energy, food intake, thirst, as well as body temperature, sexual dimorphism, sleep, and circadian rhythm (12). Therefore, studying the microstructural alterations in each HT nucleus is crucial to monitor their respective roles in the behavioral shifts associated with weight-related disorders *in vivo* in humans. However, translation of the cellular mechanisms observed in animal models to Human *in vivo* studies is not straightforward. In that context, neuroimaging has appeared as a game changer to explore eating behavior networks and the consequences of their dysregulation from an anatomical, functional, and metabolic point of view (4,13,14). BMI has been shown to correlate with HT

volume (15,16). However, a volume increase was only found in the left anterior-inferior and the right posterior parts of HT in adults living with obesity relative to healthy controls (16).

As of now, only one study has examined structural alterations in hypothalamic subregions in young females living with either anorexia nervosa or obesity (17). This study found a larger HT volume in young females living with obesity. It also found an atrophy of the inferior-tubular subregion in young females with anorexia nervosa. Additionally, regional structural HT alterations were associated with variations in appetite-regulating hormone levels (17). Indeed, a larger volume of posterior HT subregions was associated with an increase of leptin levels in the young females living with obesity. Meanwhile, ghrelin levels were negatively associated with the global HT volumes in the whole cohort (anorexia, obesity, and control) (17).

Overall, previous studies using magnetic fields of 3T or lower were unable to characterize individual HT nuclei due to challenging HT segmentation. Difficulties to segment HT nuclei emerge from a lack of spatial resolution and poor MRI contrast (18).

In this exploratory study, we combined the use of high resolution quantitative 3D-T_1 MRI sequence to a super-resolute atlas of HT nuclei (19) to uncover morpho-structural variations of HT nuclei, and their association to BMI and severity of eating disorders, in well-characterized cohorts of young females: with normal weight (HC), living with obesity (OB), or with restrictive anorexia nervosa (AN).

High spatial resolution multiparametric quantitative MRI (20) opens a new perspective to characterize individual HT nuclei in humans, and steadily narrows the gap in our understanding from rodent studies.

Materials and Methods

Questionnaires

The morning of the scan, all participants completed questionnaires regarding their eating behavior and presence of anxiety or depression.

- French version of the 'Sick, Control, One, Fat, Food' (SCOFF) with 5 questions used to screen for eating disorders (presence of eating disorders score ≥ 2).
- Yale Food Addiction Scale 2.0 (YFAS) measures food addiction with 35 items which assess 11 indicators of addictive behaviors, distress, and related clinical impairment (presence of food addiction if ≥ 2 symptoms with clinical impairment).
- Eating Attitudes Test-26 (EAT-26) is a self-reported measure with 26 items to identify the presence of eating disorder risk (presence of eating disorders score ≥ 20).
- Hospital Anxiety and Depression Scale (HADS) is an instrument used to screen for anxiety and depressive disorders. It consists of 14 items rated from 0 to 3 (7 relate to anxiety and 7 to depressive dimension, presence of anxiety or depression if ≥ 11 in either item).
- Beck Depression Inventory (BECK) measures the severity of clinical depression through 13 items (a score between 0 to 3 suggests an absence of depression, 4 to 7 a mild depression, 8 to 15 a moderate to moderately severe depression, and above 16 a severe depression).

Participants

A total of forty-four adult young females (age 18-35 years old) were recruited in this protocol between July 2020 and May 2024 (See participant flowchart in **supplemental Figure 1**): i) thirteen young females on the 'ill phase' of acute severe restrictive AN (BMI <17 kg/m^2, positive to the criteria defined by the Diagnostic and Statistical Manual of Mental Disorders 5), ii) ten OB (BMI ≥ 30 kg/m^2 and no life time or current medical condition that could potentially affect appetite or weight (e.g. diabetes, bariatric surgery history, GLP-1 analog, corticoids or

psychotropics treatment), and iii) twenty-one HC (18.5≤ BMI <25 kg/m^2, no life time or current medical condition that could potentially affect appetite or weight, no eating disorder defined by the EAT-26, SCOFF, and YFAS as well as no anxiety or depression evaluated by HADS and BECK. AN and OB were recruited from the Department of Endocrinology (CHU Nord and Hôpital de la Conception, AP-HM, Marseille, France), a national reference center for anorexia nervosa and obesity.

For this exploratory study, the sample size of n=44 allowed to detect differences among the three groups with a standard deviation of 1, an effect of 1.2 with a statistical power of 0.861.

All participants completed a dietary survey analyzed by a dietitian to assess total energy intake. Bioelectrical impedance analysis was performed on AN and OB to measure body composition.

Participants with contraindication to 7T MRI, at risk of non-compliance with the examination, unable to give their consent, with a history of head injury, neurosurgery, neurological pathology, psychosis or bipolar disorder or with a current addiction were not included in the study. A pregnancy test on urine sample was performed and pregnant and lactating females were excluded from the study. All participants were registered to a health insurance plan and gave their written informed consent after receiving detailed, understandable, and honest information. This protocol was in accordance with the Declaration of Helsinki and obtained ethics approval by the French Ethic Committee 'CPP EST I' (#20.02.13.47002 – IDRCB : 2020-A00340-39; Clinical trial Hypothalnet : NCT04451759).

Hormone assays

The day of the MRI exploration and after an overnight fasting period (no food or caloric beverages later than 8pm), blood samples were obtained from each participant for leptin and ghrelin dosages. Blood samples were centrifuged at 3000 g for 10 min and stored at –80°C for subsequent analysis. Plasma ghrelin (total: acylated + non-acylated) and leptin concentrations

were measured using commercially available kits from R&D Systems (Human Ghrelin DuoSet ELISA 5 plate, lot: P394826, assay range [31.3 - 2000 pg/mL], coefficient variation: 8.5%; Quantikine ELISA Human Leptin, lot: P387308, assay range [15.6 - 1000 pg/mL], coefficient variation: 5.2%). Different dilution ranges were used to obtain all measures within the detection limits. For leptin, we initially used a 1/100 dilution, as recommended by the supplier, followed by a 1/10 dilution for all anorexic patients. Ghrelin was first tested without dilution, followed by a second test with a 1/2 dilution for all patients. No specific bias was introduced, as a standard range was included in each test, and only samples within that range were analyzed. The only correction applied was the subtraction of the initial blank to obtain the standard curve.

5.2.1 *Image acquisition*

Participants were scanned once after an overnight fasting period using a 7T MR scanner with 40 participants (n_{AN}=12, n_{OB}=9, n_{HC}=19) explored on a 7T Terra MR system (Siemens Healthineers, Erlangen, Germany); and 4 participants (n_{AN}=1, n_{OB}=1, n_{HC}=2) explored on a 7T Siemens Magnetom step 2 system (Siemens Healthineers, Erlangen, Germany). Both scanners were equipped with the same (1Tx/32Rx) head coil (NOVA Medical, Wilmington, MA, USA). After an automatic 3D B_0 shimming procedure, a whole brain B_1^+ map was acquired using a spin-echo-based sequence by assessing the ratio of consecutive spin and stimulated echoes (WIP#658, Siemens Healthineers). Anatomical images were obtained using a 3D-MP2RAGE sequence (TR= 5ms, TE= 3ms, TI_1= 900ms/TI_2= 2.750ms, 256 slices, 0.6mm isotropic voxel, TA= 10min12s), already proven to be reliable and sensitive to characterize structural alterations in early multiple sclerosis (21), Parkinson disease (22) or partial epilepsy (20).

Unbiased T_1 maps and T_1-w-UNIDEN images were obtained after B_1^+ inhomogeneity correction (23). Qualitative high resolution T_2-weighted images (TSE) and 3D FLAIR were also acquired for radiological assessment of the HT in all participants. Diffusion-weighted

imaging, resting-state, and task-related fMRI acquisitions were also performed for in the context of a larger research protocol, but at lower spatial resolution (1.2mm isotropic voxel) limiting the possible use of these data for the current objective aiming to obtain a precise morpho-structural characterization of individual HT nuclei (See the whole study protocol in **supplemental Table 1**).

Image processing

Image quality and registration were evaluated independently by two experienced raters (CR, JPR) based on a continuous scale [0-5] obtained for 8 items (maximum global score of 40) evaluating i) the quality of T_1w-UNIDEN images, ii) quality of qT_1 maps, iii) quality of registration of MDA template onto T_1w-UNIDEN images and iv) quality of parcellation of 5 anatomically identifiable hypothalamic regions: fornix, mammillary bodies, mammillary-thalamic tracts, paraventricular nuclei and arcuate nuclei. The inter-rater reliability between the two raters was evaluated using the intra-class correlation coefficient (ICC) (**supplemental data Figure 2**). The T_1 values of grey matter (GM) and white matter (WM) masks for each participant were obtained by segmenting the T_1-weighted images using SPM12 (threshold >0.5) and applying the segmentation to the whole-brain unbiased T_1 maps. Whole brain volume (WBV) of each participant was obtained using fslbet (24). Automated segmentation of HT nuclei was performed using a similar procedure to that described by Brun and colleagues (25) for segmenting various nuclei of the basal ganglia using precise coregistration of high resolution 7T-MRI template and atlas (**Figure 1**, See the method in **supplemental data Figure 3**). The predefined open source 'MDA_990HCP_t1_MNI152b_0.5' MRI high-resolution template (0.5mm isotropic voxel) associated with the Neudorfer atlas obtained by manual segmentation of two experienced raters were employed (19). This high-resolution template was derived from datasets of 990 participants extracted from the HCP1200 data release, normalized to the

'MNI152b' space using a minimum deformation averaging (MDA) pipeline (19). The reliability of the atlas, reported in the seminal paper as a measure for voxel-wise volume overlap among two different raters, was described in (19). They reported acceptable margins of error in DICE similarity coefficients (mean ± SD = 0.63 ± 0.19) and Hausdorff distances (mean distance=1.44 ± 0.67 mm) for hypothalamic nuclei (19). In addition, to improve spatial registration centered on the hypothalamus, the T_1-weighted template was cropped using the following limits in the z axis: up-down = corpus callosum–pons; left-right = left insula-right insula; anterior-posterior = genu-splenium to obtain the 'cropped-MDA_990HCP_t1_MNI152b_0.5' template and the 'cropped-Neudorfer-Atlas'. Similar cropping was applied to the B_1^+ corrected T_1w-UNIDEN MP2RAGE images and T_1 maps for each participant. The 'cropped-MDA_990HCP_t1_MNI152b_0.5' template was then coregistered to the B_1^+ corrected 'cropped-T1w-UNIDEN MP2RAGE' of each participant by estimating non-linear warp (https://github.com/ANTsX/ANTs/blob/master/Scripts/antsRegistrationSyNQuick.sh) (**supplemental code**). Mutual information was used for rigid and affine steps, and cross-correlation for the last BSplineSyN transformation (gradientStep = 0.1, Correlation window radius=4). The corresponding spatial transform was applied to the 'cropped-MDA_990HCP_t1_MNI152b_0.5' and the 'cropped-Neudorfer-Atlas' (See supplemental data for the script).

Finally, we used the function 'Segmentation/Volumes and Statistics' of the ITK-SNAP toolbox to extract volumes and T_1 values from HT nucleus masks derived from the coregistered atlases applied to cropped-T_1 maps of individual participants and the whole brain volume derived from the brain mask extracted using fslbet. The global hypothalamic volume included the inner nuclei segmented with Neudorfer atlas.

For each subject, volumes of HT nuclei were normalized by their WBV. Then, Z-scores of normalized volumes and T_1 values of HT nuclei were computed using the control's mean and

standard deviation (Z-score done on 19 controls for the Terra MR scanner and 11 controls for the Magnetom MR scanner).

Statistical analysis

Differences of age, BMI, behavioral scores, leptin and ghrelin concentrations, whole brain volume, GM and WM T_1 values, HT volume, right and left HT volumes as well as structural HT nuclei parameters between AN, OB and HC were assessed by non-parametric tests with post-hoc corrections using the Steel-Dwass procedure (JMP 16). Additionally, we applied false discovery rate (p_{FDR} <0.05) to correct for the number of HT nuclei.

The inter-rater reliability was evaluated using the intra-class correlation coefficient (ICC) (EMP Measurement System Analysis platform, JMP16 pro) with global scores as responses, subjects as samples and raters as grouping variable.

To deal with data characterized by multicollinearity, we used multivariate Non-Linear Partial Least Square (NIPALS) analyses to determine the leading parameters associated with weight disorders including appetite-regulating hormones levels, behavior scores and MRI parameters of HT nuclei in the (AN+HC) and (OB+HC) cohorts.

A second NIPALS analysis was conducted in the whole cohort of participants (AN+OB+HC) to determine the potential association of MRI parameters of HT nuclei with the severity of eating disorders (EAT-26 scores) (**supplemental figure 4)**. Both models were constructed in two steps. First all parameters were integrated in the model and a first selection of variables was conducted according to variables' effect threshold of 1.2. The NIPALS algorithm was re-applied using these selected variables using a threshold of effect of 1. Explained variance of the model, importance (effect) and coefficients of variables were reported.

Results

General features

We did not find any significant difference between groups for age, total plasmatic ghrelin levels, WBV and T_1 values in whole brain GM and WM (**Table 1, supplemental figure 5**). In line with the inclusion criteria, BMI were significantly different between groups, with $BMI_{AN} < BMI_{HC}$ ($p<0.0003$) and $BMI_{OB} > BMI_{HC}$ ($p<0.0002$). Plasmatic leptin levels were significantly higher in OB compared to HC ($p<0.0003$) and lower in AN compared to HC ($p<0.0001$). OB showed higher percentages of fat mass compared to AN ($p<0.0004$), while percentages of lean mass were higher in AN relative to OB ($p<0.0004$). Relative to HC, AN showed a higher percentage of carbohydrates ($p=0.0022$) and lower percentages of lipids ($p=0.0046$) intake, higher eating disorders scores (EAT26 $p<0.0001$, SCOFF $p<0.0001$, YFAS symptom counts $p<0.0009$, YFAS diagnosis $p<0.0002$), anxiety (HADS anxiety $p=0.0022$), depression scales (BECK $p<0.0001$; HADS depression $p=0.003$). Relative to HC, OB also showed higher eating disorders (EAT26 $p=0.0335$), anxiety (HADS anxiety $p=0.0087$) and depression (HADS depression $p=0.0178$, BECK $p=0.0175$) scores (Table 1). The medians and ranges of global quality scores of imaging data for rater 1 and rater 2 were 39 [33-40] and 38 [31-40] respectively, with an ICC (including bias) of 0.9742.

Altered morphometric and microstructure patterns of HT nuclei in restrictive anorexia nervosa

The volume of the global HT (Zscore: 0.780±1.059; $p=0.0246$) **(Figure 2A)** and right HT (Zscore: 0.916±1.150; $p=0.0099$) **(Figure 2B)** was higher in AN**.** At the nucleus level, AN showed higher volumes of the right PaVN (Zscore: 1.824±1.455; $p_{FDR}=0.0009$) and left Fx (Zscore=1.451±1.248; $p_{FDR}=0.0022$) **(Figure 3A)**; and higher T_1 values within right PaVN (Zscore: 3.761±4.477; $p_{FDR}=0.0017$), left PaVN (Zscore: 2.249±2.367; $p_{FDR}=0.0036$) and right periventricular hypothalamic nucleus (PeVN) (Zscore: 3.734±4.811; $p_{FDR}=0.0041$) relative to

HC (**Figure 3B**) (**supplemental data Figure 6**).

Partial least square analysis conducted in the (AN+HC) cohort (explained variance of 74.1% using 13 variables) showed that the severity of weight disorders in AN (lower BMI scores) was associated with i) lower T_1 values of the right PaVN [beta=0.0129, effect size=0.8968] and the right AC [beta=0.2683, effect size=1.0624], higher T_1 values of the left PaVN [beta=-0.0219, effect size=0.8782], higher volumes of the left FX [beta=-0.1308, effect size=0.8537] and the right PaVN [beta=-0.0085, effect size=0.9089], ii) eating behavior scores (SCOFF [beta=-0.2435, effect size=1.4043]; EAT-26 [beta=-0.1365, effect size=1.1647]; YFAS diagnosis scores [beta=-0.0386, effect size=0.9778]; YFAS symptom counts [beta=-0.0495, effect size=0.8782]), iii) more severe depression (BECK scores [beta=-0.0710, effect size=1.0614]) and anxiety (HADS anxiety scores [beta=-0.1245, effect size=0.9770]), iv) lower plasmatic leptin levels [beta=0.1139, effect size=0.9002] and higher plasmatic ghrelin levels [beta=-0.2191, effect size=0.8881] (**Figure 4A**).

Alterated morphometric and microstructure patterns of HT nuclei in obesity

Relative to HC, OB showed higher volume of the global HT (Zscore: 1.434±1.515; p= 0.0039) (Figure 2A), right HT (Zscore: 1.530±1.468; p=0.0032) (Figure 2B) and left HT (Zscore: 1.187±1.486; p=0.0083) **(Figure 2C)**. However, no observed differences in the macrostructure of HT nuclei in OB relative to HC survived FDR multiple comparison corrections (Figure 3A) (supplemental data Figure 6).

Partial least square analysis conducted in the (OB+HC) cohort (explained variance of 68.5% using 14 variables) showed that the severity of weight disorders in OB (higher BMI scores) was associated with higher alterations of i) higher T_1 values of the right PaVN [beta=0.0611, effect size=0.8048] and higher volumes of left PH [beta=0.0712, effect size=0.9380], left FX [beta=0.0636, effect size=0.8380], right FX [beta=0.0627, effect size=0.8261], right AHA

[beta=0.0627, effect size=0.8257], right LH [beta=0.0611, effect size=0.8049], ii) eating behavior scores (EAT26 [beta=0.0956, effect size=1.2601]; SCOFF [beta=0.0711, effect size=0.9362]; YFAS symptom counts [beta=0.0631, effect size=0.8317]), iii) more severe depression (BECK scores [beta=0.0928, effect size=1.2232]; HADS depression [beta=0.0921, effect size=1.2139]) and anxiety (HADS anxiety [beta=0.0993, effect size=1.3087]), and iv) higher plasmatic leptin levels [beta=0.1088, effect size=1.4332] and plasmatic ghrelin levels [beta=0.0620, effect size=0.8171] (**Figure 4B**).

Association between severity of eating disorders (EAT-26) and MRI parameters of HT nuclei

Partial least square analysis conducted in the whole cohort (AN+OB+HC) using only MRI parameters of HT nuclei (explained variance of 51.08% using 10 variables) showed that the severity of eating disorders (EAT-26 score) was associated with larger micro and macrostructural alterations within the bilateral PaVN (Zscore_Vol_R_PaVN [beta=0.1024, effect size=1.2090]; Zscore_T_1_R_PaVN [beta=0.0854, effect size=1.0080]; Zscore_T_1_L_PaVN [beta=0.0945, effect size=1.1154]), the bilateral ARH (Zscore_Vol_L_ARH [beta=0.0783, effect size=0.9246], Zscore_Vol_R_ARH [beta=0.0799, effect size=0.9434]; Zscore_T_1_R_ARH [beta=0.0879, effect size=1.0382]), the right BNST (Zscore_T_1_R_BNST [beta=0.0748, effect size=0.8827]), the left MPO (Zscore_Vol_L_MPO [beta=0.0869, effect size=1.2060]), and the right TM (Zscore_T_1_R_TM [beta=0.0730, effect size=0.8616]) (**Figure 4C**).

Discussion

The current study shows that quantitative T_1 relaxometry derived from 7T MRI is sensitive enough to investigate *in vivo* morphological and microstructural alterations of individual HT nuclei in weight-related disorders. To our knowledge, this is the first study characterizing those alterations with such high granularity. It was achieved by means of registration of high-resolution *in vivo* anatomical atlas of human hypothalamic nuclei on individual subjects (19). This was applied on carefully selected young female participants according to age and sex, and constrained to a 15h fasting period. No global microstructural brain effect was observed in whole brain WM and GM of AN and OB relative to HC, however, we observed specific alterations in HT. This suggests that the observed alterations in micro and macrostructural features are not associated with a widespread phenomenon, but that they are specific to the HT. Thus, in addition to higher HT volumes present in both AN and OB, we observed significant micro and macrostructural alterations in individual HT nuclei involved in eating behavior networks (PaVN, PeVN) in AN. Furthermore, lower BMI scores in AN were associated with larger micro and macrostructural alterations of bilateral PaVN, right AC and left FX, lower plasmatic leptin levels, higher plasmatic ghrelin levels, greater severity of eating behaviors, depression, and anxiety. In contrast, higher BMI scores in OB were associated with greater micro and macrostructural alterations of right PaVN, right LH, right AHA, left PH and bilateral FX, higher plasmatic leptin and ghrelin levels, greater severity of eating behaviors, depression, and anxiety. Finally, the severity of eating disorders was associated with enhanced alterations within bilateral PaVN, bilateral AN, right BNST, left MPO, and right TM.

Macrostructural and microstructural fingerprinting of HT nuclei in restrictive anorexia nervosa

Previous works have shown that anorexia nervosa was associated with a pattern of lower HT and global brain volumes (26,27). Nevertheless, most previous studies showed that these morphological alterations in the HT did not remain after intracranial volume normalization (11,16). In contrast, in this well-controlled cohort of AN, we observed higher volumes of the global HT after normalization by the whole brain volume. High hypothalamic volume could be associated with hypothalamic inflammation, which is a well-known factor in the development of anorexia-cachexia syndrome (28). Focusing on individual HT nuclei, AN showed higher volume of the right PaVN, and higher T_1 values within bilateral PaVN, and right PeVN, possibly reflecting local inflammation. In addition, the partial least square analysis conducted on the (AN+HC) cohort, showed the association of the severity of restrictive anorexia nervosa (reflected by the lower BMI scores) with PaVN and FX higher volumes, as well as lower plasmatic leptin concentrations. Structural and functional alterations of PaVN may have major impacts on energy homeostasis since PaVN stimulation was found to inhibit food intake (29). Thus, the exchange of information between the PaVN and ARH is essential for translating nutritional signals received by the HT into actionable signals that induce metabolic alterations (30). For example, stimulation of POMC/CART neurons in the ARH releases excitatory neurotransmitters alpha-MSH in the PaVN which activate ^{PaVN}MC3/4R, resulting in reduced food intake.

An alternative hypothesis is that inflammation and mitochondrial dysfunction may alter structural connectivity between PaVN and ARH in anorexia nervosa. This altered connectivity associated with fewer fibers could trigger an aberrant glutamatergic response to food intake (14,31,32). Our results are in line with disturbances of signaling pathway between PaVN and ARH in restrictive anorexia nervosa. Interestingly, PaVN alterations and severity of depression and anxiety scores were associated with weight-disorder severities of both anorexia nervosa and obesity. As the primary driver of hypothalamo–pituitary–adrenocortical (HPA) responses, PaVN seems to be involved in handling the demands of chronic stress exposure (33). Therefore,

dysfunctions of PaVN due to inflammatory processes may induce dysfunctions of the emotional-stress systems with altered expression in PaVN of arginine vasopressin, oxytocin, neuropeptide S or orexin receptors (34).

Concurrently, PeVN belongs to the eating behavior control system and is regulated by the neocortex and the limbic system. Its activity is influenced by hippocampal outflow, which is balanced by low-affinity and high-affinity glucocorticoid receptors (35). Thus, inflammation of PeVN observed by 7T MRI might influence the allocation of energy and may play a central role in the pathogenesis of anorexia nervosa (35). Moreover, association between lower BMI and higher left FX volume observed in the present study suggests the presence of inflammation in specific WM tracts of AN. As FX is particularly involved in reward processing, damage of these WM tracts may reflect the reduced capacity for reward (anhedonia) reported in severe restrictive anorexia nervosa (36). Numerous studies using diffusion-weighted MRI have demonstrated the presence of microstructural alterations (i.e., increased mean diffusivity and reduced fractional anisotropy) within the FX in anorexia nervosa (37–39) which can be reversed by brief weight restoration therapy (40). Furthermore, we found that leptin, which stimulates POMC/CART neurons (41), shows lower levels in AN compared to HC. The role of leptin is to signal to the brain a reduction in stored energy to initiate metabolic responses and conserve energy to allow survival (42). This finding is in line with the decrease in body fat mass and very low leptin blood levels reported in anorexia nervosa patients compared to healthy controls (43).

Macrostructural and microstructural fingerprinting of HT nuclei in obesity

In this limited sample of OB patients (n=10), we were only able to observe higher global HT volume relative to HC, which is in line with other studies using much larger cohorts (17,44). Higher macrostructural HT volume can be a symptom of more intricate alterations in cellular processes. Indeed, studies on brain samples from rodents and *postmortem* humans have linked

higher HT T_2-w signal intensity in obesity to the proliferation and activation of microglia and astrocytes (45,46). Modification of T_2-weighted signal was strongly associated with systemic low-grade inflammation (47). Indeed, during inflammation, astrocytes accumulate water through aquaporin-4 which increases T_2-weighted signal intensity (48). Furthermore, numerous studies on rodents reported that high fat diet (HFD) exposure triggers chronic low-grade HT inflammation with insulin and leptin resistance (49,50). Over time, this localized inflammation impairs the sensing of anorexigenic signals, potentially disrupting brain circuits regulating the balance between energy intake and energy expenditure. This disruption promotes weight gain and leads to obesity (51).

Nevertheless, we did not observe any significant differences in micro and macrostructural characteristics at the level of HT nuclei. This may be due to the limited statistical power from the sample size of OB participants (n=10). However, in the (OB+HC) cohort, the partial least square analysis demonstrated an association between the morbid augmentation of BMI scores and higher plasmatic leptin and ghrelin levels, greater severity of eating behaviors, depression, and anxiety, as well as larger volumes and/or T_1 value alterations of the right LH, right PaVN, right AHA, left PH, and bilateral FX. Indeed, the LH is known as the ‘hunger center’ since its stimulation leads to an increase in food intake (29). Numerous studies have demonstrated that a fat-rich diet is associated with inflammation and a resistance to anorexigenic signals in the HT (49). Therefore, dependence between increased volumes of the LH and BMI scores in OB may indicate a progressive, inflammation-mediated, disruption of the integration of anorexigenic signals in the LH. This disruption could induce the observed altered eating behavior. Moreover, LH neurons are integrative sites for signals involved in the motivation to eat (52). Indeed, experiments on the LH revealed its role in adjusting self-stimulation behavior based on feeding, suggesting its involvement in reward-seeking behavior usually found in obesity (53). Additionally, the LH seems to contribute to the processing of food palatability since it is involved in forming conditioned preferences and aversions to tastes based on

gustatory stimuli (54–56). Furthermore, the LH has recently been involved in non-homeostatic feeding. The latter is linked to overconsumption of food independently of satiety levels, biased toward palatable foods (57). These findings suggest the involvement of the LH in the overconsumption of food, the leading factor for obesity in our modern world (58). In addition, while the LH is one of the main targets of ghrelin projections and is believed to mediate ghrelin-induced hyperphagia (59). The impact of higher ghrelin concentrations on BMI scores in the present study could illustrate enhancement by ghrelin of the reward value of a high-fat diet through an orexin pathway connecting the LH and ventral tegmental areas (60). As stated before, the PaVN plays a critical role in energy homeostasis as its stimulation was found to inhibit food intake (29). Its dysfunction could promote food overconsumption, as shown by the observed higher EAT-26, SCOFF, and YFAS scores, associated with higher BMI scores in OB. The observed high plasmatic leptin concentrations reflect the resistance to leptin that fails to promote satiety in obesity (8).

Nevertheless, individual HT nuclei present significant functional overlap and extensive coordination. Furthermore, the diverse range of functions attributed to a single HT nucleus can be attributed to the heterogeneous population of neurons it contains. For example, subtypes of orexigenic agouti-related peptide neurons in the arcuate nucleus (^{ARH}AgRP) show distinct transcriptional responses to fasting. This suggests they may represent separate populations, which may respond specifically to different energy states (61). Similarly, the diverse populations of neurons in the LH enable this nucleus to coordinate a range of essential behaviors, including sleep, wakefulness, feeding, stress, and motivated actions (62).

Association of MRI HT parameters with the severity of eating disorders

Presently, the severity of eating disorders (EAT-26 score) was associated with higher volumes and/or higher T_1 values not only of PaVN, ARH, and right BNST, but also of the MPO and

TM. As discussed, the first three HT nuclei (PaVN, ARH and right BNST) are the main hypothalamic centers responsible for regulating food-related homeostasis (63). They were reported to exhibit the largest structural and connectivity differences in adults with anorexia nervosa and obesity, with respect to healthy controls (14,16,17). In contrast, MPO and TM have been reported to be primarily involved in arousal, wakefulness, and sleep (64). The latter is known to be altered in eating disorders (65).

Limitations

There are several limitations to this study. First, we recruited unequal cohort sample sizes, with a particularly small sample size of OB (n=10), due to very strict inclusion criteria, with great care for age, sex, and conditions (15h fasting, blood sample collection, morning scan) control. Therefore, longitudinal studies and larger sample sizes are warranted to determine the sensitivity of variation in repeated measurements relative to the differences between cohorts and/or treatment effects. The absence of significant differences in ghrelin levels could be explained by the fact that at the time of 7T MRI assessment, there were no significant differences in total energy intake between cohorts. Indeed, we conducted scans on AN during their hospitalization in which they complied with a diet rich in carbohydrate, lipid, and protein, relative to the patients' weight and energy requirements. Furthermore, inclusion of patients with very high BMI was not possible according to the mechanical constraints related to the 60cm diameter of the 7T bore.

Although we found some altered morpho-structural common to both AN and OB, it is interesting to observe that HT alterations are pathology-specific and closely related to HT nuclei function in feeding. Ultimately, we showed that conclusive results can be obtained with fewer participants than previously required before the advent of 7T MRI. This opens new perspectives

for MRI studies, specifically those involving integrative multimodal protocols which are common in appetite-related research.

Among the forty-four scans, four were performed on a different 7T MR scanner. However, the same head coil and similar MRI sequences were used. Furthermore, B_1^+ corrections of quantitative maps minimized inter-scanner and inter-subject biases, revealing subtle microstructural differences in HT nuclei. However, it is important to note that the granularity of our investigation cannot be directly applied using magnetic field lower than 7T, which makes it currently challenging to apply this as a diagnostic tool in a clinical setting.

Although numerous studies have linked higher volume and T_1 values to inflammation, the exact cellular processes responsible for such alterations are still speculative. Furthermore, the cross-sectional design of the protocol limits its ability to determine whether HT alterations in AN and OB are causal or consequential. However, animal experiments have shown that HT inflammation precedes body weight gain (66).

In conclusion, we assessed specific micro and macrostructural alterations of individual HT nuclei involved in eating behavior networks and found relationships between these alterations with leptin levels, eating disorders, and anxiety and depression scores, in AN and OB. Future prospective studies will look into larger cohorts and integrate these morpho-structural findings with structural and functional connectivity, as well as activations patterns related to food-cues in AN and OB.

We believe this present study is a first step towards a more comprehensive characterization of HT nuclei. This is crucial for understanding how eating behavior circuits become maladaptive and recover after therapy both in AN and OB. More specifically, a better characterization of eating behavior circuits could help decipher how GLP-1 agonists modulate these networks in females living with obesity. Ultimately, this could enable early prognosis of treatment efficacy and promote better understanding of partial or complete non-responders.

Acknowledgments

CR, BG, AD, MG, PD, FY, MPR, PJC, JPR designed research; CR, AL, LP, PA, JPR conducted research; CR and JPR analyzed data, CR and JPR wrote the paper. HD and AK helped with preprocessing. CR and JPR had primary responsibility for final content. All authors read and approved the final manuscript. We thank Timothy Anderson for his contribution to proofreading this manuscript.

Data availability: Data described in the manuscript, code book, and analytic code will be made available upon request pending [application and approval].

Funding: *CR has received a PhD grant from EUR Neuroschool (ANR-17-EURE-0029), and* Agency for Science, Technology and Research, Singapore *(A*STAR).*

*This work received the support of the Merlion Program Campus France (*PHC MERLION 2019 # 43654ZK*) and the A*STAR.*

*The project leading to this publication has received funding from the French government under the "France 2030" investment plan managed by the French National Research Agency (reference : ANR-16-CONV000X / ANR-17-EURE-0029) and from Excellence Initiative of Aix-Marseille University - A*MIDEX (AMX-19-IET-004, 7TEAMS Chair).*

This work was performed by a laboratory member of France Life Imaging network (grant ANR-11-INBS-0006).

Author Disclosures: Jean-Philippe Ranjeva reports financial support was provided by French National Research Agency. Jean-Philippe Ranjeva reports financial support was provided by Excellence Initiative of Aix-Marseille University. Jean-Philippe Ranjeva reports financial support was provided by PHC MERLION 2019. Coleen Roger reports financial support was

provided by EUR Neuroschool. If there are other authors, they declare that they have no known competing financial interests or personal relationships that could have appeared to influence the work reported in this paper.

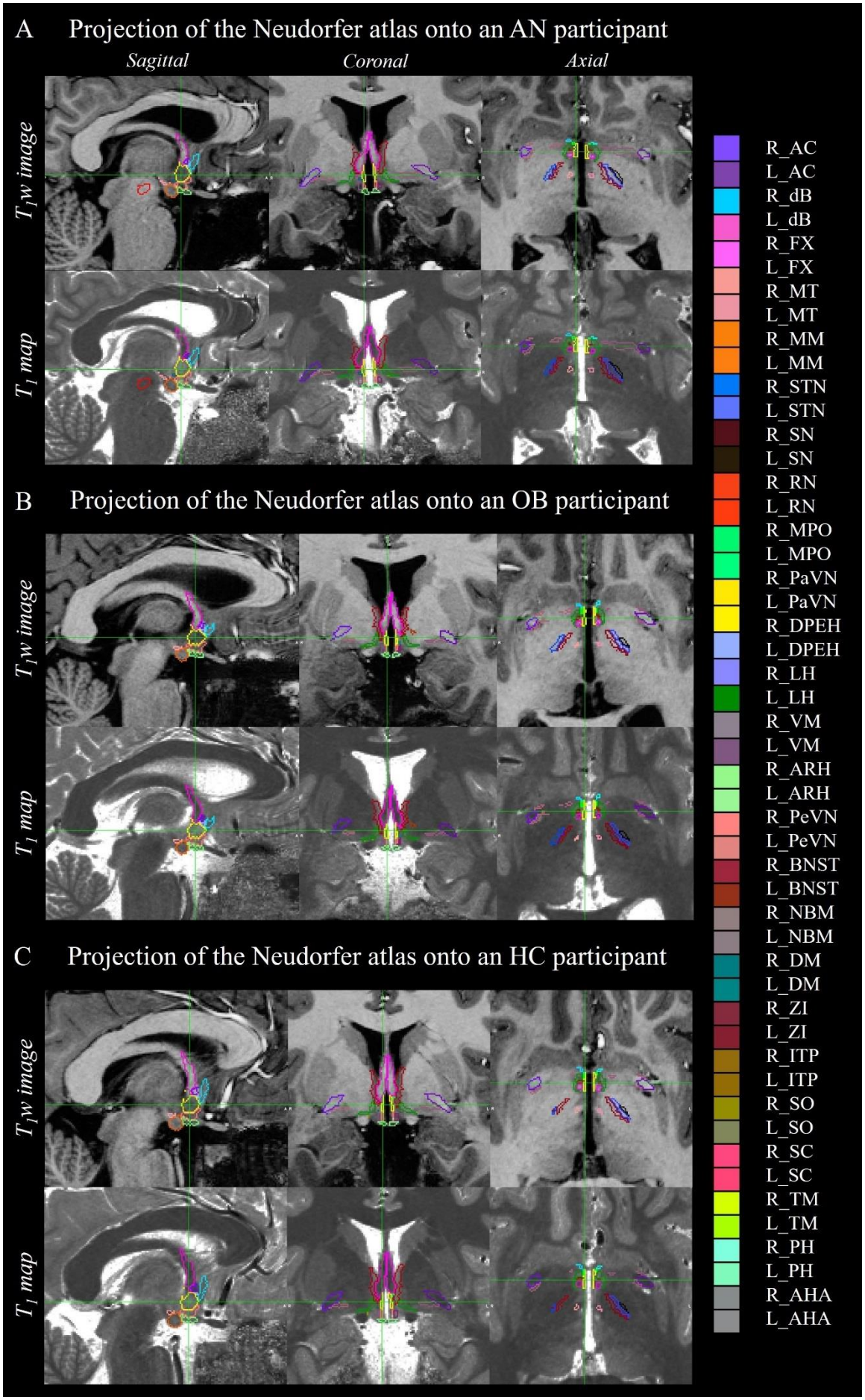
A Projection of the Neudorfer atlas onto an AN participant
Sagittal
Coronal
Axial
T1w image
T1 map
B Projection of the Neudorfer atlas onto an OB participant
T1w image
T1 map
C Projection of the Neudorfer atlas onto an HC participant
T1w image
T1 map
R_AC
L_AC
R_dB
L_dB
R_FX
L_FX
R_MT
L_MT
R_MM
L_MM
R_STN
L_STN
R_SN
L_SN
R_RN
L_RN
R_MPO
L_MPO
R_PaVN
L_PaVN
R_DPEH
L_DPEH
R_LH
L_LH
R_VM
L_VM
R_ARH
L_ARH
R_PeVN
L_PeVN
R_BNST
L_BNST
R_NBM
L_NBM
R_DM
L_DM
R_ZI
L_ZI
R_ITP
L_ITP
R_SO
L_SO
R_SC
L_SC
R_TM
L_TM
R_PH
L_PH
R_AHA
L_AHA

Figure 1: Projection of the Neudorfer atlas on individual T_1 weighted images and unbiased T_1 maps for young females living with anorexia nervosa (A), obesity (B) and healthy control (C) (resolution $(0.6\ mm)^3$). The top images represent the delineated nuclei on T1 weighted images, and the bottom images display the delineated nuclei on unbiased T_1 maps.

Abbreviations: A*C, anterior commissure; AHA, anterior hypothalamic area; AN, arcuate nucleus; BNST, bed nucleus of stria terminalis; dB, diagonal band of Broca; DM, dorsomedial hypothalamic nucleus; DPEH, dorsal periventricular hypothalamus; FX, fornix; ITP, inferior thalamic peduncle; LH, lateral hypothalamus; MM, mammillary bodies; MPO, medial preoptic nucleus of the hypothalamus; MT, mammillothalamic tract; NBM, nucleus basalis of Meynert; PaVN, paraventricular nucleus; PeVN, periventricular nucleus; PH, posterior hypothalamus; RN, red nucleus; SC, suprachiasmatic nucleus; SN, substantia nigra; SO, supraoptic nucleus; STN, subthalamic nucleus, TM, tuberomammillary nucleus; VM, ventromedial nucleus; ZI, zona incerta.*

Table 1. General features of study participants (n=44).

	AN (n= 13)	OB (n= 10)	HC (n= 21)
Age (years)	21±6.24[18-34]	26.5±3.53[23-33]	25±4.03[19-34]
BMI ($kg.m^{-2}$)	15±1.16 [13.10-16.98]	36.33±4.52 [31.43-42.87]	20.94±1.98 [18.56-24.91]
Leptin (pg/ml)	940±866.15 [128-2702]	76866±24479.39 [44164-119215]	14957±13795.9 [4210-59098]
Ghrelin (pg/ml)	240±4256 [56-15264]	221±988.04 [56-3125]	222±141.76 [45-653]
Calorie intake (Kcal)	1850±605.33 [717-2269]	1941±521.04 [1380-3025]	1922±300.76 [1380-2501]
Lipids (%)	28±7.26 [15.6-40.2]	39±5.38 [25-42.5]	42.05±15.06 [31.4-52.7]
Proteins (%)	18±3.58 [11.6-26]	14±2.46 [12-19]	19±1.91 [15.8-19.2]
Carbohydrates (%)	51.5±7.79 [43-67.6]	46±7.05 [39.9-63]	36.75±12.94 [27.6-45.9]
Fat mass (%)	7±6.17 [3-20]	49.5±4.94 [38-51]	NA
Lean mass (%)	87.5±5.82 [75-91]	47.5±4.37 [45-57]	NA
SCOFF	4±1.11[1-5]	1±0.7[0-2]	0±0.4[0-1]
YFAS # symptoms	4±1.44[2-6]	2±3.51[0-11]	0±1.34[0-5]
YFAS diagnosis	1±0.51[0-1]	0±0.32[0-1]	0±0[0-0]
EAT26	44±15.87 [7-64]	13±13.55[4-47]	5±4.87[0-17]
HADS anxiety	10±5.04[2-20]	10.5±4.85[4-19]	5±2.41[0-9]

HADS depression	8±4.78[0-14]	6±6.23[0-18]	1±2.86[0-10]
BECK	14±6.05[4-23]	8.5±7.49[0-22]	2±2.77[0-8]
WM T_1	1200.1±38.28 [1139.09-1284.02]	1188.7±33.06 [1158.34-1276.94]	1175.6±33.16 [1135.4-1254.7]
GM T_1	1776.78±60.16 [1693.91-1939.46]	1755.93±62.32 [1701.86-1915.56]	1761.15±51.28 [1705.27-1916.01]

The values are displayed as the median ± standard deviation [min-max]. *Abbreviations: AN, young females with anorexia nervosa; BECK, Beck Depression Inventory (a score between 0 to 3 suggests an absence of depression, 4 to 7 a mild depression, 8 to 15 a moderate to moderately severe depression, and above 16 a severe depression); BMI, body mass index; EAT-26, Eating Attitudes Test-26 (presence of ED score ≥ 20); GM, grey matter; HADS, Hospital Anxiety and Depression Scale (presence of anxiety or depression score ≥ 11 in either items); HC, young females with normal weight; OB, young females with obesity; SCOFF, Sick, Control, One, Fat, Food (presence of ED score ≥ 2); WM, white matter; YFAS, Yale Food Addiction Scale 2.0 (presence of ED score if diagnosis ≥ 2.*

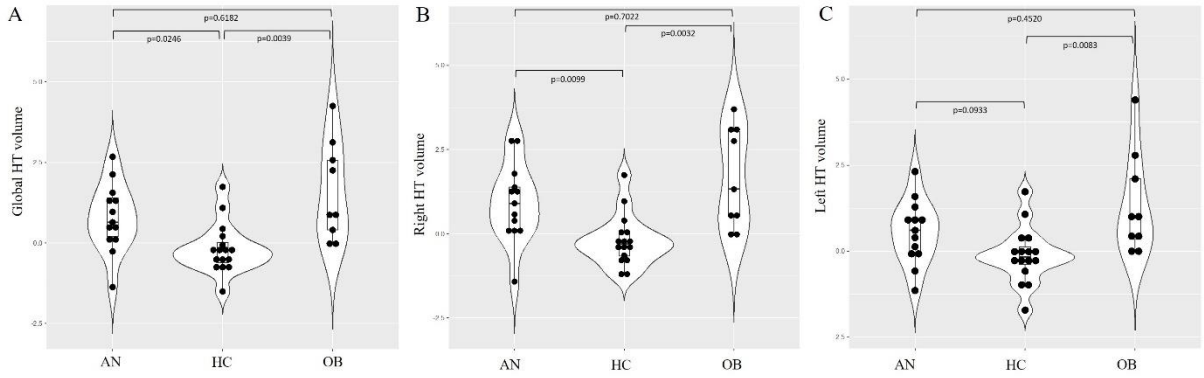

Figure 2: Global, right and left hypothalamic volume in AN, HC and OB.

Non-parametric tests corrected for multiple comparisons using the Steel-Dwass all pairs procedure (JMP 16 pro) were used to compare between AN, HC and OB groups the following parameters: A) global hypothalamic volume, B) right hypothalamic volume, C) left hypothalamic volume.

A

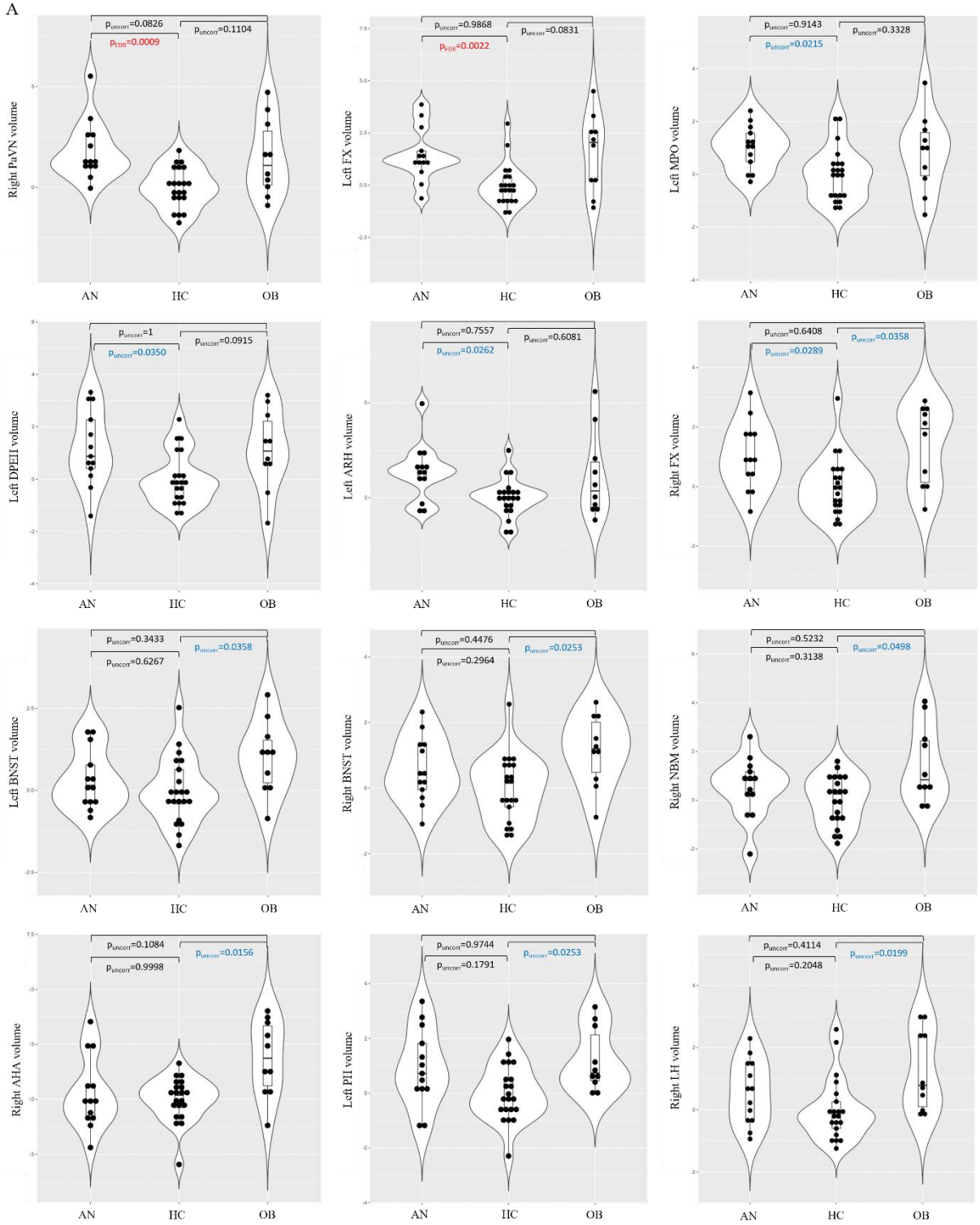
Right PaVN volume
p_{uncorr}=0.0826
p_{FDR}=0.0009
p_{uncorr}=0.1104
Left FX volume
p_{uncorr}=0.9868
p_{FDR}=0.0022
p_{uncorr}=0.0831
Left MPO volume
p_{uncorr}=0.9143
p_{uncorr}=0.0215
p_{uncorr}=0.3328
Left DPEH volume
p_{uncorr}=1
p_{uncorr}=0.0350
p_{uncorr}=0.0915
Left ARH volume
p_{uncorr}=0.7557
p_{uncorr}=0.0262
p_{uncorr}=0.6081
Right FX volume
p_{uncorr}=0.6408
p_{uncorr}=0.0289
p_{uncorr}=0.0358
Left BNST volume
p_{uncorr}=0.3433
p_{uncorr}=0.6267
p_{uncorr}=0.0358
Right BNST volume
p_{uncorr}=0.4476
p_{uncorr}=0.2964
p_{uncorr}=0.0253
Right NBM volume
p_{uncorr}=0.5232
p_{uncorr}=0.3138
p_{uncorr}=0.0498
Right AHA volume
p_{uncorr}=0.1084
p_{uncorr}=0.9998
p_{uncorr}=0.0156
Left PH volume
p_{uncorr}=0.9744
p_{uncorr}=0.1791
p_{uncorr}=0.0253
Right LH volume
p_{uncorr}=0.4114
p_{uncorr}=0.2048
p_{uncorr}=0.0199
AN
HC
OB

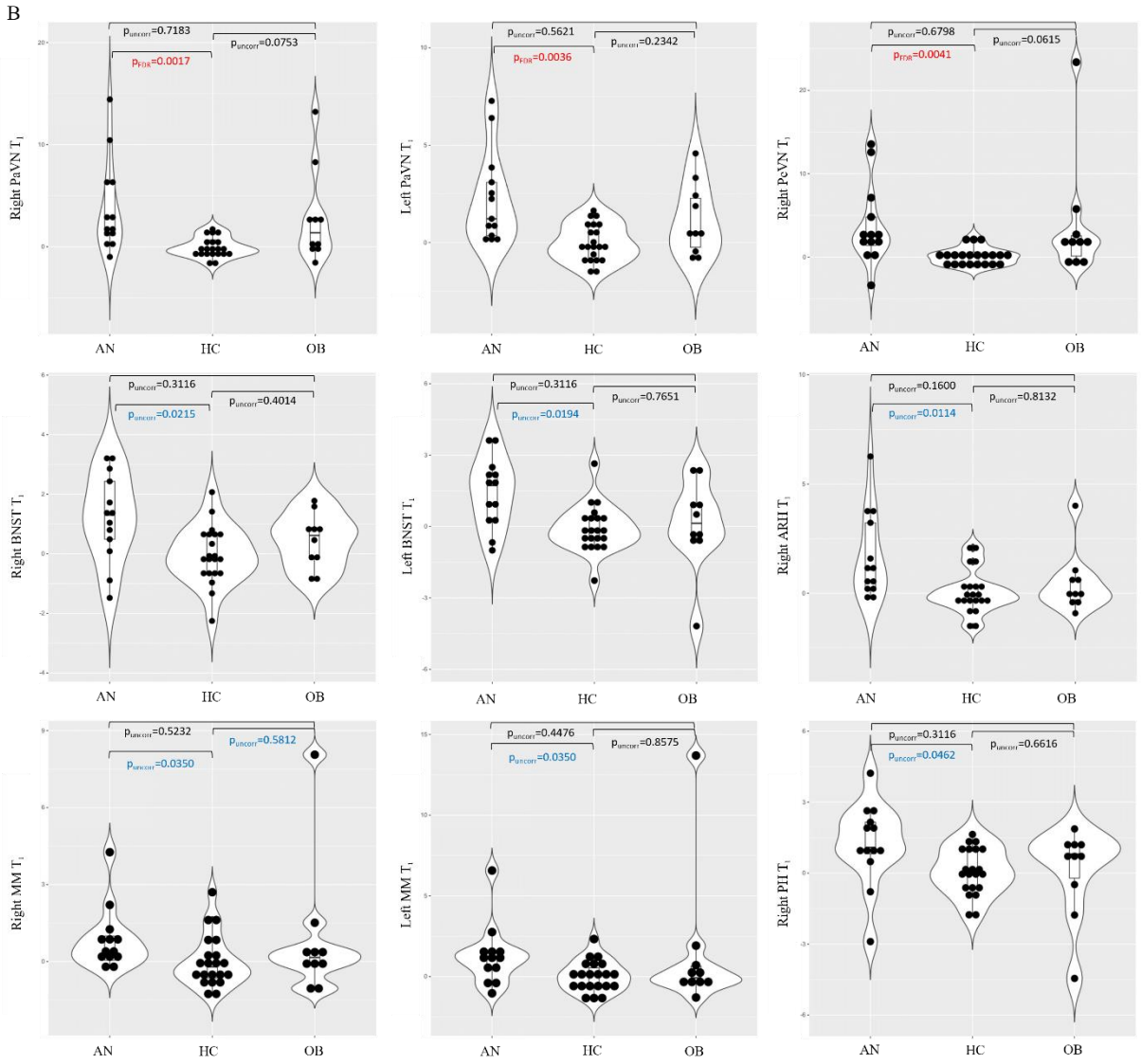

Figure 3: Macrostructural (A) and microstructural (B) modulation of hypothalamic nuclei in AN and OB relative to HC.

A) Relative to HC, AN showed significant increase (p_{FDR}<0.05) in the volumes of right PaVN and left FX while the observed differences in left ARH, left MPO, left DPEH and right FX did not survive multiple comparison corrections (p_{uncorr}<0.05). B) AN showed significant increase in T_1 values (p_{FDR}<0.05) in bilateral PaVN and right PeVN while differences observed in bilateral BNST, right ARH, bilateral MM, and right PH did not survive multiple comparison corrections (p_{uncorr}<0.05).

B) Relative to HC, OB did not show significant difference remaining after multiple comparison correction but only trends of increases (p_{uncorr}<0.05) in the volumes of right FX, right LH, bilateral BNST, right NBM, right AHA and left PH.

Abbreviations: AHA, anterior hypothalamic area; ARH, arcuate nucleus; BNST, bed nucleus of stria terminalis DPEH, dorsal periventricular hypothalamus; FX, fornix; LH, lateral hypothalamus; MM, mammillary bodies; MPO, medial preoptic nucleus of the hypothalamus; NBM, nucleus basalis of Meynert; PaVN, paraventricular nucleus; PeVN, periventricular nucleus; PH, posterior hypothalamus.

A Contributions of imaging, behavioral and hormone variables to model BMI in AN & HC

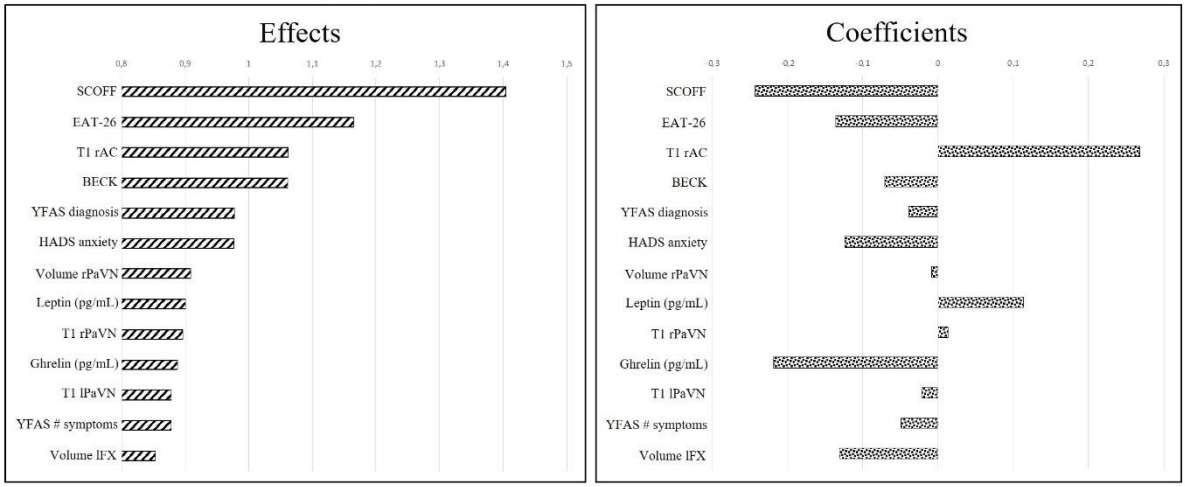

B Contributions of imaging, behavioral and hormone variables to model BMI in OB & HC

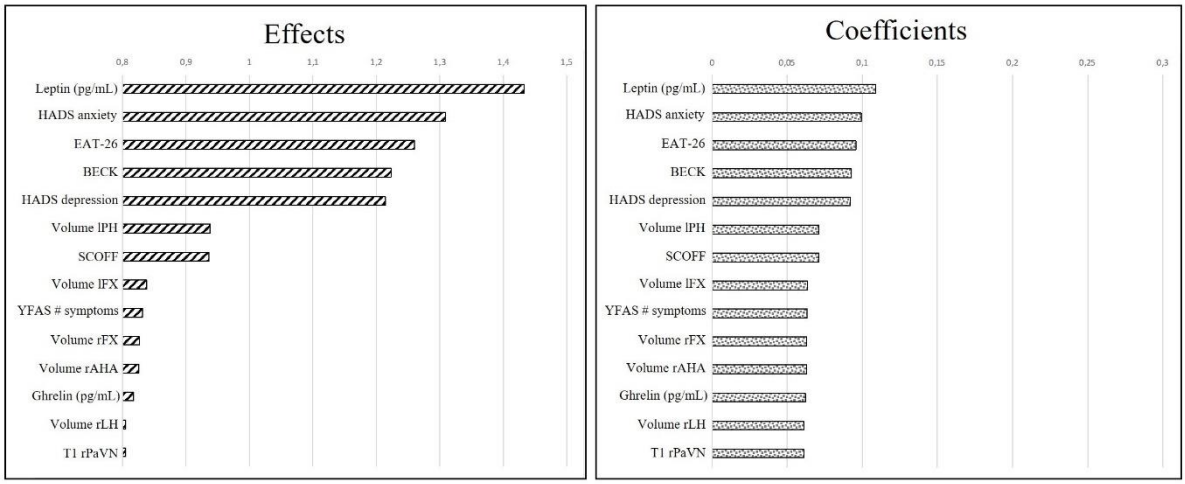

C Contributions of imaging variables of HT nuclei to model EAT-26 scores in AN, HC & OB

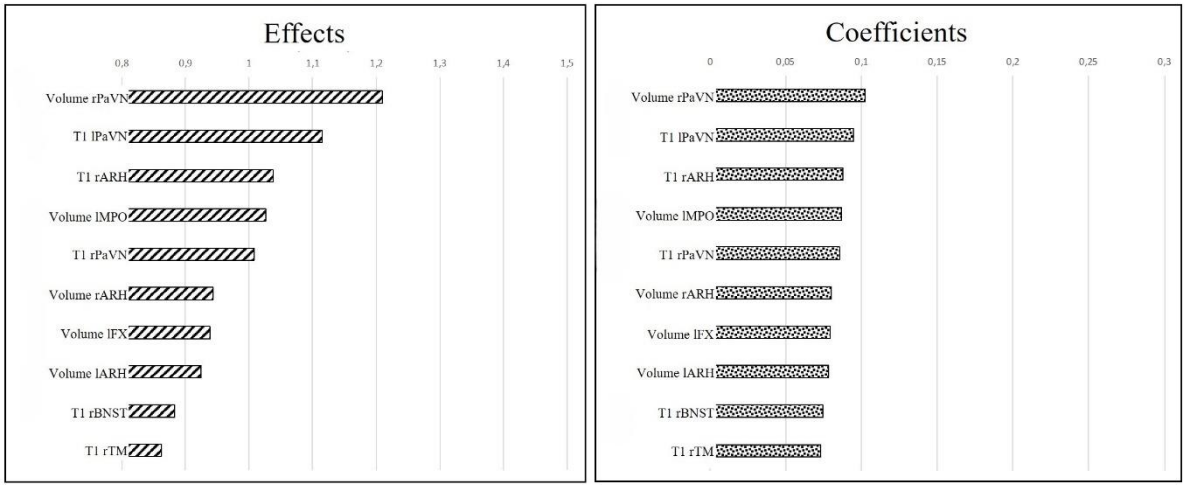

Figure 4: Relative contributions of variables to predict severity of eating disorders and weight disorders.

Figure 4 reports the size effects (left) and coefficients (right) of imaging, behavioral and hormone parameters to model, A) the severity of eating disorders (EAT-26 scores) observed in the whole subjects (explained variance = 51.08%, 10 variables used (effect >0.8), 7 cross-validations using fast SVD NIPALS, Van de Voet T^2=0, 1 factor), B) BMI scores in AN(+HC) (explained variance = 74.1%, 13 variables used (effect >0.8), 7 cross-validations using fast SVD NIPALS, Van de Voet T^2=0, 2 factors) and C) BMI scores in OB(+HC) (Explained variance = 68.5%,14 variables used (effect >0.8), 7 cross-validations using fast SVD NIPALS, Van de Voet T^2=0, 1 factor) using Non-Linear Partial Least Square (NIPALS) modeling (JMP 16 Pro).

Supplemental data

Supplemental Figure 1: Participant flowchart.

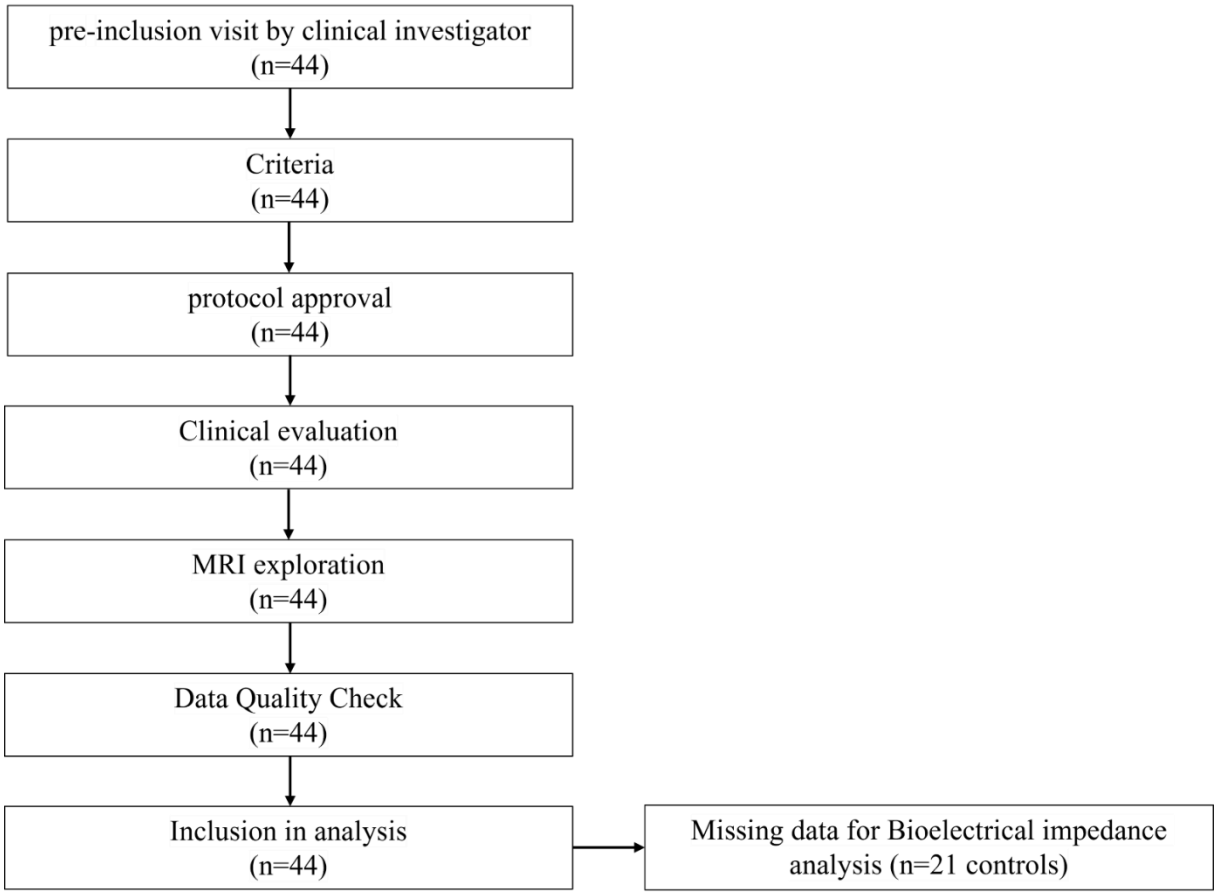

Supplemental Table 1. Database acquired in the whole protocol (HYPOTHALNET).

Sequence description	MRI sequence	Parameters
High Resolution T1 weighted images	3D-MP2RAGE Sagittal	Resolution= 0.6 mm*0.6 mm*0.6 mm Matrix= 402*402*256 FOV= 240mm*240mm*154mm TR_{MPR}= 5000 ms TR= 5 ms TE= 3 ms TI1= 900 ms/TI2= 2.750 ms α_1= 6°, α_2= 5° TA= 10 min 12 s BW= 240 Hz/ Px Acceleration factor= 3
T2 weighted images	3D-FLAIR Sagittal	Resolution= 0.8 mm*0.8 mm*0.8 mm Matrix 300*300*192 FOV= 240mm*240mm*154mm TR= 9000 ms TE= 352 ms TI1= 2300 ms TA= 7 min 32 s BW= 723 Hz/ Px Acceleration factor= 6 ETL= 210
	High Resolution 2D T2-TSE Coronal (Centered on HT)	Resolution= 0.2mm*0.2mm*1mm Matrix= 1050*1050 FOV= 210mm*210mm Slices= 31 *(interleaved acquisition)*

Functional MRI images	2D multiband single-shot EPI *7T HCP protocol* (whole brain)	TR= 3050 ms TE= 530 ms RFA= 135° TA= 5 min BW= 241 Hz/ Px Acceleration factor= 3 ETL= 11 Resolution= $(1.6\ mm)^3$ Matrix= 142*142*85 FOV=227mm*227mm Slices= 85 *(interleaved acquisition)* TR= 1080 ms TE= 25 ms Flip angle= 38° BW= 1956 Hz/ Px Multiband=5 GRAPPA=2
Diffusion tensor images	2D multiband single-shot EPI*7T HCP protocol*	Resolution= 1.13 mm*1.13 mm*1.13 mm Matrix= 186*186 FOV= 210*210 Slices= 120 TR= 5500 ms TE= 78 ms Flip angle= 90° BW= 1344 Hz/ Px TA= 2*11min 80 diffusions gradient directions, b values (1000s/mm^2 and 2000 s/mm^2) Acquisition with 2 opposite phase- encoding directions (R-L and L-R)

MR Scanners : Magnetom 7T Step 2 and Magnetom 7T TERRA (Siemens, Erlangen, Germany).

Abbreviations: *MP2RAGE=Magnetization Prepared 2 Rapid Acquisition Gradient Echoes, FLAIR= Fluid-Attenuated Inversion Inversion Recovery, TSE= Turbo Spin Echo, EPI= Echo Planar Imaging, TR= Repetition Time,* $_{MPR}$= magnetization prepared 2 *rapid gradient echo, TE= Echo Time, TI= Inversion Time, TA= Acquisition Time, FOV= Field Of View, ETL= Echo Tain Length , BW= Band Width, RFA= Refocusing Flip Angle, GRAPPA= Generalized Autocalibrating Partially Parallel Acquisition, R= Right, L= Left.*

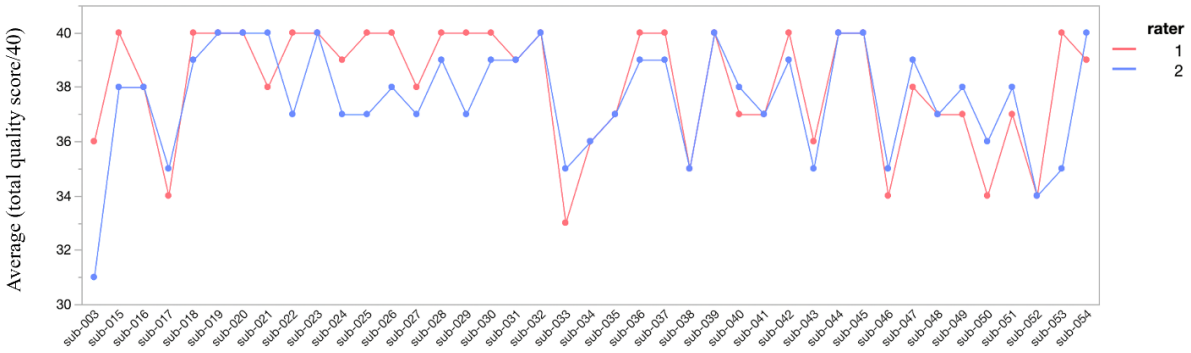

Supplemental Figure 2: Average individual rater score of the quality of T_1w-UNIDEN images and qT_1 maps, and registration of the Neudorfer's template and atlas.

The average individual rater score is shown on the y-axis for each participant represented on the x-axis. The medians and ranges of global quality scores of imaging data for rater 1 and rater 2 were 39 [33-40] and 38 [31-40] respectively, with an ICC (including bias) of 0.9742.

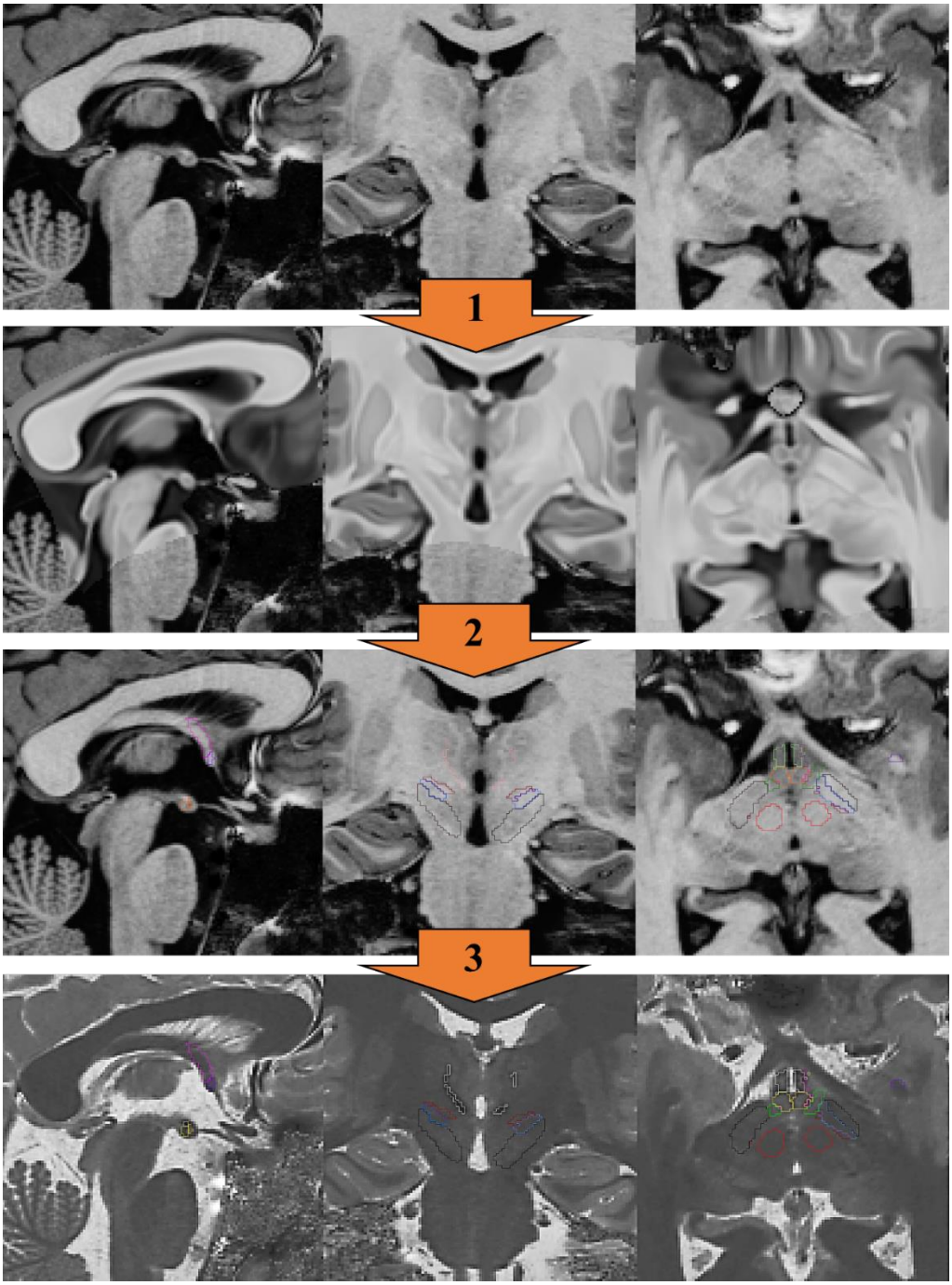

Supplemental Figure 3: Spatial registration of T_1w with the Neudorfer atlas template and labels

After cropping T_1w volumes, unbiased quantitative T_1 maps, Neudorfer templates and atlases in a similar manner, a spatial registration between the Neudorfer template and T_1w using the SyN procedure of ANTS was performed (1), and the transformation was applied to the atlas (2) and the unbiased T_1 maps (3) before extraction of parameters of each HT nucleus (resolution= $(0.6\ mm)^3$).

```
% computing of transforms %
antsRegistrationSyNQuick.sh -d 3 \
  -f crop-sub-XX_T1wUNIDEN.nii \
  -m ../cropped-MDA_990HCP_t1_MNI152b_0.5.nii.gz  \
  -o cropMDA_to_cropT1wUNIDEN_

% application of transforms %
antsApplyTransforms -d 3 \
 -i ../cropped-MDA_990HCP_atlas_labels_0.5mm.nii.gz \
 -r crop-sub-XX_T1wUNIDEN.nii \
 -o crop_MDA_Atlas_to_sub-051_T1w.nii.gz \
 -t cropMDA_to_cropT1wUNIDEN_1Warp.nii.gz \
 -t cropMDA_to_cropT1wUNIDEN_0GenericAffine.mat \
 -n genericLabel
```

Supplemental code: script used to perform the coregistration of the Neudorfer template to T1-w volume of individual subjects using the ants library.

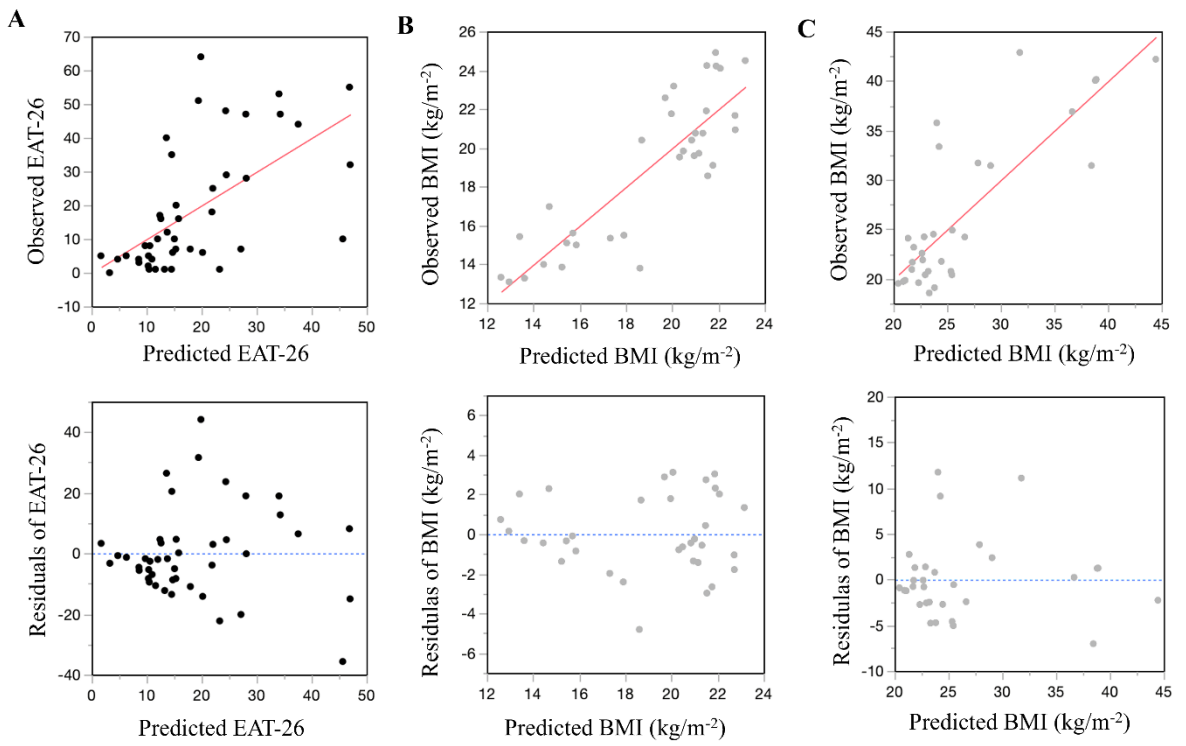

Supplemental Figure 4: Prediction and residuals of the NIPALS models

Graphics from the NIPALS models from A) MRI parameters associated with the severity of eating disorders (EAT-26) in the whole cohort, B) MRI parameters, appetite-regulating hormones levels and behavior scores associated with the severity of the BMI score in AN, C) MRI parameters, appetite-regulating hormones levels and behavior scores associated with the severity of the BMI score in OB.

The upper graphics show the quality of the fitting of the explained variances by the model. The lower graphics show the residuals of the models.

For cross-validation of each NIPALS models, the original data (n_A=44, n_B=34, n_C=21) were divided into 7 subsets (ns_A=6, ns_B=4, ns_C=3). Each of the 7 sets is used to validate the model fit on the rest of the data, fitting a total of 7 models. The model that produces the best validation statistic is chosen as the final model, and the fold that is not used in the building of that model provides the validation set performance statistics.

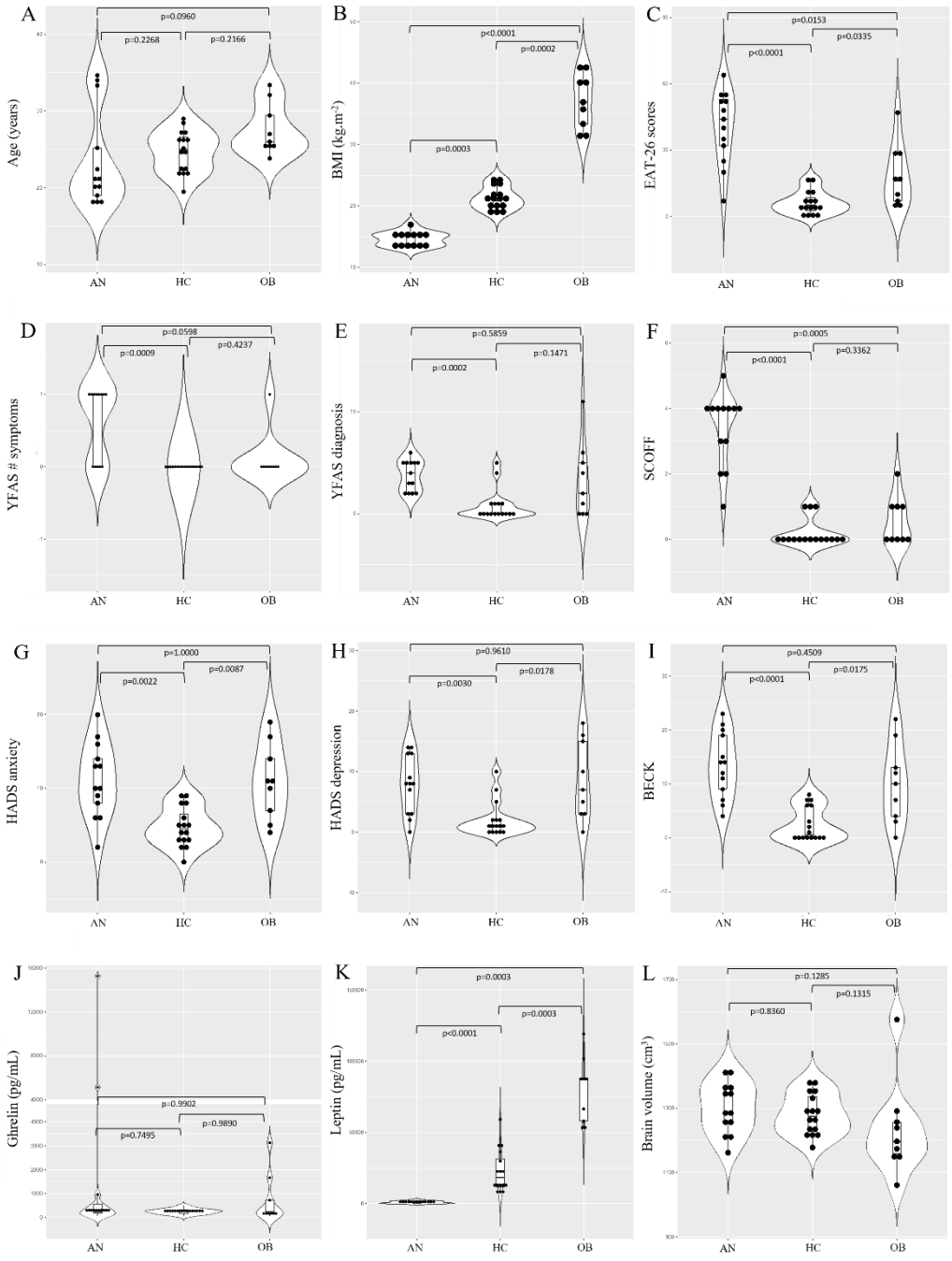

Supplemental Figure 5: Demographics, behavioural status, and hormones levels in AN, HC and OB.

Non-parametric tests corrected for multiple comparisons using the Steel-Dwass all pairs procedure (JMP 16 pro) were used to compare between AN, HC and OB groups the following parameters: A) Age, B) BMI scores, C) EAT-26 scores, D) YFAS number (#) of symptoms scores, E) YFAS diagnosis scores, F) SCOFF scores, G) HADS anxiety scores, H) HADS depression scores, I) BECK scores, J) plasmatic Ghrelin levels, K) plasmatic Leptin levels, L) Brain volumes.

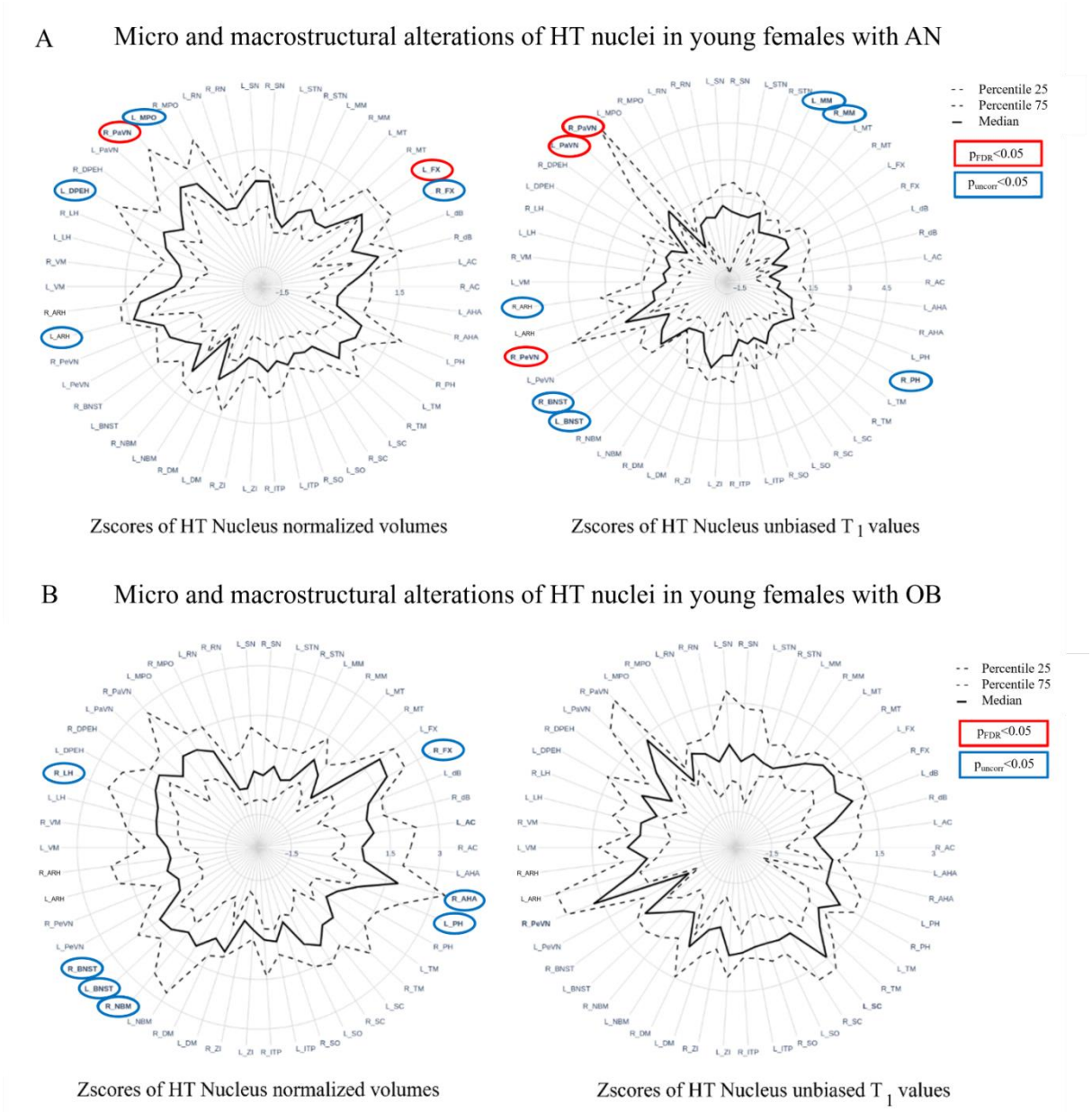

Supplemental Figure 6: Micro and macrostructural increase in AN and OB relative to HC.
A) relative to HC, AN showed significant increase (p_{FDR}<0.05) in the volumes of right PaVN and left FX while the observed differences in left ARH, left MPO, left DPEH and right FX did not survive multiple comparison corrections (p_{uncorr}<0.05) (left). Relative to HC, AN showed significant increase in T_1 values (p_{FDR}<0.05) in bilateral PaVN and right PeVN while differences observed in bilateral BNST, right ARH, bilateral MM, and right PH did not survive multiple comparison corrections (p_{uncorr}<0.05) (right).
B) Relative to HC, OB did not show significant difference remaining after multiple comparison correction but only trends of increases (p_{uncorr}<0.05) in the volumes of right FX, right LH, bilateral BNST, right NBM, right AHA and left PH.
Abbreviations: AHA, anterior hypothalamic area; ARH, arcuate nucleus; BNST, bed nucleus of stria terminalis DPEH, dorsal periventricular hypothalamus; FX, fornix; LH, lateral hypothalamus; MM, mammillary bodies; MPO, medial preoptic nucleus of the hypothalamus; NBM, nucleus basalis of Meynert; PaVN, paraventricular nucleus; PeVN, periventricular nucleus; PH, posterior hypothalamus

5.3 Concluding remarks

Using high spatial resolution 3D-MP2RAGE at 7T, combined with a tailored processing pipeline enabling the alignment of the Neudorfer atlas to individual participants images, we were able to observe macro- and micro-structural changes in the hypothalamic (HT) nuclei, consistent with inflammatory in carefully selected cohorts of young women living with obesity and anorexia nervosa. We then sought to determine whether 7T MRI could help us observe functional reorganization within the hypothalamic nuclei networks involved in regulating eating behaviors.

6 Functional reorganization of hypothalamic networks in young women with Obesity and Anorexia Nervosa – a 7T MRI study

6.1 Foreword

Preliminary results from this work were presented as a scientific poster at the Gordon Research Conference (GRC) Annual meeting 2022 in Ventura, California US. The following section presents this work, which is set to be submitted soon.

6.2 Manuscript

Functional reorganization of hypothalamic networks in young females living with Obesity and Anorexia Nervosa – a 7T MRI study

Coleen Roger[1,2,3], Adele Lasbleiz[4,5], Hugo Dary[1,2], Roy AM Haast[1,2], Lauriane Pini[1,2], Anezka Kovarova[1,2,6,7], Marie-Pierre Ranjeva[1,2], Patrice Darmon[4,5], Benedicte Gaborit[4,5], Yu Fu[3], Patrick J Cozzone[1,2], Maxime Guye[1,2], Anne Dutour[4,5], Jean-Philippe Ranjeva[1,2]

8. Aix Marseille Univ, CNRS, Centre de Résonance Magnétique Biologique et Médicale (CRMBM), Marseille, France
9. Aix Marseille Univ, Assistance Publique-Hôpitaux de Marseille (AP-HM), Centre d'Exploration Métabolique par Résonance Magnétique (CEMEREM), Hôpital Universitaire de la Timone, Marseille, France
10. A*Star, Institute of Molecular and Cell Biology (IMCB), Singapore.
11. Aix Marseille Univ, INSERM, INRAE, Centre de recherche en CardioVasculaire et Nutrition (C2VN), Marseille, France
12. Aix Marseille Univ, Assistance Publique-Hôpitaux de Marseille (AP-HM), Département d'Endocrinologie, Hôpital de la Conception, Marseille, France
13. CEITEC – Central European Institute of Technology, Masaryk University, Brno, Czech Republic
14. Faculty of Medicine of the Masaryk University, First Department of Neurology, Brno, Czech Republic

Corresponding author: Coleen ROGER

CRMBM (AMU-CNRS 7339), Faculté des Sciences Médicales et Paramédicales,

27 boulevard Jean Moulin 13385, Marseille, France

coleen.roger@etu.univ-amu.fr

Abstract

Background: The development of weight-related disorders has been associated with altered function of the hypothalamus (HT). However, the limited spatial and temporal resolution used so far has prevented its characterization at the nuclei level.

Objective: We investigated the functional alterations of HT nuclei and brain regions involved in eating behaviors in individuals with weight-related disorders, and their association with BMI and eating disorder (EAT-26) scores.

Methods: MRI exams were conducted after an overnight 15h fasting period in 46 young females living with obesity (OB, n=10) or restrictive anorexia nervosa (AN, n=15), and healthy controls (HC, n=21). We used high resolution functional MRI (fMRI) at 7T during a food- and context-cue task, along with resting-state fMRI. Differences in activation patterns, static and dynamic functional connectivity (FC) of eating behavior networks were investigated in relation to BMI and EAT-26 scores.

Results: During food vs nonfood cues, both OB and AN showed hyperactivation in the left middle cingulate and right fronto-parietal network, compared to HC. The right paraventricular nucleus (PaVN) was hyperactivated in OB, while the right mammillothalamic tracts and right posterior HT nucleus were deactivated in AN. During the context vs nonfood cues, AN showed hyperactivation in body image-related regions and deactivation of the bed nucleus of the stria terminalis and fornix, compared to HC.
FC differences across the 3 groups were found for connections involving the right PaVN and tuberomammillary nucleus. In AN, nodal alterations in the salience network were positively associated with BMI and negatively with EAT-26 scores. In OB, the left suprachiasmatic and ventromedial HT nuclei showed alterations, both positively correlated with BMI. OB also exhibited reduced fast transition dynamics in global and intra-HT networks, negatively associated with BMI.

Conclusion: Weight-related disorders are associated with numerous functional variations at the brain-wide as well as at the HT nuclei levels within eating behavior networks.

Keywords
weight-related disorders; hypothalamus; hypothalamic nuclei; eating behaviors; BMI; eating disorder; obesity; restrictive anorexia nervosa; functional MRI; resting-state fMRI.

Abbreviations
ACC, anterior cingulate cortex; AN, anorexia nervosa; EAT-26, Eating Attitudes Test-26; FC, functional connectivity; HC, healthy control; HT, hypothalamus; NAcc, nucleus accumbens; OB, obesity; PaVN, paraventricular nucleus; PFC, prefrontal cortex.

Introduction

Disturbances of hypothalamic functions are closely linked to the development of weight-related disorders, highlighting the crucial role of the hypothalamus (HT) in regulating energy homeostasis. Research from human histopathological studies and animal models have revealed that the HT is a complex brain region, composed of multiple nuclei involved in distinct aspects of energy regulation (Fong et al., 2023; Swaab, 1997). Bridging the detailed cellular-level understanding obtained *in vitro* to *in vivo* human research imposes significant challenges. Nonetheless, neuroimaging has emerged as the preferred method for investigating eating behavior networks and examining the anatomical, functional, and metabolic impacts of their dysregulation *in vivo* (Florent et al., 2020a; Neseliler et al., 2017; Salem & Dhillo, 2015a).

Among available MRI techniques, functional MRI (fMRI), which relies on blood-oxygen-level-dependent (BOLD) signal changes, has been important in identifying key brain networks involved in energy (dys)regulation. Task-related fMRI has revealed greater activation of brain networks related to the reward, emotion and motivation in response to high-fat food (HF) cues in both healthy controls (HC) and weight-related disorders (Stoeckel et al., 2008b). Moreover, activation in cortical and subcortical food reward areas in response to food images has been found to positively correlate with body mass index (BMI) (Batterink et al., 2010b). In contrast, individuals with anorexia nervosa (AN) exhibit a widespread hypoactivation of food motivation and appetite circuitries (Holsen et al., 2012b; Kaye et al., 2011), while regions associated with cognitive evaluation, attention and executive functioning show elevated activity (Kaye et al., 2011). Conversely, these regions are often hypoactive in individuals with obesity (OB) (Batterink et al., 2010b). In rare instances, fMRI successfully showed bilateral activation of HT in response to HF images in HC (Killgore et al., 2003b; Schur et al., 2009b).

In addition, functional connectivity (FC) has contributed to better characterize maladaptation of eating behavioral networks using resting-state fMRI (rs-fMRI). For example, FC analyses have shown that HT and mesocorticolimbic connectivity is crucial in regulating feeding behavior and is disrupted in weight-related disorders (Castro et al., 2015; G. K. W. Frank et al., 2021; J. J. Simon et al., 2020b). High-resolution rs-fMRI studies have revealed that HT subregions exhibit baseline differences in FC, which are influenced by BMI. For instance, individuals with higher BMI show increased FC between the medial HT and reward-related regions, including the orbitofrontal cortex and nucleus accumbens (NAcc), but reduced FC between the HT and cognitive control networks (Kullmann, Heni, et al., 2014b; Kullmann & Veit, 2021; T. M. Le et al., 2020b). In AN, disruptions in HT connectivity are also evident, including impaired satiety state-dependent FC with the reward system (J. J. Simon et al.,

2020b), and altered fronto-accumbal connectivity associated with reward and habit learning (Cha et al., 2016b).

Rs-fMRI studies using graph-theoretical analysis have revealed global and local network inefficiencies in obesity, particularly in whole-brain networks (Baek et al., 2017), while anorexia nervosa primarily affects thalamo-insular circuit (Geisler et al., 2016).

Dynamic FC (dFC) analyses, which capture temporal fluctuations in connectivity, offer additional insights into the links between brain networks and feeding behavior (Park et al., 2018). For example, BMI has been positively correlated with variability in regional dFC in visual and reward-related regions (Guo et al., 2023), highlighting the potential of these approaches to provide more sensitive and accurate measures compared to static analyses.

Despite their important contributions to our understanding of feeding behavior, many neuroimaging studies have either steered away from the HT, or treated it as a single structure, primarily due to the spatial and temporal limitations of standard MRI techniques. Studying the HT as a homogeneous structure overlooks its complex and multifaceted functions. For example, the overall hypothalamic BOLD fMRI signal in a fasted state may appear negligible as orexigenic nuclei activation and anorexigenic nuclei inhibition produce opposing signals that can cancel each other out (De Silva et al., 2012b). To better understand the role of the HT in regulating eating behavior, it is crucial to functionally characterize its different nuclei (Roger et al., 2022).

In the present study, we aimed at characterizing activation patterns, static and dynamic FC of eating behavioral networks at both the whole-brain and HT nucleus-levels. Our well-characterized cohorts consisted of young females i) living with obesity (OB), or ii) with restrictive anorexia nervosa (AN) and with iii) normal weight (healthy control, HC). Towards this goal, we employed ultra-high field (7 Tesla, 7T) MRI, utilizing high-resolution BOLD fMRI during food-cue and context-cue tasks, alongside rs-fMRI sequences, to comprehensively examine brain activity, connectivity patterns, and their relationship to BMI and eating disorder scores.

Materials and Methods

Participants

A total of forty-six adult young females (18-35 yrs) were recruited in this protocol, consisting of: i) fifteen young females on the 'ill phase' of AN (BMI <17 kg/m^2, positive to the criteria defined by the Diagnostic and Statistical Manual of Mental Disorders 5), ii) ten OB (BMI ≥ 30 kg/m^2 and no lifetime or current medical condition that could potentially affect appetite or weight (e.g. diabetes, bariatric surgery history, GLP-1 analog, corticoids or psychotropics treatment), and iii) twenty-one HC (18.5≤ BMI <25 kg/m^2, no lifetime or current medical condition that could potentially affect appetite or weight, no eating disorder, anxiety or depression). AN and OB were recruited from the Department of Endocrinology (CHU Nord and Hôpital de la Conception, AP-HM, Marseille, France) and HC from the CEMEREM (Hôpital de la Timone, AP-HM, Marseille, France).

On the morning of the scan, all participants performed the self-reported Eating Attitudes Test-26 (EAT-26) to identify the presence of eating disorder risk. We collected a total of 39 scans for the task-related fMRI (n_{AN}= 11, n_{OB}= 9, n_{HC}= 19) and 46 scans for the resting-state fMRI (n_{AN}= 15, n_{OB}= 10, n_{HC}= 21). Participants were not included in the study if they had contraindications to 7T MRI, were at risk of non-compliance with the examination, were unable to provide consent, had a history of head injury, neurosurgery, neurological conditions, psychosis, or bipolar disorder, or had a current addiction. Additionally, a urine pregnancy test was conducted, and pregnant or lactating female were excluded. All participants were enrolled in a health insurance plan and provided written informed consent after receiving clear, comprehensive, and honest information. This protocol was in accordance with the Declaration of Helsinki and obtained ethics approval by the French Ethic Committee 'CPP EST I' (#20.02.13.47002 – IDRCB : 2020-A00340-39; Clinical trial Hypothalnet : NCT04451759).

Image acquisition

After an overnight fasting period, 42 participants (n_{AN}=14, n_{OB}=9, n_{HC}=19) were explored on a 7T Terra MR system (Siemens Healthineers, Erlangen, Germany), and 4 participants (n_{AN}=1, n_{OB}=1, n_{HC}=2) explored on a 7T Siemens Magnetom step 2 system (Siemens Healthineers, Erlangen, Germany). Both scanners were equipped with the same (1Tx/32Rx) head coil (NOVA medical). The same MRI protocol was conducted on both scanners. After an automatic 3D B_0 shimming procedure, a whole brain B_1^+ map was acquired using a spin-echo-based sequence by assessing the ratio of consecutive spin and stimulated echoes (WIP#658, Siemens Healthineers). Anatomical images were obtained using a 3D-MP2RAGE sequence (TR= 5ms, TE= 3ms, TI_1= 900ms/TI_2= 2.750ms, 256 slices, 0.6mm isotropic resolution, TA= 10min12s). Unbiased T_1 maps and T_1-w-UNIDEN images were obtained after B_1^+ inhomogeneity

correction described in (Massire et al., 2016). Qualitative high resolution T_2-weighted images (TSE) and 3D FLAIR were also acquired for radiological assessment of the HT in all participants. Resting-state and task-related fMRI acquisitions were performed using a 2D multiband single-shot EPI sequence (1.6mm isotropic resolution, FOV= 227mm*227mm, flip angle (FA)= 38°, TR= 1080 ms, TE= 25 ms, Flip angle= 38°, 85 slices interleaved acquisition) with 420 volumes for rs-fMRI and 830 volumes for task-fMRI.

Food cue viewing fMRI task

The task consisted of showing to the participants a series of 120 images (60 'Food', 30 'NonFood', 30 'Context') distributed randomly (**Figure 1**). To ensure reproducibility, we selected images from a standardized databases of food and non-food images (Full4Health Image Collection) (Charbonnier et al., 2018). The food condition was composed of an equal amount of High-fat (HF) and Low-fat (LF) food. Open-sourced materials were used for context images (cooking or dining-related utensils, positive and negative valence). Each image was shown for 1 second and interspersed by a black screen with a white cross on its centre for a variable amount of time. Stimuli were presented using the Presentation software (Neurobehavioural Sys Inc, Berkeley, CA, USA) on a BOLD screen (Cambridge Research System, Rochester, UK), which participants viewed through a mirror mounted on the head coil. The paradigm lasted 15:20 min in total. Prior to begin the experiment, all participants were handled one joystick for each hand and were instructed to right-click if they saw a picture of food and left-click if they saw a photo of non-food or context, to verify they were attentive to the stimuli while in the scanner.

Image processing

Preprocessing of the anatomical scans included automatic (sub)cortical segmentation, and reconstruction of the cortical surfaces using FreeSurfer (v7.3.2). The functional scans were corrected for susceptibility-related spatial distortions using the 'topup' procedure implemented in FSL (v6.0.5) (Andersson et al., 2003). Slice timing and realignment was then performed using SPM12 (Statistical Parametric Toolbox 12, Wellcome Department of Imaging Neuroscience, London, United Kingdom) in MATLAB (R2023a, Mathworks, Inc., Sherborn, MA, United States). The anatomical scans were then registered to the functional scans using FSL's 'bbregister', before being normalized to the Montreal Neurological Institute space (MNI152NLin6Asym). Spatial smoothing of functional scans was performed with a 2-mm full width at half maximum (FWHM).

Functional activation patterns

For the task fMRI, a general linear model analysis (SPM12) was performed using a canonical hemodynamic response function (HRF) with time and dispersion derivatives. The conditions [Food], [Context], [NonFood] were defined for each participant. Motion parameters were modeled as confounds. Second-level analyses were performed to obtain activation/deactivation patterns of the [Food-NonFood] and [Context-NonFood] contrasts in HC, and differences between AN and HC, as well as OB and HC. To localize activation clusters, we used the AAL3 atlas for the whole brain (Rolls et al., 2020). For HT, regional analyses were performed using a binarized and dilated inclusion mask derived from the Neudorfer atlas (Neudorfer et al., 2020b) (**Supplementary Figure 1**). Labeling of clusters was then performed according to the Neudorfer atlas after an automated registration using ANTS (https://github.com/ANTsX/ANTs/blob/master/Scripts/antsRegistrationSyNQuick.sh) and visually validated by two investigators (CR and JPR).

Static functional connectivity (sFC)

Functional connectivity was assessed using the CONN toolbox (Whitfield-Gabrieli & Nieto-Castanon, 2012). Anatomical data were segmented into grey matter, white matter, and CSF tissue classes using SPM12 unified segmentation and normalization algorithm. The six motion parameters, signals extracted from CSF and WM were used as nuisance regressors in CONN's standard denoising pipeline. Connectivity matrices containing Fisher-transformed bivariate correlation coefficient between pairs of region-of-interest (ROI) BOLD timeseries were calculated for the 123 ROIs. ROIs were derived from a combination of 4 different atlas: the HT nuclei labels from the Neudorfer atlas (Neudorfer et al., 2020b), whole-brain regions labels from the Brainnetome atlas (Fan et al., 2016), AAL3 (Rolls et al., 2020) and ATAG (Keuken & Forstmann, 2015) (**Supplementary Table 1**). We then used the Brain Connectivity Toolbox (http://www.brain-connectivity-toolbox.net) (Rubinov & Sporns, 2010) for MATLAB to calculate different graph theory metrics at the nodal level: i) the global network properties: local efficiency [efficiency_bin]; ii) regional network properties: degree [degrees_und], betweenness centrality [betweenness_bin].

Dynamic FC functional connectivity (dFC)

Using the dFCwalk toolbox for MATLAB (https://github.com/FunDyn/dFCwalk), the dynamics of resting-state networks were assessed by measuring the typical dynamic speed, which reflects the distribution of the time-resolved rate at which FC reconfigures over time. The typical dynamic speed of the inner hypothalamic network and of the whole brain network were assessed at different ranges of temporal windows from 10s to 60s. Group differences in

typical dynamic speeds were compared for the full range of temporal windows [10s-60s], for the fast transitions [10s-30s] and the slow transitions [35s-60s].

Statistical analysis

Differences in eating behavioral scores (EAT-26) and BMI between groups were assessed using non-parametric tests corrected for multiple comparisons (Steel-Dwass procedure, $p<0.05$).

Group differences in activation patterns for the contrasts [Food-NonFood] and [Context-NonFood] were assessed using a second-level procedure based on one-way ANOVA at the whole brain level ($p_{TFCE}<0.05$, k=5, FDR-corrected at the cluster-level $p_{FDR}<0.05$) and at the regional level centered on the HT to study activation patterns of HT nuclei ($p_{TFCE}<0.05$ uncorrected).

For static rs-fMRI, between-group edge connectivity was compared using network based statistics (NBS, connectivity threshold $p_{uncorr}<0.001$, NBS threshold $p_{FDR}<0.05$) (Zalesky et al., 2010). Global differences and pair-wise differences among the groups were studied. Concurrently, nodal parameters derived from graph theory metrics of static rs-fMRI data were compared using non-parametric tests ($p_{FDR}<0.05$).

Comparisons of group FC dynamics were conducted using repeated measures ANOVA including data i) of all temporal windows [10s-60s], ii) only of short temporal windows [10s, 15s, 20s, 25s, 30s] and iii) of long temporal windows [35s, 40s, 45s, 50s, 55s, 60s] to characterize differences in global, fast and slow and transitions respectively. Non-parametric post-hoc tests (Steel-Dwass procedures) were applied for all windows to compare all pairs of groups.

Correlations of EAT-26 and BMI with altered static nodal parameters and typical dynamic speeds were determined (spearman rank test $p_{FDR}<0.05$).

Results

General features

Eating scores differed significantly among groups. Relative to HC, individuals with OB and AN showed altered scores on the EAT-26: median $EAT\text{-}26_{HC}$ = 5 [0-17], median $EAT\text{-}26_{OB}$ = 13 [4-77] (OB vs HC, p=0.0059), and median $EAT\text{-}26_{AN}$ = 40 [7-64] (AN vs HC, p<0.0001).

As expected, BMI varied significantly between groups, with $BMI_{AN} < BMI_{HC}$ (p<0.0001) and $BMI_{OB} > BMI_{HC}$ (p<0.0001). Median values were BMI_{HC} = 21.6 [18.5-24.9], BMI_{OB} = 37.7 [31.6-42.9] and BMI_{AN} = 14.7 [13.1-16.9].

Brain activation patterns in response to Food and Context cues in HC

In HC, the [Food-NonFood] contrast (**Figure 2 red, Supplementary Table 2**) induced activations in the right-hand sensorimotor system (left precentral cortex [PreCC], left postcentral cortex [PostCC], and supplementary motor area [SMA]), reflecting the motor response during forced choices (Food cue: right-hand joystick; NonFood cue: left-hand joystick). Additional activations were observed in the paracentral lobules, precuneus, left inferior parietal cortex, angular cortex, right middle temporal cortex, and right superior and middle occipital cortices. Subcortical activations included the right bed nucleus of stria terminalis (BNST) and right mammillothalamic tracts (MT) within the HT.

The [NonFood-Food] contrast (Figure 2 blue, Supplementary Table 2) recruited the left-hand sensory motor system (right PreCC, right PostCC). Deactivations during Food cues were observed in the anterior (ACC) and middle cingulate cortices (MCC), superior frontal gyrus, left medial superior frontal gyrus, left dorsolateral frontal gyrus, and the lateral hypothalamus (LH) within the HT.

For the [Context-NonFood] contrast, significant activations (Figure 2 red, Supplementary Table 2) were limited to the right MT. Conversely, the [NonFood-Context] contrast (Figure 2 blue, Supplementary Table 2) recruited the left-hand sensory motor system and revealed deactivations during Context cues of a broad network, including the left insula, the ACC and MCC, left rolandic operculum, left orbitofrontal cortex, left inferior and superior frontal cortices, left medial, opercular and triangularis inferior frontal cortices, supramarginal angular, inferior and superior parietal cortices, middle and superior temporal cortices, left temporal pole, middle and superior occipital cortices, and the left fornix (FX) within the HT.

Brain activation patterns in response to Food and Context cues in OB versus HC

Relative to HC, OB showed stronger activation during the [Food-NonFood] contrast (**Figure 3 red, Supplementary Table 3**) in the right-hand sensorimotor system, left MCC, left superior parietal cortex, right paracentral lobule, and the right paraventricular nucleus (PaVN) within

the HT. Decreased activations in OB relative to HC were observed in the right anterior commissure (AC) and the left FX within the HT (Figure 3 blue, Supplementary Table 3).

For the [Context-NonFood] contrast, OB exhibited lower activation in the left FX relative to HC (Figure 3 red, Supplementary Table 3).

Brain activation patterns in response to Food and Context cues in AN versus HC

Relative to HC, AN showed stronger activation during the [Food-NonFood] contrast (**Figure 4 red, Supplementary Table 4**) in the left-hand sensorimotor system, left MCC, right medial and superior frontal cortices, right paracentral lobule, right supramarginal, inferior and superior parietal cortices, right angular cortex, right superior temporal cortex, right middle and superior occipital cortices, right calcarine, right cuneus, and the left FX within the HT. Deactivations in AN relative to HC (Figure 4 blue, Supplementary Table 4) were observed in the right-hand sensorimotor system, left posterior cingulate (PCC), left paracentral lobule, left inferior parietal cortex, left cuneus, left calcarine and the right MT and right posterior hypothalamic nucleus (PH) within the HT.

For the [Context-NonFood] contrast, AN showed increased activation in the right PCC, supramarginal cortex and inferior parietal cortex (Figure 4 red, Supplementary Table 4). Decreased activations were observed in the BNST and the FX in the HT (Figure 4 blue, Supplementary Table 4).

Static functional connectivity

FC reorganization of edges in AN and OB

A significant global effect was observed among the three groups, with the right tuberomammillary (TM) and the right PaVN nuclei identified as key nodes in the network (**Figure 5A**). Between-group differences in FC were observed for edges linking the right TM to the right anterior hypothalamic area (AHA), right VM, right DM, right PaVN, left periventricular hypothalamic nucleus (PeVN), and left supraoptic hypothalamic nucleus (SON). Similarly, differences were observed for edges linking the right PaVN to the left SON, left VM, and left PeVN. Additional differences included edges linking the left SON with the right SON and the left thalamus pulvinar inferior, as well as the left VM with the left thalamus intralaminar.

Post-hoc pairwise comparisons showed that these differences were primarily driven by higher FC in the OB group compared to the AN group. Specifically, OB exhibited greater FC between the right TM and the right PaVN, DM, AHA, VM and internal globus pallidus, as well as between the right AHA and right LH, and between the left VM and left thalamus intralaminar (**Figure 5B**).

Conversely, lower FC in OB relative to AN was observed for edges linking the right PaVN to the left PeVN and VM, the right VM to the left MM, and the right TM to left internal globus pallidus.

Nodal FC reorganization in AN and OB

Relative to HC, AN showed significant lower nodal degree in several regions, including the NAcc (p_{FDR}=0.002), left putamen (p_{FDR}<0.001), right putamen (p_{FDR}=0.002), left caudate (p_{FDR}<0.001), and the left thalamus pulvinar medial (p_{FDR}=0.004, **Figure 6A**). Additionally, betweenness centrality was higher in the right BNST (p_{FDR}=0.005) and the left dorsal PeVN (p_{FDR}=0.007, **Figure 6B**). Nodal local efficiency was reduced in the left putamen (p_{FDR}=0.001) and the left insula (p_{FDR}=0.002, Figure 6C).

In the OB group, significant increases in nodal degree were observed in the left VM (p_{FDR}=0.010, Figure 6A). Additionally, local efficiency was higher in the right suprachiasmatic hypothalamic nucleus (SCN, p_{FDR}=0.050, **Figure 6C**).

Dynamic functional connectivity

6.2.1.1 Whole-brain network dynamics

For the whole-brain network, no significant group effects were observed for the full range of windows [10s-60s] or for slow transitions [35s-60s]. However, a significant group effect (F=4.630, p=0.015) emerged during the fast transitions [10s-30s], alongside a significant window effect (p<0.0001). Post-hoc pairwise comparisons showed that the typical speed of whole brain dynamics was slower in OB relative to HC and AN during short windows (10s, **Figure 7A**).

Intra-hypothalamic network dynamics

For the intra-hypothalamic network, a significant group effect (F=5.774, p<0.006), window effect (p<0.0001), and a window*group interaction (p=0.0205) were observed for the full range of windows. Group differences were pronounced during fast transitions (F=9.12, p=0.0005), with a significant window effect (p<0.0001) and a window*group interaction (p=0.0032). Additionally, a significant group effect was observed for slow transitions (F=3.412, p=0.042), with a window effect (p<0.0001) but no significant window*group interaction. Post-hoc analyses indicated that the typical speed of intra-hypothalamic dynamics was slower in OB relative to HC and AN for windows of 10s, 15s, 20s, 25s, 30s, and 35s (**Figure 7B**).

Association between severity of eating disorders with graph theory metrics and dFC typical speed

6.2.2 EAT-26 correlations

EAT-26 scores showed significant negative correlations with several graph-theory metrics. These included the nodal degrees of the NAcc (ρ= -0.408, p_{FDR}= 0.005), left putamen (ρ= -0.476, p_{FDR}= 0.001), and left caudate (ρ= -0.446, p_{FDR}= 0.002), as well as the local efficiency of the left putamen (ρ= -0.414, p_{FDR}= 0.004, **Figure 8A**). In contrast, positively correlations were observed between EAT-26 scores and betweenness centrality in the right BNST (ρ= 0.482, p_{FDR}= 0.001) and left PeVN (ρ= 0.410, p_{FDR}= 0.005).

BMI correlations

After false discovery rate correction (p_{FDR}<0.05), BMI scores were positively correlated with the nodal degrees of the right putamen (ρ= 0.418, p_{FDR}= 0.004), left thalamus pulvinar medial (ρ= 0.573, p_{FDR}= 0.0001, **Figure 8B**), and the local efficiency of the left insula (ρ= 0.437, p_{FDR}= 0.002, Figure 8B).

From a dynamical perspective, BMI scores were negatively associated with the typical dFC speed of the whole-brain network for the 10s window (ρ= -0.414, p_{FDR}= 0.001). Similar negative associations were observed for the intra-hypothalamic network for the 15s (ρ= -0.300, p_{FDR}= 0.004), 20s (ρ= -0.294, p_{FDR}= 0.004), and 35s (ρ= -0.303, p_{FDR}= 0.003) windows (**Figure 8C**).

Discussion

This study leveraged the high spatial and temporal resolution of 7T MRI to explore functional reorganization within eating behavior networks in young females with anorexia nervosa and obesity. Both groups exhibited altered neural responses to food and contextual stimuli across circuits related to reward, self-regulation, memory, and saliency compared to healthy controls. While static FC analysis showed limited differences in edges strengths, graph-

theory metrics highlighted significant nodal reorganization of eating behavioral networks, including several HT nuclei, in both AN and OB. Additionally, dynamic FC analysis demonstrated alterations in network dynamics, with OB showing a marked slowing of fast transitions in both whole-brain and hypothalamic networks.

Functional characterization of behavioral networks in HC

The activation of brain regions associated with self-referential processing, body image and food visualization in response to [Food-NonFood] contrast supports prior interpretations of mental simulations of eating, engaging visual, gustatory, and somatomotor systems while evaluating anticipated rewards (J. Chen et al., 2016). Notably, we observed activation of the right BNST, which coordinates HT feeding centers for the regulation of food intake (Y. Wang et al., 2019), and the MT, critical for memory retention (Barnett et al., 2021). The inverse contrast showed deactivation of self-regulatory control regions (ACC, PFC) (Neseliler et al., 2017) and the LH, a nucleus pivotal for motivated behavior and energy balance (Rossi, 2023).

Context images trigger a deactivation of the FX, a pathway mediating hippocampal-hypothalamic-prefrontal interactions for regulating food intake (Metzler-Baddeley et al., 2013b). Additional deactivation occurred in self-regulatory control regions (ACC, PFC, middle and superior temporal gyri), body image representation areas (supramarginal, angular, inferior parietal cortex), and circuits involved in food reward (orbitofrontal cortex, vmPFC), taste processing (insula), visual representation (middle and superior occipital cortices), and eating behavior regulation (inferior frontal gyrus) (J. Chen et al., 2016).

Functional reorganization of behavioral networks in AN

Relative to HC, AN showed increased activation in brain regions involved in attentional and cognitive control (right MCC, right superior temporal cortex, right paracentral lobule, left FX), food value processing (medial frontal cortex), body image representation (inferior and superior parietal cortices, right angular cortex, right supramarginal gyrus), and visual representation (right middle and superior occipital cortices, right calcarine, right cuneus). This greater activation in the frontoparietal network is in agreement with studies demonstrating heightened activation in response to food cues (Brooks et al., 2011; Brooks, O'Daly, et al., 2012; Uher et al., 2004), and executive function tasks (Lao-Kaim et al., 2015; Zastrow et al., 2009), coupled with increased connectivity within this same network in AN (Boehm et al., 2024). The posterior visual and inferior parietal hyperactivation might reflect increased inhibitory control, as seen in Go-NoGo tasks (Lock et al., 2011).

In contrast relative to HC, AN showed lower activation in the left frontoparietal network (left paracentral lobule, left inferior parietal cortex), visual system (left cuneus, left calcarine),

and self-referential processing system (left posterior cingulate) (Guterstam et al., 2015). Lower activation was also found in the right MT and right PH, regions involved in memory and vigilance, respectively (Goutagny et al., 2004).

During the [Context-NonFood] condition, the AN group showed subtle greater activation in body image-related regions (right supramarginal cortex, right inferior parietal cortex), and lower activation in HT nuclei involved in motivation (BNST) and self-regulation (FX) relative to HC. This suggests alterations in communication within and between networks responsible for proprioception and visual integration, potentially impairing the integration of homeostatic signals such as hunger and energy levels, contributing to distorted body shape perceptions (Craig, 2011; Ehrlich et al., 2015; Friederich et al., 2012). Although these results align with the hypothesis of diminished food reward processing in AN (Kaye et al., 2013), it is important to recognize that these regions also contribute to stress and anxiety regulation (Goldstein et al., 2010; Klumpp et al., 2012; S. G. Shah et al., 2009), which were heightened in our cohort (data not shown), as well as in obsessive-compulsive disorder (Schienle et al., 2005).

Furthermore, our results suggest that AN may exhibit excessive cognitive control, potentially through higher-order inhibitory function, a characteristic feature of AN (Favaro et al., 2012). Changes in motor response regions may also contribute to the hyperactivity observed in AN patients (Hebebrand & Bulik, 2011; Kullmann, Giel, et al., 2014).

In terms of FC, AN showed no significant differences in edge strength relative to HC. Nevertheless, AN showed higher FC than OB between the right PaVN and left VM, and between the right PaVN and left PeVN, all of which are nuclei involved in food intake regulation and satiety (Bray et al., 1990; Kalsbeek & Buijs, 2021; Rønnekleiv et al., 2022). Higher betweenness centrality in the left PeVN further indicated its greater influence on network organization in AN. In addition, higher FC was observed between the right VM and the left MM, both involved in memory and stress (Shetty et al., 2024).

Regarding nodal organization, AN showed reduced nodal degree in the salience network, including the NAcc, involved in reward processing, in the goal-related behavior system (putamen, left caudate, left thalamus pulvinar medial), alongside lower local efficiency in the emotional-ingestive system (left insula), supporting previous findings of decreased local network efficiency in these areas (Geisler et al., 2016). However, AN presented higher betweenness centrality in the right BNST and the left PeVN, stimulating the anorexigenic neurons within the PaVN (Rønnekleiv et al., 2022), reflecting increased influence of these HT nuclei on the network activity. These findings align with previous research showing functional and structural alterations in the salience network in AN (Ehrlich et al., 2015; Friederich et al., 2012; Frieling et al., 2012; Hayes et al., 2015; Lord et al., 2016; Shott et al., 2016). Notably,

we observed significant associations between the severity of eating disorder symptoms (high EAT-26 scores) and weight loss (low BMI) with reduced nodal degree and local efficiency in regions within the salience network.

Finally, dynamics of resting-state eating behavioral networks were not found to be altered in AN relative to HC at either the whole-brain or intra-hypothalamic scale, regardless of transition dynamics (fast or slow).

Functional reorganization of behavioral networks in OB

Relative to HC, OB showed greater activation in the frontoparietal network (right paracentral lobule, left superior parietal cortex) and regions involved the salience network (MCC) and food intake regulation (right PaVN) during the [Food-NonFood] contrast. This aligns with reports of altered FC and activity patterns in individuals leaving with obesity (García-García et al., 2012; Kullmann et al., 2013). Hyperactivation of the PaVN may be linked to its role in modulating food-related reward and aversion, similar to its involvement in drug consumption (Huang et al., 2024). Additionally, the MCC and parietal lobes have demonstrated higher activation in appetite control in OB compared to HC (Tuulari et al., 2015).

Relative decreased activation was observed in the anterior commissure and left FX, with the latter also observed during the [Context-NonFood] contrast. However, no significant reorganization of the fronto-mesolimbic circuitry typically seen in obesity (G. Li et al., 2023) was observed, likely due to the small cohort of OB (n=9). Despite this, increased sensitivity in FC differences was observed between OB and AN, particularly in hypothalamic regions. Higher FC was found in histaminergic connections within the HT, specifically between the right TM and the right PaVN, DM, AHA, VM and the internal globus pallidus. TM, a key source of histamine, is involved in arousal and appetite regulation (Contreras et al., 2016) while histamine receptors (H1R, H3R) are highly expressed in hypothalamic nuclei involved in energy homeostasis (Khouma et al., 2023). Higher FC was observed between the right AHA and right LH, with the latter being involved in goal-directed eating behaviors (Ha et al., 2024).

Concerning nodal characteristics, the OB group showed higher nodal degree in the left VM and enhanced local efficiency in the right SCN demonstrated compared to HC. The SCN, as the central clock of the circadian timing system, regulates glucose metabolism in a time-of-day dependent manner (Speksnijder et al., 2024).

Regarding dynamic transitions, OB exhibited lower fast transition dynamics within whole-brain and intra-HT networks during fasting periods, with an even more pronounced reduction in the intra-HT network. This reduction in intra-HT fast transitions was inversely

associated with BMI scores, echoing findings from a previous study linking BMI to temporal variability in FC within the reward system (Guo et al., 2023).

Limits

The current study presents several key limitations. As stated above, the modest scale of our sample might have imposed limitations on the study's statistical power. However, we still obtained substantial effect sizes between groups due to the gain in signal-to-noise ratio obtained by moving from 3T to 7T acquisitions. To limit large interindividual variability and further improve the statistical power, we opted for a stringent selection for our participants (same sex, age, fasting condition, restrictive subtype), which increases sensitivity to observe multimodal differences, at the whole-brain, as well as the HT nuclei levels. Thus, while other studies with much larger cohorts are available, the lack of a cohesive neurobiological model for anorexia nervosa and obesity involving inhomogeneities in their sample, study design, and magnetic resonance field strength, has led to a considerable variability in their results (Holsen et al., 2012b). Finally, despite the fact that conclusions of dFC analyses rely heavily on the parameters chosen by the experimenter, our multiband acquisition coupled with short TR (1080 ms) improved the accuracy of FC dynamic, as demonstrated by Sahib and colleagues (Sahib et al., 2018).

Conclusion

Our study aimed to investigate brain-wide function and network properties in rigorously selected young female participants, carefully controlling for age, sex, and a standardized 15-hour fasting period. Utilizing 7T MRI, we have identified significant alterations in food intake circuits, including key HT nuclei, affecting both neural activity and connectivity in weight-related disorders. These findings provide new insights into the complex neural mechanisms underlying anorexia nervosa and obesity, contributing to our understanding of their distinct brain network reorganizations.

Acknowledgments

CR, BG, AD, MG, PD, FY, MPR, PJC, JPR designed research; CR, AL, LP, JPR conducted research; CR and JPR analyzed data, CR and JPR wrote the paper with the help from RH. HD and AK helped with preprocessing. CR and JPR had primary responsibility for final content. All authors read and approved the final manuscript.

Data availability: Data described in the manuscript, code book, and analytic code will be made available upon request pending [application and approval].

Funding: *CR has received a PhD grant from EUR Neuroschool (ANR-17-EURE-0029), and Agency for Science, Technology and Research, Singapore (A*STAR). RAMH was supported by a Marie Sklodowska-Curie Postdoctoral Fellowship (101061988).*
*This work received the support of the Merlion Program Campus France (*PHC MERLION 2019 # 43654ZK*) and the A*STAR.*
*The project leading to this publication has received funding from the French government under the "France 2030" investment plan managed by the French National Research Agency (reference: ANR-16-CONV000X / ANR-17-EURE-0029) and from Excellence Initiative of Aix-Marseille University - A*MIDEX (AMX-19-IET-004, 7TEAMS Chair).*
This work was performed by a laboratory member of France Life Imaging network (grant ANR-11-INBS-0006).

Author Disclosures: The authors declare that the research was conducted in the absence of any commercial or financial relationships that could be construed as a potential conflict of interest.

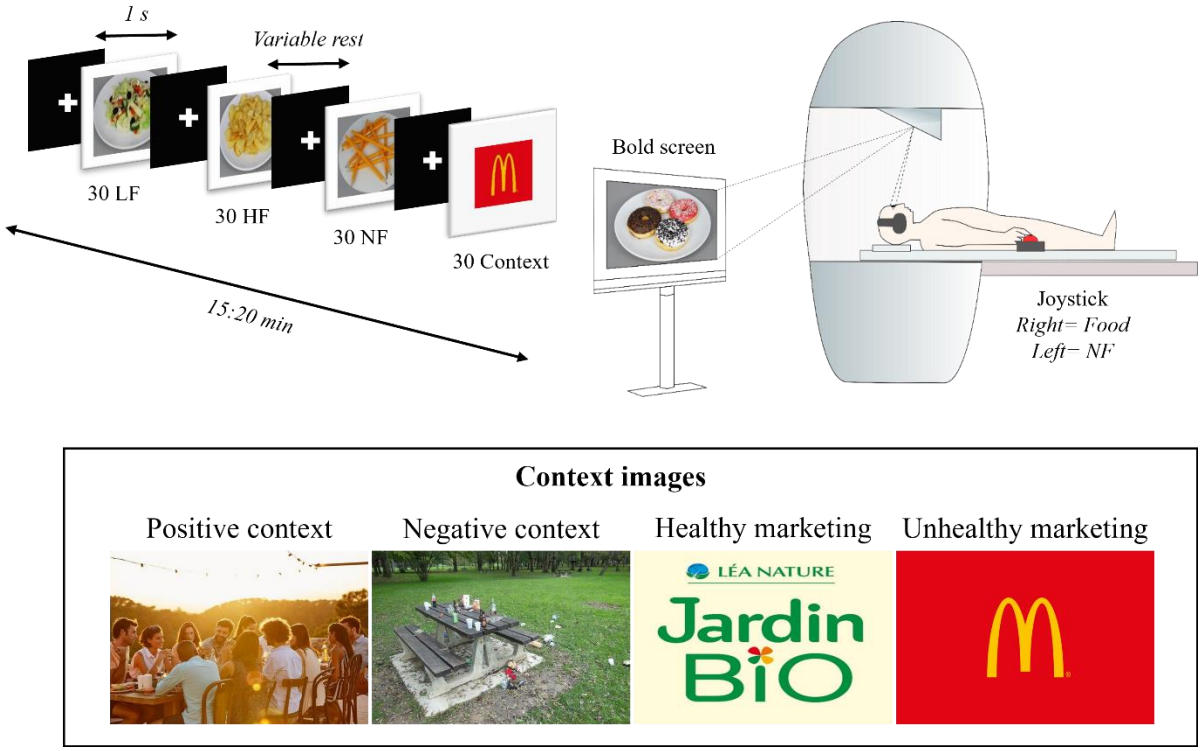

Figure 1: Schematic representation of the food-cue paradigm.
The 'Food' condition refers to Low fat (LF) and High fat (HF) food images. Context images are composed of lunch/dining context with positive or negative valences, as well as junk food or healthy food chain logos.

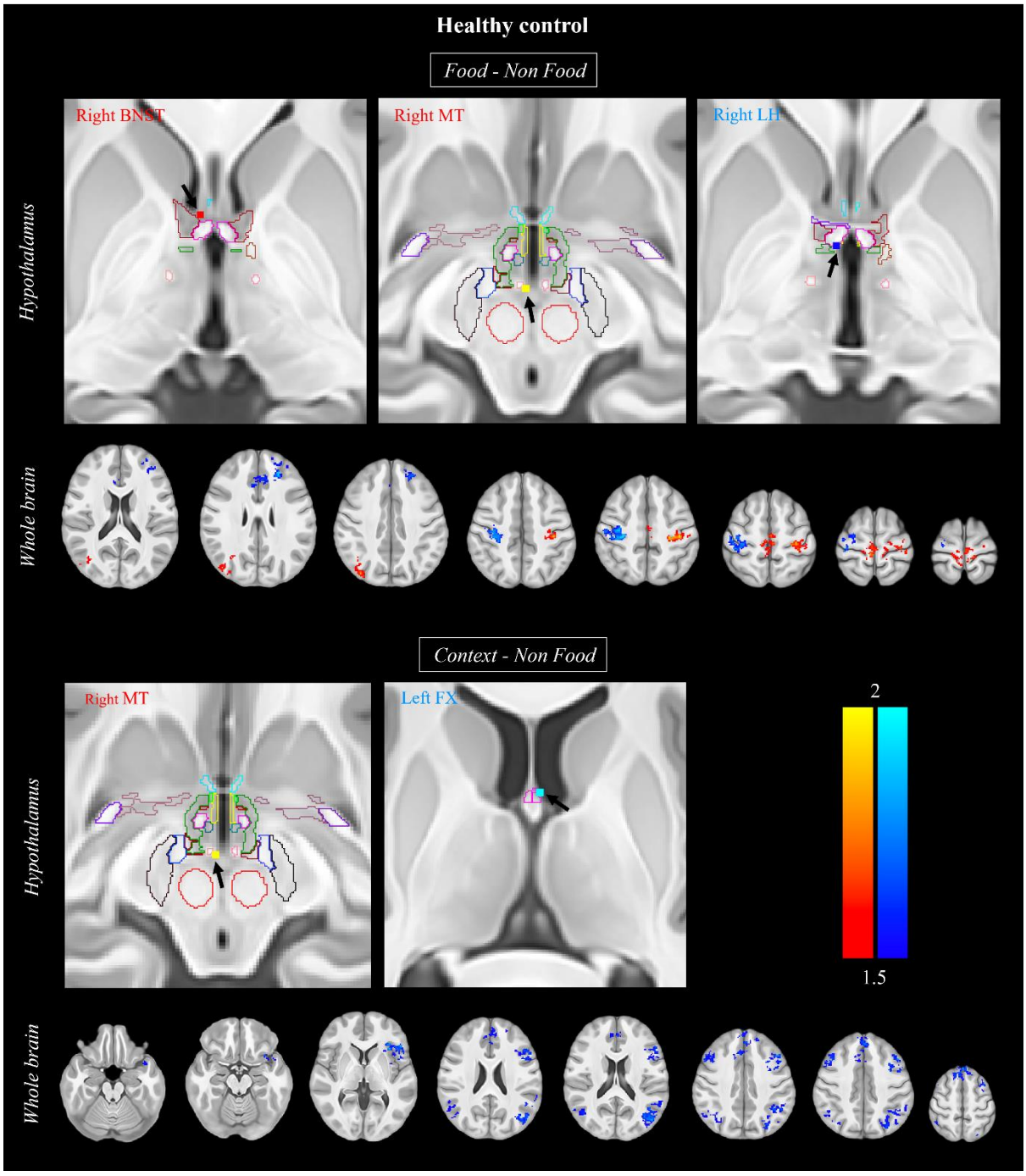

Figure 2: Activation and deactivation patterns during [Food-NonFood] and [Context-NonFood] contrasts in healthy controls (HC).

Activation is represented in red and deactivation in blue. T-maps (pTFCE<0.05 FDR corrected at the cluster level p<0.05 for the whole brain and p_{TFCE} <0.05 uncorrected for the hypothalamus).

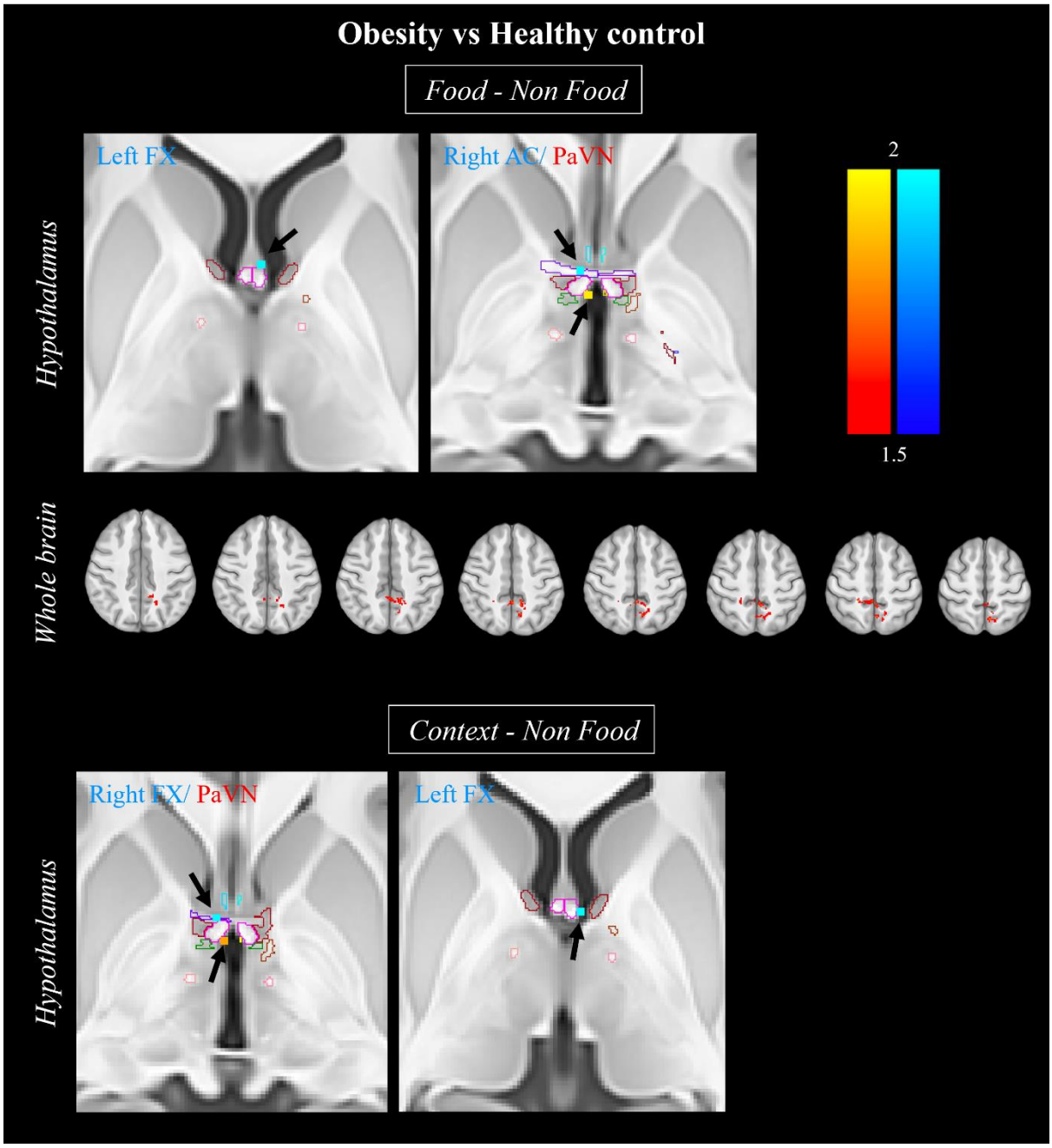

Figure 3: Modulation of activation patterns during [Food-NonFood] and [Context-NonFood] contrasts in participants living with obesity (OB) relative to controls (HC).
Activation is represented in red and deactivation in blue. T-maps (p_{TFCE}<0.05 FDR corrected at the cluster level p<0.05 for the whole brain and p_{TFCE} <0.05 uncorrected for the hypothalamus).

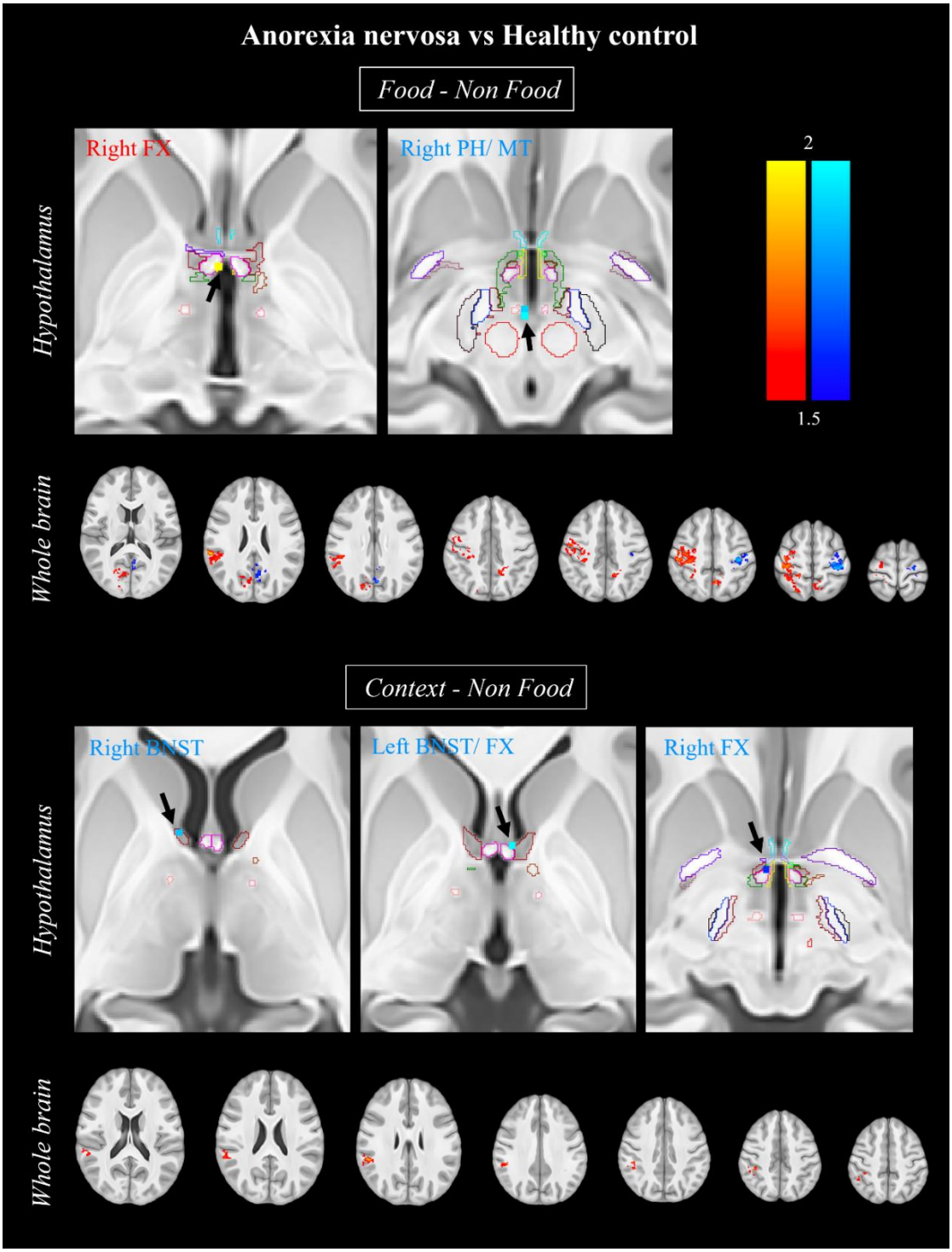

Figure 4: Modulation of activation patterns during [Food-NonFood] and [Context-NonFood] contrasts in participants living with restrictive anorexia nervosa (AN) relative to controls (HC). Activation is represented in red and deactivation in blue. T-maps (p_{TFCE}<0.05 FDR corrected at the cluster level p<0.05 for the whole brain and p_{TFCE} <0.05 uncorrected for the hypothalamus).

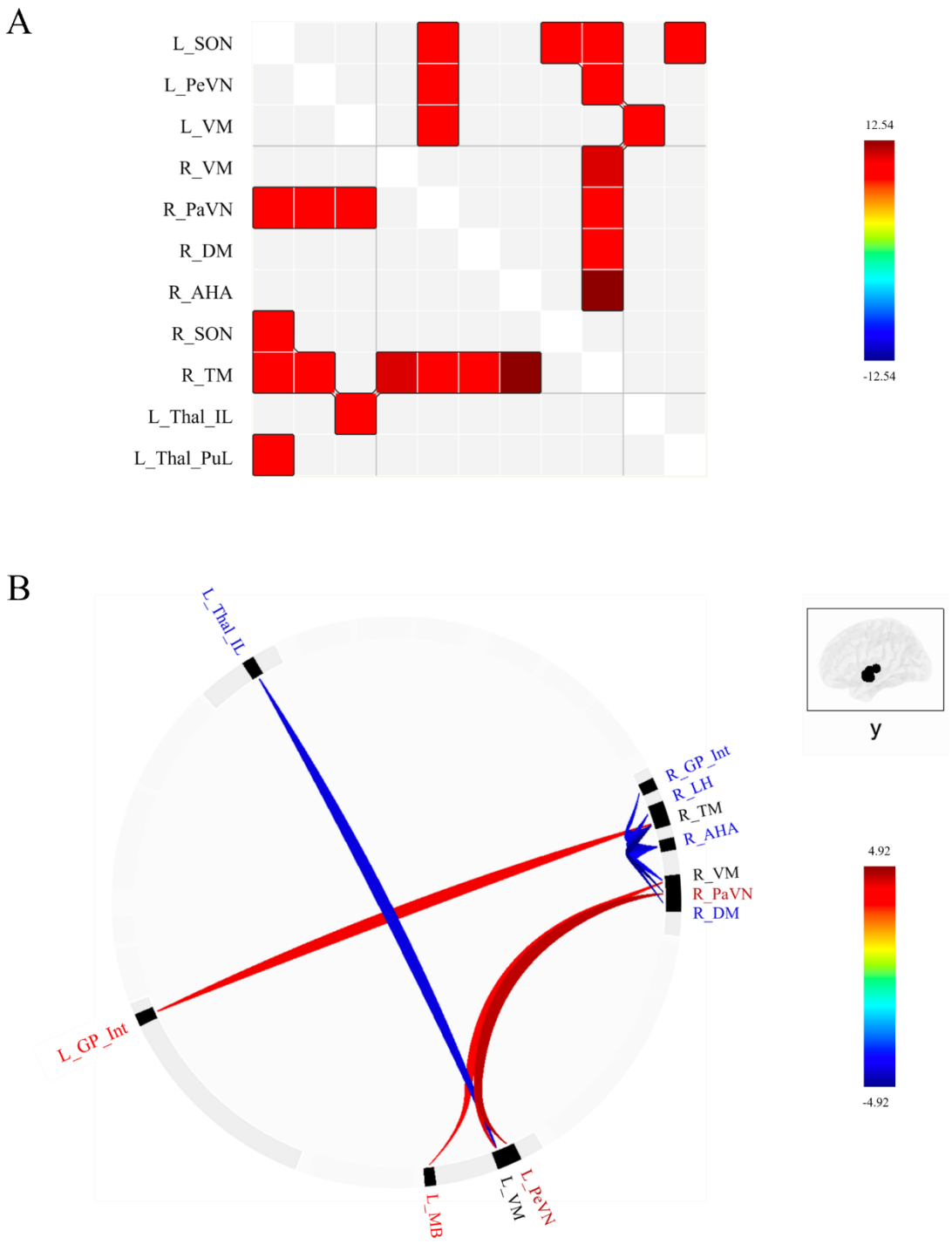

Figure 5: Functional connectivity modulation in weight-related disorders.
A) Matrix representing the global effect due to significant differences among the three groups, and B) Circos plot of the hyper- (red) and hypo- (blue) functional connectivity of young female living with obesity compared to young female living with anorexia nervosa. Shown are F-Test (NBS threshold $p_{FDR}<0.05$).

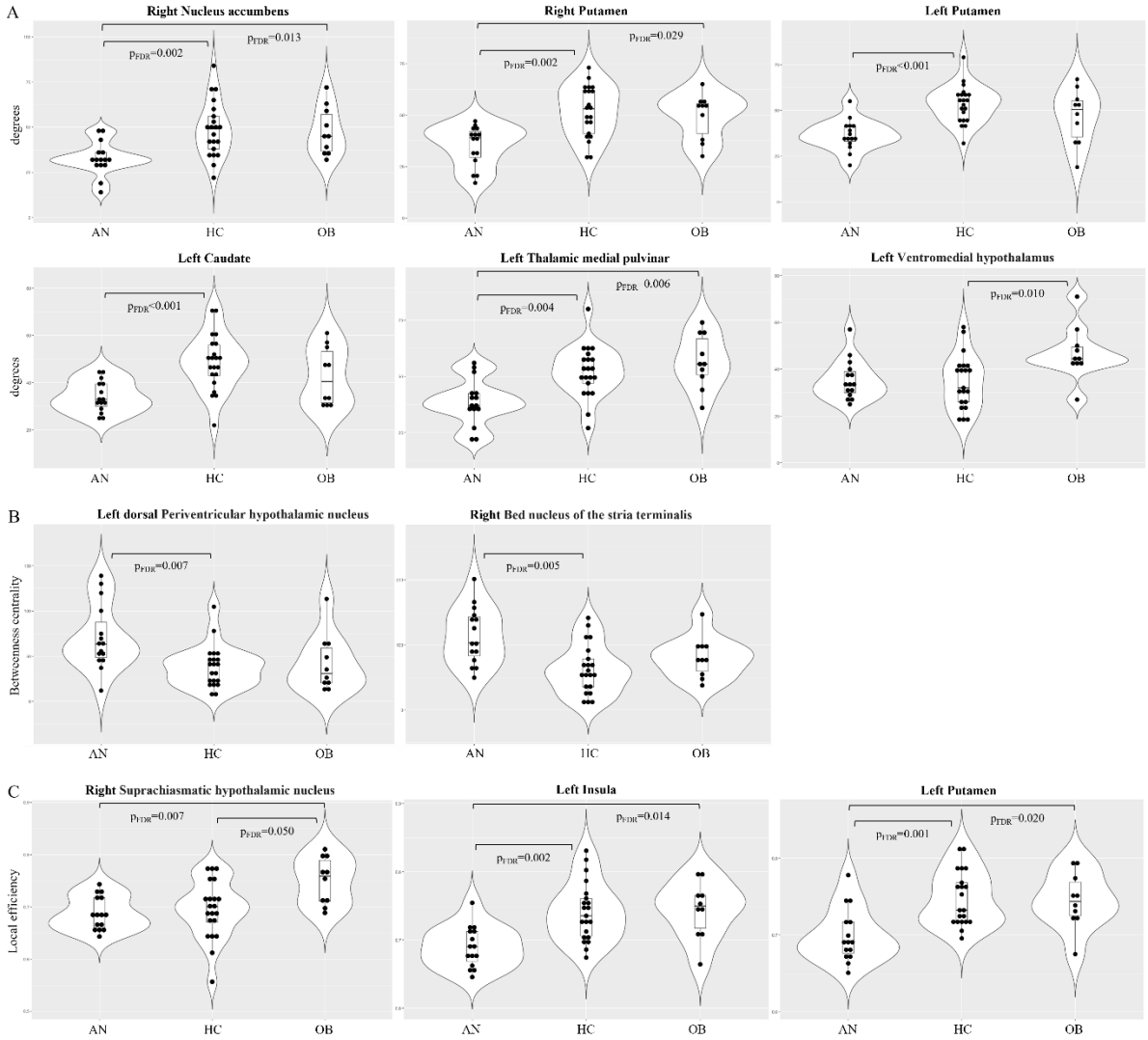

Figure 6: Modulation in node characteristics observed in young female living with restrictive anorexia nervosa (AN) or with obesity (OB) relative to healthy controls (HC).
Shown are the significant differences (p_{FDR}<0.05) of A) nodal degrees, B) betweenness centrality, and C) local efficiency between weight related disorders (AN or OB) and HC (*) and between AN and OB (£). Violin plots represent the data distribution, the box indicates the interquartile range (from 25% to 75%), the line within the box represents the median.

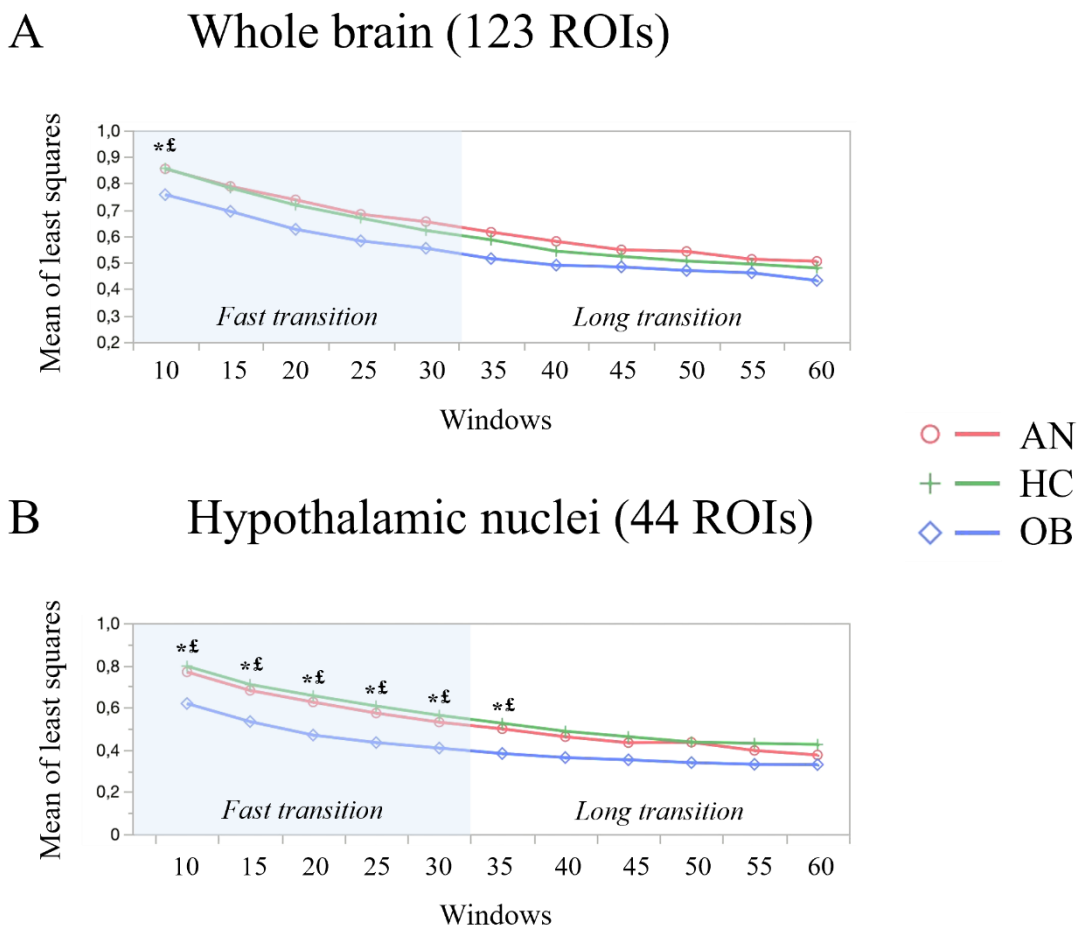

Figure 7: Representation of the typical dynamic speed of the whole brain network, A) the inner hypothalamic network, B) in the three cohorts for the different temporal windows.
Fast and long transitions in young females living with restrictive anorexia nervosa (red) or with obesity (blue) and healthy controls (green) are represented.

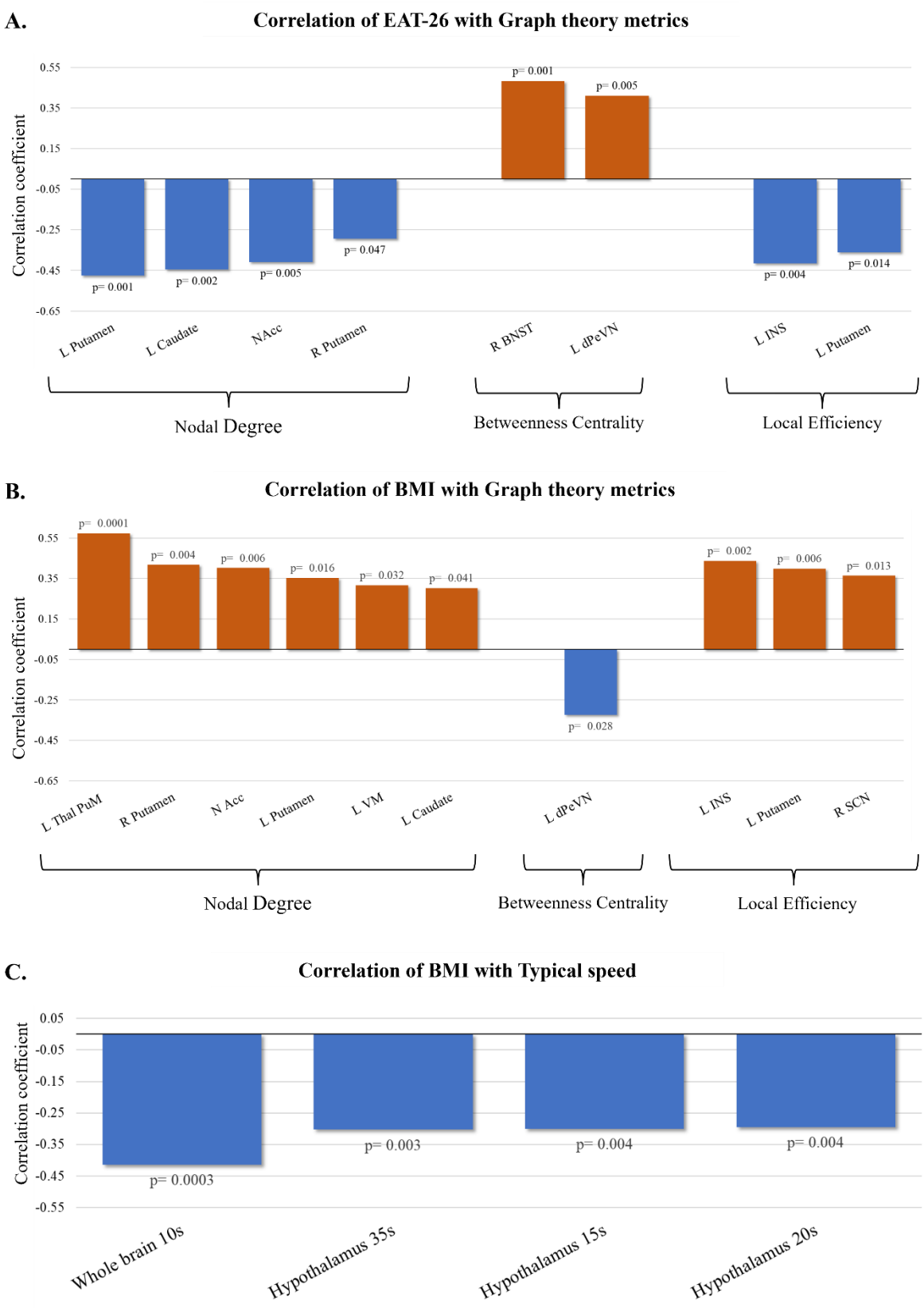

Figure 8: Bar plots representing the correlation of EAT-26 with graph metrics (A) and BMI with graph metrics (B) and dFC typical speed (C).
Shown are the $p_{FDR}<0.05$.

Supplementary data

Atlas	Anatomical description	Abbreviation
Neudorfer	Anterior hypothalamic area	R(L)_AHA
	Arcuate hypothalamic nucleus	R(L)_ARC
	Bed nucleus of the stria terminalis	R(L)_BNST
	Diagonal band of Broca	R(L)_dB
	Dorsal periventricular hypothalamic nucleus	R(L)_dPeVN
	Dorsomedial hypothalamic nucleus	R(L)_DM
	Fornix	R(L)_FX
	Lateral hypothalamus	R(L)_LH
	Mammillary bodies	R(L)_MB
	Medial preoptic nucleus	R(L)_MPO
	Nucleus basalis of Meynert	R(L)_NBM
	Paraventricular nucleus	R(L)_PaVN
	Periventricular hypothalamic nucleus	R(L)_PeVN
	Posterior hypothalamic nucleus	R(L)_PH
	Suprachiasmatic hypothalamic nucleus	R(L)_SCN
	Supraoptic hypothalamic nucleus	R(L)_SON
	Tuberomammillary hypothalamic nucleus	R(L)_TM
	Ventromedial hypothalamus	R(L)_VM
	Zona Incerta	R(L)_ZI
	Red Nucleus	R(L)_RN
	Substantia Nigra	R(L)_SN
	Subthalamic nucleus	R(L)_STN
AAL3	Cuneus	R(L)_Cuneus
	Locus coeruleus	R(L)_LC
	Caudate nucleus	R(L)_Caudate
	Pallidum	R(L)_Pallidum
	Nucleus accumbens	N_Acc
	Medial orbital gyrus	R(L)_OFCmed
	Anterior orbital gyrus	R(L)_OFCant
	Posterior orbital gyrus	R(L)_OFCpost
	Lateral orbital gyrus	R(L)_OFClat
	Putamen	R(L)_Putamen
	Olfactory cortex	R(L)_Olfactory
	Raphe nucleus dorsal	Raphe_D
	Raphe nucleus median	Raphe_M
	Thalamus anteroventral nucleus	R(L)_Thal_AV
	Thalamus intralaminar	R(L)_Thal_IL
	Thalamus lateral geniculate	R(L)_Thal_LGN
	Thalamus lateral posterior	R(L)_Thal_LP
	Thalamus mediodorsal lateral parvocellular	R(L)_ThaL_MDI
	Thalamus mediodorsal medial magnocellular	R(L)_Thal_MDm
	Thalamus medial Geniculate	R(L)_Thal_MGN
	Thalamus pulvinar anterior	R(L)_Thal_PuA
	Thalamus pulvinar inferior	R(L)_Thal_Pul
	Thalamus pulvinar lateral	R(L)_Thal_PuL
	Thalamus pulvinar medial	R(L)_Thal_PuM

	Thalamus reuniens	R(L)_Thal_Re
	Thalamus ventral anterior	R(L)_Thal_VA
	Thalamus ventral lateral	R(L)_Thal_VL
	Thalamus ventral posterolateral	R(L)_Thal_VPL
	Ventral tegmental area	R(L)_VTA
Brainnetome	Medial amygdala	R(L)_Amyg_med
	Lateral amygdala	R(L)_Amyg_lat
	Rostral hippocampus	R(L)_Hipp_rostral
	Caudal hippocampus	R(L)_Hipp_caudal
	Hypergranular insula	R(L)_INS_hG
	Ventral agranular insula	R(L)_INS_vA
	Dorsal agranular insula	R(L)_INS_dAgranular
	Ventral dysgranular and granular insula	R(L)_INS_vDG
	Dorsal granular insula	R(L)_INS_dGgranular
	Dorsal dysgranular insula	R(L)_INS_dDysgranular
ATAG	external Globus Pallidus	R(L)_GP_Ext
	internal Globus Pallidus	R(L)_ GP_Int

Supplementary Table 1: Nomenclature and abbreviations of the 123 brain areas from four different atlas (Neudorfer, AAL3, Brainnetome, ATAG) used in this study.

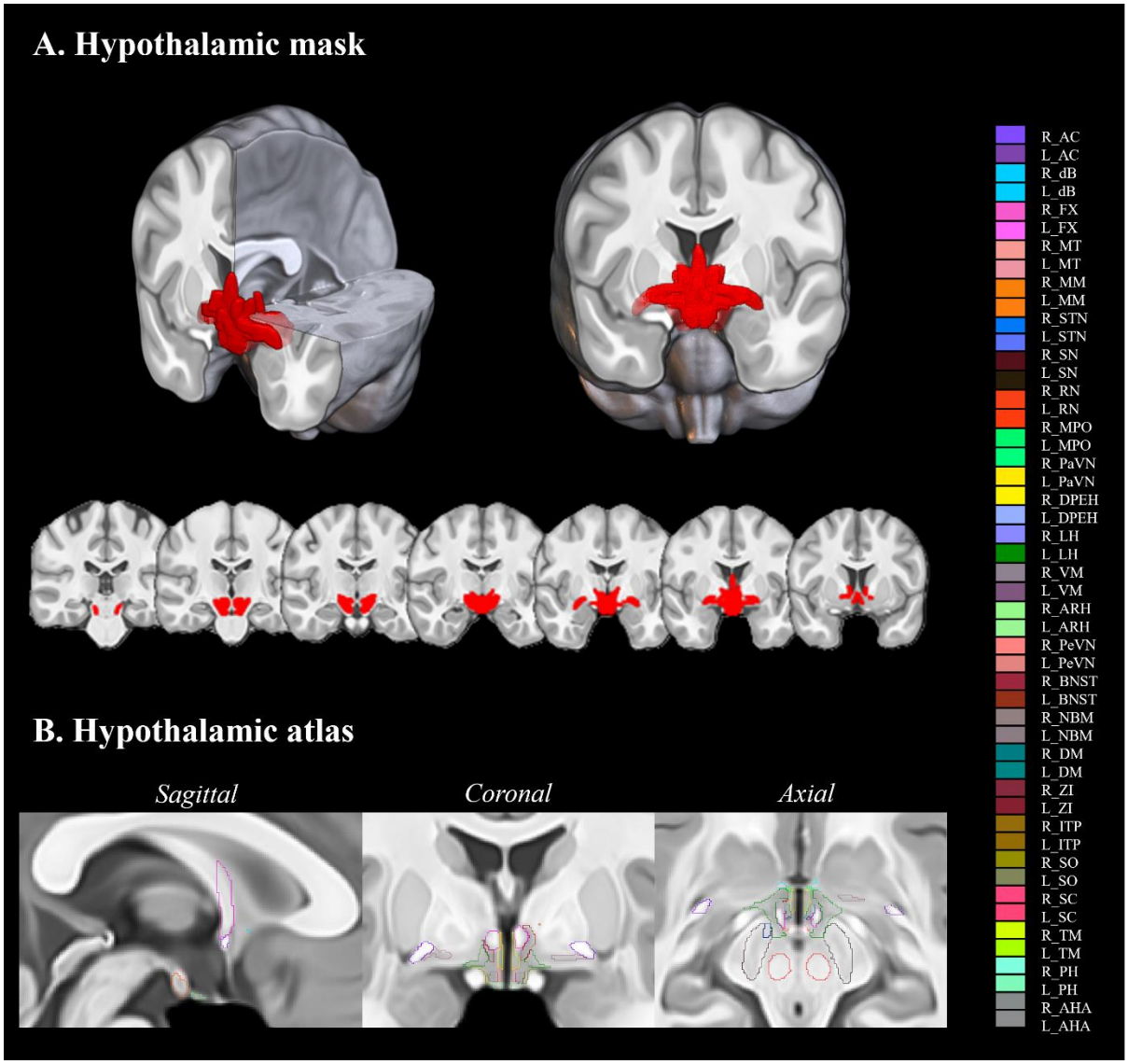

Supplementary Figure 1: Representation of the HT mask (A) and projection of the Hypothalamic Neudorfer atlas (Neudorfer et al., 2020b) **on MNI anatomical image (B).**
(A) represents the dilated HT mask used for SPM12 analysis, (B) displays the delineated nuclei (resolution 1.6 mm^3).
Abbreviations: A*C, anterior commissure; AHA, anterior hypothalamic area; ARH, arcuate nucleus; BNST, bed nucleus of stria terminalis; dB, diagonal band of Broca; DM, dorsomedial hypothalamic nucleus; DPEH, dorsal periventricular hypothalamus; FX, fornix; ITP, inferior thalamic peduncle; LH, lateral hypothalamus; MM, mammillary bodies; MPO, medial preoptic nucleus of the hypothalamus; MT, mammillothalamic tract; NBM, nucleus basalis of Meynert; PaVN, paraventricular nucleus; PeVN, periventricular nucleus; PH, posterior hypothalamus; RN, red nucleus; SC, suprachiasmatic nucleus; SN, substantia nigra; SO, supraoptic nucleus; STN, subthalamic nucleus, TM, tuberomammillary nucleus; VM, ventromedial nucleus; ZI, zona incerta.*

Contrast [Food – Non Food]						
Activation in HC						
Whole brain (p_{TFCE} <0.05 k=5; FDR corrected at the cluster level p<0.05)						
MNI coordinates (mm)			k	p_{FDR} (cluster)	T value	Regions
X	Y	Z				
-39	-24	50	764	<0.0001	4.62	Left PreCC
-28	-26	53			3.98	Left PostCC
-31	-24	61			3.96	Left paracentral lobule Left Parietal Inf
4	-32	69	869	<0.0001	5.22	Right paracentral lobule
4	-22	61			4.31	Right PreCC
-13	-29	77			4.29	Right PostCC SMA Left paracentral lobule Left Precuneus
36	-77	39	540	<0.0001	4.99	Right Mid Occipital
48	-75	26			4.34	Right Sup Occipital
38	-77	31			4.22	Right Angular
1	-43	44			3.47	Right Mid Temporal
Local analysis on HT mask (p<0.05 uncorrected)						
MNI coordinates (mm)			k	p_{uncor}	T value	HT nuclei
X	Y	Z				
1	-11	-9	4	0.027	2.05	Right MT
3	5	-1	1	0.044	1.79	Right BNST
Deactivation in HC						
Whole brain (p_{TFCE} <0.05 k=5; FDR corrected at the cluster level p<0.05)						
MNI coordinates (mm)			k	p_{FDR} (cluster)	T value	Regions
X	Y	Z				
28	-24	53	1225	<0.0001	4.65	Right PreCC
35	-18	53			4.08	Right PostCC
36	-29	55			3.90	Right SFG
-23	40	29	574	0.001	4.47	Left SFG
-24	42	37			3.33	Left SFGmedial
-36	40	26			3.01	Left IFGtriang
0	22	36	938	<0.0001	5.30	ACC
-2	34	26			4.35	MCC
-12	29	29			4.10	Left SFGmedial
Local analysis on HT mask (p<0.05 uncorrected)						
MNI coordinates (mm)			k	p_{uncor}	T value	HT nuclei
X	Y	Z				
3	-2	-3	1	0.044	1.79	Right LH

Supplementary Table 2: Activation and deactivation clusters obtained for the [Food-NonFood] condition in HC.

ACC, anterior cingulate cortex; BNST, bed nucleus of stria terminalis; IFG, inferior frontal gyrus; LH, lateral hypothalamus; MCC, middle cingulate cortex; MT, mammillothalamic tracts; PreCC, Precentral cortex; PostCC, Postcentral cortex; SFG, superior frontal gyrus; SMA, Supplementary motor area.

Contrast [Context – Non Food]						
Activation in HC						
Local analysis on HT mask (p_{TFCE} <0.05, uncorrected)						
MNI coordinates (mm)			k	p_{uncorr}	T value	HT nuclei
X	Y	Z				
1	-11	-9	1	0.004	2.93	Right MT
Deactivation in HC						
Whole brain (p_{TFCE} <0.05 k=5; FDR corrected at the cluster level p<0.05)						
MNI coordinates (mm)			k	p_{FDR} (cluster)	T value	Regions
X	Y	Z				
-48	27	4	2417	<0.0001	4.89 4.24 4.08	Left IFGtriang, SFGmedial, SFG Left PreCC Left Inf & post OFC Left Insula Left IFGoper Left Rolandic operculum Left Temporal pole Left Sup & Mid Temporal Left Sup Occipital
-34	22	4				
-37	19	-8				
-39	-50	39	2136	<0.0001	3.94 3.80 3.77	Left Sup & Inf Parietal Left Supramarginal Left Sup & Mid Temporal Left Angular Left Mid & Sup Occipital
-37	-70	20				
-47	-74	20				
0	40	56	2285	<0.0001	3.93 3.93 3.61	Left SFGmedial Right SFGmedial Left SFG Left IFGtriang SMA ACC MCC
-7	35	52				
6	29	50				
44	18	50	486	<0.0001	3.63 3.29 3.06	Right SFGmedial, IFGtriang Right PreCC
52	18	40				
51	27	32				
38	-64	39	410	0.022	3.75 3.52 3.45	Right Inf & Sup Parietal Right Angular Right Supramarginal Right Sup & Mid Temporal Right Mid and Sup Occipital
46	-53	45				
46	-48	56				
Local analysis on HT mask (p_{TFCE} <0.05, uncorrected)						
MNI coordinates			k	p_{uncorr}	T value	HT nuclei
X	Y	Z				
-2	3	10	2	0.032	1.96	Left FX

Supplementary Table 3: Activation and deactivation clusters obtained for the [Context-NonFood] condition in healthy controls (HC).

FX, Fornix; OFC, orbitofrontal cortex.

Contrast [Food – Non Food]						
OB > HC						
Whole brain (p_{TFCE} <0.05 k=5; FDR corrected at the cluster level p<0.05)						
MNI coordinates (mm)			k	p_{FDR} (cluster)	T value	Regions
X	Y	Z				
0	-45	52	392	0.018	4.00 3.06 2.95	Precuneus Left MCC Left Sup Parietal Right paracentral lobules
19	40	56				
-4	-59	56				
Local analysis on HT mask (p_{TFCE} <0.05, uncorrected)						
MNI coordinates (mm)			k	p_{uncorr}	T value	HT nuclei
X	Y	Z				
1	-2	-3	1	1.78	0.041	Right PaVN
OB < HC						
Local analysis on HT mask (p_{TFCE} <0.05, uncorrected)						
MNI coordinates (mm)			k	p_{uncorr}	T value	HT nuclei
X	Y	Z				
3	3	-3	1	0.044	1.71	Right AC
-2	5	4	1	0.049	1.69	Right FX
Contrast [Context – Non Food]						
OB < HC						
Local analysis on HT mask (p_{TFCE} <0.05, uncorrected)						
MNI coordinates (mm)			k	p_{uncorr}	T value	HT nuclei
X	Y	Z				
-4	2	4	1	0.041	1.74	Left FX

Supplementary Table 4: Differences in activation and deactivation patterns obtained for the [Context-NonFood] condition in young female living with obesity (OB) compared to healthy controls (HC).

AC, anterior commissure; PaVN, Paraventricular nucleus.

Contrast [Food – Non Food]						
AN > HC						
Whole brain (p_{TFCE} <0.05 k=5; FDR corrected at the cluster level p<0.05)						
MNI coordinates (mm)			k	p_{FDR} (cluster)	T value	Regions
X	Y	Z				
59	-34	24	667	<0.0001	5.22 3.75 3.38	Right Supramarginal Right Temporal Sup Right Angular Right Parietal Inferior
48	-34	29				
59	-43	21				
-5	-56	52	419	<0.002	4.27 3.25 2.81	Precuneus Left MCC Left Parietal Sup
-13	-50	44				
-8	-50	66				
49	-24	55	2551	<0.0001	4.54 4.49 4.03	Right PreCC & PostCC Right Sup & Inf Parietal Right paracentral lobule Right SFGmedial & SFG Right precuneus
36	-29	66				
27	-38	56				
19	-77	32	1180	<0.0001	4.18	Right cuneus Right calcarine Right Sup & Mid occipital
12	-82	20			4.11	
22	-67	15			3.96	
Local analysis on HT mask (p_{TFCE} <0.05, uncorrected)						
MNI coordinates (mm)			K	p_{uncorr}	T value	HT Nuclei
X	Y	Z				
1	0	-3	1	0.033	1.84	Right FX
AN < HC						
Whole brain (p_{TFCE} <0.05 k=5; FDR corrected at the cluster level p<0.05)						
MNI coordinates (mm)			k	p_{FDR} (cluster)	T value	Regions
X	Y	Z				
-40	-27	63	850	<0.0001	4.52 4.39 3.96	Left PreCC Left PostCC Left paracentral lobule Left Inf Parietal
-37	-26	55				
-31	-24	61				
-4	-69	31	397	0.005	3.75 3.35 2.72	Left & Right precuneus Left PCC Left cuneus Calcarine
-4	-53	20				
-7	-59	26				
Local analysis on HT mask (p_{TFCE} <0.05, uncorrected)						
MNI coordinates (mm)			k	p_{uncorr}	T value	HT Nuclei
X	Y	Z				
1	-13	-8	2	0.013	2.32	Right PH Right MT
Contrast [Context – Non Food]						
AN > HC						
Whole brain (p_{TFCE} <0.05 k=5; FDR corrected at the cluster level p<0.05)						
MNI coordinates (mm)			k	p_{FDR} (cluster)	T value	Region
X	Y	Z				
52	-38	28	367	0.022	3 .66 3.11	Right supramarginal Right PostCC
48	-35	34				

57	-34	23			2.80	Right Inf Parietal cortex Right Sup Temporal
AN < HC						
Local analysis on HT mask (p_{TFCE} <0.05, uncorrected)						
MNI coordinates (mm)			k	p_{uncorr}	T value	HT nuclei
X	Y	Z				
-4	3	0	1	0.016	2.21	Left FX Left BNST
8	5	4	1	0.020	2.12	Right BNST
3	0	-6	1	0.031	1.91	Right FX

Supplementary Table 5: Differences in activation and deactivation patterns obtained for the [Context-NonFood] condition in young female living with restrictive anorexia nervosa (AN) compared to healthy controls (HC).

PCC, posterior cingulate cortex; PH, posterior hypothalamus.

Contrast [Food – Non Food]

OB > AN						
Whole brain (p_{TFCE} <0.05 k=5; FDR corrected at the cluster level p<0.05)						
MNI coordinates (mm)			k	p_{FDR} (cluster)	T value	regions
X	Y	Z				
-37	-26	-55	1513	<0.0001	4.29	Left PreCC
-29	-38	53			3.83	Left PostCC
-31	-19	66			3.63	Left Inf & Sup Parietal Left Precuneus Left paracentral lobule
Whole brain (p_{TFCE} <0.05 k=5; FDR corrected at the cluster level p<0.05)						
MNI coordinates (mm)			k	p_{uncorr}	T value	HT nuclei
X	Y	Z				
1	-2	-3	1	0.041	1.78	Right PaVN
AN > OB						
Whole brain (p_{TFCE} <0.05 k=5; FDR corrected at the cluster level p<0.05)						
MNI coordinates (mm)			k	p_{FDR} (cluster)	T value	regions
X	Y	Z				
32	-34	66	977	<0.0001	4.80	Right PreCC
24	-30	68			3.37	Right PostCC
32	-19	66			3.12	Right Sup and Mid Frontal Right Inf Parietal
Local analysis on HT mask (p_{TFCE} <0.05, uncorrected)						
MNI coordinates (mm)			k	p_{uncorr}	T value	Regions
X	Y	Z				
-2	5	4	1	0.045	1.72	Left FX
Contrast [Context – Non Food]						
OB > AN						
Whole brain (p_{TFCE} <0.05 k=5; FDR corrected at the cluster level p<0.05)						
MNI coordinates (mm)			k	p_{FDR} (cluster)	T value	Region
X	Y	Z				
-18	-58	10	681	<0.0001	3 .75	Left & Right Calcarine
-20	-64	24			3.56	Left & Right Cuneus
16	-53	15			3.34	Left & Right Precuneus Left Sup Occipital Right Lingual
4	-40	42	354	0.009	3.02	MCC
-4	-43	45			2.99	Precuneus
14	-43	42			2.87	Paracentral lobules Right SMA
Local analysis on HT mask (p_{TFCE} <0.05, uncorrected)						
MNI coordinates			k	p_{uncorr}	T value	HT nuclei
X	Y	Z				
1	-5	-9	3	0.031	1.93	Right DM Right PaVN
1	-8	-8	1	0.038	1.81	Right PH

Supplementary Table 6: Differences in activation and deactivation patterns obtained for the [Food-NonFood] and [Context-NonFood] condition between young female living with restrictive anorexia nervosa (AN) and obesity (OB).

Abbreviations: DM, Dorsomedial hypothalamic nucleus.

Graph Theory parameters	
Nodes	**Degrees**

		AN	HC	OB
Intra-HT	L_VM	35±8	34±12	**47±11** *(p_{FDR}=0.010)
Extra-HT	L_Putamen	**37±8** *(p_{FDR}<0.001)	53±10	47±15
	R_Putamen	**35±10** *(p_{FDR}=0.002) £(p_{FDR}=0.029)	52±13	50±11
	L_Caudate	**34±7** *(p_{FDR}<0.001)	49±12	43±12
	N_Acc	**33±9** *(p_{FDR}=0.002) £(p_{FDR}=0.013)	49±15	48±13
	L_Thal_PuM	**39±10** *(p_{FDR}=0.004) £(p_{FDR}=0.006)	52±11	58±12
	Nodes	**Betweenness Centrality**		
		AN	**HC**	**OB**
Intra-HT	R_BNST	**114±44** *(p_{FDR}=0.005)	62±38	81±32
	L_dPeVN	**71±36** *(p_{FDR}=0.007)	38±23	42±31
	Nodes	**Local Efficiency**		
		AN	**HC**	**OB**
Intra-HT	R_SCN	0.687±0.032	0.694±0.056	**0.750±0.045** *(p_{FDR}=0.050) £(p_{FDR}=0.007)
Extra-HT	L_Putamen	**0.700±0.035** *(p_{FDR}=0.001) £(p_{FDR}=0.020)	0.747±0.035	0.745±0.036
	L_INS_dGranular	**0.669±0.030** *(p_{FDR}=0.002) £(p_{FDR}=0.014)	0.741±0.043	0.745±0.041

Supplementary Table 7: Modulation in node characteristics observed in young female living with restrictive anorexia nervosa (AN) or with obesity (OB) relative to healthy controls (HC). Shown are the significant higher (red) and lower (blue) node characteristics (p_{FDR}<0.05) between weight related disorders (AN or OB) and HC (*) and between AN and OB (£).

7 General conclusion

In the context of the rising prevalence of obesity, as well as the severity of restrictive anorexia nervosa, my thesis work aimed at characterizing the organization of eating behavior networks at the hypothalamic level scale and across different species.
While it is known that the HT processes sensory inputs and engages in bidirectional communication with behavioral, autonomic, and endocrine systems, ongoing research continues to refine our understanding of the circuits regulating eating behaviors. The role of hypothalamic subnuclei neuronal activity in regulating food intake and feeding has been identified through rodents' studies. However, translating these findings to humans is complex, as human eating behavior is heavily influenced by sociopsychological factors, which are difficult to replicate and study in rodents.
Furthermore, although hypothalamic nuclei have been extensively described in rodents, these studies were often invasive and/or focused on a single hypothalamic subpopulation and were using existing knowledge. Therefore, using MRI to generate a comprehensive brain-wide connectivity map of hypothalamic nuclei and its modulation in weight-related disorders is necessary to gain a deeper understanding of the networks regulating eating behavior.
The Human HT is a small brain region (around 1 cm^3), it is organized into highly distinct nuclei, which most neuroimaging studies have largely overlooked. In that context, ultra-high field (7T) MRI has appeared as a game changer to explore *in vivo* the eating behavioral networks and the consequences of their dysregulation in weight-related disorders.
Ultimately, my work demonstrates that ultra-high field MRI has advanced sufficiently to effectively investigate brain-wide functional and structural circuits underlying maladaptive behavior over different species.

In the first part of my work, I established from the ground up the MRI standard operating protocol for the in-vivo resting-state fMRI and ex-vivo DTI acquisitions of mice, as well as their processing. This protocol once optimized, I obtained the structural and functional connectome of control mice as well as in a mouse model of cue-triggered food consumption (CFC). Using those, I then focused my investigation on the TN, a nucleus which role had been recently described by my colleagues in Singapore. In addition to detailing both the structural and functional connectome of the TN in control mice, I also described functional connectivity modulation in CFC. Indeed, brain-wide circuit mapping of the TN revealed circuit changes, including both reported and novel circuits. For example, TN is hyperconnected to the hippocampus, insula, thalamus, amygdala, striatum and olfactory areas. This finding may be attributed to the nature of the conditioning related to food, which involves multiple aspects, including reward, olfaction, and memory. To validate my functional connectivity results, I initially verified whether there was a significant increase in TN-Subiculum functional connectivity in CFC mice, as previously reported by Mohammad and colleagues (Mohammad et al., 2021). In addition, the feasibility of using fMRI-based connectivity for screening brain-wide circuits underlying maladaptive behavior was validated by my colleagues using a lighsheet method in the same cohort, serving as 'gold standard'. Using fMRI, my work revealed the functional changes underlying the structural connectome observed through lightsheet imaging.

I believe that this multi-modal, brain-wide neural circuit mapping represents a substantial breakthrough in systems neuroscience research, as it provides a more thorough method for identifying potential circuit mechanisms linked to specific conditioned behaviors.
The last development of my work consists in linking the amount of food consumed on the last day of CFC (test day) with the increase in TN FC in CFC mice. For example, linear regression of the TN-Subiculum connectivity with the amount of food intake showed significant correlation, which supports previous finding that Subiculum-TN circuit plays a critical role in CFC (Mohammad et al., 2021).
However, ex-vivo DTI did not allow me to study the modulation of the mice's structural connectome in the context of cue-triggered food consumption. This disappointing result could be attributed to the deformation the brain experienced after their fixation or to the preprocessing pipeline, which was challenged by the limited presence of large white matter fibers in mouse brains. Currently, there is no widely accepted pipeline for rodents and the existing software for DTI preprocessing (MRtrix3) is optimized for human brains, which have large white matter tracts.

In the second part of my work, I characterize in fasted young females living with obesity (OB), restrictive anorexia nervosa (AN) or healthy control (HC), the structural and functional alterations of HT nuclei in weight-related disorders, using ultra high field MRI (7T) including high resolution quantitative anatomical sequences, along with BOLD task related fMRI and rs-fMRI. The lack of spatial resolution and signal contrast used in previous studies prevented the precise individual anatomo-functional characterization of HT nuclei. By improving selectivity and spatial resolution, 7T MRI has opened new perspectives to reach this goal.
First, the macro- and microstructural exploration revealed that both OB and AN have higher volumes of specific HT nuclei relative to HC, with AN showing significant HT structural modulation. Furthermore, we found a significant correlation between the observed structural alterations and leptin/ghrelin plasmatic levels, as well as with the severity of eating disorders, depression and anxiety. I hypothesized that hypothalamic inflammation plays a key role in rewiring the neural circuits governing energy homeostasis in pathological conditions such as obesity and anorexia nervosa. Indeed, recent research has made it evident that hypothalamic inflammation is a significant contributor to the disruption of energy regulation in both conditions. Interestingly, although we found some commonly abnormal morpho-structural in both YWAN and YWOB, it is interesting to observe that HT alterations are pathology specific and closely related to HT nuclei function in feeding.
In the same cohort, I then applied task-related fMRI to investigate activation patterns of cortical, subcortical and HT nuclei of eating behavior networks using highcalories/low-calories/non-food cues as well as images displaying environments prone or aversive to have a satisfying meal. I observed reorganization of static functional connectivity (FC), particularly within the inner-HT network and between the HT and reward-related areas in AN and OB. AN also displayed abnormal nodal network organization within the salience network. Both inner-HT and whole brain network dynamic FC were significantly altered in OB, characterized by a slowdown in rapid transitions. These changes were also found to be correlated with disordered eating behaviors, as assessed by the EAT-26. Finally, both AN and OB presented abnormal responses to images of food and context relative to non-food.

In sum, we have successfully demonstrated changes in food intake circuits, including at the HT nuclei level, affecting morpho-structure, activity and overall connectivity in weight-related disorders.
However, my work presented a few limitations. First, further analyses with a larger sample size are necessary, as the strict inclusion criteria controlling for factors like age, sex, and conditions (12-hour fasting, blood sample collection, morning scan) resulted in small and unequal group sizes. Then, although the Neudorfer atlas (Neudorfer et al., 2020a) is suitable for hypothalamic segmentation in volumetric analyses, its reliability and effectiveness in clinical subjects still require thorough methodological validation.

To conclude, my PhD work has laid the foundation for developing precise, in vivo, non-invasive imaging biomarkers to map the microstructure, connectivity, and function of individual hypothalamic nuclei involved in Human eating behavior. Additionally, I set up MRI-based multi-modal brain-wide neural circuit mapping in mice, revealing functional modulation of the TN in CFC mice.

This PhD work opens many perspectives across different species. In mice, employing multi-modal circuit mapping tools will significantly enhance neuroscience research by offering an unbiased and comprehensive understanding of underlying mechanisms, revealing new neural circuit targets that may not be readily apparent in existing literature, and ultimately fostering the development of novel ideas and hypotheses that advance our comprehension of specific behaviors.
In Human, a more detailed characterization of hypothalamic nuclei involved in eating behavior networks is crucial for understanding how eating behavior circuits become maladaptive in weight-related disorders. This deeper insight could reduce short-term relapses after treatment and help answer key questions, such as how GLP-1 agonists modulate these networks in females with obesity, ultimately enabling early prognosis of treatment efficacy and a better understanding of partial or complete non-responders. I showed that conclusive results can be obtained with fewer subjects than previously required before the advent of 7T MRI. This offers a new perspective for MRI studies, specifically those involving intensive protocols, which are commonly employed in appetite-related research. Regarding the context, I would like to explore the effects of positive context versus negative context on hypothalamic activity in weight-related disorders. Finally, precise parcellation of HT nuclei requires the creation of new atlas derived from high resolution 7T acquisitions.

8 Bibliography

A, S., & Y, T. (2014). CRF and urocortin peptides as modulators of energy balance and feeding behavior during stress. *Frontiers in Neuroscience*, *8*. https://doi.org/10.3389/fnins.2014.00052

Affinati, A. H., & Martin G. Myers, J. (2021). Neuroendocrine Control of Body Energy Homeostasis. In *Endotext [Internet]*. MDText.com, Inc. https://www.ncbi.nlm.nih.gov/sites/books/NBK570658/

Aggarwal, M., Zhang, J., Miller, M. I., Sidman, R. L., & Mori, S. (2009). Magnetic resonance imaging and micro-computed tomography combined atlas of developing and adult mouse brains for stereotaxic surgery. *Neuroscience*, *162*(4), 1339–1350. https://doi.org/10.1016/j.neuroscience.2009.05.070

Al-Zubaidi, A., Iglesias, S., Stephan, K. E., Buades-Rotger, M., Heldmann, M., Nolde, J. M., Kirchner, H., Mertins, A., Jauch-Chara, K., & Münte, T. F. (2020). Effects of hunger, satiety and oral glucose on effective connectivity between hypothalamus and insular cortex. *NeuroImage*, *217*, 116931. https://doi.org/10.1016/j.neuroimage.2020.116931

Amunts, K., Mohlberg, H., Bludau, S., & Zilles, K. (2020). Julich-Brain: A 3D probabilistic atlas of the human brain's cytoarchitecture. *Science (New York, N.Y.)*, *369*(6506), 988–992. https://doi.org/10.1126/science.abb4588

Anand, B. K., & Brobeck, J. R. (1951a). Hypothalamic Control of Food Intake in Rats and Cats. *The Yale Journal of Biology and Medicine*, *24*(2), 123–140.

Anand, B. K., & Brobeck, J. R. (1951b). Localization of a “feeding center” in the hypothalamus of the rat. *Proceedings of the Society for Experimental Biology and Medicine. Society for Experimental Biology and Medicine (New York, N.Y.)*, *77*(2), 323–324. https://doi.org/10.3181/00379727-77-18766

Andermann, M. L., & Lowell, B. B. (2017). Towards a Wiring-Diagram Understanding of Appetite Control. *Neuron*, *95*(4), 757–778. https://doi.org/10.1016/j.neuron.2017.06.014

Andersson, J. L. R., Skare, S., & Ashburner, J. (2003). How to correct susceptibility distortions in spin-echo echo-planar images: Application to diffusion tensor imaging. *NeuroImage*, *20*(2), 870–888. https://doi.org/10.1016/S1053-8119(03)00336-7

Aponte, Y., Atasoy, D., & Sternson, S. M. (2011). AGRP neurons are sufficient to orchestrate feeding behavior rapidly and without training. *Nature Neuroscience*, *14*(3), 351–355. https://doi.org/10.1038/nn.2739

Arcelus, J., Mitchell, A. J., Wales, J., & Nielsen, S. (2011). Mortality rates in patients with anorexia nervosa and other eating disorders. A meta-analysis of 36 studies. *Archives of General Psychiatry*, *68*(7), 724–731. https://doi.org/10.1001/archgenpsychiatry.2011.74

A/RES/70/1 Transforming our world: The 2030 Agenda for Sustainable Development. (2030).

Artmann, H., Grau, H., Adelmann, M., & Schleiffer, R. (1985). Reversible and non-reversible enlargement of cerebrospinal fluid spaces in anorexia nervosa. *Neuroradiology*, *27*(4), 304–312. https://doi.org/10.1007/BF00339562

Atasoy, D., Betley, J. N., Su, H. H., & Sternson, S. M. (2012). Deconstruction of a neural circuit for hunger. *Nature*, *488*(7410), 172–177. https://doi.org/10.1038/nature11270

Atlas of the Human Hypothalamus—1st Edition. (n.d.). Retrieved July 7, 2021, from https://www.elsevier.com/books/atlas-of-the-human-hypothalamus/dudas/978-0-12-822051-1

Ávalos, Y., Kerr, B., Maliqueo, M., & Dorfman, M. (2018a). Cell and molecular mechanisms behind diet-induced hypothalamic inflammation and obesity. *Journal of Neuroendocrinology*, *30*(10), e12598. https://doi.org/10.1111/jne.12598

Ávalos, Y., Kerr, B., Maliqueo, M., & Dorfman, M. (2018b). Cell and molecular mechanisms behind diet-induced hypothalamic inflammation and obesity. *Journal of Neuroendocrinology*, *30*(10), e12598. https://doi.org/10.1111/jne.12598

Avants, B. B., Epstein, C. L., Grossman, M., & Gee, J. C. (2008). Symmetric diffeomorphic image registration with cross-correlation: Evaluating automated labeling of elderly and neurodegenerative brain. *Medical Image Analysis*, *12*(1), 26–41. https://doi.org/10.1016/j.media.2007.06.004

Avants, B. B., Tustison, N. J., Song, G., Cook, P. A., Klein, A., & Gee, J. C. (2011). A reproducible evaluation of ANTs similarity metric performance in brain image registration. *NeuroImage*, *54*(3), 2033–2044. https://doi.org/10.1016/j.neuroimage.2010.09.025

Avants, B., Tustison, N. J., & Song, G. (2009). Advanced Normalization Tools: V1.0. *The Insight Journal*. https://doi.org/10.54294/uvnhin

Avena, N. M., & Bocarsly, M. E. (2012). Dysregulation of brain reward systems in eating disorders: Neurochemical information from animal models of binge eating, bulimia nervosa, and anorexia nervosa. *Neuropharmacology*, *63*(1), 87–96. https://doi.org/10.1016/j.neuropharm.2011.11.010

Azevedo, E. P., Ivan, V. J., Friedman, J. M., & Stern, S. A. (2022). Top-down control of appetite. *Biological Psychiatry*, *91*(10), 869–878. https://doi.org/10.1016/j.biopsych.2021.07.015

Azevedo, E. P., Pomeranz, L., Cheng, J., Schneeberger, M., Vaughan, R., Stern, S. A., Tan, B., Doerig, K., Greengard, P., & Friedman, J. M. (2019). A Role of Drd2 Hippocampal Neurons in Context-Dependent Food Intake. *Neuron*, *102*(4), 873-886.e5. https://doi.org/10.1016/j.neuron.2019.03.011

Baek, K., Morris, L. S., Kundu, P., & Voon, V. (2017). Disrupted resting-state brain network properties in obesity: Decreased global and putaminal cortico-striatal network efficiency. *Psychological Medicine*, *47*(4), 585–596. https://doi.org/10.1017/S0033291716002646

Baggio, H. C., Abos, A., Segura, B., Campabadal, A., Garcia-Diaz, A., Uribe, C., Compta, Y., Marti, M. J., Valldeoriola, F., & Junque, C. (2018). Statistical inference in brain graphs using threshold-free network-based statistics. *Human Brain Mapping*, *39*(6), 2289–2302. https://doi.org/10.1002/hbm.24007

Baldo, B. A., Spencer, R. C., Sadeghian, K., & Mena, J. D. (2016). GABA-Mediated Inactivation of Medial Prefrontal and Agranular Insular Cortex in the Rat: Contrasting Effects on Hunger- and Palatability-Driven Feeding. *Neuropsychopharmacology*, *41*(4), 960–970. https://doi.org/10.1038/npp.2015.222

Bang, L., Bahrami, S., Hindley, G., Smeland, O. B., Rødevand, L., Jaholkowski, P. P., Shadrin, A., Connell, K. S. O., Frei, O., Lin, A., Rahman, Z., Cheng, W., Parker, N., Fan, C. C., Dale, A. M., Djurovic, S., Bulik, C. M., & Andreassen, O. A. (2023). Genome-wide analysis of anorexia nervosa and major psychiatric disorders and related traits reveals genetic overlap and identifies novel risk loci for anorexia nervosa. *Translational Psychiatry*, *13*(1), 1–9. https://doi.org/10.1038/s41398-023-02585-1

Banks, W. A., Coon, A. B., Robinson, S. M., Moinuddin, A., Shultz, J. M., Nakaoke, R., & Morley, J. E. (2004). Triglycerides induce leptin resistance at the blood-brain barrier. *Diabetes*, *53*(5), 1253–1260. https://doi.org/10.2337/diabetes.53.5.1253

Barbato, G., Fichele, M., Senatore, I., Casiello, M., & Muscettola, G. (2006). Increased dopaminergic activity in restricting-type anorexia nervosa. *Psychiatry Research*, *142*(2), 253–255. https://doi.org/10.1016/j.psychres.2005.07.031

Barnett, S. C., Parr-Brownlie, L. C., Perry, B. A. L., Young, C. K., Wicky, H. E., Hughes, S. M., McNaughton, N., & Dalrymple-Alford, J. C. (2021). Anterior thalamic nuclei neurons sustain

memory. *Current Research in Neurobiology*, *2*, 100022. https://doi.org/10.1016/j.crneur.2021.100022

Baroncini, M., Jissendi, P., Balland, E., Besson, P., Pruvo, J.-P., Francke, J.-P., Dewailly, D., Blond, S., & Prevot, V. (2012). MRI atlas of the human hypothalamus. *NeuroImage*, *59*(1), 168–180. https://doi.org/10.1016/j.neuroimage.2011.07.013

Baroncini, M., Jissendi, P., Catteau-Jonard, S., Dewailly, D., Pruvo, J.-P., Francke, J.-P., & Prevot, V. (2010). Sex steroid hormones-related structural plasticity in the human hypothalamus. *NeuroImage*, *50*(2), 428–433. https://doi.org/10.1016/j.neuroimage.2009.11.074

Barone, F. C., Wayner, M. J., Scharoun, S. L., Guevara-Aguilar, R., & Aguilar-Baturoni, H. U. (1981). Afferent connections to the lateral hypothalamus: A horseradish peroxidase study in the rat. *Brain Research Bulletin*, *7*(1), 75–88. https://doi.org/10.1016/0361-9230(81)90101-5

Batterham, R. L., Cowley, M. A., Small, C. J., Herzog, H., Cohen, M. A., Dakin, C. L., Wren, A. M., Brynes, A. E., Low, M. J., Ghatei, M. A., Cone, R. D., & Bloom, S. R. (2002). Gut hormone PYY(3-36) physiologically inhibits food intake. *Nature*, *418*(6898), 650–654. https://doi.org/10.1038/nature00887

Batterink, L., Yokum, S., & Stice, E. (2010a). Body mass correlates inversely with inhibitory control in response to food among adolescent girls: An fMRI study. *NeuroImage*, *52*(4), 1696–1703. https://doi.org/10.1016/j.neuroimage.2010.05.059

Batterink, L., Yokum, S., & Stice, E. (2010b). Body mass correlates inversely with inhibitory control in response to food among adolescent girls: An fMRI study. *NeuroImage*, *52*(4), 1696–1703. https://doi.org/10.1016/j.neuroimage.2010.05.059

Beck, A. T., & Beamesderfer, A. (1974). Assessment of depression: The depression inventory. *Modern Problems of Pharmacopsychiatry*, *7*(0), 151–169. https://doi.org/10.1159/000395074

Beckstead, R. M., Domesick, V. B., & Nauta, W. J. H. (1979). Efferent connections of the substantia nigra and ventral tegmental area in the rat. *Brain Research*, *175*(2), 191–217. https://doi.org/10.1016/0006-8993(79)91001-1

Beier, K. T., Kim, C. K., Hoerbelt, P., Hung, L. W., Heifets, B. D., DeLoach, K. E., Mosca, T. J., Neuner, S., Deisseroth, K., Luo, L., & Malenka, R. C. (2017). Rabies screen reveals GPe control of cocaine-triggered plasticity. *Nature*, *549*(7672), 345. https://doi.org/10.1038/nature23888

Beier, K. T., Steinberg, E. E., DeLoach, K. E., Xie, S., Miyamichi, K., Schwarz, L., Gao, X. J., Kremer, E. J., Malenka, R. C., & Luo, L. (2015). Circuit Architecture of VTA Dopamine Neurons Revealed by Systematic Input-Output Mapping. *Cell*, *162*(3), 622–634. https://doi.org/10.1016/j.cell.2015.07.015

Bellinger, L. L., & Bernardis, L. L. (2002). The dorsomedial hypothalamic nucleus and its role in ingestive behavior and body weight regulation: Lessons learned from lesioning studies. *Physiology & Behavior*, *76*(3), 431–442. https://doi.org/10.1016/s0031-9384(02)00756-4

Benoit, S. C., Kemp, C. J., Elias, C. F., Abplanalp, W., Herman, J. P., Migrenne, S., Lefevre, A.-L., Cruciani-Guglielmacci, C., Magnan, C., Yu, F., Niswender, K., Irani, B. G., Holland, W. L., & Clegg, D. J. (2009). Palmitic acid mediates hypothalamic insulin resistance by altering PKC-θ subcellular localization in rodents. *The Journal of Clinical Investigation*, *119*(9), 2577–2589. https://doi.org/10.1172/JCI36714

Benzo, C. A. (1983). Minireview. The hypothalamus and blood glucose regulation. *Life Sciences*, *32*(22), 2509–2515. https://doi.org/10.1016/0024-3205(83)90231-x

Bergen, A. W., Yeager, M., Welch, R. A., Haque, K., Ganjei, J. K., van den Bree, M. B. M., Mazzanti, C., Nardi, I., Fichter, M. M., Halmi, K. A., Kaplan, A. S., Strober, M., Treasure, J., Woodside, D. B., Bulik, C. M., Bacanu, S.-A., Devlin, B., Berrettini, W. H., Goldman, D., & Kaye, W. H. (2005). Association of Multiple DRD2 Polymorphisms with Anorexia Nervosa. *Neuropsychopharmacology*, *30*(9), 1703–1710. https://doi.org/10.1038/sj.npp.1300719

Bergh, C., & Södersten, P. (1996a). Anorexia nervosa, self–starvation and the reward of stress. *Nature Medicine*, *2*(1), 21–22. https://doi.org/10.1038/nm0196-21

Bergh, C., & Södersten, P. (1996b). Anorexia nervosa, self–starvation and the reward of stress. *Nature Medicine*, *2*(1), Article 1. https://doi.org/10.1038/nm0196-21

Bernardoni, F., King, J. A., Geisler, D., Birkenstock, J., Tam, F. I., Weidner, K., Roessner, V., White, T., & Ehrlich, S. (2018). Nutritional Status Affects Cortical Folding: Lessons Learned From Anorexia Nervosa. *Biological Psychiatry*, *84*(9), 692–701. https://doi.org/10.1016/j.biopsych.2018.05.008

Bernardoni, F., King, J. A., Geisler, D., Stein, E., Jaite, C., Nätsch, D., Tam, F. I., Boehm, I., Seidel, M., Roessner, V., & Ehrlich, S. (2016). Weight restoration therapy rapidly reverses cortical thinning in anorexia nervosa: A longitudinal study. *NeuroImage*, *130*, 214–222. https://doi.org/10.1016/j.neuroimage.2016.02.003

Berridge, K. C., & Valenstein, E. S. (1991). What psychological process mediates feeding evoked by electrical stimulation of the lateral hypothalamus? *Behavioral Neuroscience*, *105*(1), 3–14. https://doi.org/10.1037//0735-7044.105.1.3

Berthoud, H.-R. (2002a). Multiple neural systems controlling food intake and body weight. *Neuroscience and Biobehavioral Reviews*, *26*(4), 393–428. https://doi.org/10.1016/s0149-7634(02)00014-3

Berthoud, H.-R. (2002b). Multiple neural systems controlling food intake and body weight. *Neuroscience and Biobehavioral Reviews*, *26*(4), 393–428. https://doi.org/10.1016/s0149-7634(02)00014-3

Berthoud, H.-R. (2012a). The neurobiology of food intake in an obesogenic environment. *The Proceedings of the Nutrition Society*, *71*(4), 478–487. https://doi.org/10.1017/S0029665112000602

Berthoud, H.-R. (2012b). The neurobiology of food intake in an obesogenic environment. *The Proceedings of the Nutrition Society*, *71*(4), 478–487. https://doi.org/10.1017/S0029665112000602

Berthoud, H.-R., & Morrison, C. (2008a). The Brain, Appetite, and Obesity. *Annual Review of Psychology*, *59*(Volume 59, 2008), 55–92. https://doi.org/10.1146/annurev.psych.59.103006.093551

Berthoud, H.-R., & Morrison, C. (2008b). *The Brain, Appetite, and Obesity* (SSRN Scholarly Paper ID 1141913). Social Science Research Network. https://papers.ssrn.com/abstract=1141913

Berthoud, H.-R., Sutton, G. M., Townsend, R. L., Patterson, L. M., & Zheng, H. (2006). Brainstem mechanisms integrating gut-derived satiety signals and descending forebrain information in the control of meal size. *Physiology & Behavior*, *89*(4), 517–524. https://doi.org/10.1016/j.physbeh.2006.08.018

Betley, J. N., Cao, Z. F. H., Ritola, K. D., & Sternson, S. M. (2013). Parallel, Redundant Circuit Organization for Homeostatic Control of Feeding Behavior. *Cell*, *155*(6), 1337–1350. https://doi.org/10.1016/j.cell.2013.11.002

Betley, J. N., Xu, S., Cao, Z. F. H., Gong, R., Magnus, C. J., Yu, Y., & Sternson, S. M. (2015). Neurons for hunger and thirst transmit a negative-valence teaching signal. *Nature*, *521*(7551), 180–185. https://doi.org/10.1038/nature14416

Bi, S., Ladenheim, E. E., Schwartz, G. J., & Moran, T. H. (2001). A role for NPY overexpression in the dorsomedial hypothalamus in hyperphagia and obesity of OLETF rats. *American Journal of Physiology. Regulatory, Integrative and Comparative Physiology*, *281*(1), R254-260. https://doi.org/10.1152/ajpregu.2001.281.1.R254

Biswal, B., Yetkin, F. Z., Haughton, V. M., & Hyde, J. S. (1995a). Functional connectivity in the motor cortex of resting human brain using echo-planar MRI. *Magnetic Resonance in Medicine*, *34*(4), 537–541. https://doi.org/10.1002/mrm.1910340409

Biswal, B., Yetkin, F. Z., Haughton, V. M., & Hyde, J. S. (1995b). Functional connectivity in the motor cortex of resting human brain using echo-planar MRI. *Magnetic Resonance in Medicine*, *34*(4), 537–541. https://doi.org/10.1002/mrm.1910340409

Blechert, J., Meule, A., Busch, N. A., & Ohla, K. (2014). Food-pics: An image database for experimental research on eating and appetite. *Frontiers in Psychology*, *5*. https://doi.org/10.3389/fpsyg.2014.00617

Bleich, S. N., Cutler, D., Murray, C., & Adams, A. (2008). Why Is the Developed World Obese? *Annual Review of Public Health*, *29*(Volume 29, 2008), 273–295. https://doi.org/10.1146/annurev.publhealth.29.020907.090954

Boehm, I., Geisler, D., King, J. A., Ritschel, F., Seidel, M., Deza Araujo, Y., Petermann, J., Lohmeier, H., Weiss, J., Walter, M., Roessner, V., & Ehrlich, S. (2014). Increased resting state functional connectivity in the fronto-parietal and default mode network in anorexia nervosa. *Frontiers in Behavioral Neuroscience*, *8*. https://doi.org/10.3389/fnbeh.2014.00346

Boehm, I., Geisler, D., Tam, F., King, J. A., Ritschel, F., Seidel, M., Bernardoni, F., Murr, J., Goschke, T., Calhoun, V. D., Roessner, V., & Ehrlich, S. (2016). Partially restored resting-state functional connectivity in women recovered from anorexia nervosa. *Journal of Psychiatry & Neuroscience: JPN*, *41*(6), 377–385. https://doi.org/10.1503/jpn.150259

Boehm, I., Mennigen, E., Geisler, D., Poller, N. W., Gramatke, K., Calhoun, V. D., Roessner, V., King, J. A., & Ehrlich, S. (2024). Dynamic functional connectivity in anorexia nervosa: Alterations in states of low connectivity and state transitions. *Journal of Child Psychology and Psychiatry, and Allied Disciplines*. https://doi.org/10.1111/jcpp.13970

Boersma, G. J., Liang, N.-C., Lee, R. S., Albertz, J. D., Kastelein, A., Moody, L. A., Aryal, S., Moran, T. H., & Tamashiro, K. L. (2016). Failure to upregulate Agrp and Orexin in response to activity based anorexia in weight loss vulnerable rats characterized by passive stress coping and prenatal stress experience. *Psychoneuroendocrinology*, *67*, 171–181. https://doi.org/10.1016/j.psyneuen.2016.02.002

Boghi, A., Sterpone, S., Sales, S., D'Agata, F., Bradac, G. B., Zullo, G., & Munno, D. (2011). In vivo evidence of global and focal brain alterations in anorexia nervosa. *Psychiatry Research*, *192*(3), 154–159. https://doi.org/10.1016/j.pscychresns.2010.12.008

Borg, W. P., During, M. J., Sherwin, R. S., Borg, M. A., Brines, M. L., & Shulman, G. I. (1994). Ventromedial hypothalamic lesions in rats suppress counterregulatory responses to

hypoglycemia. *The Journal of Clinical Investigation*, *93*(4), 1677–1682. https://doi.org/10.1172/JCI117150

Bray, G., Fisler, J., & York, D. (1990). Neuroendocrine control of the development of obesity: Understanding gained from studies of experimental animal models. *Frontiers in Neuroendocrinology*. https://www.semanticscholar.org/paper/Neuroendocrine-control-of-the-development-of-%3A-from-Bray-Fisler/c9733711eba4fd8c5ca17879ca09bba1b13e7414

Briggs, D. I., Enriori, P. J., Lemus, M. B., Cowley, M. A., & Andrews, Z. B. (2010). Diet-induced obesity causes ghrelin resistance in arcuate NPY/AgRP neurons. *Endocrinology*, *151*(10), 4745–4755. https://doi.org/10.1210/en.2010-0556

Brodmann, K. (1909). *Vergleichende Lokalisationslehre der Grosshirnrinde in ihren Prinzipien dargestellt auf Grund des Zellenbaues.* Barth.

Brooks, S. J., O'Daly, O. G., Uher, R., Friederich, H.-C., Giampietro, V., Brammer, M., Williams, S. C. R., Schiöth, H. B., Treasure, J., & Campbell, I. C. (2011). Differential Neural Responses to Food Images in Women with Bulimia versus Anorexia Nervosa. *PLoS ONE*, *6*(7). https://doi.org/10.1371/journal.pone.0022259

Brooks, S. J., O'Daly, O., Uher, R., Friederich, H.-C., Giampietro, V., Brammer, M., Williams, S. C. R., Schiöth, H. B., Treasure, J., & Campbell, I. C. (2012). Thinking about Eating Food Activates Visual Cortex with Reduced Bilateral Cerebellar Activation in Females with Anorexia Nervosa: An fMRI Study. *PLoS ONE*, *7*(3). https://doi.org/10.1371/journal.pone.0034000

Brooks, S. J., Rask-Andersen, M., Benedict, C., & Schiöth, H. B. (2012). A debate on current eating disorder diagnoses in light of neurobiological findings: Is it time for a spectrum model? *BMC Psychiatry*, *12*, 76. https://doi.org/10.1186/1471-244X-12-76

Brown, S. S. G., Westwater, M. L., Seidlitz, J., Ziauddeen, H., & Fletcher, P. C. (2023). Hypothalamic volume is associated with body mass index. *NeuroImage. Clinical*, *39*, 103478. https://doi.org/10.1016/j.nicl.2023.103478

Brunault, P., Ballon, N., Gaillard, P., Réveillère, C., & Courtois, R. (2014). Validation of the French version of the yale food addiction scale: An examination of its factor structure, reliability, and construct validity in a nonclinical sample. *Canadian Journal of Psychiatry. Revue Canadienne De Psychiatrie*, *59*(5), 276–284. https://doi.org/10.1177/070674371405900507

Buffenstein, R., Poppitt, S. D., McDevitt, R. M., & Prentice, A. M. (1995). Food intake and the menstrual cycle: A retrospective analysis, with implications for appetite research. *Physiology & Behavior*, *58*(6), 1067–1077. https://doi.org/10.1016/0031-9384(95)02003-9

Buresova, O. (1956). [Effect of spreading EEG depression on unconditioned and natural conditioned digestive reflexes during the depression]. *Physiologia Bohemoslovenica*, *5*(3), 350–358.

Byerly, M. S., Swanson, R., Wei, Z., Seldin, M. M., McCulloh, P. S., & Wong, G. W. (2013). A Central Role for C1q/TNF-Related Protein 13 (CTRP13) in Modulating Food Intake and Body Weight. *PLOS ONE*, *8*(4), e62862. https://doi.org/10.1371/journal.pone.0062862

Cai, D., & Khor, S. (2019a). "Hypothalamic Microinflammation" Paradigm in Aging and Metabolic Diseases. *Cell Metabolism*, *30*(1), 19–35. https://doi.org/10.1016/j.cmet.2019.05.021

Cai, D., & Khor, S. (2019b). "Hypothalamic Microinflammation" Paradigm in Aging and Metabolic Diseases. *Cell Metabolism*, *30*(1), 19–35. https://doi.org/10.1016/j.cmet.2019.05.021

Calabrese, E., Badea, A., Cofer, G., Qi, Y., & Johnson, G. A. (2015). A Diffusion MRI Tractography Connectome of the Mouse Brain and Comparison with Neuronal Tracer Data. *Cerebral Cortex*, *25*(11), 4628–4637. https://doi.org/10.1093/cercor/bhv121

Campbell, J. N., Macosko, E. Z., Fenselau, H., Pers, T. H., Lyubetskaya, A., Tenen, D., Goldman, M., Verstegen, A. M. J., Resch, J. M., McCarroll, S. A., Rosen, E. D., Lowell, B. B., & Tsai, L. T. (2017). A molecular census of arcuate hypothalamus and median eminence cell types. *Nature Neuroscience*, *20*(3), 484–496. https://doi.org/10.1038/nn.4495

Carlén, M. (2017). What constitutes the prefrontal cortex? *Science*, *358*(6362), 478–482. https://doi.org/10.1126/science.aan8868

Castañeda, T. R., Tong, J., Datta, R., Culler, M., & Tschöp, M. H. (2010). Ghrelin in the regulation of body weight and metabolism. *Frontiers in Neuroendocrinology*, *31*(1), 44–60. https://doi.org/10.1016/j.yfrne.2009.10.008

Castro, D. C., Cole, S. L., & Berridge, K. C. (2015). Lateral hypothalamus, nucleus accumbens, and ventral pallidum roles in eating and hunger: Interactions between homeostatic and reward circuitry. *Frontiers in Systems Neuroscience*, *9*, 90. https://doi.org/10.3389/fnsys.2015.00090

Çavdar, S., Esen Aydın, A., Algin, O., & Aydoğmuş, E. (2020). Fiber dissection and 3-tesla diffusion tensor tractography of the superior cerebellar peduncle in the human brain: Emphasize on the cerebello-hypthalamic fibers. *Brain Structure & Function*, *225*(1), 121–128. https://doi.org/10.1007/s00429-019-01985-8

Ceccarini, M., Fittipaldi, S., Ciccacci, C., Granese, E., Centofanti, F., Dalla Ragione, L., Bertelli, M., Beccari, T., & Botta, A. (2022). *Association Between DRD2 and DRD4 Polymorphisms and Eating Disorders in an Italian Population*. https://doi.org/10.3389/fnut.2022.838177

Cha, J., Ide, J. S., Bowman, F. D., Simpson, H. B., Posner, J., & Steinglass, J. E. (2016a). Abnormal reward circuitry in anorexia nervosa: A longitudinal, multimodal MRI study. *Human Brain Mapping*, *37*(11), 3835–3846. https://doi.org/10.1002/hbm.23279

Cha, J., Ide, J. S., Bowman, F. D., Simpson, H. B., Posner, J., & Steinglass, J. E. (2016b). Abnormal reward circuitry in anorexia nervosa: A longitudinal, multimodal MRI study. *Human Brain Mapping*, *37*(11), 3835–3846. https://doi.org/10.1002/hbm.23279

Chang, Y.-H. A., Marshall, A., Bahrami, N., Mathur, K., Javadi, S. S., Reyes, A., Hegde, M., Shih, J. J., Paul, B. M., Hagler, D. J., & McDonald, C. R. (2019). Differential sensitivity of structural, diffusion, and resting-state functional MRI for detecting brain alterations and verbal memory impairment in temporal lobe epilepsy. *Epilepsia*, *60*(5), 935–947. https://doi.org/10.1111/epi.14736

Chapelot, D., Aubert, R., Marmonier, C., Chabert, M., & Louis-Sylvestre, J. (2000). An endocrine and metabolic definition of the intermeal interval in humans: Evidence for a role of leptin on the

prandial pattern through fatty acid disposal. *The American Journal of Clinical Nutrition*, *72*(2), 421–431. https://doi.org/10.1093/ajcn/72.2.421

Charbonnier, L., van Meer, F., Johnstone, A. M., Crabtree, D., Buosi, W., Manios, Y., Androutsos, O., Giannopoulou, A., Viergever, M. A., Smeets, P. a. M., & Full4Health consortium. (2018). Effects of hunger state on the brain responses to food cues across the life span. *NeuroImage*, *171*, 246–255. https://doi.org/10.1016/j.neuroimage.2018.01.012

Charbonnier, L., van Meer, F., van der Laan, L. N., Viergever, M. A., & Smeets, P. A. M. (2016). Standardized food images: A photographing protocol and image database. *Appetite*, *96*, 166–173. https://doi.org/10.1016/j.appet.2015.08.041

Charles, M.-A., Eschwège, E., & Basdevant, A. (2008). Monitoring the Obesity Epidemic in France: The Obepi Surveys 1997–2006. *Obesity*, *16*(9), 2182–2186. https://doi.org/10.1038/oby.2008.285

Chen, E. Y., & Zeffiro, T. A. (2020a). Hunger and BMI modulate neural responses to sweet stimuli: fMRI meta-analysis. *International Journal of Obesity (2005)*, *44*(8), 1636–1652. https://doi.org/10.1038/s41366-020-0608-5

Chen, E. Y., & Zeffiro, T. A. (2020b). Hunger and BMI modulate neural responses to sweet stimuli: fMRI meta-analysis. *International Journal of Obesity*, *44*(8), Article 8. https://doi.org/10.1038/s41366-020-0608-5

Chen, J., Papies, E. K., & Barsalou, L. W. (2016). A core eating network and its modulations underlie diverse eating phenomena. *Brain and Cognition*, *110*, 20–42. https://doi.org/10.1016/j.bandc.2016.04.004

Chen, Y., Lin, Y.-C., Kuo, T.-W., & Knight, Z. A. (2015). Sensory detection of food rapidly modulates arcuate feeding circuits. *Cell*, *160*(5), 829–841. https://doi.org/10.1016/j.cell.2015.01.033

Chin, S.-H., Kahathuduwa, C. N., Stearns, M. B., Davis, T., & Binks, M. (2018). Is hunger important to model in fMRI visual food-cue reactivity paradigms in adults with obesity and how should this be done? *Appetite*, *120*, 388–397. https://doi.org/10.1016/j.appet.2017.09.012

Chou, T. C., Scammell, T. E., Gooley, J. J., Gaus, S. E., Saper, C. B., & Lu, J. (2003). Critical Role of Dorsomedial Hypothalamic Nucleus in a Wide Range of Behavioral Circadian Rhythms. *Journal of Neuroscience*, *23*(33), 10691–10702. https://doi.org/10.1523/JNEUROSCI.23-33-10691.2003

Clarke, R. E., Voigt, K., Reichenbach, A., Stark, R., Bharania, U., Dempsey, H., Lockie, S. H., Mequinion, M., Lemus, M., Wei, B., Reed, F., Rawlinson, S., Nunez-Iglesias, J., Foldi, C. J., Kravitz, A. V., Verdejo-Garcia, A., & Andrews, Z. B. (2023). Identification of a Stress-Sensitive Anorexigenic Neurocircuit From Medial Prefrontal Cortex to Lateral Hypothalamus. *Biological Psychiatry*, *93*(4), 309–321. https://doi.org/10.1016/j.biopsych.2022.08.022

Coletta, M., Platek, S., Mohamed, F. B., van Steenburgh, J. J., Green, D., & Lowe, M. R. (2009). Brain activation in restrained and unrestrained eaters: An fMRI study. *Journal of Abnormal Psychology*, *118*(3), 598–609. https://doi.org/10.1037/a0016201

Collantoni, E., Michelon, S., Tenconi, E., Degortes, D., Titton, F., Manara, R., Clementi, M., Pinato, C., Forzan, M., Cassina, M., Santonastaso, P., & Favaro, A. (2016). Functional connectivity correlates of response inhibition impairment in anorexia nervosa. *Psychiatry Research. Neuroimaging*, *247*, 9–16. https://doi.org/10.1016/j.pscychresns.2015.11.008

Connan, F., Campbell, I. C., Katzman, M., Lightman, S. L., & Treasure, J. (2003). A neurodevelopmental model for anorexia nervosa. *Physiology & Behavior*, *79*(1), 13–24. https://doi.org/10.1016/s0031-9384(03)00101-x

Considine, R. V., Sinha, M. K., Heiman, M. L., Kriauciunas, A., Stephens, T. W., Nyce, M. R., Ohannesian, J. P., Marco, C. C., McKee, L. J., & Bauer, T. L. (1996). Serum immunoreactive-leptin concentrations in normal-weight and obese humans. *The New England Journal of Medicine*, *334*(5), 292–295. https://doi.org/10.1056/NEJM199602013340503

Contreras, M., Riveros, M. E., Quispe, M., Sánchez, C., Perdomo, G., Torrealba, F., & Valdés, J. L. (2016). The Histaminergic Tuberomamillary Nucleus Is Involved in Appetite for Sex, Water

and Amphetamine. *PLOS ONE*, *11*(2), e0148484. https://doi.org/10.1371/journal.pone.0148484

Coons, E. E., & Cruce, J. A. F. (1968). Lateral Hypothalamus: Food Current Intensity in Maintaining Self-Stimulation of Hunger. *Science*, *159*(3819), 1117–1119. https://doi.org/10.1126/science.159.3819.1117

Corbetta, M., & Shulman, G. L. (2002). Control of goal-directed and stimulus-driven attention in the brain. *Nature Reviews Neuroscience*, *3*(3), Article 3. https://doi.org/10.1038/nrn755

Cowdrey, F. A., Filippini, N., Park, R. J., Smith, S. M., & McCabe, C. (2014). Increased resting state functional connectivity in the default mode network in recovered anorexia nervosa. *Human Brain Mapping*, *35*(2), 483–491. https://doi.org/10.1002/hbm.22202

Cox, R. W. (1996). AFNI: Software for Analysis and Visualization of Functional Magnetic Resonance Neuroimages. *Computers and Biomedical Research*, *29*(3), 162–173. https://doi.org/10.1006/cbmr.1996.0014

Craig, A. D. B. (2011). Significance of the insula for the evolution of human awareness of feelings from the body. *Annals of the New York Academy of Sciences*, *1225*, 72–82. https://doi.org/10.1111/j.1749-6632.2011.05990.x

Csifáry, A., Görcs, T. J., & Palkovits, M. (1990). Neuropeptide Y innervation of ACTH-immunoreactive neurons in the arcuate nucleus of rats: A correlated light and electron microscopic double immunolabeling study. *Brain Research*, *506*(2), 215–222. https://doi.org/10.1016/0006-8993(90)91253-d

Cummings, D. E. (2006). Ghrelin and the short- and long-term regulation of appetite and body weight. *Physiology & Behavior*, *89*(1), 71–84. https://doi.org/10.1016/j.physbeh.2006.05.022

Cummings, D. E., & Foster, K. E. (2003). Ghrelin-leptin tango in body-weight regulation. *Gastroenterology*, *124*(5), 1532–1535. https://doi.org/10.1016/s0016-5085(03)00350-0

Davidson, T. L., Chan, K., Jarrard, L. E., Kanoski, S. E., Clegg, D. J., & Benoit, S. C. (2009). Contributions of the Hippocampus and Medial Prefrontal Cortex to Energy and Body Weight Regulation. *Hippocampus*, *19*(3), 235–252. https://doi.org/10.1002/hipo.20499

de Araujo, I. E., Schatzker, M., & Small, D. M. (2020). Rethinking Food Reward. *Annual Review of Psychology*, *71*, 139–164. https://doi.org/10.1146/annurev-psych-122216-011643

De Silva, A., Salem, V., Matthews, P. M., & Dhillo, W. S. (2012a). The Use of Functional MRI to Study Appetite Control in the CNS. *Experimental Diabetes Research*, *2012*, 1–13. https://doi.org/10.1155/2012/764017

De Silva, A., Salem, V., Matthews, P. M., & Dhillo, W. S. (2012b). The use of functional MRI to study appetite control in the CNS. *Experimental Diabetes Research*, *2012*, 764017. https://doi.org/10.1155/2012/764017

De Souza, C. T., Araujo, E. P., Bordin, S., Ashimine, R., Zollner, R. L., Boschero, A. C., Saad, M. J. A., & Velloso, L. A. (2005a). Consumption of a fat-rich diet activates a proinflammatory response and induces insulin resistance in the hypothalamus. *Endocrinology*, *146*(10), 4192–4199. https://doi.org/10.1210/en.2004-1520

De Souza, C. T., Araujo, E. P., Bordin, S., Ashimine, R., Zollner, R. L., Boschero, A. C., Saad, M. J. A., & Velloso, L. A. (2005b). Consumption of a fat-rich diet activates a proinflammatory response and induces insulin resistance in the hypothalamus. *Endocrinology*, *146*(10), 4192–4199. https://doi.org/10.1210/en.2004-1520

Dekkers, I. A., Jansen, P. R., & Lamb, H. J. (2019). Obesity, Brain Volume, and White Matter Microstructure at MRI: A Cross-sectional UK Biobank Study. *Radiology*, *291*(3), 763–771. https://doi.org/10.1148/radiol.2019181012

Delgado, J. M. R., & Anand, B. K. (1953). Increase of food intake induced by electrical stimulation of the lateral hypothalamus. *The American Journal of Physiology*, *172*(1), 162–168. https://doi.org/10.1152/ajplegacy.1952.172.1.162

DelParigi, A., Chen, K., Salbe, A. D., Hill, J. O., Wing, R. R., Reiman, E. M., & Tataranni, P. A. (2004). Persistence of abnormal neural responses to a meal in postobese individuals. *International Journal of Obesity and Related Metabolic Disorders: Journal of the International Association for the Study of Obesity*, *28*(3), 370–377. https://doi.org/10.1038/sj.ijo.0802558

Desikan, R. S., Ségonne, F., Fischl, B., Quinn, B. T., Dickerson, B. C., Blacker, D., Buckner, R. L., Dale, A. M., Maguire, R. P., Hyman, B. T., Albert, M. S., & Killiany, R. J. (2006). An automated labeling system for subdividing the human cerebral cortex on MRI scans into gyral based regions of interest. *NeuroImage*, *31*(3), 968–980. https://doi.org/10.1016/j.neuroimage.2006.01.021

Desrosiers-Gregoire, G., Devenyi, G. A., Grandjean, J., & Chakravarty, M. M. (2022). *Rodent Automated Bold Improvement of EPI Sequences (RABIES): A standardized image processing and data quality platform for rodent fMRI* (p. 2022.08.20.504597). bioRxiv. https://doi.org/10.1101/2022.08.20.504597

Dhillon, H., Zigman, J. M., Ye, C., Lee, C. E., McGovern, R. A., Tang, V., Kenny, C. D., Christiansen, L. M., White, R. D., Edelstein, E. A., Coppari, R., Balthasar, N., Cowley, M. A., Chua, S., Elmquist, J. K., & Lowell, B. B. (2006). Leptin directly activates SF1 neurons in the VMH, and this action by leptin is required for normal body-weight homeostasis. *Neuron*, *49*(2), 191–203. https://doi.org/10.1016/j.neuron.2005.12.021

Di Martino, A., Scheres, A., Margulies, D. S., Kelly, A. M. C., Uddin, L. Q., Shehzad, Z., Biswal, B., Walters, J. R., Castellanos, F. X., & Milham, M. P. (2008). Functional connectivity of human striatum: A resting state FMRI study. *Cerebral Cortex (New York, N.Y.: 1991)*, *18*(12), 2735–2747. https://doi.org/10.1093/cercor/bhn041

DiMicco, J. A., Samuels, B. C., Zaretskaia, M. V., & Zaretsky, D. V. (2002). The dorsomedial hypothalamus and the response to stress: Part renaissance, part revolution. *Pharmacology, Biochemistry, and Behavior*, *71*(3), 469–480. https://doi.org/10.1016/s0091-3057(01)00689-x

Dimicco, J. A., & Zaretsky, D. V. (2007). The dorsomedial hypothalamus: A new player in thermoregulation. *American Journal of Physiology. Regulatory, Integrative and Comparative Physiology*, *292*(1), R47-63. https://doi.org/10.1152/ajpregu.00498.2006

Ding, S.-L., Royall, J. J., Sunkin, S. M., Ng, L., Facer, B. A. C., Lesnar, P., Guillozet-Bongaarts, A., McMurray, B., Szafer, A., Dolbeare, T. A., Stevens, A., Tirrell, L., Benner, T., Caldejon, S., Dalley, R. A., Dee, N., Lau, C., Nyhus, J., Reding, M., … Lein, E. S. (2016). Comprehensive cellular-resolution atlas of the adult human brain. *Journal of Comparative Neurology*, *524*(16), 3127–3481. https://doi.org/10.1002/cne.24080

Dosenbach, N. U. F., Visscher, K. M., Palmer, E. D., Miezin, F. M., Wenger, K. K., Kang, H. C., Burgund, E. D., Grimes, A. L., Schlaggar, B. L., & Petersen, S. E. (2006). A core system for the implementation of task sets. *Neuron*, *50*(5), 799–812. https://doi.org/10.1016/j.neuron.2006.04.031

E, N., A, B., E, B., C, T., L, D., L, B., G, R., E, M., F, C., & Mo, C. (2007). D2 dopamine receptor (DRD2) gene Taq1A polymorphism and the eating-related psychological traits in eating disorders (anorexia nervosa and bulimia) and obesity. *Eating and Weight Disorders : EWD*, *12*(2). https://doi.org/10.1007/BF03327583

Eddy, K., Plessow, F., Breithaupt, L., Becker, K., Slattery, M., Mancuso, C., Izquierdo, A., Water, A. V. D., Kahn, D., Dreier, M., Deckersbach, T., Thomas, J., Holsen, L., Misra, M., & Lawson, E. (2022). *Neural activation of food reward and cognitive control regions in young females with anorexia nervosa and atypical anorexia nervosa versus healthy controls*. https://doi.org/10.21203/rs.3.rs-2211452/v1

Ehrlich, S., Lord, A. R., Geisler, D., Borchardt, V., Boehm, I., Seidel, M., Ritschel, F., Schulze, A., King, J. A., Weidner, K., Roessner, V., & Walter, M. (2015). Reduced functional connectivity in the thalamo-insular subnetwork in patients with acute anorexia nervosa. *Human Brain Mapping*, *36*(5), 1772–1781. https://doi.org/10.1002/hbm.22736

Elias, C. F., Lee, C., Kelly, J., Aschkenasi, C., Ahima, R. S., Couceyro, P. R., Kuhar, M. J., Saper, C. B., & Elmquist, J. K. (1998). Leptin activates hypothalamic CART neurons projecting to the spinal cord. *Neuron*, *21*(6), 1375–1385. https://doi.org/10.1016/s0896-6273(00)80656-x

Elmquist, J. K., Elias, C. F., & Saper, C. B. (1999). From lesions to leptin: Hypothalamic control of food intake and body weight. *Neuron*, *22*(2), 221–232. https://doi.org/10.1016/s0896-6273(00)81084-3

Erdur, L., Kallenbach-Dermutz, B., Lehmann, V., Zimmermann-Viehoff, F., Köpp, W., Weber, C., & Deter, H.-C. (2012). Somatic comorbidity in anorexia nervosa: First results of a 21-year follow-up study on female inpatients. *Biopsychosocial Medicine*, *6*, 4. https://doi.org/10.1186/1751-0759-6-4

Exner, C., Hebebrand, J., Remschmidt, H., Wewetzer, C., Ziegler, A., Herpertz, S., Schweiger, U., Blum, W. F., Preibisch, G., Heldmaier, G., & Klingenspor, M. (2000). Leptin suppresses semi-starvation induced hyperactivity in rats: Implications for anorexia nervosa. *Molecular Psychiatry*, *5*(5), 476–481. https://doi.org/10.1038/sj.mp.4000771

Faber, C. L., Deem, J. D., Phan, B. A., Doan, T. P., Ogimoto, K., Mirzadeh, Z., Schwartz, M. W., & Morton, G. J. (2021, February 2). *Leptin receptor neurons in the dorsomedial hypothalamus regulate diurnal patterns of feeding, locomotion, and metabolism*. eLife; eLife Sciences Publications Limited. https://doi.org/10.7554/eLife.63671

Faber, C. L., Matsen, M. E., Velasco, K. R., Damian, V., Phan, B. A., Adam, D., Therattil, A., Schwartz, M. W., & Morton, G. J. (2018). Distinct Neuronal Projections From the Hypothalamic Ventromedial Nucleus Mediate Glycemic and Behavioral Effects. *Diabetes*, *67*(12), 2518–2529. https://doi.org/10.2337/db18-0380

Fan, L., Li, H., Zhuo, J., Zhang, Y., Wang, J., Chen, L., Yang, Z., Chu, C., Xie, S., Laird, A. R., Fox, P. T., Eickhoff, S. B., Yu, C., & Jiang, T. (2016). The Human Brainnetome Atlas: A New Brain Atlas Based on Connectional Architecture. *Cerebral Cortex (New York, NY)*, *26*(8), 3508–3526. https://doi.org/10.1093/cercor/bhw157

Farooqi, I. S., & O'Rahilly, S. (2006). Genetics of Obesity in Humans. *Endocrine Reviews*, *27*(7), 710–718. https://doi.org/10.1210/er.2006-0040

Farr, O. M., Gavrieli, A., & Mantzoros, C. S. (2015). Leptin applications in 2015: What have we learned about leptin and obesity? *Current Opinion in Endocrinology, Diabetes, and Obesity*, *22*(5), 353–359. https://doi.org/10.1097/MED.0000000000000184

Favaro, A., Santonastaso, P., Manara, R., Bosello, R., Bommarito, G., Tenconi, E., & Di Salle, F. (2012). Disruption of visuospatial and somatosensory functional connectivity in anorexia nervosa. *Biological Psychiatry*, *72*(10), 864–870. https://doi.org/10.1016/j.biopsych.2012.04.025

Ferssiwi, A., Cardo, B., & Velley, L. (1987). Gustatory preference-aversion thresholds are increased by ibotenic acid lesion of the lateral hypothalamus in the rat. *Brain Research*, *437*(1), 142–150. https://doi.org/10.1016/0006-8993(87)91535-6

Fetissov, S. O., Hallman, J., Oreland, L., af Klinteberg, B., Grenbäck, E., Hulting, A.-L., & Hökfelt, T. (2002). Autoantibodies against α-MSH, ACTH, and LHRH in anorexia and bulimia nervosa patients. *Proceedings of the National Academy of Sciences*, *99*(26), 17155–17160. https://doi.org/10.1073/pnas.222658699

Fladung, A.-K., Grön, G., Grammer, K., Herrnberger, B., Schilly, E., Grasteit, S., Wolf, R. C., Walter, H., & von Wietersheim, J. (2010). A Neural Signature of Anorexia Nervosa in the Ventral Striatal Reward System. *American Journal of Psychiatry*, *167*(2), 206–212. https://doi.org/10.1176/appi.ajp.2009.09010071

Fladung, A.-K., Schulze, U. M. E., Schöll, F., Bauer, K., & Grön, G. (2013). Role of the ventral striatum in developing anorexia nervosa. *Translational Psychiatry*, *3*(10), e315. https://doi.org/10.1038/tp.2013.88

Flier, J. S. (2006). AgRP in energy balance: Will the real AgRP please stand up? *Cell Metabolism*, *3*(2), 83–85. https://doi.org/10.1016/j.cmet.2006.01.003

Florent, V., Baroncini, M., Jissendi-Tchofo, P., Lopes, R., Vanhoutte, M., Rasika, S., Pruvo, J.-P., Vignau, J., Verdun, S., Johansen, J. E., Pigeyre, M., Bouret, S. G., Nilsson, I. A. K., & Prevot, V.

(2020a). Hypothalamic Structural and Functional Imbalances in Anorexia Nervosa. *Neuroendocrinology*, *110*(6), 552–562. https://doi.org/10.1159/000503147

Florent, V., Baroncini, M., Jissendi-Tchofo, P., Lopes, R., Vanhoutte, M., Rasika, S., Pruvo, J.-P., Vignau, J., Verdun, S., Johansen, J. E., Pigeyre, M., Bouret, S. G., Nilsson, I. A. K., & Prevot, V. (2020b). Hypothalamic Structural and Functional Imbalances in Anorexia Nervosa. *Neuroendocrinology*, *110*(6), 552–562. https://doi.org/10.1159/000503147

Föcker, M., Timmesfeld, N., Scherag, S., Bühren, K., Langkamp, M., Dempfle, A., Sheridan, E. M., de Zwaan, M., Fleischhaker, C., Herzog, W., Egberts, K., Zipfel, S., Herpertz-Dahlmann, B., & Hebebrand, J. (2011). Screening for anorexia nervosa via measurement of serum leptin levels. *Journal of Neural Transmission (Vienna, Austria: 1996)*, *118*(4), 571–578. https://doi.org/10.1007/s00702-010-0551-z

Fong, H., Zheng, J., & Kurrasch, D. (2023). The structural and functional complexity of the integrative hypothalamus. *Science (New York, N.Y.)*, *382*(6669), 388–394. https://doi.org/10.1126/science.adh8488

Fontbonne, A., Currie, A., Tounian, P., Picot, M.-C., Foulatier, O., Nedelcu, M., & Nocca, D. (2023). Prevalence of Overweight and Obesity in France: The 2020 Obepi-Roche Study by the "Ligue Contre l'Obésité." *Journal of Clinical Medicine*, *12*(3), Article 3. https://doi.org/10.3390/jcm12030925

Foster-Schubert, K. E., & Cummings, D. E. (2006). Emerging therapeutic strategies for obesity. *Endocrine Reviews*, *27*(7), 779–793. https://doi.org/10.1210/er.2006-0041

Fox, M. D., Snyder, A. Z., Vincent, J. L., Corbetta, M., Van Essen, D. C., & Raichle, M. E. (2005). The human brain is intrinsically organized into dynamic, anticorrelated functional networks. *Proceedings of the National Academy of Sciences of the United States of America*, *102*(27), 9673–9678. https://doi.org/10.1073/pnas.0504136102

Frank, G. K., Bailer, U. F., Henry, S. E., Drevets, W., Meltzer, C. C., Price, J. C., Mathis, C. A., Wagner, A., Hoge, J., Ziolko, S., Barbarich-Marsteller, N., Weissfeld, L., & Kaye, W. H. (2005a).

Increased Dopamine D2/D3 Receptor Binding After Recovery from Anorexia Nervosa Measured by Positron Emission Tomography and [11C]Raclopride. *Biological Psychiatry*, *58*(11), 908–912. https://doi.org/10.1016/j.biopsych.2005.05.003

Frank, G. K., Bailer, U. F., Henry, S. E., Drevets, W., Meltzer, C. C., Price, J. C., Mathis, C. A., Wagner, A., Hoge, J., Ziolko, S., Barbarich-Marsteller, N., Weissfeld, L., & Kaye, W. H. (2005b). Increased dopamine D2/D3 receptor binding after recovery from anorexia nervosa measured by positron emission tomography and [11c]raclopride. *Biological Psychiatry*, *58*(11), 908–912. https://doi.org/10.1016/j.biopsych.2005.05.003

Frank, G. K. W., Shott, M. E., Stoddard, J., Swindle, S., & Pryor, T. L. (2021). Association of Brain Reward Response With Body Mass Index and Ventral Striatal-Hypothalamic Circuitry Among Young Women With Eating Disorders. *JAMA Psychiatry*, *78*(10), 1123–1133. https://doi.org/10.1001/jamapsychiatry.2021.1580

Friederich, H.-C., Walther, S., Bendszus, M., Biller, A., Thomann, P., Zeigermann, S., Katus, T., Brunner, R., Zastrow, A., & Herzog, W. (2012). Grey matter abnormalities within cortico-limbic-striatal circuits in acute and weight-restored anorexia nervosa patients. *NeuroImage*, *59*(2), 1106–1113. https://doi.org/10.1016/j.neuroimage.2011.09.042

Friedman, J. M., & Halaas, J. L. (1998). Leptin and the regulation of body weight in mammals. *Nature*, *395*(6704), 763–770. https://doi.org/10.1038/27376

Frieling, H., Fischer, J., Wilhelm, J., Engelhorn, T., Bleich, S., Hillemacher, T., Dörfler, A., Kornhuber, J., de Zwaan, M., & Peschel, T. (2012). Microstructural abnormalities of the posterior thalamic radiation and the mediodorsal thalamic nuclei in females with anorexia nervosa—A voxel based diffusion tensor imaging (DTI) study. *Journal of Psychiatric Research*, *46*(9), 1237–1242. https://doi.org/10.1016/j.jpsychires.2012.06.005

Fritz, F. J., Sengupta, S., Harms, R. L., Tse, D. H., Poser, B. A., & Roebroeck, A. (2019). Ultra-high resolution and multi-shell diffusion MRI of intact ex vivo human brains using kT-dSTEAM at 9.4T. *NeuroImage*, *202*, 116087. https://doi.org/10.1016/j.neuroimage.2019.116087

Frohman, L. A., & Bernardis, L. L. (1971). Effect of hypothalamic stimulation on plasma glucose, insulin, and glucagon levels. *The American Journal of Physiology*, *221*(6), 1596–1603. https://doi.org/10.1152/ajplegacy.1971.221.6.1596

Fulwiler, C. E., & Saper, C. B. (1984). Subnuclear organization of the efferent connections of the parabrachial nucleus in the rat. *Brain Research*, *319*(3), 229–259. https://doi.org/10.1016/0165-0173(84)90012-2

García-García, I., Jurado, M. Á., Garolera, M., Segura, B., Sala-Llonch, R., Marqués-Iturria, I., Pueyo, R., Sender-Palacios, M. J., Vernet-Vernet, M., Narberhaus, A., Ariza, M., & Junqué, C. (2012). Alterations of the salience network in obesity: A resting-state fMRI study. *Human Brain Mapping*, *34*(11), 2786. https://doi.org/10.1002/hbm.22104

Garner, D. M., Olmsted, M. P., Bohr, Y., & Garfinkel, P. E. (1982). The eating attitudes test: Psychometric features and clinical correlates. *Psychological Medicine*, *12*(4), 871–878. https://doi.org/10.1017/s0033291700049163

Gaudio, S., Wiemerslage, L., Brooks, S. J., & Schiöth, H. B. (2016). A systematic review of resting-state functional-MRI studies in anorexia nervosa: Evidence for functional connectivity impairment in cognitive control and visuospatial and body-signal integration. *Neuroscience and Biobehavioral Reviews*, *71*, 578–589. https://doi.org/10.1016/j.neubiorev.2016.09.032

Gautier, J. F., Chen, K., Salbe, A. D., Bandy, D., Pratley, R. E., Heiman, M., Ravussin, E., Reiman, E. M., & Tataranni, P. A. (2000). Differential brain responses to satiation in obese and lean men. *Diabetes*, *49*(5), 838–846. https://doi.org/10.2337/diabetes.49.5.838

Gautier, J. F., Del Parigi, A., Chen, K., Salbe, A. D., Bandy, D., Pratley, R. E., Ravussin, E., Reiman, E. M., & Tataranni, P. A. (2001). Effect of satiation on brain activity in obese and lean women. *Obesity Research*, *9*(11), 676–684. https://doi.org/10.1038/oby.2001.92

Gautron, L., & Layé, S. (2010). Neurobiology of Inflammation-Associated Anorexia. *Frontiers in Neuroscience*, *3*, 59. https://doi.org/10.3389/neuro.23.003.2009

Geha, P., Cecchi, G., Todd Constable, R., Abdallah, C., & Small, D. M. (2017). Reorganization of brain connectivity in obesity: Obesity and Altered Brain Connectivity. *Human Brain Mapping*, *38*(3), 1403–1420. https://doi.org/10.1002/hbm.23462

Geha, P. Y., Aschenbrenner, K., Felsted, J., O'Malley, S. S., & Small, D. M. (2013). Altered hypothalamic response to food in smokers. *The American Journal of Clinical Nutrition*, *97*(1), 15–22. https://doi.org/10.3945/ajcn.112.043307

Gehrlach, D. A., Weiand, C., Gaitanos, T. N., Cho, E., Klein, A. S., Hennrich, A. A., Conzelmann, K.-K., & Gogolla, N. (2020). A whole-brain connectivity map of mouse insular cortex. *eLife*, *9*, e55585. https://doi.org/10.7554/eLife.55585

Geisler, D., Borchardt, V., Lord, A. R., Boehm, I., Ritschel, F., Zwipp, J., Clas, S., King, J. A., Wolff-Stephan, S., Roessner, V., Walter, M., & Ehrlich, S. (2016). Abnormal functional global and local brain connectivity in female patients with anorexia nervosa. *Journal of Psychiatry & Neuroscience : JPN*, *41*(1), 6–15. https://doi.org/10.1503/jpn.140310

Glasser, M. F., Sotiropoulos, S. N., Wilson, J. A., Coalson, T. S., Fischl, B., Andersson, J. L., Xu, J., Jbabdi, S., Webster, M., Polimeni, J. R., Van Essen, D. C., Jenkinson, M., & WU-Minn HCP Consortium. (2013). The minimal preprocessing pipelines for the Human Connectome Project. *NeuroImage*, *80*, 105–124. https://doi.org/10.1016/j.neuroimage.2013.04.127

Goldstein, J. M., Jerram, M., Abbs, B., Whitfield-Gabrieli, S., & Makris, N. (2010). Sex Differences in Stress Response Circuitry Activation Dependent on Female Hormonal Cycle. *The Journal of Neuroscience*, *30*(2), 431–438. https://doi.org/10.1523/JNEUROSCI.3021-09.2010

Gong, R., Xu, S., Hermundstad, A., Yu, Y., & Sternson, S. M. (2020). Hindbrain Double-Negative Feedback Mediates Palatability-Guided Food and Water Consumption. *Cell*, *182*(6), 1589-1605.e22. https://doi.org/10.1016/j.cell.2020.07.031

Gooley, J. J., Schomer, A., & Saper, C. B. (2006). The dorsomedial hypothalamic nucleus is critical for the expression of food-entrainable circadian rhythms. *Nature Neuroscience*, *9*(3), 398–407. https://doi.org/10.1038/nn1651

Gorgolewski, K. J., Auer, T., Calhoun, V. D., Craddock, R. C., Das, S., Duff, E. P., Flandin, G., Ghosh, S. S., Glatard, T., Halchenko, Y. O., Handwerker, D. A., Hanke, M., Keator, D., Li, X., Michael, Z., Maumet, C., Nichols, B. N., Nichols, T. E., Pellman, J., … Poldrack, R. A. (2016). The brain imaging data structure, a format for organizing and describing outputs of neuroimaging experiments. *Scientific Data*, *3*(1), Article 1. https://doi.org/10.1038/sdata.2016.44

Goutagny, R., Verret, L., Fort, P., Salvert, D., Léger, L., Luppi, P. H., & Peyron, C. (2004). Posterior hypothalamus and regulation of vigilance states. *Archives Italiennes De Biologie*, *142*(4), 487–500.

Grandjean, J., Canella, C., Anckaerts, C., Ayrancı, G., Bougacha, S., Bienert, T., Buehlmann, D., Coletta, L., Gallino, D., Gass, N., Garin, C. M., Nadkarni, N. A., Hübner, N. S., Karatas, M., Komaki, Y., Kreitz, S., Mandino, F., Mechling, A. E., Sato, C., … Gozzi, A. (2020). Common functional networks in the mouse brain revealed by multi-centre resting-state fMRI analysis. *NeuroImage*, *205*, 116278. https://doi.org/10.1016/j.neuroimage.2019.116278

Grandjean, J., Desrosiers-Gregoire, G., Anckaerts, C., Angeles-Valdez, D., Ayad, F., Barrière, D. A., Blockx, I., Bortel, A. B., Broadwater, M., Cardoso, B. M., Célestine, M., Chavez-Negrete, J. E., Choi, S., Christiaen, E., Clavijo, P., Colon-Perez, L., Cramer, S., Daniele, T., Dempsey, E., … Hess, A. (2022). *StandardRat: A multi-center consensus protocol to enhance functional connectivity specificity in the rat brain* (p. 2022.04.27.489658). bioRxiv. https://doi.org/10.1101/2022.04.27.489658

Grandjean, J., Desrosiers-Gregoire, G., Anckaerts, C., Angeles-Valdez, D., Ayad, F., Barrière, D. A., Blockx, I., Bortel, A., Broadwater, M., Cardoso, B. M., Célestine, M., Chavez-Negrete, J. E., Choi, S., Christiaen, E., Clavijo, P., Colon-Perez, L., Cramer, S., Daniele, T., Dempsey, E., … Hess, A. (2023). A consensus protocol for functional connectivity analysis in the rat brain. *Nature Neuroscience*, 1–9. https://doi.org/10.1038/s41593-023-01286-8

Grinevich, V., Fournier, A., & Pelletier, G. (1997). Effects of pituitary adenylate cyclase-activating polypeptide (PACAP) on corticotropin-releasing hormone (*CRH*) gene expression in the rat

hypothalamic paraventricular nucleus. *Brain Research*, *773*(1), 190–196. https://doi.org/10.1016/S0006-8993(97)01011-1

Gulban, O. F., De Martino, F., Vu, A. T., Yacoub, E., Uğurbil, K., & Lenglet, C. (2018). Cortical fibers orientation mapping using in-vivo whole brain 7 T diffusion MRI. *NeuroImage*, *178*, 104–118. https://doi.org/10.1016/j.neuroimage.2018.05.010

Guo, Y., Xia, Y., & Chen, K. (2023). The body mass index is associated with increased temporal variability of functional connectivity in brain reward system. *Frontiers in Nutrition*, *10*. https://doi.org/10.3389/fnut.2023.1210726

Guterstam, A., Björnsdotter, M., Gentile, G., & Ehrsson, H. H. (2015). Posterior cingulate cortex integrates the senses of self-location and body ownership. *Current Biology: CB*, *25*(11), 1416–1425. https://doi.org/10.1016/j.cub.2015.03.059

Ha, L. J., Yeo, H.-G., Kim, Y. G., Baek, I., Baeg, E., Lee, Y. H., Won, J., Jung, Y., Park, J., Jeon, C.-Y., Kim, K., Min, J., Song, Y., Park, J.-H., Nam, K. R., Son, S., Yoo, S. B. M., Park, S., Choi, W. S., … Choi, H. J. (2024). Hypothalamic neuronal activation in non-human primates drives naturalistic goal-directed eating behavior. *Neuron*, *112*(13), 2218-2230.e6. https://doi.org/10.1016/j.neuron.2024.03.029

Haleem, D. J. (2012). Serotonin neurotransmission in anorexia nervosa. *Behavioural Pharmacology*, *23*(5–6), 478–495. https://doi.org/10.1097/FBP.0b013e328357440d

Haltia, L. T., Viljanen, A., Parkkola, R., Kemppainen, N., Rinne, J. O., Nuutila, P., & Kaasinen, V. (2007). Brain white matter expansion in human obesity and the recovering effect of dieting. *The Journal of Clinical Endocrinology and Metabolism*, *92*(8), 3278–3284. https://doi.org/10.1210/jc.2006-2495

Harris, R. B. S. (Ed.). (2017a). *Appetite and Food Intake: Central Control* (2nd ed.). CRC Press/Taylor & Francis. http://www.ncbi.nlm.nih.gov/books/NBK453148/

Harris, R. B. S. (Ed.). (2017b). *Appetite and Food Intake: Central Control* (2nd ed.). CRC Press/Taylor & Francis. http://www.ncbi.nlm.nih.gov/books/NBK453148/

Hasan, T. F., & Hasan, H. (2011). Anorexia Nervosa: A Unified Neurological Perspective. *International Journal of Medical Sciences*, *8*(8), 679–703.

Hayes, D. J., Lipsman, N., Chen, D. Q., Woodside, D. B., Davis, K. D., Lozano, A. M., & Hodaie, M. (2015). Subcallosal Cingulate Connectivity in Anorexia Nervosa Patients Differs From Healthy Controls: A Multi-tensor Tractography Study. *Brain Stimulation: Basic, Translational, and Clinical Research in Neuromodulation*, *8*(4), 758–768. https://doi.org/10.1016/j.brs.2015.03.005

Haynos, A. F., Hall, L. M. J., Lavender, J. M., Peterson, C. B., Crow, S. J., Klimes-Dougan, B., Cullen, K. R., Lim, K. O., & Camchong, J. (2019). Resting state functional connectivity of networks associated with reward and habit in anorexia nervosa. *Human Brain Mapping*, *40*(2), 652–662. https://doi.org/10.1002/hbm.24402

Hebben, N., Corkin, S., Eichenbaum, H., & Shedlack, K. (1985). Diminished ability to interpret and report internal states after bilateral medial temporal resection: Case H.M. *Behavioral Neuroscience*, *99*(6), 1031–1039. https://doi.org/10.1037//0735-7044.99.6.1031

Hebebrand, J., & Bulik, C. M. (2011). Critical appraisal of the provisional DSM-5 criteria for anorexia nervosa and an alternative proposal. *International Journal of Eating Disorders*, *44*(8), 665–678. https://doi.org/10.1002/eat.20875

Herb, B. R., Glover, H. J., Bhaduri, A., Colantuoni, C., Bale, T. L., Siletti, K., Hodge, R., Lein, E., Kriegstein, A. R., Doege, C. A., & Ament, S. A. (2023). Single-cell genomics reveals region-specific developmental trajectories underlying neuronal diversity in the human hypothalamus. *Science Advances*, *9*(45), eadf6251. https://doi.org/10.1126/sciadv.adf6251

Herman, J. P., McKlveen, J. M., Ghosal, S., Kopp, B., Wulsin, A., Makinson, R., Scheimann, J., & Myers, B. (2016). Regulation of the Hypothalamic-Pituitary-Adrenocortical Stress Response. *Comprehensive Physiology*, *6*(2), 603–621. https://doi.org/10.1002/cphy.c150015

Herrmann, C. (1997). International experiences with the Hospital Anxiety and Depression Scale—A review of validation data and clinical results. *Journal of Psychosomatic Research*, *42*(1), 17–41. https://doi.org/10.1016/s0022-3999(96)00216-4

Herwig, U., Dhum, M., Hittmeyer, A., Opialla, S., Scherpiet, S., Keller, C., Brühl, A. B., & Siegrist, M. (2016). Neural Signaling of Food Healthiness Associated with Emotion Processing. *Frontiers in Aging Neuroscience*, *8*, 16. https://doi.org/10.3389/fnagi.2016.00016

Hetherington, A. W., & Ranson, S. W. (1940). Hypothalamic lesions and adiposity in the rat. *The Anatomical Record*, *78*(2), 149–172. https://doi.org/10.1002/ar.1090780203

Heymsfield, S. B., Greenberg, A. S., Fujioka, K., Dixon, R. M., Kushner, R., Hunt, T., Lubina, J. A., Patane, J., Self, B., Hunt, P., & McCamish, M. (1999). Recombinant leptin for weight loss in obese and lean adults: A randomized, controlled, dose-escalation trial. *JAMA*, *282*(16), 1568–1575. https://doi.org/10.1001/jama.282.16.1568

Hill, J. W. (2012). PVN pathways controlling energy homeostasis. *Indian Journal of Endocrinology and Metabolism*, *16*(Suppl 3), S627–S636. https://doi.org/10.4103/2230-8210.105581

Hillebrand, J. J. G., Kas, M. J. H., & Adan, R. A. H. (2005). A-MSH enhances activity-based anorexia. *Peptides*, *26*(10), 1690–1696. https://doi.org/10.1016/j.peptides.2004.11.027

Hillebrand, J. J. G., Kas, M. J. H., Scheurink, A. J. W., van Dijk, G., & Adan, R. A. H. (2006). AgRP(83–132) and SHU9119 differently affect activity-based anorexia. *European Neuropsychopharmacology*, *16*(6), 403–412. https://doi.org/10.1016/j.euroneuro.2005.11.004

Hillebrand, J. J. G., Koeners, M. P., de Rijke, C. E., Kas, M. J. H., & Adan, R. A. H. (2005). Leptin Treatment in Activity-Based Anorexia. *Biological Psychiatry*, *58*(2), 165–171. https://doi.org/10.1016/j.biopsych.2005.03.011

Hinkle, W., Cordell, M., Leibel, R., Rosenbaum, M., & Hirsch, J. (2013). Effects of reduced weight maintenance and leptin repletion on functional connectivity of the hypothalamus in obese humans. *PloS One*, *8*(3), e59114. https://doi.org/10.1371/journal.pone.0059114

Hirose, S., Osada, T., Ogawa, A., Tanaka, M., Wada, H., Yoshizawa, Y., Imai, Y., Machida, T., Akahane, M., Shirouzu, I., & Konishi, S. (2016). Lateral-Medial Dissociation in Orbitofrontal Cortex-Hypothalamus Connectivity. *Frontiers in Human Neuroscience*, *10*, 244. https://doi.org/10.3389/fnhum.2016.00244

Hoebel, B. G., & Teitelbaum, P. (1962). Hypothalamic Control of Feeding and Self-Stimulation. *Science*, *135*(3501), 375–377. https://doi.org/10.1126/science.135.3501.375

Hollmann, M., Hellrung, L., Pleger, B., Schlögl, H., Kabisch, S., Stumvoll, M., Villringer, A., & Horstmann, A. (2012). Neural correlates of the volitional regulation of the desire for food. *International Journal of Obesity (2005)*, *36*(5), 648–655. https://doi.org/10.1038/ijo.2011.125

Holsen, L. M., Lawson, E. A., Blum, J., Ko, E., Makris, N., Fazeli, P. K., Klibanski, A., & Goldstein, J. M. (2012a). Food motivation circuitry hypoactivation related to hedonic and nonhedonic aspects of hunger and satiety in women with active anorexia nervosa and weight-restored women with anorexia nervosa. *Journal of Psychiatry & Neuroscience: JPN*, *37*(5), 322–332. https://doi.org/10.1503/jpn.110156

Holsen, L. M., Lawson, E. A., Blum, J., Ko, E., Makris, N., Fazeli, P. K., Klibanski, A., & Goldstein, J. M. (2012b). Food motivation circuitry hypoactivation related to hedonic and nonhedonic aspects of hunger and satiety in women with active anorexia nervosa and weight-restored women with anorexia nervosa. *Journal of Psychiatry & Neuroscience: JPN*, *37*(5), 322–332. https://doi.org/10.1503/jpn.110156

Hoyt, E. C., Lund, P. K., Winesett, D. E., Fuller, C. R., Ghatei, M. A., Bloom, S. R., & Ulshen, M. H. (1996). Effects of fasting, refeeding, and intraluminal triglyceride on proglucagon expression in jejunum and ileum. *Diabetes*, *45*(4), 434–439. https://doi.org/10.2337/diab.45.4.434

Hsu, T. M., Noble, E. E., Liu, C. M., Cortella, A. M., Konanur, V. R., Suarez, A. N., Reiner, D. J., Hahn, J. D., Hayes, M. R., & Kanoski, S. E. (2018). A hippocampus to prefrontal cortex neural pathway inhibits food motivation through glucagon-like peptide-1 signaling. *Molecular Psychiatry*, *23*(7), 1555–1565. https://doi.org/10.1038/mp.2017.91

Huang, S., Shi, C., Tao, D., Yang, C., & Luo, Y. (2024). Modulating reward and aversion: Insights into addiction from the paraventricular nucleus. *CNS Neuroscience & Therapeutics*, *30*(9), e70046. https://doi.org/10.1111/cns.70046

Hübel, C., Marzi, S. J., Breen, G., & Bulik, C. M. (2019). Epigenetics in eating disorders: A systematic review. *Molecular Psychiatry*, *24*(6), 901. https://doi.org/10.1038/s41380-018-0254-7

Huston, J. P., & Bures, J. (1970). Drinking and eating elicited by cortical spreading depression. *Science (New York, N.Y.)*, *169*(3946), 702–704. https://doi.org/10.1126/science.169.3946.702

Izquierdo, A. G., Crujeiras, A. B., Casanueva, F. F., & Carreira, M. C. (2019). Leptin, Obesity, and Leptin Resistance: Where Are We 25 Years Later? *Nutrients*, *11*(11), Article 11. https://doi.org/10.3390/nu11112704

Jacobs, V. L. (1965). *The Cerebellofugal System in the Tarsius (Tarsiidae Carbonarius) and the Marmoset (Oedipomidas Oedipus)*. University of Kansas, Anatomy.

Jais, A., & Brüning, J. C. (n.d.). Hypothalamic inflammation in obesity and metabolic disease. *The Journal of Clinical Investigation*, *127*(1), 24–32. https://doi.org/10.1172/JCI88878

Janak, P. H., & Tye, K. M. (2015). From circuits to behaviour in the amygdala. *Nature*, *517*(7534), 284–292. https://doi.org/10.1038/nature14188

Jastreboff, A. M., Sinha, R., Lacadie, C., Small, D. M., Sherwin, R. S., & Potenza, M. N. (2013). Neural Correlates of Stress- and Food Cue–Induced Food Craving in Obesity. *Diabetes Care*, *36*(2), 394–402. https://doi.org/10.2337/dc12-1112

Jennings, J. H., Rizzi, G., Stamatakis, A. M., Ung, R. L., & Stuber, G. D. (2013). The Inhibitory Circuit Architecture of the Lateral Hypothalamus Orchestrates Feeding. *Science (New York, N.Y.)*, *341*(6153), 1517–1521. https://doi.org/10.1126/science.1241812

Jf, M., F, R., & Jh, L. (1999). The SCOFF questionnaire: Assessment of a new screening tool for eating disorders. *BMJ (Clinical Research Ed.)*, *319*(7223). https://doi.org/10.1136/bmj.319.7223.1467

Kalsbeek, A., & Buijs, R. M. (2021). Chapter 4—Organization of the neuroendocrine and autonomic hypothalamic paraventricular nucleus. In D. F. Swaab, F. Kreier, P. J. Lucassen, A. Salehi, & R. M. Buijs (Eds.), *Handbook of Clinical Neurology* (Vol. 180, pp. 45–63). Elsevier. https://doi.org/10.1016/B978-0-12-820107-7.00004-5

Kamali, A., Ghazi Sherbaf, F., Rahmani, F., Khayat-Khoei, M., Aein, A., Gandhi, A., Shah, E. G., Sair, H. I., Riascos, R. F., Esquenazi, Y., Zhu, J.-J., Keser, Z., & Hasan, K. M. (2020). A direct visuosensory cortical connectivity of the human limbic system. Dissecting the trajectory of the parieto-occipito-hypothalamic tract in the human brain using diffusion weighted tractography. *Neuroscience Letters*, *728*, 134955. https://doi.org/10.1016/j.neulet.2020.134955

Kamali, A., Karbasian, N., Ghazi Sherbaf, F., Wilken, L. A., Aein, A., Sair, H. I., Arevalo Espejo, O., Rabiei, P., Choi, S. J., Mirbagheri, S., Riascos, R. F., & Hasan, K. M. (2020). Uncovering the Dorsal Thalamo-hypothalamic Tract of the Human Limbic System. *Neuroscience*, *432*, 55–62. https://doi.org/10.1016/j.neuroscience.2020.02.021

Kamali, A., Karbasian, N., Rabiei, P., Cano, A., Riascos, R. F., Tandon, N., Arevalo, O., Ocasio, L., Younes, K., Khayat-Khoei, M., Mirbagheri, S., & Hasan, K. M. (2018). Revealing the cerebello-ponto-hypothalamic pathway in the human brain. *Neuroscience Letters*, *677*, 1–5. https://doi.org/10.1016/j.neulet.2018.04.024

Kamali, A., Sair, H. I., Blitz, A. M., Riascos, R. F., Mirbagheri, S., Keser, Z., & Hasan, K. M. (2016). Revealing the ventral amygdalofugal pathway of the human limbic system using high spatial resolution diffusion tensor tractography. *Brain Structure & Function*, *221*(7), 3561–3569. https://doi.org/10.1007/s00429-015-1119-3

Kamali, A., Yousem, D. M., Lin, D. D., Sair, H. I., Jasti, S. P., Keser, Z., Riascos, R. F., & Hasan, K. M. (2015). Mapping the trajectory of the stria terminalis of the human limbic system using high spatial resolution diffusion tensor tractography. *Neuroscience Letters*, *608*, 45–50. https://doi.org/10.1016/j.neulet.2015.09.035

Kanoski, S. E., Fortin, S. M., Ricks, K. M., & Grill, H. J. (2013). Ghrelin signaling in the ventral hippocampus stimulates learned and motivational aspects of feeding via PI3K-Akt signaling. *Biological Psychiatry*, *73*(9), 915–923. https://doi.org/10.1016/j.biopsych.2012.07.002

Kas, M. J. H., van Dijk, G., Scheurink, A. J. W., & Adan, R. a. H. (2003). Agouti-related protein prevents self-starvation. *Molecular Psychiatry*, *8*(2), 235–240. https://doi.org/10.1038/sj.mp.4001206

Kassotis, C. D., Vandenberg, L. N., Demeneix, B. A., Porta, M., Slama, R., & Trasande, L. (2020). Endocrine-disrupting chemicals: Economic, regulatory, and policy implications. *The Lancet Diabetes & Endocrinology*, *8*(8), 719–730. https://doi.org/10.1016/S2213-8587(20)30128-5

Kaurijoki, S., Kuikka, J. T., Niskanen, E., Carlson, S., Pietiläinen, K. H., Pesonen, U., Kaprio, J. M., Rissanen, A., Tiihonen, J., & Karhunen, L. (2008). Association of serotonin transporter promoter regulatory region polymorphism and cerebral activity to visual presentation of food. *Clinical Physiology and Functional Imaging*, *28*(4), 270–276. https://doi.org/10.1111/j.1475-097X.2008.00804.x

Kaye, W. H., Berrettini, W., Gwirtsman, H., & George, D. T. (1990). Altered cerebrospinal fluid neuropeptide Y and peptide YY immunoreactivity in anorexia and bulimia nervosa. *Archives of General Psychiatry*, *47*(6), 548–556. https://doi.org/10.1001/archpsyc.1990.01810180048008

Kaye, W. H., Frank, G. K. W., & McConaha, C. (1999). Altered Dopamine Activity after Recovery from Restricting-Type Anorexia Nervosa. *Neuropsychopharmacology*, *21*(4), 503–506. https://doi.org/10.1016/S0893-133X(99)00053-6

Kaye, W. H., Wagner, A., Fudge, J. L., & Paulus, M. (2011). Neurocircuity of eating disorders. *Current Topics in Behavioral Neurosciences*, *6*, 37–57. https://doi.org/10.1007/7854_2010_85

Kaye, W. H., Wierenga, C. E., Bailer, U. F., Simmons, A. N., Wagner, A., & Bischoff-Grethe, A. (2013). Does a shared neurobiology for foods and drugs of abuse contribute to extremes of food ingestion in anorexia and bulimia nervosa? *Biological Psychiatry*, *73*(9), 836–842. https://doi.org/10.1016/j.biopsych.2013.01.002

Keating, C., Tilbrook, A. J., Rossell, S. L., Enticott, P. G., & Fitzgerald, P. B. (2012). Reward processing in anorexia nervosa. *Neuropsychologia*, *50*(5), 567–575. https://doi.org/10.1016/j.neuropsychologia.2012.01.036

Kelley, A. E., Baldo, B. A., & Pratt, W. E. (2005). A proposed hypothalamic-thalamic-striatal axis for the integration of energy balance, arousal, and food reward. *The Journal of Comparative Neurology*, *493*(1), 72–85. https://doi.org/10.1002/cne.20769

Kenny, P. J. (2011). Reward mechanisms in obesity: New insights and future directions. *Neuron*, *69*(4), 664–679. https://doi.org/10.1016/j.neuron.2011.02.016

Keuken, M. C., & Forstmann, B. U. (2015). A probabilistic atlas of the basal ganglia using 7 T MRI. *Data in Brief*, *4*, 577–582. https://doi.org/10.1016/j.dib.2015.07.028

Khouma, A., Moeini, M. M., Plamondon, J., Richard, D., Caron, A., & Michael, N. J. (2023). Histaminergic regulation of food intake. *Frontiers in Endocrinology*, *14*. https://doi.org/10.3389/fendo.2023.1202089

Killgore, W. D. S., Young, A. D., Femia, L. A., Bogorodzki, P., Rogowska, J., & Yurgelun-Todd, D. A. (2003a). Cortical and limbic activation during viewing of high- versus low-calorie foods. *NeuroImage*, *19*(4), 1381–1394. https://doi.org/10.1016/s1053-8119(03)00191-5

Killgore, W. D. S., Young, A. D., Femia, L. A., Bogorodzki, P., Rogowska, J., & Yurgelun-Todd, D. A. (2003b). Cortical and limbic activation during viewing of high- versus low-calorie foods. *NeuroImage*, *19*(4), 1381–1394. https://doi.org/10.1016/s1053-8119(03)00191-5

Killgore, W. D. S., & Yurgelun-Todd, D. A. (2005a). Body mass predicts orbitofrontal activity during visual presentations of high-calorie foods. *Neuroreport*, *16*(8), 859–863. https://doi.org/10.1097/00001756-200505310-00016

Killgore, W. D. S., & Yurgelun-Todd, D. A. (2005b). Developmental changes in the functional brain responses of adolescents to images of high and low-calorie foods. *Developmental Psychobiology*, *47*(4), 377–397. https://doi.org/10.1002/dev.20099

Killgore, W. D. S., & Yurgelun-Todd, D. A. (2006). Affect modulates appetite-related brain activity to images of food. *The International Journal of Eating Disorders*, *39*(5), 357–363. https://doi.org/10.1002/eat.20240

Kim, D.-H., D'Alessio, D. A., Woods, S. C., & Seeley, R. J. (2009). The effects of GLP-1 infusion in the hepatic portal region on food intake. *Regulatory Peptides*, *155*(1–3), 110–114. https://doi.org/10.1016/j.regpep.2009.03.002

Kim, K. R., Ku, J., Lee, J.-H., Lee, H., & Jung, Y.-C. (2012). Functional and effective connectivity of anterior insula in anorexia nervosa and bulimia nervosa. *Neuroscience Letters*, *521*(2), 152–157. https://doi.org/10.1016/j.neulet.2012.05.075

King, J. A., Geisler, D., Ritschel, F., Boehm, I., Seidel, M., Roschinski, B., Soltwedel, L., Zwipp, J., Pfuhl, G., Marxen, M., Roessner, V., & Ehrlich, S. (2015). Global cortical thinning in acute anorexia nervosa normalizes following long-term weight restoration. *Biological Psychiatry*, *77*(7), 624–632. https://doi.org/10.1016/j.biopsych.2014.09.005

Klenotich, S. J., Ho, E. V., McMurray, M. S., Server, C. H., & Dulawa, S. C. (2015a). Dopamine D2/3 receptor antagonism reduces activity-based anorexia. *Translational Psychiatry*, *5*(8), e613. https://doi.org/10.1038/tp.2015.109

Klenotich, S. J., Ho, E. V., McMurray, M. S., Server, C. H., & Dulawa, S. C. (2015b). Dopamine D2/3 receptor antagonism reduces activity-based anorexia. *Translational Psychiatry*, *5*, e613. https://doi.org/10.1038/tp.2015.109

Klump, K. L., Kaye, W. H., & Strober, M. (2001). The evolving genetic foundations of eating disorders. *The Psychiatric Clinics of North America*, *24*(2), 215–225. https://doi.org/10.1016/s0193-953x(05)70218-5

Klumpp, H., Angstadt, M., & Phan, K. L. (2012). Insula Reactivity and Connectivity to Anterior Cingulate Cortex When Processing Threat in Generalized Social Anxiety Disorder. *Biological Psychology*, *89*(1), 273–276. https://doi.org/10.1016/j.biopsycho.2011.10.010

Koutcherov, Y., Mai, J. K., & Paxinos, G. (2003). Hypothalamus of the human fetus. *Journal of Chemical Neuroanatomy*, *26*(4), 253–270. https://doi.org/10.1016/j.jchemneu.2003.07.002

Krashes, M. J., Koda, S., Ye, C., Rogan, S. C., Adams, A. C., Cusher, D. S., Maratos-Flier, E., Roth, B. L., & Lowell, B. B. (2011). Rapid, reversible activation of AgRP neurons drives feeding behavior in mice. *The Journal of Clinical Investigation*, *121*(4), 1424–1428. https://doi.org/10.1172/JCI46229

Krettek, J. E., & Price, J. L. (1978). Amygdaloid projections to subcortical structures within the basal forebrain and brainstem in the rat and cat. *The Journal of Comparative Neurology*, *178*(2), 225–254. https://doi.org/10.1002/cne.901780204

Kreutzer, C., Peters, S., Schulte, D. M., Fangmann, D., Türk, K., Wolff, S., van Eimeren, T., Ahrens, M., Beckmann, J., Schafmayer, C., Becker, T., Kerby, T., Rohr, A., Riedel, C., Heinsen, F.-A., Degenhardt, F., Franke, A., Rosenstiel, P., Zubek, N., … Laudes, M. (2017). Hypothalamic Inflammation in Human Obesity Is Mediated by Environmental and Genetic Factors. *Diabetes*, *66*(9), 2407–2415. https://doi.org/10.2337/db17-0067

Krieg, W. J. S. (1932). The hypothalamus of the albino rat. *Journal of Comparative Neurology*, *55*(1), 19–89. https://doi.org/10.1002/cne.900550104

Kullmann, S., Giel, K. E., Teufel, M., Thiel, A., Zipfel, S., & Preissl, H. (2014). Aberrant network integrity of the inferior frontal cortex in women with anorexia nervosa. *NeuroImage: Clinical*, *4*, 615–622. https://doi.org/10.1016/j.nicl.2014.04.002

Kullmann, S., Heni, M., Linder, K., Zipfel, S., Häring, H.-U., Veit, R., Fritsche, A., & Preissl, H. (2014a). Resting-state functional connectivity of the human hypothalamus. *Human Brain Mapping*, *35*(12), 6088–6096. https://doi.org/10.1002/hbm.22607

Kullmann, S., Heni, M., Linder, K., Zipfel, S., Häring, H.-U., Veit, R., Fritsche, A., & Preissl, H. (2014b). Resting-state functional connectivity of the human hypothalamus. *Human Brain Mapping*, *35*(12), 6088–6096. https://doi.org/10.1002/hbm.22607

Kullmann, S., Pape, A.-A., Heni, M., Ketterer, C., Schick, F., Häring, H.-U., Fritsche, A., Preissl, H., & Veit, R. (2013). Functional network connectivity underlying food processing: Disturbed salience and visual processing in overweight and obese adults. *Cerebral Cortex (New York, N.Y.: 1991)*, *23*(5), 1247–1256. https://doi.org/10.1093/cercor/bhs124

Kullmann, S., & Veit, R. (2021). Resting-state functional connectivity of the human hypothalamus. *Handbook of Clinical Neurology*, *179*, 113–124. https://doi.org/10.1016/B978-0-12-819975-6.00005-4

Kullmann, S., Veit, R., Crabtree, D. R., Buosi, W., Androutsos, O., Johnstone, A. M., Manios, Y., Preissl, H., & Smeets, P. A. M. (2023). The effect of hunger state on hypothalamic functional connectivity in response to food cues. *Human Brain Mapping*, *44*(2), 418–428. https://doi.org/10.1002/hbm.26059

Lancaster, J. L., Tordesillas-Gutiérrez, D., Martinez, M., Salinas, F., Evans, A., Zilles, K., Mazziotta, J. C., & Fox, P. T. (2007). Bias between MNI and Talairach coordinates analyzed using the ICBM-152 brain template. *Human Brain Mapping*, *28*(11), 1194–1205. https://doi.org/10.1002/hbm.20345

Lao-Kaim, N. P., Fonville, L., Giampietro, V. P., Williams, S. C. R., Simmons, A., & Tchanturia, K. (2015). Aberrant Function of Learning and Cognitive Control Networks Underlie Inefficient Cognitive Flexibility in Anorexia Nervosa: A Cross-Sectional fMRI Study. *PLOS ONE*, *10*(5), e0124027. https://doi.org/10.1371/journal.pone.0124027

Le, D. S. N. T., Chen, K., Pannacciulli, N., Gluck, M., Reiman, E. M., & Krakoff, J. (2009). Reanalysis of the obesity-related attenuation in the left dorsolateral prefrontal cortex response to a satiating meal using gyral regions-of-interest. *Journal of the American College of Nutrition*, *28*(6), 667–673. https://doi.org/10.1080/07315724.2009.10719799

Le, T. M., Liao, D.-L., Ide, J., Zhang, S., Zhornitsky, S., Wang, W., & Li, C.-S. R. (2020a). The interrelationship of body mass index with gray matter volume and resting-state functional

connectivity of the hypothalamus. *International Journal of Obesity*, *44*(5), 1097–1107. https://doi.org/10.1038/s41366-019-0496-8

Le, T. M., Liao, D.-L., Ide, J., Zhang, S., Zhornitsky, S., Wang, W., & Li, C.-S. R. (2020b). The interrelationship of body mass index with gray matter volume and resting-state functional connectivity of the hypothalamus. *International Journal of Obesity (2005)*, *44*(5), 1097–1107. https://doi.org/10.1038/s41366-019-0496-8

Lee, S., Ran Kim, K., Ku, J., Lee, J.-H., Namkoong, K., & Jung, Y.-C. (2014). Resting-state synchrony between anterior cingulate cortex and precuneus relates to body shape concern in anorexia nervosa and bulimia nervosa. *Psychiatry Research*, *221*(1), 43–48. https://doi.org/10.1016/j.pscychresns.2013.11.004

Legrand, R., Lucas, N., Breton, J., Azhar, S., do Rego, J.-C., Déchelotte, P., Coëffier, M., & Fetissov, S. O. (2016). Ghrelin treatment prevents development of activity based anorexia in mice. *European Neuropsychopharmacology*, *26*(6), 948–958. https://doi.org/10.1016/j.euroneuro.2016.03.010

Lemaire, J.-J., Frew, A. J., McArthur, D., Gorgulho, A. A., Alger, J. R., Salomon, N., Chen, C., Behnke, E. J., & De Salles, A. A. F. (2011). White matter connectivity of human hypothalamus. *Brain Research*, *1371*, 43–64. https://doi.org/10.1016/j.brainres.2010.11.072

Lemaire, J.-J., Nezzar, H., Sakka, L., Boirie, Y., Fontaine, D., Coste, A., Coll, G., Sontheimer, A., Sarret, C., Gabrillargues, J., & De Salles, A. (2013a). Maps of the adult human hypothalamus. *Surgical Neurology International*, *4*(Suppl 3), S156–S163. https://doi.org/10.4103/2152-7806.110667

Lemaire, J.-J., Nezzar, H., Sakka, L., Boirie, Y., Fontaine, D., Coste, A., Coll, G., Sontheimer, A., Sarret, C., Gabrillargues, J., & De Salles, A. (2013b). Maps of the adult human hypothalamus. *Surgical Neurology International*, *4*(Suppl 3), S156–S163. https://doi.org/10.4103/2152-7806.110667

Li, G., Hu, Y., Zhang, W., Wang, J., Ji, W., Manza, P., Volkow, N. D., Zhang, Y., & Wang, G.-J. (2023). Brain functional and structural magnetic resonance imaging of obesity and weight loss

interventions. *Molecular Psychiatry*, *28*(4), 1466–1479. https://doi.org/10.1038/s41380-023-02025-y

Li, H. Y., & Sawchenko, P. E. (1998). Hypothalamic effector neurons and extended circuitries activated in “neurogenic” stress: A comparison of footshock effects exerted acutely, chronically, and in animals with controlled glucocorticoid levels. *The Journal of Comparative Neurology*, *393*(2), 244–266.

Li, J. X., Yoshida, T., Monk, K. J., & Katz, D. B. (2013). Lateral Hypothalamus Contains Two Types of Palatability-Related Taste Responses with Distinct Dynamics. *Journal of Neuroscience*, *33*(22), 9462–9473. https://doi.org/10.1523/JNEUROSCI.3935-12.2013

Lips, M. A., Wijngaarden, M. A., van der Grond, J., van Buchem, M. A., de Groot, G. H., Rombouts, S. A. R. B., Pijl, H., & Veer, I. M. (2014). Resting-state functional connectivity of brain regions involved in cognitive control, motivation, and reward is enhanced in obese females. *The American Journal of Clinical Nutrition*, *100*(2), 524–531. https://doi.org/10.3945/ajcn.113.080671

Liu, Y., Gao, J. H., Liu, H. L., & Fox, P. T. (2000). The temporal response of the brain after eating revealed by functional MRI. *Nature*, *405*(6790), 1058–1062. https://doi.org/10.1038/35016590

Liu, Z., Patil, I. Y., Jiang, T., Sancheti, H., Walsh, J. P., Stiles, B. L., Yin, F., & Cadenas, E. (2015). High-fat diet induces hepatic insulin resistance and impairment of synaptic plasticity. *PloS One*, *10*(5), e0128274. https://doi.org/10.1371/journal.pone.0128274

Lock, J., Garrett, A., Beenhakker, J., & Reiss, A. (2011). Aberrant Brain Activation During a Response Inhibition Task in Adolescent Eating Disorder Subtypes. *The American Journal of Psychiatry*, *168*(1), 55. https://doi.org/10.1176/appi.ajp.2010.10010056

Lopez, R. B., Hofmann, W., Wagner, D. D., Kelley, W. M., & Heatherton, T. F. (2014). Neural predictors of giving in to temptation in daily life. *Psychological Science*, *25*(7), 1337–1344. https://doi.org/10.1177/0956797614531492

Lord, A., Ehrlich, S., Borchardt, V., Geisler, D., Seidel, M., Huber, S., Murr, J., & Walter, M. (2016). Brain parcellation choice affects disease-related topology differences increasingly from global to local network levels. *Psychiatry Research: Neuroimaging*, *249*, 12–19. https://doi.org/10.1016/j.pscychresns.2016.02.001

Lotter, L. D., von Polier, G., Offermann, J., Buettgen, K., Stanetzky, L., Eickhoff, S. B., Konrad, K., Seitz, J., & Dukart, J. (2021). Recovery-Associated Resting-State Activity and Connectivity Alterations in Anorexia Nervosa. *Biological Psychiatry. Cognitive Neuroscience and Neuroimaging*, S2451-9022(21)00083-5. https://doi.org/10.1016/j.bpsc.2021.03.006

Low, A. Y. T., Goldstein, N., Gaunt, J. R., Huang, K.-P., Zainolabidin, N., Yip, A. K. K., Carty, J. R. E., Choi, J. Y., Miller, A. M., Ho, H. S. T., Lenherr, C., Baltar, N., Azim, E., Sessions, O. M., Ch'ng, T. H., Bruce, A. S., Martin, L. E., Halko, M. A., Brady, R. O., … Betley, J. N. (2021). Reverse-translational identification of a cerebellar satiation network. *Nature*, *600*, 269–273. https://doi.org/10.1038/s41586-021-04143-5

Lucas, A. R., Beard, C. M., O'Fallon, W. M., & Kurland, L. T. (1991). 50-year trends in the incidence of anorexia nervosa in Rochester, Minn.: A population-based study. *The American Journal of Psychiatry*, *148*(7), 917–922. https://doi.org/10.1176/ajp.148.7.917

Luo, S. X., Huang, J., Li, Q., Mohammad, H., Lee, C.-Y., Krishna, K., Kok, A. M.-Y., Tan, Y. L., Lim, J. Y., Li, H., Yeow, L. Y., Sun, J., He, M., Grandjean, J., Sajikumar, S., Han, W., & Fu, Y. (2018). Regulation of feeding by somatostatin neurons in the tuberal nucleus. *Science*, *361*(6397), 76–81. https://doi.org/10.1126/science.aar4983

Luquet, S., Perez, F. A., Hnasko, T. S., & Palmiter, R. D. (2005). NPY/AgRP neurons are essential for feeding in adult mice but can be ablated in neonates. *Science (New York, N.Y.)*, *310*(5748), 683–685. https://doi.org/10.1126/science.1115524

M, S., A, R.-L., L, G., G, L., Jl, V., P, J., & M, C. (2012). An investigation of Goodman's addictive disorder criteria in eating disorders. *European Eating Disorders Review : The Journal of the Eating Disorders Association*, *20*(3). https://doi.org/10.1002/erv.1140

Machado, C. J., & Bachevalier, J. (2007). Measuring reward assessment in a semi-naturalistic context. *Neuroscience*, *148*(3), 599–611. https://doi.org/10.1016/j.neuroscience.2007.06.035

Mai, J. K., Majtanik, M., & Paxinos, G. (2015). *Atlas of the Human Brain*. Academic Press.

Majdic, G., Young, M., Gomez-Sanchez, E., Anderson, P., Szczepaniak, L. S., Dobbins, R. L., McGarry, J. D., & Parker, K. L. (2002). Knockout mice lacking steroidogenic factor 1 are a novel genetic model of hypothalamic obesity. *Endocrinology*, *143*(2), 607–614. https://doi.org/10.1210/endo.143.2.8652

Makris, N., Swaab, D. F., van der Kouwe, A., Abbs, B., Boriel, D., Handa, R. J., Tobet, S., & Goldstein, J. M. (2013). Volumetric parcellation methodology of the human hypothalamus in neuroimaging: Normative data and sex differences. *NeuroImage*, *69*, 1–10. https://doi.org/10.1016/j.neuroimage.2012.12.008

Mapping, O. for H. B. (2024). Abstract Book 5: OHBM 2024 Annual Meeting. *Aperture Neuro*, *4*(Suppl 1). https://doi.org/10.52294/001c.120595

Marino, R. A. M., McDevitt, R. A., Gantz, S. C., Shen, H., Pignatelli, M., Xin, W., Wise, R. A., & Bonci, A. (2020). Control of food approach and eating by a GABAergic projection from lateral hypothalamus to dorsal pons. *Proceedings of the National Academy of Sciences of the United States of America*, *117*(15), 8611–8615. https://doi.org/10.1073/pnas.1909340117

Marques, J. P., Kober, T., Krueger, G., van der Zwaag, W., Van de Moortele, P.-F., & Gruetter, R. (2010). MP2RAGE, a self bias-field corrected sequence for improved segmentation and T1-mapping at high field. *NeuroImage*, *49*(2), 1271–1281. https://doi.org/10.1016/j.neuroimage.2009.10.002

Martin, G. F., Dom, R., Katz, S., & King, J. S. (1974). The organization of projection neurons in the opossum red nucleus. *Brain Research*, *78*(1), 17–34. https://doi.org/10.1016/0006-8993(74)90350-3

Martin Monzon, B., Hay, P., Foroughi, N., & Touyz, S. (2016). White matter alterations in anorexia nervosa: A systematic review of diffusion tensor imaging studies. *World Journal of Psychiatry*, *6*(1), 177–186. https://doi.org/10.5498/wjp.v6.i1.177

Martínez-González, L., Fernández-Villa, T., Molina, A. J., Delgado-Rodríguez, M., & Martín, V. (2020). Incidence of Anorexia Nervosa in Women: A Systematic Review and Meta-Analysis. *International Journal of Environmental Research and Public Health*, *17*(11), 3824. https://doi.org/10.3390/ijerph17113824

Martín-Pérez, C., Contreras-Rodríguez, O., Vilar-López, R., & Verdejo-García, A. (2019). Hypothalamic Networks in Adolescents With Excess Weight: Stress-Related Connectivity and Associations With Emotional Eating. *Journal of the American Academy of Child & Adolescent Psychiatry*, *58*(2), 211-220.e5. https://doi.org/10.1016/j.jaac.2018.06.039

Massire, A., Taso, M., Besson, P., Guye, M., Ranjeva, J.-P., & Callot, V. (2016). High-resolution multi-parametric quantitative magnetic resonance imaging of the human cervical spinal cord at 7T. *NeuroImage*, *143*, 58–69. https://doi.org/10.1016/j.neuroimage.2016.08.055

Matsuda, M., Liu, Y., Mahankali, S., Pu, Y., Mahankali, A., Wang, J., DeFronzo, R. A., Fox, P. T., & Gao, J. H. (1999). Altered hypothalamic function in response to glucose ingestion in obese humans. *Diabetes*, *48*(9), 1801–1806. https://doi.org/10.2337/diabetes.48.9.1801

Mawe, G. M., & Hoffman, J. M. (2013). Serotonin signalling in the gut—Functions, dysfunctions and therapeutic targets. *Nature Reviews. Gastroenterology & Hepatology*, *10*(8), 473–486. https://doi.org/10.1038/nrgastro.2013.105

Mayer, J., & Barrnett, R. J. (1955). Obesity following unilateral hypothalamic lesions in rats. *Science (New York, N.Y.)*, *121*(3147), 599–600. https://doi.org/10.1126/science.121.3147.599

Meek, T. H., Nelson, J. T., Matsen, M. E., Dorfman, M. D., Guyenet, S. J., Damian, V., Allison, M. B., Scarlett, J. M., Nguyen, H. T., Thaler, J. P., Olson, D. P., Myers, M. G., Schwartz, M. W., & Morton, G. J. (2016). Functional identification of a neurocircuit regulating blood glucose.

Proceedings of the National Academy of Sciences of the United States of America, *113*(14), E2073–E2082. https://doi.org/10.1073/pnas.1521160113

Mehta, S., Melhorn, S. J., Smeraglio, A., Tyagi, V., Grabowski, T., Schwartz, M. W., & Schur, E. A. (2012). Regional brain response to visual food cues is a marker of satiety that predicts food choice. *The American Journal of Clinical Nutrition*, *96*(5), 989–999. https://doi.org/10.3945/ajcn.112.042341

Méquinion, M., Langlet, F., Zgheib, S., Dickson, S., Dehouck, B., Chauveau, C., & Viltart, O. (2013). Ghrelin: Central and Peripheral Implications in Anorexia Nervosa. *Frontiers in Endocrinology*, *4*, 15. https://doi.org/10.3389/fendo.2013.00015

Metzler-Baddeley, C., Baddeley, R. J., Jones, D. K., Aggleton, J. P., & O'Sullivan, M. J. (2013a). Individual Differences in Fornix Microstructure and Body Mass Index. *PLOS ONE*, *8*(3), e59849. https://doi.org/10.1371/journal.pone.0059849

Metzler-Baddeley, C., Baddeley, R. J., Jones, D. K., Aggleton, J. P., & O'Sullivan, M. J. (2013b). Individual Differences in Fornix Microstructure and Body Mass Index. *PLOS ONE*, *8*(3), e59849. https://doi.org/10.1371/journal.pone.0059849

Mickelsen, L. E., Bolisetty, M., Chimileski, B. R., Fujita, A., Beltrami, E. J., Costanzo, J. T., Naparstek, J. R., Robson, P., & Jackson, A. C. (2019). Single-cell transcriptomic analysis of the lateral hypothalamic area reveals molecularly distinct populations of inhibitory and excitatory neurons. *Nature Neuroscience*, *22*(4), 642–656. https://doi.org/10.1038/s41593-019-0349-8

Mieda, M., Williams, S. C., Richardson, J. A., Tanaka, K., & Yanagisawa, M. (2006). The dorsomedial hypothalamic nucleus as a putative food-entrainable circadian pacemaker. *Proceedings of the National Academy of Sciences*, *103*(32), 12150–12155. https://doi.org/10.1073/pnas.0604189103

Miles, A. E., Kaplan, A. S., French, L., & Voineskos, A. N. (2020). White matter microstructure in women with acute and remitted anorexia nervosa: An exploratory neuroimaging study. *Brain Imaging and Behavior*, *14*(6), 2429–2437. https://doi.org/10.1007/s11682-019-00193-6

Miles, A. E., Voineskos, A. N., French, L., & Kaplan, A. S. (2018). Subcortical volume and cortical surface architecture in women with acute and remitted anorexia nervosa: An exploratory neuroimaging study. *Journal of Psychiatric Research*, *102*, 179–185. https://doi.org/10.1016/j.jpsychires.2018.04.010

Milgram, N. W. (1969). Effect of hippocampal stimulation on feeding in the rat. *Physiology & Behavior*, *4*(5), 665–670. https://doi.org/10.1016/0031-9384(69)90098-5

Moga, M. M., Weis, R. P., & Moore, R. Y. (1995). Efferent projections of the paraventricular thalamic nucleus in the rat. *The Journal of Comparative Neurology*, *359*(2), 221–238. https://doi.org/10.1002/cne.903590204

Mogenson, G. J., & Stevenson, J. A. (1967). Drinking induced by electrical stimulation of the lateral hypothalamus. *Experimental Neurology*, *17*(2), 119–127. https://doi.org/10.1016/0014-4886(67)90139-2

Mohammad, H., Senol, E., Graf, M., Lee, C.-Y., Li, Q., Liu, Q., Yeo, X. Y., Wang, M., Laskaratos, A., Xu, F., Luo, S. X., Jung, S., Augustine, G. J., & Fu, Y. (2021). A neural circuit for excessive feeding driven by environmental context in mice. *Nature Neuroscience*, *24*(8), Article 8. https://doi.org/10.1038/s41593-021-00875-9

Moran, T. H., & Kinzig, K. P. (2004). Gastrointestinal satiety signals II. Cholecystokinin. *American Journal of Physiology. Gastrointestinal and Liver Physiology*, *286*(2), G183-188. https://doi.org/10.1152/ajpgi.00434.2003

Morrison, S. F., & Nakamura, K. (2011). Central neural pathways for thermoregulation. *Frontiers in Bioscience (Landmark Edition)*, *16*(1), 74–104. https://doi.org/10.2741/3677

Morselli, E., Fuente-Martin, E., Finan, B., Kim, M., Frank, A., Garcia-Caceres, C., Navas, C. R., Gordillo, R., Neinast, M., Kalainayakan, S. P., Li, D. L., Gao, Y., Yi, C.-X., Hahner, L., Palmer, B. F., Tschöp, M. H., & Clegg, D. J. (2014). Hypothalamic PGC-1α Protects Against High-Fat Diet Exposure by Regulating ERα. *Cell Reports*, *9*(2), 633–645. https://doi.org/10.1016/j.celrep.2014.09.025

Morton, G. J., Meek, T. H., & Schwartz, M. W. (2014). Neurobiology of food intake in health and disease. *Nature Reviews. Neuroscience*, *15*(6), 367–378. https://doi.org/10.1038/nrn3745

Mueller, K., Anwander, A., Möller, H. E., Horstmann, A., Lepsien, J., Busse, F., Mohammadi, S., Schroeter, M. L., Stumvoll, M., Villringer, A., & Pleger, B. (2011). Sex-Dependent Influences of Obesity on Cerebral White Matter Investigated by Diffusion-Tensor Imaging. *PLoS ONE*, *6*(4). https://doi.org/10.1371/journal.pone.0018544

Nagahara, Y., Nakamae, T., Nishizawa, S., Mizuhara, Y., Moritoki, Y., Wada, Y., Sakai, Y., Yamashita, T., Narumoto, J., Miyata, J., Yamada, K., & Fukui, K. (2014). A tract-based spatial statistics study in anorexia nervosa: Abnormality in the fornix and the cerebellum. *Progress in Neuro-Psychopharmacology & Biological Psychiatry*, *51*, 72–77. https://doi.org/10.1016/j.pnpbp.2014.01.009

Nauck, M. A., Niedereichholz, U., Ettler, R., Holst, J. J., Orskov, C., Ritzel, R., & Schmiegel, W. H. (1997). Glucagon-like peptide 1 inhibition of gastric emptying outweighs its insulinotropic effects in healthy humans. *The American Journal of Physiology*, *273*(5), E981-988. https://doi.org/10.1152/ajpendo.1997.273.5.E981

Nectow, A. R., Schneeberger, M., Zhang, H., Field, B. C., Renier, N., Azevedo, E., Patel, B., Liang, Y., Mitra, S., Tessier-Lavigne, M., Han, M.-H., & Friedman, J. M. (2017). Identification of a Brainstem Circuit Controlling Feeding. *Cell*, *170*(3), 429-442.e11. https://doi.org/10.1016/j.cell.2017.06.045

Neseliler, S., Han, J.-E., & Dagher, A. (2017). The Use of Functional Magnetic Resonance Imaging in the Study of Appetite and Obesity. In R. B. S. Harris (Ed.), *Appetite and Food Intake: Central Control* (2nd ed.). CRC Press/Taylor & Francis. http://www.ncbi.nlm.nih.gov/books/NBK453146/

Neudorfer, C., Germann, J., Elias, G. J. B., Gramer, R., Boutet, A., & Lozano, A. M. (2020a). A high-resolution in vivo magnetic resonance imaging atlas of the human hypothalamic region. *Scientific Data*, *7*(1), 305. https://doi.org/10.1038/s41597-020-00644-6

Neudorfer, C., Germann, J., Elias, G. J. B., Gramer, R., Boutet, A., & Lozano, A. M. (2020b). A high-resolution in vivo magnetic resonance imaging atlas of the human hypothalamic region. *Scientific Data*, *7*(1), 305. https://doi.org/10.1038/s41597-020-00644-6

Nieh, E. H., Matthews, G. A., Allsop, S. A., Presbrey, K. N., Leppla, C. A., Wichmann, R., Neve, R., Wildes, C. P., & Tye, K. M. (2015). Decoding Neural Circuits that Control Compulsive Sucrose-Seeking. *Cell*, *160*(3), 528–541. https://doi.org/10.1016/j.cell.2015.01.003

Nieh, E. H., Vander Weele, C. M., Matthews, G. A., Presbrey, K. N., Wichmann, R., Leppla, C. A., Izadmehr, E. M., & Tye, K. M. (2016). Inhibitory Input from the Lateral Hypothalamus to the Ventral Tegmental Area Disinhibits Dopamine Neurons and Promotes Behavioral Activation. *Neuron*, *90*(6), 1286–1298. https://doi.org/10.1016/j.neuron.2016.04.035

Nieuwenhuys, R., Voogd, J., & Huijzen, C. van. (1988). *The Human Central Nervous System: A Synopsis and Atlas* (3rd ed.). Springer-Verlag. https://doi.org/10.1007/978-3-662-10343-2

Noback, C. R., Ruggiero, D. A., Demarest, R. J., & Strominger, N. L. (Eds.). (2007). *The Human Nervous System: Structure and Function* (6th ed. 2005 edition). Humana Press.

Nolte, J., & Sundsten, J. W. (2002). *The Human Brain: An Introduction to Its Functional Anatomy*. Mosby.

O'Connor, E. C., Kremer, Y., Lefort, S., Harada, M., Pascoli, V., Rohner, C., & Lüscher, C. (2015). Accumbal D1R Neurons Projecting to Lateral Hypothalamus Authorize Feeding. *Neuron*, *88*(3), 553–564. https://doi.org/10.1016/j.neuron.2015.09.038

O'Doherty, J. P. (2004). Reward representations and reward-related learning in the human brain: Insights from neuroimaging. *Current Opinion in Neurobiology*, *14*(6), 769–776. https://doi.org/10.1016/j.conb.2004.10.016

Ogawa, A., Osada, T., Tanaka, M., Suda, A., Nakajima, K., Oka, S., Kamagata, K., Aoki, S., Oshima, Y., Tanaka, S., Hattori, N., & Konishi, S. (2022). Hypothalamic interaction with reward-related regions during subjective evaluation of foods. *NeuroImage*, *264*, 1–11. https://doi.org/10.1016/j.neuroimage.2022.119744

Oh, S. W., Harris, J. A., Ng, L., Winslow, B., Cain, N., Mihalas, S., Wang, Q., Lau, C., Kuan, L., Henry, A. M., Mortrud, M. T., Ouellette, B., Nguyen, T. N., Sorensen, S. A., Slaughterbeck, C. R., Wakeman, W., Li, Y., Feng, D., Ho, A., … Zeng, H. (2014). A mesoscale connectome of the mouse brain. *Nature*, *508*(7495), 207–214. https://doi.org/10.1038/nature13186

O'Mahony, S. M., Clarke, G., Borre, Y. E., Dinan, T. G., & Cryan, J. F. (2015). Serotonin, tryptophan metabolism and the brain-gut-microbiome axis. *Behavioural Brain Research*, *277*, 32–48. https://doi.org/10.1016/j.bbr.2014.07.027

Osada, T., Suzuki, R., Ogawa, A., Tanaka, M., Hori, M., Aoki, S., Tamura, Y., Watada, H., Kawamori, R., & Konishi, S. (2017). Functional subdivisions of the hypothalamus using areal parcellation and their signal changes related to glucose metabolism. *NeuroImage*, *162*, 1–12. https://doi.org/10.1016/j.neuroimage.2017.08.056

Pannacciulli, N., Del Parigi, A., Chen, K., Le, D. S. N. T., Reiman, E. M., & Tataranni, P. A. (2006). Brain abnormalities in human obesity: A voxel-based morphometric study. *NeuroImage*, *31*(4), 1419–1425. https://doi.org/10.1016/j.neuroimage.2006.01.047

Pardo, M., Roca-Rivada, A., Al-Massadi, O., Seoane, L. M., Camiña, J. P., & Casanueva, F. F. (2010). Peripheral leptin and ghrelin receptors are regulated in a tissue-specific manner in activity-based anorexia. *Peptides*, *31*(10), 1912–1919. https://doi.org/10.1016/j.peptides.2010.06.022

Park, B., Moon, T., & Park, H. (2018). Dynamic functional connectivity analysis reveals improved association between brain networks and eating behaviors compared to static analysis. *Behavioural Brain Research*, *337*, 114–121. https://doi.org/10.1016/j.bbr.2017.10.001

Pauli, W. M., Nili, A. N., & Tyszka, J. M. (2018). A high-resolution probabilistic in vivo atlas of human subcortical brain nuclei. *Scientific Data*, *5*(1), Article 1. https://doi.org/10.1038/sdata.2018.63

Petrovich, G. D. (2011). Learning and the motivation to eat: Forebrain circuitry. *Physiology & Behavior*, *104*(4), 582–589. https://doi.org/10.1016/j.physbeh.2011.04.059

Petrovich, G. D., Ross, C. A., Holland, P. C., & Gallagher, M. (2007). Medial Prefrontal Cortex Is Necessary for an Appetitive Contextual Conditioned Stimulus to Promote Eating in Sated Rats. *Journal of Neuroscience*, *27*(24), 6436–6441. https://doi.org/10.1523/JNEUROSCI.5001-06.2007

Phillipou, A., Abel, L. A., Castle, D. J., Hughes, M. E., Nibbs, R. G., Gurvich, C., & Rossell, S. L. (2016). Resting state functional connectivity in anorexia nervosa. *Psychiatry Research. Neuroimaging*, *251*, 45–52. https://doi.org/10.1016/j.pscychresns.2016.04.008

Pike, K. M. (1998). Long-term course of anorexia nervosa: Response, relapse, remission, and recovery. *Clinical Psychology Review*, *18*(4), 447–475. https://doi.org/10.1016/s0272-7358(98)00014-2

Pimentel, G. D., Ganeshan, K., & Carvalheira, J. B. C. (2014). Hypothalamic inflammation and the central nervous system control of energy homeostasis. *Molecular and Cellular Endocrinology*, *397*(1–2), 15–22. https://doi.org/10.1016/j.mce.2014.06.005

Posey, K. A., Clegg, D. J., Printz, R. L., Byun, J., Morton, G. J., Vivekanandan-Giri, A., Pennathur, S., Baskin, D. G., Heinecke, J. W., Woods, S. C., Schwartz, M. W., & Niswender, K. D. (2009). Hypothalamic proinflammatory lipid accumulation, inflammation, and insulin resistance in rats fed a high-fat diet. *American Journal of Physiology-Endocrinology and Metabolism*, *296*(5), E1003–E1012. https://doi.org/10.1152/ajpendo.90377.2008

Poulin, A.-M., & Timofeeva, E. (2008). The dynamics of neuronal activation during food anticipation and feeding in the brain of food-entrained rats. *Brain Research*, *1227*, 128–141. https://doi.org/10.1016/j.brainres.2008.06.039

Pruim, R. H. R., Mennes, M., van Rooij, D., Llera, A., Buitelaar, J. K., & Beckmann, C. F. (2015). ICA-AROMA: A robust ICA-based strategy for removing motion artifacts from fMRI data. *NeuroImage*, *112*, 267–277. https://doi.org/10.1016/j.neuroimage.2015.02.064

Puig, J., Blasco, G., Daunis-I-Estadella, J., Molina, X., Xifra, G., Ricart, W., Pedraza, S., Fernández-Aranda, F., & Fernández-Real, J. M. (2015). Hypothalamic damage is associated with

inflammatory markers and worse cognitive performance in obese subjects. *The Journal of Clinical Endocrinology and Metabolism*, *100*(2), E276-281. https://doi.org/10.1210/jc.2014-2682

Purnell, J. Q., Klopfenstein, B. A., Stevens, A. A., Havel, P. J., Adams, S. H., Dunn, T. N., Krisky, C., & Rooney, W. D. (2011). Brain functional magnetic resonance imaging response to glucose and fructose infusions in humans. *Diabetes, Obesity & Metabolism*, *13*(3), 229–234. https://doi.org/10.1111/j.1463-1326.2010.01340.x

Quarta, C., Claret, M., Zeltser, L. M., Williams, K. W., Yeo, G. S. H., Tschöp, M. H., Diano, S., Brüning, J. C., & Cota, D. (2021). POMC neuronal heterogeneity in energy balance and beyond: An integrated view. *Nature Metabolism*, *3*(3), 299–308. https://doi.org/10.1038/s42255-021-00345-3

Raji, C. A., Ho, A. J., Parikshak, N. N., Becker, J. T., Lopez, O. L., Kuller, L. H., Hua, X., Leow, A. D., Toga, A. W., & Thompson, P. M. (2009). Brain structure and obesity. *Human Brain Mapping*, *31*(3), 353–364. https://doi.org/10.1002/hbm.20870

Rask-Andersen, M., Olszewski, P. K., Levine, A. S., & Schiöth, H. B. (2010). Molecular mechanisms underlying anorexia nervosa: Focus on human gene association studies and systems controlling food intake. *Brain Research Reviews*, *62*(2), 147–164. https://doi.org/10.1016/j.brainresrev.2009.10.007

Rasmussen, A. T. (1938). The hypothalamus: Morphological, Functional, Clinical and Surgical Aspects. By W. E. Le Gros Clark, D.Sc., F.R.C.S., F.R.S.; John Beattie, M.D., D.Sc.; George Riddoch, M.D., F.R.C.P. and Norman M. Dott, F.R.C.S. Ed. Published for the William Ramsay Henderson Trust by Oliver and Boyd, Edinburgh and London, 1938. xii + 211 pp. 12 s. 6 d. *The Anatomical Record*, *72*(3), 395–396. https://doi.org/10.1002/ar.1090720311

Rijke, C. E. de, Hillebrand, J. J. G., Verhagen, L. a. W., Roeling, T. a. P., & Adan, R. a. H. (2005). Hypothalamic neuropeptide expression following chronic food restriction in sedentary and

wheel-running rats. *Journal of Molecular Endocrinology*, *35*(2), 381–390. https://doi.org/10.1677/jme.1.01808

Risold, P. Y., Thompson, R. H., & Swanson, L. W. (1997a). The structural organization of connections between hypothalamus and cerebral cortex. *Brain Research. Brain Research Reviews*, *24*(2–3), 197–254. https://doi.org/10.1016/s0165-0173(97)00007-6

Risold, P. Y., Thompson, R. H., & Swanson, L. W. (1997b). The structural organization of connections between hypothalamus and cerebral cortex. *Brain Research. Brain Research Reviews*, *24*(2–3), 197–254. https://doi.org/10.1016/s0165-0173(97)00007-6

Rivera, B., Miller, S. R., Brown, E. M., & Price, R. E. (2005). *A Novel Method for Endotracheal Intubation of Mice and Rats Used in Imaging Studies*. *44*(2), 4.

Roger, C., Lasbleiz, A., Guye, M., Dutour, A., Gaborit, B., & Ranjeva, J.-P. (2022). The Role of the Human Hypothalamus in Food Intake Networks: An MRI Perspective. *Frontiers in Nutrition*, *8*. https://doi.org/10.3389/fnut.2021.760914

Rolls, E. T. (2004). The functions of the orbitofrontal cortex. *Brain and Cognition*, *55*(1), 11–29. https://doi.org/10.1016/S0278-2626(03)00277-X

Rolls, E. T. (2015). Taste, olfactory, and food reward value processing in the brain. *Progress in Neurobiology*, *127–128*, 64–90. https://doi.org/10.1016/j.pneurobio.2015.03.002

Rolls, E. T. (2016a). Functions of the anterior insula in taste, autonomic, and related functions. *Brain and Cognition*, *110*, 4–19. https://doi.org/10.1016/j.bandc.2015.07.002

Rolls, E. T. (2016b). Reward Systems in the Brain and Nutrition. *Annual Review of Nutrition*, *36*, 435–470. https://doi.org/10.1146/annurev-nutr-071715-050725

Rolls, E. T., Huang, C.-C., Lin, C.-P., Feng, J., & Joliot, M. (2020). Automated anatomical labelling atlas 3. *NeuroImage*, *206*, 116189. https://doi.org/10.1016/j.neuroimage.2019.116189

Roman, C. W., Derkach, V. A., & Palmiter, R. D. (2016). Genetically and functionally defined NTS to PBN brain circuits mediating anorexia. *Nature Communications*, *7*(1), 11905. https://doi.org/10.1038/ncomms11905

Rønnekleiv, O. K., Qiu, J., & Kelly, M. J. (2022). Hypothalamic Kisspeptin Neurons and the Control of Homeostasis. *Endocrinology*, *163*(2), bqab253. https://doi.org/10.1210/endocr/bqab253

Rossi, M. A. (2023). Control of energy homeostasis by the lateral hypothalamic area. *Trends in Neurosciences*, *46*(9), 738–749. https://doi.org/10.1016/j.tins.2023.05.010

Rothemund, Y., Preuschhof, C., Bohner, G., Bauknecht, H.-C., Klingebiel, R., Flor, H., & Klapp, B. F. (2007). Differential activation of the dorsal striatum by high-calorie visual food stimuli in obese individuals. *NeuroImage*, *37*(2), 410–421. https://doi.org/10.1016/j.neuroimage.2007.05.008

Routtenberg, A., & Kuznesof, A. W. (1967). Self-starvation of rats living in activity wheels on a restricted feeding schedule. *Journal of Comparative and Physiological Psychology*, *64*(3), 414–421. https://doi.org/10.1037/h0025205

Rozin, P., Dow, S., Moscovitch, M., & Rajaram, S. (1998). What Causes Humans to Begin and End a Meal? A Role for Memory for What Has Been Eaten, as Evidenced by a Study of Multiple Meal Eating in Amnesic Patients. *Psychological Science*, *9*(5), 392–396. https://doi.org/10.1111/1467-9280.00073

Rubinov, M., & Sporns, O. (2010). Complex network measures of brain connectivity: Uses and interpretations. *NeuroImage*, *52*(3), 1059–1069. https://doi.org/10.1016/j.neuroimage.2009.10.003

Sahib, A. K., Erb, M., Marquetand, J., Martin, P., Elshahabi, A., Klamer, S., Vulliemoz, S., Scheffler, K., Ethofer, T., & Focke, N. K. (2018). Evaluating the impact of fast-fMRI on dynamic functional connectivity in an event-based paradigm. *PLoS ONE*, *13*(1), e0190480. https://doi.org/10.1371/journal.pone.0190480

Sainsbury, A., & Zhang, L. (2010). Role of the arcuate nucleus of the hypothalamus in regulation of body weight during energy deficit. *Molecular and Cellular Endocrinology*, *316*(2), 109–119. https://doi.org/10.1016/j.mce.2009.09.025

Salem, V., & Dhillo, W. S. (2015a). IMAGING IN ENDOCRINOLOGY: The use of functional MRI to study the endocrinology of appetite. *European Journal of Endocrinology*, *173*(2), R59-68. https://doi.org/10.1530/EJE-14-0716

Salem, V., & Dhillo, W. S. (2015b). IMAGING IN ENDOCRINOLOGY: The use of functional MRI to study the endocrinology of appetite. *European Journal of Endocrinology*, *173*(2), R59–R68. https://doi.org/10.1530/EJE-14-0716

Sanders, N., Smeets, P. A. M., van Elburg, A. A., Danner, U. N., van Meer, F., Hoek, H. W., & Adan, R. A. H. (2015). Altered food-cue processing in chronically ill and recovered women with anorexia nervosa. *Frontiers in Behavioral Neuroscience*, *9*, 46. https://doi.org/10.3389/fnbeh.2015.00046

Saneyasu, T., Honda, K., Kamisoyama, H., Nakayama, Y., Ikegami, K., & Hasegawa, S. (2011). Alpha-melanocyte stimulating hormone plays an important role in the regulation of food intake by the central melanocortin system in chicks. *Peptides*, *32*(5), 996–1000. https://doi.org/10.1016/j.peptides.2011.03.006

Saper, C. B., & Lowell, B. B. (2014). The hypothalamus. *Current Biology: CB*, *24*(23), R1111-1116. https://doi.org/10.1016/j.cub.2014.10.023

Scaife, J. C., Godier, L. R., Filippini, N., Harmer, C. J., & Park, R. J. (2017). Reduced Resting-State Functional Connectivity in Current and Recovered Restrictive Anorexia Nervosa. *Frontiers in Psychiatry*, *8*, 30. https://doi.org/10.3389/fpsyt.2017.00030

Scammell, T. E., Arrigoni, E., & Lipton, J. O. (2017). Neural Circuitry of Wakefulness and Sleep. *Neuron*, *93*(4), 747–765. https://doi.org/10.1016/j.neuron.2017.01.014

Schachter, S. (1968). Obesity and eating. Internal and external cues differentially affect the eating behavior of obese and normal subjects. *Science (New York, N.Y.)*, *161*(3843), 751–756. https://doi.org/10.1126/science.161.3843.751

Schalla, M. A., & Stengel, A. (2018). The Role of Ghrelin in Anorexia Nervosa. *International Journal of Molecular Sciences*, *19*(7), 2117. https://doi.org/10.3390/ijms19072117

Scharner, S., Prinz, P., Goebel-Stengel, M., Kobelt, P., Hofmann, T., Rose, M., & Stengel, A. (2016). Activity-Based Anorexia Reduces Body Weight without Inducing a Separate Food Intake Microstructure or Activity Phenotype in Female Rats—Mediation via an Activation of Distinct Brain Nuclei. *Frontiers in Neuroscience*, *10*. https://doi.org/10.3389/fnins.2016.00475

Schienle, A., Schäfer, A., Stark, R., Walter, B., & Vaitl, D. (2005). Neural responses of OCD patients towards disorder-relevant, generally disgust-inducing and fear-inducing pictures. *International Journal of Psychophysiology: Official Journal of the International Organization of Psychophysiology*, *57*(1), 69–77. https://doi.org/10.1016/j.ijpsycho.2004.12.013

Schirra, J., & Göke, B. (2005). The physiological role of GLP-1 in human: Incretin, ileal brake or more? *Regulatory Peptides*, *128*(2), 109–115. https://doi.org/10.1016/j.regpep.2004.06.018

Schönknecht, P., Anwander, A., Petzold, F., Schindler, S., Knösche, T. R., Möller, H. E., Hegerl, U., Turner, R., & Geyer, S. (2013). Diffusion imaging-based subdivision of the human hypothalamus: A magnetic resonance study with clinical implications. *European Archives of Psychiatry and Clinical Neuroscience*, *263*(6), 497–508. https://doi.org/10.1007/s00406-012-0389-5

Schouten, T. M., Koini, M., de Vos, F., Seiler, S., van der Grond, J., Lechner, A., Hafkemeijer, A., Möller, C., Schmidt, R., de Rooij, M., & Rombouts, S. A. R. B. (2016). Combining anatomical, diffusion, and resting state functional magnetic resonance imaging for individual classification of mild and moderate Alzheimer's disease. *NeuroImage: Clinical*, *11*, 46–51. https://doi.org/10.1016/j.nicl.2016.01.002

Schur, E. A., Kleinhans, N. M., Goldberg, J., Buchwald, D., Schwartz, M. W., & Maravilla, K. (2009a). Activation in brain energy regulation and reward centers by food cues varies with choice of visual stimulus. *International Journal of Obesity (2005)*, *33*(6), 653–661. https://doi.org/10.1038/ijo.2009.56

Schur, E. A., Kleinhans, N. M., Goldberg, J., Buchwald, D., Schwartz, M. W., & Maravilla, K. (2009b). Activation in brain energy regulation and reward centers by food cues varies with choice of

visual stimulus. *International Journal of Obesity (2005)*, *33*(6), 653–661. https://doi.org/10.1038/ijo.2009.56

Schwartz, M. W., Seeley, R. J., Campfield, L. A., Burn, P., & Baskin, D. G. (1996). Identification of targets of leptin action in rat hypothalamus. *Journal of Clinical Investigation*, *98*(5), 1101–1106.

Schwartz, N. B., & Kling, A. (1964). The effect of amygdaloid lesions on feeding, grooming and reproduction in rats. *Acta Neurovegetativa*, *26*(1), 12–34. https://doi.org/10.1007/BF01227295

Selvini-Palazzoli, M., & Viaro, M. (1988). The anorectic process in the family: A six-stage model as a guide for individual therapy. *Family Process*, *27*(2), 129–148. https://doi.org/10.1111/j.1545-5300.1988.00129.x

Shah, B. P., Vong, L., Olson, D. P., Koda, S., Krashes, M. J., Ye, C., Yang, Z., Fuller, P. M., Elmquist, J. K., & Lowell, B. B. (2014). MC4R-expressing glutamatergic neurons in the paraventricular hypothalamus regulate feeding and are synaptically connected to the parabrachial nucleus. *Proceedings of the National Academy of Sciences of the United States of America*, *111*(36), 13193–13198. https://doi.org/10.1073/pnas.1407843111

Shah, S. G., Klumpp, H., Angstadt, M., Nathan, P. J., & Phan, K. L. (2009). Amygdala and insula response to emotional images in patients with generalized social anxiety disorder. *Journal of Psychiatry & Neuroscience : JPN*, *34*(4), 296–302.

Shetty, S., Duesman, S. J., Patel, S., Huynh, P., Toh, P., Shroff, S., Das, A., Chowhan, D., Keller, B., Alvarez, J., Fisher-Foye, R., Sebra, R., Beaumont, K., McAlpine, C. S., Rajbhandari, P., & Rajbhandari, A. K. (2024). Sex-specific role of high-fat diet and stress on behavior, energy metabolism, and the ventromedial hypothalamus. *Biology of Sex Differences*, *15*(1), 55. https://doi.org/10.1186/s13293-024-00628-w

Shimazu, T., Matsushita, H., & Ishikawa, K. (1978). Hypothalamic control of liver glycogen metabolism in adult and aged rats. *Brain Research*, *144*(2), 343–352. https://doi.org/10.1016/0006-8993(78)90159-2

Shott, M. E., Pryor, T. L., Yang, T. T., & Frank, G. K. W. (2016). Greater Insula White Matter Fiber Connectivity in Women Recovered from Anorexia Nervosa. *Neuropsychopharmacology*, *41*(2), 498–507. https://doi.org/10.1038/npp.2015.172

Simon, H., Le Moal, M., & Calas, A. (1979). Efferents and afferents of the ventral tegmental-A10 region studied after local injection of [3H]leucine and horseradish peroxidase. *Brain Research*, *178*(1), 17–40. https://doi.org/10.1016/0006-8993(79)90085-4

Simon, J. J., Stopyra, M. A., Mönning, E., Sailer, S., Lavandier, N., Kihm, L. P., Bendszus, M., Preissl, H., Herzog, W., & Friederich, H.-C. (2020a). Neuroimaging of hypothalamic mechanisms related to glucose metabolism in anorexia nervosa and obesity. *Journal of Clinical Investigation*, 10.1172/JCI136782. https://doi.org/10.1172/JCI136782

Simon, J. J., Stopyra, M. A., Mönning, E., Sailer, S., Lavandier, N., Kihm, L. P., Bendszus, M., Preissl, H., Herzog, W., & Friederich, H.-C. (2020b). Neuroimaging of hypothalamic mechanisms related to glucose metabolism in anorexia nervosa and obesity. *The Journal of Clinical Investigation*, *130*(8), 4094–4103. https://doi.org/10.1172/JCI136782

Sims, J. S., & Lorden, J. F. (1986). Effect of paraventricular nucleus lesions on body weight, food intake and insulin levels. *Behavioural Brain Research*, *22*(3), 265–281. https://doi.org/10.1016/0166-4328(86)90071-9

Skibicka, K. P., Hansson, C., Egecioglu, E., & Dickson, S. L. (2012). Role of ghrelin in food reward: Impact of ghrelin on sucrose self-administration and mesolimbic dopamine and acetylcholine receptor gene expression. *Addiction Biology*, *17*(1), 95–107. https://doi.org/10.1111/j.1369-1600.2010.00294.x

Smeets, P. A. M., de Graaf, C., Stafleu, A., van Osch, M. J. P., & van der Grond, J. (2005). Functional MRI of human hypothalamic responses following glucose ingestion. *NeuroImage*, *24*(2), 363–368. https://doi.org/10.1016/j.neuroimage.2004.07.073

Smink, F. R. E., van Hoeken, D., Donker, G. A., Susser, E. S., Oldehinkel, A. J., & Hoek, H. W. (2016). Three decades of eating disorders in Dutch primary care: Decreasing incidence of bulimia nervosa but not of anorexia nervosa. *Psychological Medicine*, *46*(6), 1189–1196. https://doi.org/10.1017/S003329171500272X

Smith, J. B., Watson, G. D. R., Liang, Z., Liu, Y., Zhang, N., & Alloway, K. D. (2019). A Role for the Claustrum in Salience Processing? *Frontiers in Neuroanatomy*, *13*. https://doi.org/10.3389/fnana.2019.00064

Smith, P. M., & Ferguson, A. V. (2008). Neurophysiology of hunger and satiety. *Developmental Disabilities Research Reviews*, *14*(2), 96–104. https://doi.org/10.1002/ddrr.13

Södersten, P., Bergh, C., & Leon, M. (2016). Commentary: New Insights in Anorexia Nervosa. *Frontiers in Neuroscience*, *10*. https://doi.org/10.3389/fnins.2016.00483

Speksnijder, E. M., Bisschop, P. H., Siegelaar, S. E., Stenvers, D. J., & Kalsbeek, A. (2024). Circadian desynchrony and glucose metabolism. *Journal of Pineal Research*, *76*(4), e12956. https://doi.org/10.1111/jpi.12956

Stanek, K. M., Grieve, S. M., Brickman, A. M., Korgaonkar, M. S., Paul, R. H., Cohen, R. A., & Gunstad, J. J. (2011). Obesity is associated with reduced white matter integrity in otherwise healthy adults. *Obesity (Silver Spring, Md.)*, *19*(3), 500–504. https://doi.org/10.1038/oby.2010.312

Steinglass, J. E., & Walsh, B. T. (2016). Neurobiological model of the persistence of anorexia nervosa. *Journal of Eating Disorders*, *4*(1), 19. https://doi.org/10.1186/s40337-016-0106-2

Stern, S. A., Azevedo, E. P., Pomeranz, L. E., Doerig, K. R., Ivan, V. J., & Friedman, J. M. (2021). Top-down control of conditioned overconsumption is mediated by insular cortex Nos1 neurons. *Cell Metabolism*, *33*(7), 1418-1432.e6. https://doi.org/10.1016/j.cmet.2021.03.001

Stern, S. A., Doerig, K. R., Azevedo, E. P., Stoffel, E., & Friedman, J. M. (2018). *Control of non-homeostatic feeding in sated mice using associative learning of contextual food cues* (p. 247825). bioRxiv. https://doi.org/10.1101/247825

Stern, S. A., Doerig, K. R., Azevedo, E. P., Stoffel, E., & Friedman, J. M. (2020). Control of non-homeostatic feeding in sated mice using associative learning of contextual food cues. *Molecular Psychiatry*, *25*(3), 666–679. https://doi.org/10.1038/s41380-018-0072-y

Sternson, S. M., & Eiselt, A.-K. (2017). Three Pillars for the Neural Control of Appetite. *Annual Review of Physiology*, *79*, 401–423. https://doi.org/10.1146/annurev-physiol-021115-104948

Stice, E., Spoor, S., Bohon, C., Veldhuizen, M. G., & Small, D. M. (2008). Relation of reward from food intake and anticipated food intake to obesity: A functional magnetic resonance imaging study. *Journal of Abnormal Psychology*, *117*(4), 924–935. https://doi.org/10.1037/a0013600

Stice, E., Yokum, S., Bohon, C., Marti, N., & Smolen, A. (2010). Reward Circuitry Responsivity to Food Predicts Future Increases in Body Mass: Moderating Effects of DRD2 and DRD4. *NeuroImage*, *50*(4), 1618–1625. https://doi.org/10.1016/j.neuroimage.2010.01.081

Stoeckel, L. E., Weller, R. E., Cook, E. W., Twieg, D. B., Knowlton, R. C., & Cox, J. E. (2008a). Widespread reward-system activation in obese women in response to pictures of high-calorie foods. *NeuroImage*, *41*(2), 636–647. https://doi.org/10.1016/j.neuroimage.2008.02.031

Stoeckel, L. E., Weller, R. E., Cook, E. W., Twieg, D. B., Knowlton, R. C., & Cox, J. E. (2008b). Widespread reward-system activation in obese women in response to pictures of high-calorie foods. *NeuroImage*, *41*(2), 636–647. https://doi.org/10.1016/j.neuroimage.2008.02.031

Strader, A. D., & Woods, S. C. (2005). Gastrointestinal hormones and food intake. *Gastroenterology*, *128*(1), 175–191. https://doi.org/10.1053/j.gastro.2004.10.043

Stroe-Kunold, E., Buckert, M., Friederich, H.-C., Wesche, D., Kopf, S., Herzog, W., & Wild, B. (2016). Time Course of Leptin in Patients with Anorexia Nervosa during Inpatient Treatment:

Longitudinal Relationships to BMI and Psychological Factors. *PLOS ONE*, *11*(12), e0166843. https://doi.org/10.1371/journal.pone.0166843

Sun, X., Kroemer, N. B., Veldhuizen, M. G., Babbs, A. E., de Araujo, I. E., Gitelman, D. R., Sherwin, R. S., Sinha, R., & Small, D. M. (2015). Basolateral amygdala response to food cues in the absence of hunger is associated with weight gain susceptibility. *The Journal of Neuroscience: The Official Journal of the Society for Neuroscience*, *35*(20), 7964–7976. https://doi.org/10.1523/JNEUROSCI.3884-14.2015

Sutton, A. K., Myers, M. G., & Olson, D. P. (2016). The Role of PVH Circuits in Leptin Action and Energy Balance. *Annual Review of Physiology*, *78*, 207–221. https://doi.org/10.1146/annurev-physiol-021115-105347

Swaab, D. F. (1997). Chapter II Neurobiology and neuropathology of the human hypothalamus. In F. E. Bloom, A. Björklund, & T. Hökfelt (Eds.), *Handbook of Chemical Neuroanatomy* (Vol. 13, pp. 39–137). Elsevier. https://doi.org/10.1016/S0924-8196(97)80004-8

Sweeney, P., & Yang, Y. (2015). An excitatory ventral hippocampus to lateral septum circuit that suppresses feeding. *Nature Communications*, *6*(1), 10188. https://doi.org/10.1038/ncomms10188

Sweet, L. H., Hassenstab, J. J., McCaffery, J. M., Raynor, H. A., Bond, D. S., Demos, K. E., Haley, A. P., Cohen, R. A., Del Parigi, A., & Wing, R. R. (2012). Brain response to food stimulation in obese, normal weight, and successful weight loss maintainers. *Obesity (Silver Spring, Md.)*, *20*(11), 2220–2225. https://doi.org/10.1038/oby.2012.125

Swick, D., Ashley, V., & Turken, A. U. (2008). Left inferior frontal gyrus is critical for response inhibition. *BMC Neuroscience*, *9*, 102. https://doi.org/10.1186/1471-2202-9-102

Takizawa, R., Danese, A., Maughan, B., & Arseneault, L. (2015). Bullying victimization in childhood predicts inflammation and obesity at mid-life: A five-decade birth cohort study. *Psychological Medicine*, *45*(13), 2705–2715. https://doi.org/10.1017/S0033291715000653

Tan, H.-E., Sisti, A. C., Jin, H., Vignovich, M., Villavicencio, M., Tsang, K. S., Goffer, Y., & Zuker, C. S. (2020). The gut-brain axis mediates sugar preference. *Nature*, *580*(7804), 511–516. https://doi.org/10.1038/s41586-020-2199-7

Tataranni, P. A., Gautier, J.-F., Chen, K., Uecker, A., Bandy, D., Salbe, A. D., Pratley, R. E., Lawson, M., Reiman, E. M., & Ravussin, E. (1999). Neuroanatomical correlates of hunger and satiation in humans using positron emission tomography. *Proceedings of the National Academy of Sciences of the United States of America*, *96*(8), 4569–4574.

Thaler, J. P., & Schwartz, M. W. (2010). Minireview: Inflammation and Obesity Pathogenesis: The Hypothalamus Heats Up. *Endocrinology*, *151*(9), 4109–4115. https://doi.org/10.1210/en.2010-0336

Thaler, J. P., Yi, C.-X., Schur, E. A., Guyenet, S. J., Hwang, B. H., Dietrich, M. O., Zhao, X., Sarruf, D. A., Izgur, V., Maravilla, K. R., Nguyen, H. T., Fischer, J. D., Matsen, M. E., Wisse, B. E., Morton, G. J., Horvath, T. L., Baskin, D. G., Tschöp, M. H., & Schwartz, M. W. (2012a). Obesity is associated with hypothalamic injury in rodents and humans. *The Journal of Clinical Investigation*, *122*(1), 153–162. https://doi.org/10.1172/JCI59660

Thaler, J. P., Yi, C.-X., Schur, E. A., Guyenet, S. J., Hwang, B. H., Dietrich, M. O., Zhao, X., Sarruf, D. A., Izgur, V., Maravilla, K. R., Nguyen, H. T., Fischer, J. D., Matsen, M. E., Wisse, B. E., Morton, G. J., Horvath, T. L., Baskin, D. G., Tschöp, M. H., & Schwartz, M. W. (2012b). Obesity is associated with hypothalamic injury in rodents and humans. *The Journal of Clinical Investigation*, *122*(1), 153–162. https://doi.org/10.1172/JCI59660

Thomas, K., Beyer, F., Lewe, G., Zhang, R., Schindler, S., Schönknecht, P., Stumvoll, M., Villringer, A., & Witte, A. V. (2019). Higher body mass index is linked to altered hypothalamic microstructure. *Scientific Reports*, *9*(1), 17373. https://doi.org/10.1038/s41598-019-53578-4

Thompson, R. H., & Swanson, L. W. (1998). Organization of inputs to the dorsomedial nucleus of the hypothalamus: A reexamination with Fluorogold and PHAL in the rat. *Brain Research Reviews*, *27*(2), 89–118. https://doi.org/10.1016/S0165-0173(98)00010-1

Tian, Y., Margulies, D. S., Breakspear, M., & Zalesky, A. (2020). Topographic organization of the human subcortex unveiled with functional connectivity gradients. *Nature Neuroscience*, *23*(11), Article 11. https://doi.org/10.1038/s41593-020-00711-6

Timper, K., & Brüning, J. C. (2017). Hypothalamic circuits regulating appetite and energy homeostasis: Pathways to obesity. *Disease Models & Mechanisms*, *10*(6), 679–689. https://doi.org/10.1242/dmm.026609

Titova, O. E., Hjorth, O. C., Schiöth, H. B., & Brooks, S. J. (2013). Anorexia nervosa is linked to reduced brain structure in reward and somatosensory regions: A meta-analysis of VBM studies. *BMC Psychiatry*, *13*, 110. https://doi.org/10.1186/1471-244X-13-110

Tomasi, D., & Volkow, N. D. (2013). Striatocortical pathway dysfunction in addiction and obesity: Differences and similarities. *Critical Reviews in Biochemistry and Molecular Biology*, *48*(1), 1–19. https://doi.org/10.3109/10409238.2012.735642

Tournier, J.-D., Smith, R., Raffelt, D., Tabbara, R., Dhollander, T., Pietsch, M., Christiaens, D., Jeurissen, B., Yeh, C.-H., & Connelly, A. (2019). MRtrix3: A fast, flexible and open software framework for medical image processing and visualisation. *NeuroImage*, *202*, 116137. https://doi.org/10.1016/j.neuroimage.2019.116137

Touzani, K., & Sclafani, A. (2001). Conditioned flavor preference and aversion: Role of the lateral hypothalamus. *Behavioral Neuroscience*, *115*(1), 84–93. https://doi.org/10.1037/0735-7044.115.1.84

Tracy, A. L., Jarrard, L. E., & Davidson, T. L. (2001). The hippocampus and motivation revisited: Appetite and activity. *Behavioural Brain Research*, *127*(1–2), 13–23. https://doi.org/10.1016/s0166-4328(01)00364-3

Travers, J. B., Dinardo, L. A., & Karimnamazi, H. (1997). Motor and premotor mechanisms of licking. *Neuroscience and Biobehavioral Reviews*, *21*(5), 631–647. https://doi.org/10.1016/s0149-7634(96)00045-0

Troisi, A., Di Lorenzo, G., Lega, I., Tesauro, M., Bertoli, A., Leo, R., Iantorno, M., Pecchioli, C., Rizza, S., Turriziani, M., Lauro, R., & Siracusano, A. (2005). Plasma ghrelin in anorexia, bulimia, and binge-eating disorder: Relations with eating patterns and circulating concentrations of cortisol and thyroid hormones. *Neuroendocrinology*, *81*(4), 259–266. https://doi.org/10.1159/000087923

Tschöp, M., Weyer, C., Tataranni, P. A., Devanarayan, V., Ravussin, E., & Heiman, M. L. (2001). Circulating ghrelin levels are decreased in human obesity. *Diabetes*, *50*(4), 707–709. https://doi.org/10.2337/diabetes.50.4.707

Turton, M. D., O'Shea, D., Gunn, I., Beak, S. A., Edwards, C. M., Meeran, K., Choi, S. J., Taylor, G. M., Heath, M. M., Lambert, P. D., Wilding, J. P., Smith, D. M., Ghatei, M. A., Herbert, J., & Bloom, S. R. (1996). A role for glucagon-like peptide-1 in the central regulation of feeding. *Nature*, *379*(6560), 69–72. https://doi.org/10.1038/379069a0

Tuulari, J. J., Karlsson, H. K., Hirvonen, J., Salminen, P., Nuutila, P., & Nummenmaa, L. (2015). Neural Circuits for Cognitive Appetite Control in Healthy and Obese Individuals: An fMRI Study. *PLOS ONE*, *10*(2), e0116640. https://doi.org/10.1371/journal.pone.0116640

Uher, R., Murphy, T., Brammer, M. J., Dalgleish, T., Phillips, M. L., Ng, V. W., Andrew, C. M., Williams, S. C. R., Campbell, I. C., & Treasure, J. (2004). Medial prefrontal cortex activity associated with symptom provocation in eating disorders. *The American Journal of Psychiatry*, *161*(7), 1238–1246. https://doi.org/10.1176/appi.ajp.161.7.1238

Uher, R., Treasure, J., Heining, M., Brammer, M. J., & Campbell, I. C. (2006). Cerebral processing of food-related stimuli: Effects of fasting and gender. *Behavioural Brain Research*, *169*(1), 111–119. https://doi.org/10.1016/j.bbr.2005.12.008

Valdearcos, M., Robblee, M. M., Benjamin, D. I., Nomura, D. K., Xu, A. W., & Koliwad, S. K. (2014). Microglia Dictate the Impact of Saturated Fat Consumption on Hypothalamic Inflammation and Neuronal Function. *Cell Reports*, *9*(6), 2124–2138. https://doi.org/10.1016/j.celrep.2014.11.018

van de Sande-Lee, S., Pereira, F. R. S., Cintra, D. E., Fernandes, P. T., Cardoso, A. R., Garlipp, C. R., Chaim, E. A., Pareja, J. C., Geloneze, B., Li, L. M., Cendes, F., & Velloso, L. A. (2011). Partial reversibility of hypothalamic dysfunction and changes in brain activity after body mass reduction in obese subjects. *Diabetes*, *60*(6), 1699–1704. https://doi.org/10.2337/db10-1614

Van den Eynde, F., & Treasure, J. (2009). Neuroimaging in Eating Disorders and Obesity: Implications for Research. *Child and Adolescent Psychiatric Clinics of North America*, *18*(1), 95–115. https://doi.org/10.1016/j.chc.2008.07.016

van der Laan, L. N., de Ridder, D. T. D., Viergever, M. A., & Smeets, P. A. M. (2011). The first taste is always with the eyes: A meta-analysis on the neural correlates of processing visual food cues. *NeuroImage*, *55*(1), 296–303. https://doi.org/10.1016/j.neuroimage.2010.11.055

van Dielen, F. M., van't Veer, C., Schols, A. M., Soeters, P. B., Buurman, W. A., & Greve, J. W. (2001). Increased leptin concentrations correlate with increased concentrations of inflammatory markers in morbidly obese individuals. *International Journal of Obesity and Related Metabolic Disorders: Journal of the International Association for the Study of Obesity*, *25*(12), 1759–1766. https://doi.org/10.1038/sj.ijo.0801825

van Eeden, A. E., van Hoeken, D., & Hoek, H. W. (2021). Incidence, prevalence and mortality of anorexia nervosa and bulimia nervosa. *Current Opinion in Psychiatry*, *34*(6), 515–524. https://doi.org/10.1097/YCO.0000000000000739

van Opstal, A. M., Westerink, A. M., Teeuwisse, W. M., van der Geest, M. A. M., van Furth, E. F., & van der Grond, J. (2015). Hypothalamic BOLD response to glucose intake and hypothalamic volume are similar in anorexia nervosa and healthy control subjects. *Frontiers in Neuroscience*, *9*, 159. https://doi.org/10.3389/fnins.2015.00159

Verhagen, L. A. W., Egecioglu, E., Luijendijk, M. C. M., Hillebrand, J. J. G., Adan, R. A. H., & Dickson, S. L. (2011). Acute and chronic suppression of the central ghrelin signaling system reveals a role in food anticipatory activity. *European Neuropsychopharmacology*, *21*(5), 384–392. https://doi.org/10.1016/j.euroneuro.2010.06.005

Verhagen, L. A. W., Luijendijk, M. C. M., & Adan, R. A. H. (2011). Leptin reduces hyperactivity in an animal model for anorexia nervosa via the ventral tegmental area. *European Neuropsychopharmacology*, *21*(3), 274–281. https://doi.org/10.1016/j.euroneuro.2010.11.006

Verhagen, L. A. W., Luijendijk, M. C. M., de Groot, J.-W., van Dommelen, L. P. G., Klimstra, A. G., Adan, R. A. H., & Roeling, T. A. P. (2011). Anticipation of meals during restricted feeding increases activity in the hypothalamus in rats. *European Journal of Neuroscience*, *34*(9), 1485–1491. https://doi.org/10.1111/j.1460-9568.2011.07880.x

Viskaitis, P., Irvine, E. E., Smith, M. A., Choudhury, A. I., Alvarez-Curto, E., Glegola, J. A., Hardy, D. G., Pedroni, S. M. A., Paiva Pessoa, M. R., Fernando, A. B. P., Katsouri, L., Sardini, A., Ungless, M. A., Milligan, G., & Withers, D. J. (2017). Modulation of SF1 Neuron Activity Coordinately Regulates Both Feeding Behavior and Associated Emotional States. *Cell Reports*, *21*(12), 3559–3572. https://doi.org/10.1016/j.celrep.2017.11.089

Walther, K., Birdsill, A. C., Glisky, E. L., & Ryan, L. (2010). Structural brain differences and cognitive functioning related to body mass index in older females. *Human Brain Mapping*, *31*(7), 1052–1064. https://doi.org/10.1002/hbm.20916

Wang, D., He, X., Zhao, Z., Feng, Q., Lin, R., Sun, Y., Ding, T., Xu, F., Luo, M., & Zhan, C. (2015). Whole-brain mapping of the direct inputs and axonal projections of POMC and AgRP neurons. *Frontiers in Neuroanatomy*, *9*. https://doi.org/10.3389/fnana.2015.00040

Wang, G. J., Volkow, N. D., Logan, J., Pappas, N. R., Wong, C. T., Zhu, W., Netusil, N., & Fowler, J. S. (2001). Brain dopamine and obesity. *Lancet (London, England)*, *357*(9253), 354–357. https://doi.org/10.1016/s0140-6736(00)03643-6

Wang, G.-J., Volkow, N. D., Telang, F., Jayne, M., Ma, Y., Pradhan, K., Zhu, W., Wong, C. T., Thanos, P. K., Geliebter, A., Biegon, A., & Fowler, J. S. (2009). Evidence of gender differences in the ability to inhibit brain activation elicited by food stimulation. *Proceedings of the National*

Academy of Sciences of the United States of America, *106*(4), 1249–1254. https://doi.org/10.1073/pnas.0807423106

Wang, K., Zhang, H., Bloss, C. S., Duvvuri, V., Kaye, W., Schork, N. J., Berrettini, W., Hakonarson, H., & Price Foundation Collaborative Group. (2011). A genome-wide association study on common SNPs and rare CNVs in anorexia nervosa. *Molecular Psychiatry*, *16*(9), 949–959. https://doi.org/10.1038/mp.2010.107

Wang, Q., Ding, S.-L., Li, Y., Royall, J., Feng, D., Lesnar, P., Graddis, N., Naeemi, M., Facer, B., Ho, A., Dolbeare, T., Blanchard, B., Dee, N., Wakeman, W., Hirokawa, K. E., Szafer, A., Sunkin, S. M., Oh, S. W., Bernard, A., … Ng, L. (2020). The Allen Mouse Brain Common Coordinate Framework: A 3D Reference Atlas. *Cell*, *181*(4), 936-953.e20. https://doi.org/10.1016/j.cell.2020.04.007

Wang, S., Peterson, D. J., Gatenby, J. C., Li, W., Grabowski, T. J., & Madhyastha, T. M. (2017). Evaluation of Field Map and Nonlinear Registration Methods for Correction of Susceptibility Artifacts in Diffusion MRI. *Frontiers in Neuroinformatics*, *11*, 17. https://doi.org/10.3389/fninf.2017.00017

Wang, Y., Kim, J., Schmit, M. B., Cho, T. S., Fang, C., & Cai, H. (2019). A bed nucleus of stria terminalis microcircuit regulating inflammation-associated modulation of feeding. *Nature Communications*, *10*(1), 2769. https://doi.org/10.1038/s41467-019-10715-x

Wardle, J. (1990). Conditioning processes and cue exposure in the modification of excessive eating. *Addictive Behaviors*, *15*(4), 387–393. https://doi.org/10.1016/0306-4603(90)90047-2

Wareham, N. J., Young, E. H., & Loos, R. J. F. (2008). Epidemiological study designs to investigate gene-behavior interactions in the context of human obesity. *Obesity (Silver Spring, Md.)*, *16 Suppl 3*(Suppl 3), S66-71. https://doi.org/10.1038/oby.2008.521

Watabe-Uchida, M., Zhu, L., Ogawa, S. K., Vamanrao, A., & Uchida, N. (2012). Whole-Brain Mapping of Direct Inputs to Midbrain Dopamine Neurons. *Neuron*, *74*(5), 858–873. https://doi.org/10.1016/j.neuron.2012.03.017

Watson, H. J., Yilmaz, Z., Thornton, L. M., Hübel, C., Coleman, J. R. I., Gaspar, H. A., Bryois, J., Hinney, A., Leppä, V. M., Mattheisen, M., Medland, S. E., Ripke, S., Yao, S., Giusti-Rodríguez, P., Anorexia Nervosa Genetics Initiative, Hanscombe, K. B., Purves, K. L., Eating Disorders Working Group of the Psychiatric Genomics Consortium, Adan, R. A. H., … Bulik, C. M. (2019). Genome-wide association study identifies eight risk loci and implicates metabo-psychiatric origins for anorexia nervosa. *Nature Genetics*, *51*(8), 1207–1214. https://doi.org/10.1038/s41588-019-0439-2

Willett, W. C., & Leibel, R. L. (2002). Dietary fat is not a major determinant of body fat. *The American Journal of Medicine*, *113 Suppl 9B*, 47S-59S. https://doi.org/10.1016/s0002-9343(01)00992-5

Wise, R. A. (2004). Dopamine, learning and motivation. *Nature Reviews Neuroscience*, *5*(6), 483–494. https://doi.org/10.1038/nrn1406

Wren, A. M., Seal, L. J., Cohen, M. A., Brynes, A. E., Frost, G. S., Murphy, K. G., Dhillo, W. S., Ghatei, M. A., & Bloom, S. R. (2001). Ghrelin enhances appetite and increases food intake in humans. *The Journal of Clinical Endocrinology and Metabolism*, *86*(12), 5992. https://doi.org/10.1210/jcem.86.12.8111

Wright, H., Li, X., Fallon, N. B., Crookall, R., Giesbrecht, T., Thomas, A., Halford, J. C. G., Harrold, J., & Stancak, A. (2016). Differential effects of hunger and satiety on insular cortex and hypothalamic functional connectivity. *The European Journal of Neuroscience*, *43*(9), 1181–1189. https://doi.org/10.1111/ejn.13182

Xu, J., Li, Y., Lin, H., Sinha, R., & Potenza, M. N. (2013). Body mass index correlates negatively with white matter integrity in the fornix and corpus callosum: A diffusion tensor imaging study. *Human Brain Mapping*, *34*(5), 1044–1052. https://doi.org/10.1002/hbm.21491

Yazdi, F. T., Clee, S. M., & Meyre, D. (2015). Obesity genetics in mouse and human: Back and forth, and back again. *PeerJ*, *3*, e856. https://doi.org/10.7717/peerj.856

Yiannakas, A., & Rosenblum, K. (2017). The Insula and Taste Learning. *Frontiers in Molecular Neuroscience*, *10*. https://doi.org/10.3389/fnmol.2017.00335

Yilmaz, Z., Hardaway, J. A., & Bulik, C. M. (2015). Genetics and Epigenetics of Eating Disorders. *Advances in Genomics and Genetics*, *5*, 131–150. https://doi.org/10.2147/AGG.S55776

Yokum, S., Ng, J., & Stice, E. (2011). Attentional bias to food images associated with elevated weight and future weight gain: An fMRI study. *Obesity (Silver Spring, Md.)*, *19*(9), 1775–1783. https://doi.org/10.1038/oby.2011.168

Yokum, S., Ng, J., & Stice, E. (2012). Relation of Regional Grey and White Matter Volumes to Current BMI and Future Increases in BMI: A Prospective MRI Study. *International Journal of Obesity (2005)*, *36*(5), 656–664. https://doi.org/10.1038/ijo.2011.175

Zald, D. H. (2009). Orbitofrontal cortex contributions to food selection and decision making. *Annals of Behavioral Medicine: A Publication of the Society of Behavioral Medicine*, *38 Suppl 1*, S18-24. https://doi.org/10.1007/s12160-009-9117-4

Zalesky, A., Fornito, A., & Bullmore, E. T. (2010). Network-based statistic: Identifying differences in brain networks. *NeuroImage*, *53*(4), 1197–1207. https://doi.org/10.1016/j.neuroimage.2010.06.041

Zastrow, A., Kaiser, S., Stippich, C., Walther, S., Herzog, W., Tchanturia, K., Belger, A., Weisbrod, M., Treasure, J., & Friederich, H.-C. (2009). Neural correlates of impaired cognitive-behavioral flexibility in anorexia nervosa. *The American Journal of Psychiatry*, *166*(5), 608–616. https://doi.org/10.1176/appi.ajp.2008.08050775

Zhang, J., Chen, D., Sweeney, P., & Yang, Y. (2020). An excitatory ventromedial hypothalamus to paraventricular thalamus circuit that suppresses food intake. *Nature Communications*, *11*(1), 6326. https://doi.org/10.1038/s41467-020-20093-4

Zhang, Y., Proenca, R., Maffei, M., Barone, M., Leopold, L., & Friedman, J. M. (1994). Positional cloning of the mouse obese gene and its human homologue. *Nature*, *372*(6505), 425–432. https://doi.org/10.1038/372425a0

Zhang-Molina, C., Schmit, M. B., & Cai, H. (2020). Neural Circuit Mechanism Underlying the Feeding Controlled by Insula-Central Amygdala Pathway. *iScience*, *23*(4), 101033. https://doi.org/10.1016/j.isci.2020.101033

Zheng, J., Anderson, K. L., Leal, S. L., Shestyuk, A., Gulsen, G., Mnatsakanyan, L., Vadera, S., Hsu, F. P. K., Yassa, M. A., Knight, R. T., & Lin, J. J. (2017). Amygdala-hippocampal dynamics during salient information processing. *Nature Communications*, *8*(1), 14413. https://doi.org/10.1038/ncomms14413

Zhu, J.-N., & Wang, J.-J. (2008). The cerebellum in feeding control: Possible function and mechanism. *Cellular and Molecular Neurobiology*, *28*(4), 469–478. https://doi.org/10.1007/s10571-007-9236-z

Zigman, J. M., & Elmquist, J. K. (2003). Minireview: From anorexia to obesity--the yin and yang of body weight control. *Endocrinology*, *144*(9), 3749–3756. https://doi.org/10.1210/en.2003-0241

Zink, C. F., & Weinberger, D. R. (2010). Cracking the moody brain: The rewards of self starvation. *Nature Medicine*, *16*(12), Article 12. https://doi.org/10.1038/nm1210-1382

9 Appendix

The final part of the project in Singapore involves the functional validation of the previously identified circuits using lightsheet microscopy and resting-state fMRI. During the last two months of my time in Singapore, I focused on optimizing viral injections and lens implantation, in preparation for in-vivo imaging sessions. My first target was the Red nucleus, my colleagues are currently continuing this work.

Calcium imaging
Stereotactic Surgery

Animals were anesthetized with Ketamine/Xylazine mixture (0.1 µl/10g) for surgical procedures. During the surgeries artificial tears ointment and heating pad at 33°C were used to maintain homeostasis. Atipamezole (revearsal) and buprenorphine (analgesic) were administered to animals. Dexamethasone is injected to animals who underwent implantation surgery.
In order to image glutamatergic Red nucleus neurons projecting to TN, VglutT2 mice were unilaterally injected with 0.2 µl AAV2-Retro-Cre into TN (AP: -1.55, ML: ±0.8, DV: -5.6) and 0.05 µl AAV9-Syn-FLEX-GCAMP6s into RN (AP: -3.5, ML: ±0.5, DV: -3.5) by 10 µl NANOFIL syringes and Micro syringe pump.
A microendoscopic GRIN (0.5 mm diameter, 8 mm length; Doric Snap-in Cannula) was implanted above the injection site. The lens was slowly lowered 0.1 mm/min and retracted 0.5 mm in every 1 mm starting at 1.5mm to allow tissue penetration. The focusing ring was used to make sure to target the region of interest and ensure fixation of the lens to the skull. Glue and dental cement were applied to stabilize the lens on the skull. Animals were single housed after implantation until in vivo imaging sessions.

Checking the targeting

To check the targeting of the virus injection, 14-days post-rabies injection mice were sacrificed for histological processing. Animals were overdosed with a Ketamine/Xylazine mixture, and transcardially perfused with phosphate buffered saline (PBS) and 4% paraformaldehyde (PFA) in PBS. Subsequently, collected brains were placed in 4% PFA overnight and transferred the next day into 15% sucrose for 4 hours and 30% sucrose overnight. Brains were prepared for cryostat sectioning by freezing in OCT compound. Brains were sectioned at 50 µm in the coronal plane with Leica Cryostat (CM1950) and placed in 1X PBS. Brains slices were then mounted into SuperFrost (Fisherbrand, #12-550-15) microscope slides and coverslips were sealed with Fluoromount-G (Southern Biotech, 0100-01). Sections were imaged using Nikon Ti eclipse.